UNIVERSITY OF SOUTHAMPTON

Faculty of Social Science
Southampton Business School

Economic Speed and Repositioning of a Tramp Ship under Uncertain Fuel Consumption and Future Profit Potential

by

Yuanming Song

MSc Operational Research and Statistics
BSc Applied Mathematics

ORCiD: 0000-0003-2847-3013

A thesis for the degree of
Doctor of Philosophy

June 2024

University of Southampton

Abstract

Faculty of Social Science
Southampton Business School

Doctor of Philosophy

Economic Speed and Repositioning of a Tramp Ship under Uncertain Fuel Consumption and Future Profit Potential

by Yuanming Song

Given the nature of sailing and the unique features of tramp shipping, the decision-maker who is considered to be the carrier in a shipping contract may face uncertainties from the natural environment, ports, shipping markets, and the counter-party. This impacts decisions about not only the journey itself, i.e., job acceptance, shipping route, schedule, and selection of terms, but also future operations after the vessel terminates at the destination port. The topic of economic decision-making of speed for tramp ships has been addressed in existing research from the following perspectives: deterministic framework (Ronen, 1982; Ge et al., 2021); uncertain weather performance (also known as weather routing and scheduling problems in the marine engineering community) (Zis et al., 2020); and other uncertainties (Hwang et al., 2008; Agra et al., 2013; Lindstad et al., 2013; Christiansen and Fagerholt, 2014). This thesis provides insights on both the development of fundamental optimisation models, including mean-risk optimisation models and Markov Decision Processes (MDPs), and practical analysis for decision-making about job acceptance, route and speed scheduling, and the selection of freight payment terms. In Chapter 3, we develop a new perspective on the problem of economic (average) ship speed by considering the impact of the decision maker's risk attitude. This impacts decisions about both speed and job acceptance. A ship is used to transport bulk cargoes in the spot market. A job consists of moving a cargo from a port A to a port B. Whether a ship owner can accept a job is determined by (i) the profitability of this job, and (ii) the commercial value of having its ship in port B when the job is finished. The time needed to travel from A to B affects both (i) and (ii). We consider that the decision maker wishes to maximise the Net Present Value (NPV) of the ship under uncertainty. This uncertainty is associated with the fuel consumption on the journey and the future profit potential of the ship at the next port. Underlying factors for these risks include adverse fuel consumption rates, and randomness in freight markets. We develop mean-risk optimisation models based on either long-term or short-term risk perspectives, justify why this distinction is worthwhile to consider, and introduce stochastic programming methods to solve the set of models. Numerical experiments illustrate the approach and show the sensitivity of the optimal strategy to context parameters and risk attitude of the decision maker. The mean-risk speed optimisation models can be extended to account for risk from different sources, e.g. failure-to-pay. In Chapter 4, we develop a method of dynamic stochastic programming for

solving a ship routing and scheduling problem when fuel consumption as a function of speed depends on the location of the ship and time. More specifically, a framework of a Markov Decision Process (MDP) incorporates the stochasticities beyond and after terminating at the destination port, as well as the information updating through the decision process. In this study, the decision-maker expects to maximise the long-term profitability, which includes not only the profit obtainable from the current journey but also the profitability after termination. We employ the approach of Net Present Value (NPV) and exploit the Future Profit Potential (FPP) to represent profitability after completing the current journey. The model is established in 3D states that include the spatial and temporal constituents of the vessel and solved by the value iteration algorithm. Subsequently, a simulation-enhanced value iteration (SEVI) is proposed to generate the distribution profile of NPV in the short- and long-term for decision-makers with a variety of risk attitudes. Numerical experiments show the methods proposed in this paper generate a higher NPV under a wide range of scenarios under risk. Experiments in reference to alternative delivery time-windows offer insights into how to secure an ideal delivery time-window before reaching agreement with due consideration of risk attitudes and long-term profitability. In Chapter 5, we agrue for the consideration of non-payment risk into the decision-making problems for the carrier in tramp shipping. We employ a Net Present Value (NPV) model to generally describe payment structures under a variety of freight payment terms, including Freight Prepaid (FP) and Freight Collect (FC), and shipment terms, including Free-on-Board Origin (FOB-O), Free-on-Board Destination (FOB-D), Cost and Freight (CFR), Cost, Insurance, and Freight (CIF). We demonstrate the cash-flows are symmetric when all parties have extended trust when conducting business activities with each other, which means there is no non-payment risk with freight charges. While the trust among all parties is weaker than extended trust, i.e., basic trust or guarded trust, additional monitoring mechanisms are required to assure all parties are liable to comply with the contract. Letter of Credit (LC), as a financial instrument that has been widely used in international trade, is discussed in this paper, especially for the transaction for freight charges. Variations in Letters of Credit are addressed in the payment structure. Computational results reveal that when the unit freight rate is determined, Red Clause Letters of Credit (RCLC) are more advantageous than other types of LC, i.e., Irrevocable Confirmed Letters of Credit (ICLC), and Letters of Credit at sight (LC at sight), especially when the carrier has inadequate liquidity cash flows. Whereas, LC at sight first-order stochastic dominants RCLC under specific conditions.

Contents

List of Figures

List of Tables

Declaration of Authorship

I, Yuanming Song, declare that this thesis titled, 'Economic Speed and Repositioning of a Tramp Ship under Uncertain Fuel Consumption and Future Profit Potential', and the work presented in it is my own and has been generated by me as the result of my own original research.

I confirm that:

1. This work was done wholly or mainly while in candidature for a research degree at this University;
2. Where any part of this thesis has previously been submitted for a degree or any other qualification at this University or any other institution, this has been clearly stated;
3. Where I have consulted the published work of others, this is always clearly attributed;
4. Where I have quoted from the work of others, the source is always given. With the exception of such quotations, this thesis is entirely my own work;
5. I have acknowledged all main sources of help;
6. Where the thesis is based on work done by myself jointly with others, I have made clear exactly what was done by others and what I have contributed myself;
7. None of this work has been published before submission

Signed:..... Date:.....

Acknowledgements

First and foremost, I would like to express my sincere gratitude to my supervisors, Dr. Patrick Beullens, and Prof. Dominic Hudson for giving me the opportunity to work on this project, for all their excellent guidance, encouragement, and outstanding feedback. An immense thank you to Patrick, who guides me with his extensive knowledge of operational research and shipping. I always leave our discussions with fresh research ideas. The creation of this thesis would not have been possible without them.

I would like to thank my parents, for their support and understanding all these years. I would like to thank my friends and colleagues, without their accompany and support my life will be quite boring and lonely.

Finally, I would like to thank Southampton Marine and Maritime Institute, Southampton Business School, and Shell, for funding my PhD and providing the opportunity.

List of Symbols and Abbreviations

Chapter 3

TCH	Time Charter Hire
FPP	Future Profit Potential
v	Average speed (nm per hour)
$v_{\min}$	Lower limit of design speed
$v_{\max}$	Higher limit of design speed
S	Sailing distance (nm)
T^l	Loading time (days)
T^s	Sailing time/Travel time (days)
T^{s*}	Optimal travel time (days)
T^w	Waiting time (days)
T^u	Unloading time (days)
T	Total time for completing the leg (days)
f^{TCH}	Daily hire rate (USD per day)
α	Opportunity cost of capital rate (per day)
G_0	Future profit potential (USD per day)
$C^l(v,z)$	Loading cost (USD)
C^u	Unloading cost (USD)
C^h	Handling cost (USD)
$C^f(v,w,z)$	Fuel cost (USD)
c^f	Fuel price (USD per tonne)
r^l	Loading rate (per hour)
r^u	Discharging rate (per hour)
$c^{f_{aux}}$	Auxiliary fuel price (USD per tonne)
c^p	Fixed Port Access Costs (USD)
c^l	Loading charge
c^u	Unloading charge
k	Fuel consumption function parameter
k_r	Random variable of fuel consumption rate
p	Fuel consumption function parameter
g	Fuel consumption function parameter

h	Fuel consumption function parameter
R^j	Revenue of the job (USD)
$\mathbb{E}[h(T,z)]$	Expected NPV excluding the FPP (USD)
$\mathbb{E}[H(T,z,G_0)]$	Expected NPV including the FPP (USD)
DWT^{cap}	Ship capacity (tonne)
DWT^{dsg}	Ship design weight (tonne)
DWT^{lgt}	Ship lightweight (tonne)
DWT^{bal}	Ballast tank capacity (tonne)
$r^{\mathrm{f}}_{\min}$	Minimum fill-rate (per hour)
Q^l	Loading quantity (barrel or tonne)
R^{unit}	Unit revenue (USD per barrel per 1000 nm)
μ_s	Profit target in short-term (USD)
μ_l	Profit target in long-term (USD)
R	Risk tolerance level
β_s	Percentage of freight payment after shipment
β_d	Percentage of freight payment after delivery
B_s	Deadline of payment for $\beta_s \cdot R^j$ (days)
B_d	Deadline of payment for $\beta_d \cdot R^j$ (days)
l_A	Additional penalty rate if the payment is delayed
B_{lA}	Allowed payment period after the deadline (days)
$\tilde{\beta_d}$	Actual percentage of freight payment after delivery
$\tilde{B_d}$	Actual payment time for $\beta_d \cdot R^j$ (days)
$\tilde{l_A}$	Actual rate of payment for $l_A \cdot R^j$
$\tilde{B_{lA}}$	Actual payment time for $\tilde{l_A} \cdot R^j$
Chapter 4	
TSRSP	Tramp Ship Routing and Scheduling Problem
MDP	Markov decision process
WRSP	Weather Routing and Scheduling Problem
SOP	Speed Optimisation Problem
SEVI	Simulation-enhanced value iteration algorithm
T^{ED}	Earliest delivery time by contract (days)
T^{LD}	Latest delivery time by contract (days)
$\overline{T^{w_B}}$	Maximum of estimation for waiting time at port B (hours)
T^{EDp}	Minimum travelling time (days)
T^{LDp}	Maximum travelling time (days)
$s = (x,y,t)$	3D state includes spatial coordinate x and y, and temporal element t
W	Parameter vector of oceanic weather conditions
H_s	Coefficients about wave height
T_z	Coefficients about wave period
$S_w(H_s,T_z)$	Coefficients about wave spectrum

C	Coefficient of current
V_{wu}	Coefficient of wind direction
V_{wv}	Coefficient of wind velocity
$L_{\overrightarrow{P_{ij}P_{i+1j'}}}$	Length of the segment $P_{ij}P_{i+1j'}$
$\mathbb{I}_W(s)$	Newest updated information set about oceanic weather conditions at state s
$\mathbb{I}_W(s)^{past}$	Matrix of certain information about oceanic weather conditions for states at the approached stages
$\mathbb{I}_W(s)^{future}$	Information set about oceanic weather conditions for the rest of the states
N_{future}	Total number of future states
$T^{w_B}(s)$	Random variable of the waiting time at port B estimated when the vessel is at state s
$\alpha G_0(s)$	Random variable of the FPP estimated when the vessel is at state s
$\mathcal{M}$	Markov decision process, $\mathcal{M} = \langle \mathbf{S}, \mathbf{A}, \mathbf{L}, R, \alpha \rangle$
$\mathbf{S}$	Discrete state space
$\mathbf{A}$	Discrete action space
$\mathbf{L}$	Likelihood space
$\mathrm{R}(s, a, s')$	Reward function
$S_{P_{ij}}$	The set of states that derived by the the waypoint P_{ij}
$A_{P_{ij}}$	The set of actions for the waypoint P_{ij}
$\mathrm{CF}(\tau)$	Cash flow function where τ indicates the time consumed in the transition
N_{Simul}	The amount of run times for the simulation
$\mathrm{Q}(s, a)$	Action-value function
$\mathrm{V}(s)$	Value function
$\mathrm{V}^*(s)$	The maximum of value function
ψ	Policy
ψ^*	Optimal policy
H^*	The expected NPV including FPP at the destination port after applying the optimal policy ψ^* (USD)
h^*	The expected obtained NPV from completing the voyage after applying the optimal policy ψ^* (USD)

Chapter 5

FOB	Free on Board
CFR	Cost and Freight
CIF	Cost, Insurance, and Freight
FP	Freight Prepaid
FC	Freight Collect
LC	Letter of Credit

ICLC	Irrevocable and Confirmed Letter of Credit
LC at sight	Letter of Credit at sight
RCLC	Red Clause Letter of Credit
CAR	Carrier
SHPR	Shipper
CNEE	Consignee
FOB-O-FC	FOB Origin Freight Collect
FOB-O-FP	FOB Origin Freight Prepaid
FOB-O-FPCB	FOB Origin Freight Prepaid Charge Back
FOB-D-FC	FOB Destination Freight Collect
FOB-D-FP	FOB Destination Freight Prepaid
FOB-D-FCA	FOB Destination Freight Collect Allowed
BoL	Bill of Lading
TCI	Trade Credit Insurance
t^{billi_b}	Time that carrier send the bill i, $i = 1,2,3$ (years)
t^{billi_c}	Time that the party who is liable to pay the bill i completes the payment, $i = 1,2,3$ (years)
β	Matrix about freight payment
γ	Matrix about insurance claim
L^{billi}	Period of completing payment after receipt of the bill i, $i = 1,2,3$ (days)
L^{claim}	Period of filing the claim if there is any loss or damage (days)
R^{os}	Amount of outstanding bill i, $i = 1,2,3$ (USD)
R_j^{late}	Amount of payments made later than the last bill's deadline, $j = 1,2,\ldots,n$ (USD)
t_j^{late}	Time of payments made later than the last bill's deadline, $j = 1,2,\ldots,n$ (years)
R^{aosi}	Remaining amount of outstanding bill, $i = 1,2,3$ (USD)
t^{aosi}	Overdue time for the remaining amount of outstanding bill R^{aosi}, $i = 1,2,3$ (days)
NPV_{CAR}	NPV for carrier (USD)
NPV_{SHRP}	NPV for shipper (USD)
NPV_{CNEE}	NPV for consignee (USD)
CDT^{fc}	Amount of credit authorised for freight charges (USD)
$r^{\text{LC}^{fc}}$	Rate of cost for having the LC
$t^{\text{LC}_a^{fc}}$	Time that the shipper or consignee request the ICLC or LC at sight (years)
$t_{IB/CB}^{\text{CDT}}$	Time that the issuing bank sends credit to the confirming bank (years)
t^{load}	Time that shipment starts (years)
t_e^{sail}	Time that shipment ends (years)

$t^{CAR_{\text{BoL}}}$	Time that carrier present the BoL (years)
$t^{fc}_{(party)/IB}$	Time that shipper or consignee pays the freight charges to the issuing bank (years)
$t^{fc}_{CB/CAR}$	Time that confirming bank pays the carrier (years)
σ	Time difference in asymmetric cash-flows (days)
$\text{FC}^{\text{LC}}_{(party)}$	Freight charges paid by the party indicated (USD)
$\text{FC}^{\text{LC}}_{CAR}$	Freight charges received by the carrier with letters of credit (USD)
$\text{NPV}^{\text{LC}}_{CAR}$	NPV for carrier with letters of credit (USD)
$\text{NPV}^{\text{RCLC}}_{CAR}$	NPV for carrier with red clause letters of credit (USD)
$\text{NPV}^{\text{LCatsight}}_{CAR}$	NPV for carrier with letters of credit at sight (USD)
$\triangle\text{FC}^{\text{LC}}_{CAR}$	Difference of total freight charges in consequence by σ (USD)
$\triangle\text{NPV}^{\text{LC}}_{CAR}$	Difference of total NPV in consequence by σ (USD)
$G^{\text{LC at sight}}$	Distributions of the utility function $\text{NPV}^{\text{LC}}_{CAR}$ for LC at sight
G^{ICLC}	Distributions of the utility function $\text{NPV}^{\text{LC}}_{CAR}$ for ICLC
$F^{\text{LC at sight}}$	Distributions of σ for LC at sight
F^{ICLC}	Distributions of σ for ICLC
$r^{\text{RCLC}^{fc}}$	Rate of cost for having the RCLC
R^{fci}	Amount of freight charges received by carrier, $i = 1, 2$ (USD)
t^{fci}	Time of receipt R^{fci}, $i = 1, 2$ (years)
$\text{FC}^{\text{RCLC}}_{CAR}$	Freight charges received by the carrier with red clause letters of credit (USD)
$\text{NPV}^{\text{LC}}_{CAR}$	NPV for carrier with red clause letters of credit (USD)
$\Delta\text{FC}^{\text{RCLC}}_{CAR}(\theta_1, \theta_2)$	Difference in freight charges between ICLC and RCLC for θ_1 and θ_2 (USD)
$\Delta\text{NPV}^{\text{RCLC}}_{CAR}(\theta_1, \theta_2)$	Difference in NPV between ICLC and RCLC for θ_1 and θ_2 (USD)

Chapter 1

Introduction

In this chapter, the research topics addressed in this thesis will be introduced by illustrating the research background, explaining the research aims, and provide a brief outline for the whole thesis. Connections among three independent research papers are provided at the end of this part for readers' better understanding.

1.1 Research background

Maritime transport and trade systems have faced challenges from the variety of uncertainties, that working singly or in combination, leading to increased volatility and risk in the shipping market. Tramp shipping market, which handles over 75 percent of cargo volumes in international maritime trade and usually deal with dry bulk cargo like coal, grains, and minerals (on Trade and Development). The performance of freight markets in tramp shipping is highly corresponding to the Baltic Dry Index (BDI) which measures the average cost of dry bulk material transportation across more than 23 routes (on Trade and Development). During last two years, BDI reached an over 13-year high of 5526 points at September of 2021, and fell to 538 points at February 2023 [1]. The fluctuation from bulk cargo freight markets not only impact the profitability for the current journey undertaken by the decision maker in tramp shipping, but also plays a vital role for future profitability that obtainable after completing the job at the destination port (Ge et al., 2021).

In addition to the volatility in freight markets, uncertainties during the sailing process and after calling at ports, such as weather conditions and fuel costs, and rising port congestion also cause the risk of delay and affect profitability (Fagerholt et al., 2010a; Alvarez et al., 2011; Schinas and Stefanakos, 2012; Magirou et al., 2015; Guan et al., 2017).

Tramp shipping is one of three shipping modes in marine transportation; the other two are liner shipping and industrial shipping (Ronen, 1983). Vessels in liner shipping are comparable to bus

[1] The data is collected from a public resource: https://tradingeconomics.com/commodity/baltic.

services in passenger transport: they typically follow fixed routes and have to meet time windows for the earliest and latest arrival times at the ports within the route. Vessels in industrial shipping are working under contracts in order to meet service schedules or frequencies at minimal cost (Barnhart and Laporte, 2006). In tramp shipping, vessels have no pre-defined routes and schedules (Ronen, 1983). The operator of vessels in tramp shipping is responsible for evaluating potential jobs, operating the vessel from route scheduling to speed control, selecting the optimal policy of contracts and attached terms, etc. Decisions are made from both capacity and profitability standpoints.

With the vital role of tramp shipping in maritime trade as well as the nature of ever-changing stochasticities, vessels operated as tramp ship are more flexible when choosing potential jobs and planning sailing routes and speeds. Less restrictions existed in satisfying service frequencies and delivery time-window when compared to vessels operated in liner shipping. This kind of flexibility brings more opportunities for decision makers to achieve higher objectives by making better decisions, and more associated uncertainties and risk at the mean time.

Economic speed optimisation problem is a classic topic that is discussed in the operational research community to optimise decisions about speed. Specifically, the decision maker in tramp shipping is represented by the shipowner or the time-charterer who play an equivalent role in making decisions about the ship's operation. Conventional speed optimisation models aim to minimise the cost of the shipping operations or maximise the ship owner's profit earned either per unit of time, per nautical mile, or per journey (Ronen, 1982; Norstad et al., 2011; Magirou et al., 2015). Ge et al. (2021) introduces the concept of Future Profit Potential (FPP) into the deterministic speed optimisation problem in tramp shipping, using maximisation of the ship's Net Present Value (NPV) as a criterion. These models are established on a deterministic basis, where parameters related to the freight market and fuel consumption are assumed to be fixed numbers. Some other speed optimisation models take uncertainties about either weather condition, i.e., comprehensively addressed by Zis et al. (2020), freight rates (Magirou et al., 2015); bunker price (Wang et al., 2013); and cargo availability (Li et al., 2022a); and so on. From the perspective of the decision maker, willingness to accept a job offer (of transporting a certain amount of cargo from port A to port B or other routes) depends on the profitability based on his or her own risk preference. The decisions of different shipowners for the same job could be various. For example, a high-return, high-risk job might be acceptable for a risk-taking shipowner but might not be for a risk-averse shipowner. Besides, the cash-flow liquidity will also affect the decisions about the ship's operation.

Another important nature of information through decision process in tramp shipping that cannot be neglectable is that the information about the above uncertainties is usually not well studied at the beginning of the journey but will become more clear over time. For example, oceanic weather conditions are considered the main factor that causes speed loss or a higher fuel consumption rate if keeping the same speed level (speed over ground) (Yu et al., 2017; Hinnenthal and Clauss, 2010). The prediction of oceanic weather conditions is 80 percent correct 7 days behind and will fall to 50 percent if it is 10 days behind (Oceanic and of Commerce). Directly

using the weather predictions in an optimisation model to optimise routes and speeds for a tramp shipping journey, which usually takes more than a month, is unrealistic and inefficient. Similarly, in the estimation of port congestion and freight markets, updating the information through the decision process are likewise necessary.

What's more, besides optimising the job acceptance or ship's routing and scheduling based on the offered contract and terms from the shipper, the shipowner or time charterer, who takes on the responsibility as carrier in tramp shipping, has alternatives to evaluate and negotiate for a more beneficial offer. Alternatives are from a wide range of delivery time-windows, loading or unloading time, terms of freight payments, or other factors that are involved in the decision maker's concern, i.e., profitability and risk.

1.2 Research aims and main contributions

This thesis initially suggests the following research problem on the research gap and relevance given such a research background, discuss the application of the problems, and utilise techniques to address the identified concern after that.

The overall objectives of the research are to develop efficient models for improving the decision-making problems in tramp shipping with multiple dimension needs, in particular towards including the diversity of risk attitudes when choosing between potential jobs and planning the travel time and route; modelling uncertainties within the decision process introduced by phenomena taking place either before or after the sailing process; addressing how estimates about the uncertainties may need to be adapted during a decision process with multiple decision points over time; and analysing different payment structures of freight payment protocols under risk.

More specifically, we can raise the following research questions:

1. Will decision-makers with different risk attitudes make different decisions about choosing potential jobs in the freight market?

2. What is the role of uncertainties in the decision process, and to what extent will these impact the decisions about choosing jobs in the freight market and corresponding optimal economic sailing speeds?

3. How can we better match the decision process about job selection and economic ship deployment to the risk attitude regarding cash liquidity?

4. How to incorporate more accurately the fact that information about weather conditions, port conditions, and freight markets, change dynamically during the sailing process; what types of operational research tools could be employed?

5. How can we update the dynamic information in the decision process to help the decision maker make decisions after the sailing starts?

6. How and to what extent will different types of payment structures and freight payment terms influence the NPV of the carrier?

7. When considering the additional financial instruments, for example, the letters of credit when paying the freight charges, which party will benefit from which type of credit from the perspective of NPV?

To investigate the listed research questions, three main topics are proposed, and each of them corresponds to an independent chapter. The proposed topics are as follows:

Chapter 3: ***Job Acceptance and Economic Travel Time of a Tramp Ship under Risk***

Chapter 4: ***A Framework of Markov Decision Processes for Economic Tramp Ship Routing and Scheduling Problems***

Chapter 5: ***Payment Structures, NPV Analysis and Letters of Credit in Tramp Shipping***

In Chapter 3, research questions 1-3 are solved by introducing the mean-risk optimisation problems to address the risk of not achieving the NPV, excluding and including the FPP for decision makers with various risk attitudes. The decision makers are categorised based on their risk tolerance level and profit target, whether short- or long-term. The mean-risk optimisation models with short- or long-term NPV constraints are designed to solve job acceptance and economic speed for different decision makers. In Chapter 4, research questions 4-5 are accomplished by building an information updating Markov Decision Process (MDP) framework. The approach introduces a novel update procedure about the stochastic uncertainty on future voyage days and improves upon current methods in the literature that aim to account for updating weather forecasts. In Chapter 5, research questions 6-7 are answered step by step for a wide range of freight payment terms and letters of credit. The NPV analysis for the main counterparty involved in the freight payment is also being discussed. The framework can be used by all parties involved to analysis the relative benefits of various credit mechanisms.

We further illustrate the main contributions of this thesis could be concluded as follows:

1. Uncertainty about fuel consumption is addressed in the optimisation model in Chapter 3. The fuel consumption rate function ($tonne/day$) is considered as a function of speed v and deadweight w, introduced by Psaraftis and Kontovas (2014) as follows:

$$f(v,w) = k \cdot (p + v^g)(w + A)^h, \tag{1.1}$$

We convert the rate k from a constant into a random variable k_r to represent the uncertainty:

$$f(v,w,k_r) = k_r \cdot (p + v^g)(w + A)^h. \tag{1.2}$$

Let $k_r = k$ represent the usual fuel consumption rate, then an unusual fuel consumption rate is $k_r < k$ or $k_r > k$. For example, a ship having to battle a rough weather day may

well consume double the amount of fuel, i.e. $k_r = 2k$. The stochastic fuel consumption rate is formulated into a random variable k_r.

2. Uncertainty about future profit potential (FPP) is addressed in the optimisation model in Chapter 3 in order to capture changes in job acceptance and speeds when the estimation of FPP changes. Decision makers are assumed to have a desire to maximise profitability, which is obtainable not only from the current evaluated journey but also from potential journeys afterwards. The latter is accounted for in the model by the FPP calculated by NPV.

3. Mean-risk optimisation models are established in Chapter 3 for considering decision makers having different tolerance levels to risk and whether they consider short-term or long-term risk. The uncertainties captured by the stochastic modelling are mapped to a probabilistic space of long- and short-term NPV. The model is applicable to finding the optimal travel time under a risk tolerance and profit target.

4. Stochastic information such as conditions of weather, port congestion, and FPP are considered as dynamic and will be updated through the decision process. Based on that, a framework of MDP is formulated to optimise the sailing routes and schedules in Chapter 4. The framework incorporate the technique of 3D states in space and temporal backward from the termination states the starting states.

5. An adjusted value iteration algorithm is formulated in Chapter 4 to derive optimum solution for risk-neutral decision makers and a simulation-enhanced value iteration algorithm (SEVI) for decision makers have a variety of risk tolerance levels, profit target in short- or long-term. The risk performance of simulated NPV in the short- and long-term as well as the intuitive graphs are suggested rather than a single optimal solution.

6. Alternative delivery time-window are compared in Chapter 4 to help decision makers who are not satisfied with the risk performance of NPV that derived from current delivery time window in Chapter 4 as a way to mitigate risk of delivering late when the estimation of weather or port congestion is undesirable.

7. A variety of freight payment terms are described by a general payment structure model and employed by the approach of NPV in Chapter 5.

8. The non-payment risk is addressed by considering the business in shipping when all parties have an extended trust and a relatively weaker trust. Further, documentary credit, such as LC, is proven to be necessary when there is a lack of trustworthiness in the business. LC plays a role in reducing the wide range of risks raised by the party entitled to the ownership of cargo and the carrier, which means the cost of the transaction will increase owing to the lower level of trust.

9. A wide range of options for LC and an analysis of NPV for the carrier are discussed in Chapter 5. The NPV analysis and discussions about non-payment risk could help carriers better choose terms and clauses before negotiating the agreements. Also, our model provides insights for professionals in the shipping industry about how to select the best freight charge terms for different types of carriers.

In this thesis, we concentrate on solving decision-making problems for shipowners or time-charterer in tramp shipping by optimising decisions including job acceptance and economic travel time (Chapter 3); sailing routes and speeds (Chapter 4); and selection of terms of freight payment (Chapter 5). The decision maker is considered to be provident that has the objective of maximising profitability in the long term, which includes the NPV from the current journey and the FPP. The risk attitudes of different types of decision makers are also taken into account during the model establishment and numerical experiments in each chapter.

1.3 Research methodology, data collection, and analysis

The research focuses on utilising methodologies from the field of operational research, which is concerned with the art and science of solving decision-making problems. To model and solve the three proposed research topics, several research methodologies are chosen. For Chapter 3, stochastic modelling for fuel consumption rate and FPP; mean-risk optimisation models are employed to the problem; For Chapter 4, the speed correction model, Markov decision process, information updating during the MDP, and simulation method are applied; for Chapter 5, the NPV approach is utilised to describe the cash-flow functions for the shipper, consignee, and carrier involved in the shipping contract. Becaause the nature of the problem often dictates which OR methods are most suited, a detailed motivation of why these particular methods have been chosen is given in the corresponding chapters where these problems are also discussed in detail.

Data used in this research are all public data that acquired from the public accessed websites or publications. The websites include:

`https://tradingeconomics.com/commodity/baltic`;

`https://www.bimco.org/news/market_analysis/2021/20210601_dry_bulk_shipping`;

`https://www.sea.live/intelligent-marketplace/vessel-tracking/`;

`https://www.passageweather.com/`.

The vessel characteristics for Suezmax is obtained from (Stopford, 2008), as shown in Appendix A. The vessel characteristics for PANAMANA is obtained from the website https://www.sea.live/, and estimated by the fuel consumption rate function. This is no confidential data utilised.

1.4 Outline

The remaining of thesis is organised as follows: *Job Acceptance and Economic Travel Time of a Tramp Ship under Risk* is presented in Chapter 3; *A Framework of Markov Decision Processes for Economic Tramp Ship Routing and Scheduling Problems* is given in Chapter 4; *Payment Structures, NPV Analysis and Letters of Credit in Tramp Shipping* is discussed in Chapter 5; the main conclusion of this thesis and the PhD study is presented in Chapter 6; supplementary contents for the thesis is given in Appendix A-G. The overview of the thesis structure and research questions is presented in Figure 1.

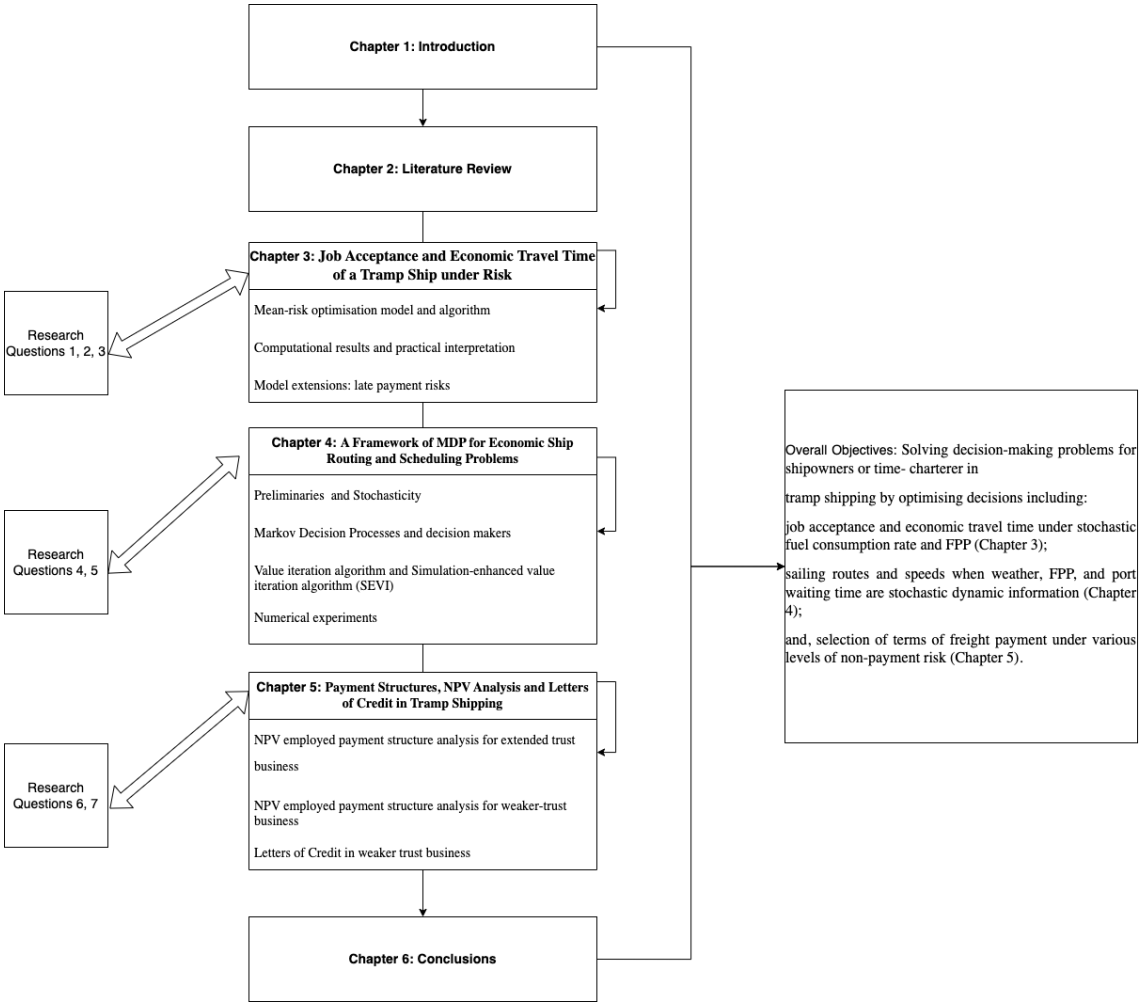

FIGURE 1: Overview of the thesis structure and research questions

The thesis follows a three-paper format and Chapters 3, 4, and 5 are intended to be publishable as independent research papers in the peer-reviewed literature.

Chapter 2

Literature Review

This chapter provides a comprehensive overview of optimisation in economic speed strategy with regards to ship routing and scheduling problems for tramp shipping. Tramp shipping is one of three ocean transportation modes, next to liner and industrial shipping. The vessels operated by liner shipping are usually compared to buses in land transportation due to them have predefined routes and schedules. The objectives of liner shipping businesses include maintaining the service frequency withing operation cost constraints. The industrial shipping vessels, on the other side, usually aims to minimise the cost Stopford (2008); Christiansen et al. (2004) within the confines of a service contract that may, for example, involve delivering an agreed volume on an annual basis. Tramp shipping is a shipping mode that can be compared to a taxi service, due to the flexibility regarding the choice of journeys, sailing routes, and speed. The decision maker in tramp shipping is typically a vessel owner, or a person in an equivalent position such as a charterer having time-chartered ships, and who is responsible for providing instructions to the master of the vessels about taking shipping jobs. Given the importance of considering the stochasticity and concept of future profit potential in tramp shipping, literature about uncertainties in marine optimisation problems is also included as an individual chapter; see Chapter 2.2. The purpose of this part is to provide a better understanding of knowledge, modelling approaches, and solving methods and algorithms in the field of ship routing and scheduling problems before carrying out further investigations. Meanwhile, the research gap and motivation for topics discussed within this study are illustrated in the debates for existing studies in Chapter 2.3.

2.1 Ship routing and scheduling problems

Investigations for ship routing and scheduling problems between 1967 to 1993 are comprehensively addressed in Ronen (1993). Then, due to the fast developments in computer science, researchers be aware of the significant improvements which are lead by the economic scheduling of the ship. During this decade, literature in this ship routing and scheduling problems concentrated on optimising the fleet size and mix, deployment, inventory routing, cruising speed and

ship scheduling. Benford (1981) provides a procedure for the shipowner to choose the most profitable mix of fleet and corresponding speed. He mentioned that the potential profitability exists in exceeding the ship's capacity when fuel price goes high. For the same question, Perakis (1985) argues that in the case of fuel price keeps in high level, use more slow steaming ships could be a better option than exceeding all using ship's capacity. The structure of optimal deployment policy which contains the fleet size, type and speed for each ship strengthen the importance of speed in such optimisation problems. Ronen (1982) extended the work of impact from fuel price, he investigated the optimal ship speed in three different modes, income generating leg, positioning leg and speed related income. A conclusion was drawn from this paper that the optimal speed is highly related to the model formulation that concludes design speed limit, objectives, fuel price and contract details.

Literature for ship routing and scheduling problems in the last decade of 2004 is provided by Christiansen et al. (2004). Bausch et al. (1998) introduced a spreadsheet-based optimisation decision support system for short-term bulk product transport and used speed as one of the decision variables. Brown et al. (1987) and Fagerholt (2001) also used speed as their major decision variables in the model formulation. Brown et al. (1987) formulated a crude oil transportation scheduling problem as an Elastic Set Partitioning Problem (ESPP), by taking the potential economic profitability during waiting time in the harbour as one of the cost components for the fleet to find the optimal speed and scheduling. The most common objectives in tramp shipping routing and scheduling problems are minimising costs or maximising profits (Appelgren, 1969, 1971; Kim and Lee, 1997; Bausch et al., 1998; Fagerholt, 2004). Cost components can be different according to the contract type and operating mode. Basically, it concludes daily operation cost, bunker fuel cost, auxiliary fuel cost, port and canal fees, and demurrage (Stopford, 2008).

A mixed-integer programming model is presented by Agarwal and Ergun (2008) for solving a cargo routing problem in liner shipping. Deeply analysis on the application of greedy heuristic, column generation and benders decomposition algorithms are given, which lead to the dominance of benders decomposition-based algorithms perform better than others in computational experiment. The model focus on routing problem for single ship type, single service route and fixed service frequency, while the model can be adjusted for changing service frequency. According to the segmentation in Christiansen et al. (2004), LNG inventory routing problem is a component of commercial vessels routing and scheduling and ship routing and scheduling in supply chains. Grønhaug et al. (2010) used a path flow model to simulate procedures and parts included in LNG supply chain and presents how to solve the model by branch-and-price algorithm and column generation method. There are more constraints in LNG-IRP than typical inventory routing problems, such as the producing level and capacity for each port are varied, thus demand can be fluctuating during the whole horizon.

Moreover, due to the chemical characteristics of LNG, loss during liquefaction and transportation is also worth considering. Norstad et al. (2011) presented an optimisation model which set the objective as minimising the cost. Different from Benford (1981); Perakis (1985); Perakis and Papadakis (1987a,b), this model set the speed of each leg as decision variable and exclude time

window of loading and discharging. Several algorithms are mentioned for solving the model in this paper, firstly is nonlinear programming, which is practical theoretically, but the computing time will depend on solver and model size. Secondly is discretising arrival time and transfer the model to the shortest path problem. The advantage of this method is relatively intuitive. And the drawback is concluding too much useless branch in the discretising tree which will waste time in computing. The last one is recursive smoothing algorithm, choose a speed in range as the start point, narrow the time window range step by step through comparing the objective function value in the neighbourhood of current speed. The computational experiment shows that recursive smoothing algorithm can competitively improve the computation efficiency. Norstad et al. (2011) argued that total average fuel consumption of the vessel will be lower if the speed is set as the decision variable when assigning cargoes. This argument is helpful for the multi-fleet optimisation problem. Wen et al. (2017) presented a multiple ship routing and scheduling problem that set speed as a decision variable, minimising cost as objective. In logistical context, the model helps a pickup and delivery problem to allocate proper ship to target route and schedule optimal average speed for each leg. When dealing with the speed, the model contains a default optimal speed which is obtained before solving the optimisation problem by finding the minimum point of the cost function. Then determine the optimal speed v^* through the feasible range. Heuristic branch-and-price and constraint programming are proposed for solving the optimisation problem. Although the title of Wen et al. (2017) contained multiple objectives, there is no exact multi-objective model established in this paper. And most of the related parts about objectives concentrate on comparing different optimal speed results when altering objective function to minimising cost, minimising cost when ignore cargo inventory cost, minimising emission and minimising total trip time.

For example, Perakis and Bremer (1992) described a crude oil tanker scheduling problem for minimum costs. Ronen (1982) presented a speed optimisation model for three voyage legs, income generating leg, positioning leg and mixed leg. By maximising the profit per day with the constraint of nominal speed asked by the physical performance of the vessel, an optimal speed is driven for each type of leg. Ronen's model can be seen as a typical mathematical formulation for optimal speed in ship routing and scheduling problems. There are also some improvements in the accuracy of model components, for example, Psaraftis and Kontovas (2014) stated a lot of treatments of factors in ship speed optimisation model from the operational view and provide several variants which the model formulation can be reorganised. For treatments of fuel consumption, approximation function contains a cubic function of ship speed, regression function of ship speed and vessel payload and more complex regression function that consider the impact from the external environment such as weather condition, wave condition, temperature and others. Ronen (2011) investigated the effect of oil price on ship speed and fleet size for a liner shipping optimisation problem. Through handling the balance between saving fuel cost and completing service frequency on time, whether to slow up the speed is influenced by the specific oil price. Psaraftis and Kontovas (2014) used an example of path and tour problem to prove that changes of freight rate will influence the optimal visiting sequence which indicates

the value of input parameters in ship speed optimisation problem. Such papers explain the limitations of deterministic operational methods in ship speed optimisation problem and declare that introducing dynamic stochastic modelling formulations is quite necessary. Magirou et al. (2015) added stochastic economic data in the process for determining optimal ship speed and voyage sequence. They used the journey model of Ronen (1982) in which the objective is to maximise the dollars earned per unit of time, and also proposed a discounted profit model in infinite horizon case. The deterministic speed optimisation model established by Ge et al. (2021) consider to employ the approach of Net Present Value (NPV) and maximise the NPV and FPP for the trip.

2.2 Uncertainties in shipping optimisation problems

There are many unknowns involved in operating a vessel at sea and doing business in freight markets. Particularly, the flexibility of routing and scheduling for tramp ships makes considering the uncertainties in the decision-making process more vital. A lot of uncertainties are addressed in the literature, and we summarise those according to its consequence in decision maker's objective-maximising profitability and control the risk below his or her own tolerance level. The objective in tramp shipping decision making, or routing and scheduling problems, is maximising the profit, which is equivalent to the total freight income minus the operating cost (Norstad et al., 2011). For decision makers consider the future potential profitability after completing the current job, Ge et al. (2021) proposes the concept of future profit potential (FPP) and calculate the objective as maximising the NPV of the ship. Both approaches look at freight income versus operational costs.

The freight rates are often negotiated among the shipper, carrier, or a third-party working on their behalf and may be put into a contract upon accepting a transport job. This explains why it is not included as a decision variable in the optimisation process. Thus, the freight income for the 'current' journey can be considered fixed and known. The operating cost for a vessel is consists of the port costs (fixed), the fuel cost depending on sailing route and speeds, hiring cost depending on the type of charterer, and other handling fees (Stopford, 2008; Wen et al., 2016). Fuel costs contribute to a significant portion of the many costs associated with maritime transportation. As an example, fuel costs may account for over 50% of the overall operating costs of a tramp shipping firm (Meng et al., 2015). As fuel costs are highly related to the sailing speeds and weather conditions, they from a source of stochasticity on the costs of a journey during the sailing process. The uncertainty on the fuel cost is further discussed in Section 2.2.1.

The condition of the departure or destination port when the vessel departs from or arrives at is also uncertain, whereas either of them influences the rate of loading or unloading and the expected time of arrival. It impacts the decisions of speeds and routes due to the ship usually aims to deliver the cargo within the negotiated time-windows. We further discuss the uncertainty from port congestion in Section 2.2.2.

When comparing the tramp ship to a taxi in land transportation, the driver should consider the profitability after completing the job before accepting the job. The decision maker in tramp shipping should have the same concern when comparing the potential jobs to undertake. Ge et al. (2021) proposes the concept of FPP and illustrate with numerical experiments the significance of applying the method of NPV to calculate the objective as well as using a concept of the FPP to express the financial desirability of the destination port in the tramp shipping context. Our investigation indicates that the FPP as a likely source of uncertainty affecting the future prospect in shipping optimisation problems and is further discussed in Section 2.2.3.

Thus, we conclude the following parts as the uncertainties that considered in this research due to its importance in tramp shipping decision making problems: fuel cost, port congestion, and future prospects. Other factors of likely importance are discussed in Appendix G.

2.2.1 Fuel cost

Fuel cost is a considerable component in the cost of shipping services. Regularly, fuel cost is consists of two parts, practical fuel consumption and surcharges. Notteboom and Vernimmen (2009) illustrated the impact of increasing fuel price on liner shipping services and some deals to release the influence. Due to the non-linear relationship between fuel consumption and vessel speed, there will have a significant impact if the fuel price fluctuated in the short term. Liner shipping services ask for a regular inventory supplement. Thus some complements such as add new liner shipping route, increase the amount of service vessel should be done after comparing to increase current vessel speed. In the same year, Notteboom and Cariou (2009) investigated the relationship between actual fuel cost and fuel surcharges and concluded new methods to calculate the fuel surcharges based on bunker price, vessel type, speed, deadweight tonnage and navigation distance. Yao et al. (2012) gave a thorough analysis of how can bunker price and availability of bunker in each port influence the bunker fuel management strategy in the optimisation model. They concluded the bunker fuel management as three parts, the port selection, the amount to bunker and the speed schedule. After applying their optimisation model to two classic liner shipping service routes, Asia-Europe Express (AEX) and Atlantic Pacific Express (APX), they made some comments about impacts lead by bunker price and availability. Firstly, fluctuations in fuel price will impact the bunker fuel management in some sense. Depending on specific background, the optimal bunker port could change, different amount of bunker will be determined, or sometimes the vessel speed could be altered. Changes in optimal strategy conclude mixed decision information and vary in different cases. Secondly, the vessel speed is mainly influenced by the time window of the liner shipping services when the bunker fuel price primarily impacts the decision of bunker amount and port. Thirdly, the current bunker fuel strategy could be improved by applying the optimisation model proposed in this paper that bunker in some specific ports will limit choosing options. Availability of the bunker in first calling port should be ensured, and additional discounts should also be negotiated for minimising the fuel cost. Stefanakos and Schinas (2014) proposed a multivariate non-stationary stochastic model for forecasting future bunker price. They considered the bunker fuel price from the view of world-wide trade and finance development view. Fuel price is a complicated stochastic factor mainly

related to the world trade situation and can change in different port and time point. Fuel price and fuel consumption make up more than others in the component of cost in ship optimisation problem which leads to the fuel price we use in the model will highly impact the optimal policy and numerical results.

Freight rate is important components of the revenue in cash flow. For different operating mode and contract type, the freight rate could be different. Abdelwahab and Sargious (1990) investigated the relationship between freight rate and shipment size when solving the optimisation problem of economic order quantity. Ottaviano et al. (2002) improved the modelling strategy to economic geography and gave an analysis of agglomeration process and economic clusters. Kavussanos and Alizadeh-M (2002) inspected the seasonality of freight rate and proves that the seasonality pattern in tanker spot freight rate markets could impact decisions such as port positioning, vessel speed schedule and investment. Ottaviano et al. (2002) considered the transportation cost as a fixed cost per unit without the count influence from agglomeration. Koekebakker et al. (2006) concluded the reason for failure to accept stationary and design an empirical experiment as a non-linear version of the Augmented Dickey-Fuller test. They proved the non-linear stationary character of freight rates in the dry-bulk and tanker market by applying an exponentially smooth-transition auto-regressive model. Koekebakker et al. (2007) argued that there is a research gap in the pricing of freight rate, particularly in the Asian options traded in freight derivative market. Jing et al. (2008) investigated the freight rate volatility in the dry bulk market. They divided the dry bulk market into three parts based on the vessel size, capsize shipping, panama shipping and handysize shipping. Then they applied GARCH(1,1) model to prove the impact from daily return persistently increase in the long term. Furthermore, for testing the asymmetric influence between past innovation and future development, they apply the EGARCH model and conclude that the influence could be varied in different vessel sizes and market conditions. The reason for this variation mainly comes from the flexibility of different shipping routes. Behrens et al. (2009) investigated the relationship between industry location and welfare when transport costs are endogenous. Their findings can be summarised as four steps that firstly the freight rate is positively related to the manufacturing agglomeration, then freight rate leads to carriers increase, then the marginal costs of transportation fall, and finally cause negative influence to agglomeration. At this point, consumers will benefit from the process. But if the influence leads to the change of industry location, the benefit will be the opposite. In the model, they concluded goods in two categories, homogeneous and horizontally differential goods. The transportation for homogeneous goods is considered as costless as the value in every region is equal. Moreover, the transportation for horizontally differential goods are costly, and the cost of each unit is called freight rate. Behrens and Picard (2011) proposed that when the demand for export from region A to B increase, the freight rate will reflect correspondingly. The increasing transportation cost will lead to region A lost competitively in some sense. When the imbalance of demand between two regions exceeds full agglomeration, which means that the freight rate from region B to region A close to 0, cooperation will consider establishing factories or manufactures in region B. Based on the theory of endogenous freight rate, firms will have an incentive to spread around its manufacture or others under the interior equilibrium

where the interior equilibrium means the balance between setting up cost and freight rate saving in essence. Goulielmos and Psifia (2011) doubted the assumption of short-term forecasting of freight rate follows the normal distribution. They illustrated the forecasting of freight rate over the last 30 years then observe the existence of fat tails and high peaks. By applying the rescaled range analysis and exponent H test, the normality of the freight rate is rejected.

Generally, weather condition within navigation includes wave, wind, tide, current conditions and environmental factors such as ocean and tidal currents, fog, surface temperature and ice conditions (Perera and Soares, 2017). Exceptionally weather condition like typhoons also causes influence weather in ship routing before navigation, ship performance during navigation or safe navigation handling. And due to global warming, massive typhoons or extreme weather condition becomes severe in recent years due to global warming (Chen et al., 2013).

Perera and Soares (2017) illustrated ship resistances caused by weather which conclude frictional resistance, residual resistance, added wave resistance and wind resistance. The combination of frictional resistance and residual resistance is called calm water resistance and mainly depends on the ship design of shape and surface material. Added wave resistance depends on the ship speed and parameters of wave contains height, angel and period. Wind resistance is determined by the ship speed and parameters of wind which conclude wind speed and direction, also the superstructure shape and area. Thus resistance caused by weather is mainly caused by wave and wind. When investigating the connection between weather and ship speed or forecast future weather, we can concentrate on parameters of wave (i.e. wave height, wave angel and period) and wind (i.e. wind speed and direction).

Weather routing problems are different with general ship routing and scheduling problems because not only financial Hinnenthal and Clauss (2010) introduced a Pareto-optimum approach for solving a multi-objective nonlinear constrained optimisation problem. They point this method will find the most advantageous route by making a compromise between the estimated time of arrival, fuel consumption, safety, and comfort. Walther et al. (2016) modified a weather routing problem by nonlinear continuous optimisation model and discrete optimisation model and introduces multiple algorithms for each of them, such as Isopone Method, Dijkstra's Algorithm, Real-Coded Genetic Algorithm, Multi-Objective Genetic Algorithm, Multi-Objective Evolutionary Algorithm and combined approach. Advantages and disadvantages of each algorithm are introduced in the paper. Perera and Soares (2017) introduced the importance of combining weather routing and safe ship handling for obtaining optimal and safe ship navigation condition. Weather can be considered as stochastic or constant in weather routine optimisation problem. In the case of stochastic, the weather is presented by forecasting value and possible error according to historical data. In the case of constant, weather is deterministic and equal to forecast number (Jewson and Brix, 2005).

Fuel consumption models for vessels different but adopt assumptions about the relationship between ship speed and power settings (Wen et al., 2016; IMO, 2021). Speed-dependent methods explain why the fuel savings from a downward speed change become less significant at lower

vessel speeds. A threshold of the speed where this change in dependency occurs is vessel-dependent. In Adland et al. (2020), for example, the threshold is around 10 knots for the studied oil tankers. An alternative to the threshold method is the cubic technique that, typically, sets the propulsive power needs in proportion to the third power of speed and to the power of $2/3$ to draft (IMO, 2014; Psaraftis and Kontovas, 2014).

2.2.2 Port congestion

The types of port congestion can be illustrated as: ship berth congestion, ship work congestion, vehicle gate congestion, vehicle work congestion, cargo stack congestion and ship entry-exit route congestion (Pruyn et al., 2020). Disregarding the variety of ports, the reason of port congestion contains the damage or shortage of port equipment for entry, berthing or operations, labour shortage, sudden increased trade demand, ground traffic congestion (Gidado, 2015). Queuing and longer waiting times are the immediate effects of port congestion.

Time consumed at port should be taken into account when estimating the expected time of arrival for the ship at the destination port. It is composed by the waiting time before berthing, and operation time which is influenced by the port discharging and loading rate. Port discharging and loading rate are also considered as indicators to evaluate the port performance. Port discharging and loading rate, which is related to the time vessel calling at the port is part of the port economics content. The port interchange services could be described as the carriers provides vessels for transporting goods from the shippers that the loading or discharging of these goods will be completed in specific ports. Port service fees conclude berth occupancy fees, loading and discharging fees, inland-carrier vehicle berth occupancy fees, inland-carrier loading and discharging fees. Each of the fees could be calculated by multiplying the specific service time and the service rate (Talley, 2006, 2013). Decision variables or effective indicators such as annual average port charge, annual average discharging service rate, annual average loading service rate are found to be related to the effectiveness operating objective of the port. Modelling for port congestion is further discussed in Appendix E.

2.2.3 Future prospects

One of the main areas of interest in our research is the degree by which the future should affect decisions about current operations in maritime shipping. This kind of thinking is encountered in primarily the field of corporate finance, and discussed in the first subsection. We then proceed describing the kinds of technologies which may help shape the future in shipping.

In corporate finance, future profitability is always discussed together with dividend changes, earnings or market value of a company. Lintner (1956) introduced firms will only increase their dividends when they believe future profitability is better than current earnings level. Nissim and Ziv (2001) suggested future profitability is assessed by the forecasting of firm's future earnings and abnormal earnings. Grullon et al. (2005) argued that dividend changes do not help forecast future profitability. Based on the non-linear evolution model introduced by Fama and French (2000), the estimation of the relationship between current dividend changes and

future profitability is not consistent with signalling hypothesis even sometimes the increase of dividends are considered as a signal. Choi et al. (2011) suggested information content of dividends hypothesis should be applied carefully based on firms features, for example, corporate geographical location, ownership structure and development stage.

Also, Cook Jr (1985) presented an exploratory model of market share that decision maker can choose factor they consider and add them in the market share evaluating model. They conclude four key concepts that highly mentioned in past research about market share which are demand, supply, performance and method. Managers pursue higher future profitability by applying the established profit-maximising model. Buzzell and Chussil (1985) defined a business's economic value as the sum of its cash flows over its planning period plus its 'market value' at the end of the planning period. They point out the requirement to evaluate decision strategies' future influence on the decision process horizon. As for assessing performance among corporations, a conclusion is drawn that companies with high market shares will have a better ability to operate future businesses at their current value. Two key factors are demonstrated in this paper to influence future profitability performance: marketing aggressiveness and investment support.

Besides, stock split announcements are demonstrated to have a negative influence on future profitability in subsequent years (Huang et al., 2006). The resulting analysis of regression models for split factors and earnings change, split factors and earnings, split factors and abnormal earnings shows significantly evidence that whether future profitability is evaluated by which kind of earnings, the negative relation between split factors and future profitability always holds.

Future profitability is a evaluation characteristic in economic life of replacement problems. According to the argument proposed by Taylor (1923), economic life will alternatively change by operating cost or requirement service time. Preinreich (1940) put forward that there are segmentation for the problem of economic life and categorise according scope, limitations and economic conditions. Future profitability sometimes is considered to be a factor in equipment replacement problem beyond the planning horizon. Preinreich (1940) introduced a finite chain of replacement as $V = B + G$ where V is capital value, B is original cost of a single machine in a finite chain of replacement, G is goodwill.

The economic life of industrial equipment does not only depends on unit cost, but also relates to market price of the product (Preinreich, 1940). Terborgh et al. (1949) explained the importance of setting period duration when comparing alternatives with different replacements life. When determining the span of prediction, there are segments for service lives involve economic factors or not. For economic replacements, correct life can only be determined when its successor is known. Discount for futurity is considered as necessary content when making dynamic equipment replacement decision.

2.3 Research gap and motivations

We conclude the research gap as follows: firstly, current research on ships' optimisation problems lacks consideration of the risk attitude of decision makers. For the same job in the freight market, decision-makers with different risk tolerance levels, profit targets, and even cash flow liquidity may make different decisions about taking the job or not, sailing routes and speeds, and negotiations for contracts and terms. Secondly, models of uncertainties in the decision process are not established and solved by stochastic dynamic programming. Some research employs the technique of dynamic programming, such as 3D Dijkstra's algorithm or subsequent algorithms, to solve the weather routing and scheduling problem. However, the uncertainties are imported as deterministic values, which restrict the possibilities of utilising the model under a variety of risk profiles or updating the distribution of random variables throughout the decision process. Thirdly, non-payment risk is not sufficiently discussed in the literature in the shipping industry. To the best of our knowledge, there is no literature using mathematical models or methods to analyse payment terms in tramp shipping.

We aim to fill the underlying research gap to a certain extent. By establishing the decision-making optimisation model for shipowners or time-charterers in tramp shipping, they can achieve their own goal of profit, either short- or long-term, while mitigating the risk of undertaking the journey. Table 1 furher illustrates this gap by comparing the contributions of this thesis (Chapter 3, 4, and 5) to existing literature.

As shown in Table 1, existing literature in tramp ship routing and scheduling problems have limitations of taking the stochasticity including future profit potential into account (Ronen, 1982; Theocharis et al., 2019; Magirou et al., 2015; Norstad et al., 2011; Ge et al., 2021). Wu et al. (2021) model the cost of a voyage as a random variable and proposes that this uncertainty is not well known at the beginning stage of the planning. However, no literature exists that considers the dynamics of information updating through decision process. Indeed, while the ship travels one gets updates on weather forecasts, for example. This introduces a change in the level of uncertainty one should take into account. Another non-negligible research gap is that the non-payment risk is not addressed by any existing literature. When the revenue of a tramp ship is calculated by the unit cargo transportation revenue times the loading weight, it assumes the carrier will receive the payment from the shipping or the consignee in full and on time. However, it is not always the best assumption in practice, in particular when one aims to work with a party that one is not yet familiar with, and may have jurisdictions in other countries. This research addresses these limitations and research gap to some extent by proposing ways to better model these situations and proposing efficient algorithms to solve these novel problem formulations. The comparisons of model formulation in stochasticity, dynamics of information, payment risk, and risk attitudes of decision makers between this research and others are shown in Table 1.

TABLE 1: Summary of literature review and research gap

Paper	Applications	Objectives	Decision Variables	Stochasticity	Dynamics of information	Payment risk	Risk	Methodology	
Fagerholt et al. (2010b)	Liner shipping	Min fuel consumption for given route	Speed or Sailing time	×	×	×	×	Shortest path problem on a directed acyclic graph	
Norstad et al. (2011)	Tramp shipping (fleet)	Max total profit for given journeys	Sailing speed; Ship assignment	×	×	×	×	Multi-start local search heuristic	
Norstad et al. (2011)	Tramp shipping	Max total profit	Ship assignment, route, and speed	×	×	×	×	Discretising arrival times; Algorithm for the TSRSPSO	
Gatica and Miranda (2011)	Tramp shipping (fleet)	Min total operating cost for given journeys	Ship assignment and speed	×	×	×	×	Time windows discretisation	
Wong et al. (2015)	All types of vessels	Min weighted potential failure function	Sailing speed	×	×	×	Utility-based decision support	Sustainability model	
Magirou et al. (2015)	Tramp shipping (single vessel)	Max net average daily revenue	Sailing Speed; Voyage sequence	✓	×	×	×	Dynamic programming	Stochastic approximation
Beşikçi et al. (2016)	All types of vessels	Max energy efficiency	Sailing speed; RPM	Data driven	×	×	×	Artificial neural networks	
Wen et al. (2016)	Tramp shipping	Min sum of the transportation cost minus the total reward of the served cargoes	Ship assignment, route, and speed	×	×	×	×	Set packing problem; Column generation	
Wang et al. (2018b)	Container liner shipping	Min operating cost; bunker purchase cost	Sailing speed;Fuel purchase	✓	×	×	×	Mixed-integer programming; Stochastic approximation	
Theocharis et al. (2019)	Routes evaluation(Northern Sea Route)	Min cost per tonne	Sailing speed	×	×	×	×	Linear programming	
Wang et al. (2019)	All types of vessels	Min fuel consumption or fuel cost	Waypoints (Route) and speed	×	✓	×	✓	3D-dijkstra's algorithm	
Ge et al. (2021)	All types of vessels	Max NPV including FPP	Sailing speed; Repetitions	×	×	×	×	Net profit value (NPV); Dynamic Programming	
Wu et al. (2021)	Bulk ships	Max total profit	Fleet adjustment	✓	×	×	×	Tailored branch-and-price-and-cut algorithm; multi-cut generation technique	
Merkel et al. (2022)	Tramp shipping	Max CO_2 emission savings	Port call	×	×	×	×	Virtual arrival (VA)	Data analysis
Gao and Sun (2023)	Tramp shipping	Min total cost of travelling and charter	Ship assignment, route, and speed	×	×	×	×	Branch-and-Price algorithm	
Chapter 3	Tramp shipping	Max NPV including FPP	Job acceptance and travel time	✓	×	×	✓	Mean-risk optimisation	
Chapter 4	Tramp shipping	Max NPV including FPP	Waypoints (route) and speed	✓	✓	×	✓	Markov Decision process with dynamic information update; Simulation enhanced value iteration algorithm	
Chapter 5	Tramp shipping	Max NPV including FPP	Payment terms	✓		×	✓	Net present value (NPV)	

Chapter 3

Job Acceptance and Economic Travel Time of a Tramp Ship under Risk

In this chapter we develop a new perspective on the problem of economic (average) ship speed by considering the impact of the decision maker's risk attitude. This impacts decisions about both speed and job acceptance. A ship is used to transport bulk cargoes in the spot market. A job consists of moving a cargo from a port A to a port B. Whether a ship owner can accept a job is determined by (i) the profitability of this job, and (ii) the commercial value of having its ship in port B when the job is finished. The time needed to travel from A to B affects both (i) and (ii). We consider that the decision maker wishes to maximize the Net Present Value (NPV) of the ship under uncertainty. This uncertainty is associated with the fuel consumption on the journey and the future profit potential of the ship at the next port. Underlying factors for these risks include adverse fuel consumption rates, and randomness in freight markets. We further extend the consideration of stochasticity in the decision making problem from the view of decision makers, who may hold different risk tolerance levels, have different cash liquidity positions, face different debt situations and have different expectations regarding profit targets. We develop mean-risk optimization models based on either long-term or short-term risk perspectives, justify why this distinction is worthwhile to consider, and introduce stochastic programming methods to solve the set of models. Numerical experiments illustrate the approach and show the sensitivity of the optimal strategy to context parameters and risk attitude of the decision maker. The mean-risk speed optimization models can be extended to account for risk from different sources, e.g. failure-to-pay.

3.1 Introduction

In this chapter we develop a set of decision models that help capture the risk attitude of the decision maker when deciding on the future usage of a tramp ship operating in the spot market. This decision maker is typically the vessel owner, or a person in an equivalent position such as the charterer for a time chartered ship, and who is responsible for providing instructions to

the master of the vessel about taking shipping jobs. The major variable cost component when accepting a job is the cost associated with the fuel consumption[2], which is impacted by route choices and speed decisions (Stopford, 2008).

In the context of this study we can compare a tramp ship with a taxi. A job consists of moving cargo across the ocean from one port to another. We assume that the freight rate received if the job is accepted is fixed, as well as the fuel price paid for the associated journey. Whether a job is worthwhile is determined by the profitability of this job, and the commercial value of having the ship in the destination port upon job completion. The two sources of uncertainty considered are the amount of fuel consumed during the journey, and the commercial value of the ship at the destination port at the time when it will be available for a next job. Considering the stochasticity of fuel consumption and the future profit potential at the destination port while evaluating jobs before taking them is more realistic compared to deterministic assumptions. The former is affected by e.g. variations in ocean weather, while the latter is strongly affected by future spot market values. Both are in general not known with certainty at the time of making the decision.

Most optimisation problems in the economic literature on shipping adopt one of the following strategies: minimising the cost of the current shipping operations on a series of already planned for legs or a set of available jobs, or maximising the decision makers' profit earned either per unit of time, per nautical mile, or per journey. These models do not look into the future beyond a planning horizon. From talking to ship owners, we know that they also consider the area where the ship will end up after completion of the job, in particular about the availability and profitability of future job opportunities in the destination port, or in the vicinity of that port. In addition, and similar to the stock market, foresighted decision makers in the freight market schedule their transport based on their anticipations about the future evolution of freight rates, fuel prices, and other influencing factors (Stopford, 2008; Branch, 2012). We view decisions about job acceptance and ideal travel plan of the ship as an investment decision driven by Net Present Value (NPV) considerations. This framework allows us to also consider future anticipated (yet uncertain) cash-flow streams into decisions about current operations.

Few optimisation models on job acceptance or route/speed decisions in the literature consider stochastic elements, and those that do focus on expected value maximisation. This criterion, however, has limitations when representing how most decisions under risk are made. Because of differences in risk attitude, different decision makers are likely to make different decisions even when confronted with the same stochastic problem (Anderson, 2013).

Thus, given the importance to optimise the strategy of job taking and travel time with the consideration of stochasticity, this study formulates uncertainties in two phases: (1) during the execution of the journey, where e.g. stochastic weather conditions at sea may impact fuel consumption, and (2) after termination of the journey, where the randomness in freight markets will

[2]Discussions about other potentially important costs are in Section 3.6.

influence the future profit potential at the destination port. It is determined that the decision maker's attitude to these risks in both phases influences the decisions.

The mean-risk optimisation models developed in this paper allow for considering decision makers having different tolerance levels to risk and whether they consider short-term or long-term risk. The uncertainties captured by the stochastic modelling are mapped to a probabilistic space of long- and short-term NPV. This type of optimisation result allows for a more careful exploration of the financial risk associated with a potential job than that which only provides a solution that maximises the expected value. Decision makers can use the distributions of NPVs to make their decisions about job acceptance and ideal travel time for the target voyage that account for their individual risk profile. Even if a decision maker may not exactly know a priori how much risk they can carry, the models can be used to explore how sensitive the job selection and speed decisions are to different risk profiles and context parameters.

The proposed decision problem is solved by mean-risk optimization models for finding the optimal travel time under a risk tolerance and profit target. In particular, we examine the performance of risk measures VaR and CVaR under the various distribution of uncertainties attributed to stochastic weather conditions and fluctuating freight markets. It is worthwhile to note that the mechanisms presented to capture the influence of weather and freight markets on fuel consumption and future profit potential are not the focus on this paper, and are hence somewhat rudimentary in their development and will need further research or may better be replaced by more sophisticated approaches.

The distinction between short-term and long-term risk perspectives is a novel feature that we have not yet seen elsewhere in the literature, and which helps to characterize differences in decision maker's desire to minimize the probability of negative short-term cash-flows. Computational results show the practical significance of the models.

Most of the mentioned points have not been addressed in any paper in this field (see Section 3.2). The models developed in this paper can be extended in future research towards more complex payment structures, multiple journeys in an extended time horizon, or in general explicitly consider more sources of stochasticity.

The paper is organised as follows. Section 3.2 covers literature on the speed optimisation problem in maritime shipping, and highlights the novel characteristics of this paper. Section 3.3 introduces the basic modelling components, including aspects of the two-phases stochasticity. Section 3.4 proposes mean-risk optimisation models and algorithms for solving the problem. Section 3.5 presents numerical experiments for different risk measures and distributions of the stochastic variables. The significance of using risk-adjusted decision models as in this paper is also examined through comparison with other speed optimisation model from the literature. Section 3.6 illustrates how to extend the models by considering variations in payment structures of a contract and including the risk associated with untrustworthy shippers not being able to pay on time or even failing to pay.

TABLE 2: Related ship speed optimisation literature

Paper	Applications	Objectives	Decision Variables	Stochasticity	Risk	Methods
Fagerholt et al. (2010b)	Liner shipping	Min fuel consumption for given route	Speed or Sailing time	×	×	Shortest path problem on a directed acyclic graph
Norstad et al. (2011)	Tramp shipping (fleet)	Max total profit for given journeys	Sailing speed Ship assignment	×	×	Multi-start local search heuristic
Gatica and Miranda (2011)	Tramp shipping (fleet)	Min total operating cost for given journeys	Sailing speed Ship assignment	×	×	Time windows discretisation
Wong et al. (2015)	All types of vessels	Min weighted potential failure function	Sailing speed	×	✓	Utility-based decision support sustainability model
Magirou et al. (2015)	Tramp shipping (single vessel)	Max net average daily revenue	Sailing Speed Voyage sequence	✓	×	Dynamic programming Stochastic approximation
Beşikçi et al. (2016)	All types of vessels	Max energy efficiency	Sailing speed RPM	Data driven	×	Artificial neural networks
Wang et al. (2018b)	Container liner shipping	Min operating cost & bunker purchase cost	Sailing speed Fuel purchase	✓	×	Mixed-integer programming Stochastic approximation
Theocharis et al. (2019)	Routes evaluation (Northern Sea Route)	Min cost per tonne	Sailing speed	×	×	Linear programming
Ge et al. (2021)	All types of vessels	Max NPV including FPP	Sailing speed Repetitions	×	×	Dynamic Programming
This Paper	Tramp shipping	Max NPV including FPP	Travel time	✓	✓	Stochastic programming

3.2 Literature review

Ship routing and scheduling problems provide a rich ground for operational research. In general, there are three modes of operation in shipping: liner, industrial, and tramp. Vessels in liner shipping are comparable to bus services in passenger transport: they typically follow fixed routes and have to meet time windows for earliest and latest arrival time at ports within the route. Vessels in industrial shipping are working under contracts in order need to meet service schedules or frequencies at minimal cost (Barnhart and Laporte, 2006). In tramp shipping, vessels have no defined routes and schedules (Ronen, 1983). The operator of vessels in tramp shipping evaluates and selects from potential contracts, often single voyage charters, from both eligibility and profitability standpoints.

Related literature in recent years are reviewed according to various decision variables, objective functions, and factors in the modeling methods. Note that determining the optimal travel time is equivalent to determining an optimal average sailing speed when the distance of the journey is known. Thus, we listed the literature with a focus on this kind of objective, see also Table 2. Fagerholt et al. (2010b) propose a continuous non-linear optimisation problem for reducing the fuel emission by optimising the speed for a fixed shipping routes scheduling problem in liner shipping. In tramp shipping, Norstad et al. (2011) propose to use the sailing speed for each ship within the fleet in each leg as the decision variable for the fleet routing and scheduling problems. Another example in this field is from Gatica and Miranda (2011) who include time windows into the problem and minimise the total operations cost for the given journey. For single vessel speed optimisation problems in tramp shipping, Magirou et al. (2015) build a speed and voyage sequence optimisation problem to maximise net average daily revenues, while considering uncertainty on the freight rates. Speed optimisation models are also formulated for various types of fuel consuming vessels in (Wong et al., 2015; Beşikçi et al., 2016). In this paper, we also determine speed as a decision variable but in addition consider the decision whether to accept the potential job under investigation.

Somewhat differently to conventional ship speed optimisation problems that maximise profit or

minimise cost per journey or per unit of time, the objective function in this problem is maximising the Net Present Value (NPV) in the long term. Recently, Ge et al. (2021) have introduced the concept of *future profit potential* (FPP) into the deterministic speed optimisation problem in tramp shipping, using maximisation of the ship's net present value (NPV) as criterion. In this paper, we adopt their methodology, but transform this to a stochastic setting, while also accounting for the decision maker's risk attitude. As a result, the decision is now whether a given job offer is worthwhile given the risks involved, and if so, which travel time the ship would ideally consume to complete this journey[3].

In comparison to land-based logistics, uncertainties in ship routing and scheduling optimisation have received much less attention (Christiansen and Fagerholt, 2014). The necessity of considering uncertainties in optimisation problems lies in the lack of robustness of optimal solutions when deterministic models are used. Both internal and external origins can influence the economic activities at sea. In particular, Ronen (1983, 1993) demonstrates that there are more uncertainties in tramp shipping than in the other two modes and arising from: (1) human behaviour and errors during operations, (2) vessel performance, (3) journey conditions, and (4) freight market factors. The effect of uncertainties on ship routing, scheduling and speed planning arise mainly from (3) and (4).

For (3), ocean weather can influence the sailing time and fuel consumption and leads to weather routing problems (Lo and McCord, 1998; Azaron and Kianfar, 2003; Zis et al., 2020), and may cause uncertain service frequency in liner shipping and industrial shipping (Wang and Meng, 2012a; Aydin et al., 2017).

For (4), Magirou et al. (2015) examine the fluctuations in freight rates for a single vessel routing and scheduling problem applied in tramp shipping. Both independent freight rates and Markovian freight market states are included in their experiments. Besbes and Savin (2009) provide a stochastic dynamic setting for the bunker price with the objective to maximise profit from operating.

In addition, uncertain demand, available capacity and joint uncertainties with travelling times were discussed in research for liner shipping (Meng et al., 2012; Wang and Meng, 2020; Kuhlemann et al., 2021). Meng et al. (2015) introduce a tramp shipping routing and bunkering problem when dynamic bunker prices are assumed in different ports. The problem is solved by a branch-and-price approach in the to minimise the total bunkering cost over a rolling horizon.

Next to the inclusion of uncertainties, efforts have been reported about the integration of ship routing and scheduling features into decision support frameworks that can consider more real-life features. Bausch et al. (1998) introduce a spreadsheet-based optimisation decision problem

[3]We assume that speed is chosen from within a feasible interval. We recognise that, in reality, there may be several constraints imposed that further limit choices about ship speeds. To aid the analysis, we do not consider these, but the algorithms could be easily adjusted to account for more complex situations, e.g., the consideration of a union of disjoint speed ranges. Situations in which the ship must arrive at port B on a specific date and thus at a specific average speed are, of course, a special case in which only the journey acceptance decision must be made.

for finding optimal speed for short-term bulk commodities. Fagerholt and Lindstad (2007) introduce a decision support system named TurboRouter that could help shipping companies find the most profitable strategy for sailing speed, fleet size and bidding strategy.

Ship routing and scheduling have received high attention from researchers whether in the field of the information system or marine transportation in the last decade. Other research in the area of decision making in shipping concentrates on how to improve the interaction between computer and the decision maker, or achieve multi-objective solutions. Risk in decision making, however, is mostly discussed in the context of safety in navigation, including ship collision avoidance, or risk through legislation or emissions (Bichou, 2008; Kulkarni et al., 2020; Pastra et al., 2021).

To our best knowledge, there is no published research addressing the risk inherent in the journey acceptance and travel time optimisation problem in tramp shipping. As it is a decision context subject to lots of uncertainty, incorporating the risk preference of the decision maker seems useful. As shown in Table 2, our study extends the investigation of economic travelling strategy to a stochastic dimension while uncertainties from fuel consumption and freight markets are taken into account. Novel to the literature, our study includes various risk attitudes while making a decision about journey acceptance and ideal travel time.

3.3 Problem description

This section describes a stochastic single leg job acceptance and travel time optimisation problem for a tramp ship. It is assumed that the ship, currently in port A, has an option to take a particular job sailing from port A to port B. No voluntary waiting time, repositioning legs, or execution of other work first are permitted[4]. The ship could take the job and complete the journey within ideal travel time T^{s*} (for notation, see also Table 3) at any willing speed inside the limit boundaries, or reject the job. The latter decision will be reached, loosely speaking, if the job is deemed not sufficiently profitable, or too risky to undertake (this is will be formalised in Section 3.4). Information about ship performance, sailing route, revenue received if the job is accepted, and port economic parameters are known and deterministic when the job is evaluated. Meanwhile, fuel consumption rate is uncertain and related to ocean weather conditions. The future profitability after completion time at the destination port is also considered as uncertain.

The problem considered in this paper falls into the class of $\mathcal{P}(1,1,G_0)$ problems, according to the framework of Ge et al. (2021), i.e. it solves a single leg speed optimisation problem with the consideration of the FPP in the destination port. However, we propose a stochastic problem framework $\mathcal{P}_{\Omega_z \times \Omega_{G_0}}(1,1,G_0)$, where Ω_z and Ω_{G_0} denote the sample space of random variables during and after sailing.

[4]This keeps the problem formulation tidy. Extensions that include more complex ship routing options will be left for research in the future. The modelling framework presented in this paper captures the basic characteristics of modelling journey acceptance and ship speed optimisation under risk and will remain applicable.

3.3.1 Stochasticity

Uncertainties are considered in two phases. During sailing time, or the first phase, the vessel takes the risk of consuming more fuel in order to arrive at the destination port B within the ideal travel time. Uncertainties in the second phase relate to the future profitability of the vessel after if would have unloaded the cargo in port B, and which we incorporate by considering the FPP as a random variable. We refer to the time of completing the unloading in the destination port B as the termination time.

3.3.1.1 Uncertainty before termination time

Uncertainty in the first phase is about various fuel consumption rates experienced during the journey. It is known that for a given ship and deadweight and set speed, fuel consumption can fluctuate and is impacted by the environment, including the wind direction, wind speed, wave direction, wave height and so on. Our paper considers the uncertainties of fuel consumption rate rather than the various ocean weather conditions. For the fuel consumption rate function ($tonne/day$), we adopt the function introduced by Psaraftis and Kontovas (2014):

$$f(v,w) = k \cdot (p + v^g)(w + A)^h, \tag{3.1}$$

where v denotes the average sailing speed, w denotes the deadweight tonnage carried, A denotes the lightweight tonnage of the ship, while the values of the parameters p, g, h depend on the ship's characteristics and its condition. The reason that we choose to apply the cubic technique for fuel consumption of speed is due its advantage of estimating parameters when limited historical data is available. See also Appendix B and Appendix F for an illustration. Moreover, in conditions in which full track of vessel's historical fuel consumption data is available, the thresholds in speed-dependent modelling can be determined, which then also allows for a tailored fuel consumption rate function to be implemented in our model.

We convert the rate k from a constant into a random variable k_r to represent the uncertainty:

$$f(v,w,k_r) = k_r \cdot (p + v^g)(w + A)^h. \tag{3.2}$$

Let $k_r = k$ represent the usual fuel consumption rate, then an unusual fuel consumption rate is $k_r < k$ or $k_r > k$. For example, a ship having to battle a rough weather day may well consume double the amount of fuel, i.e. $k_r = 2k$. For more detailed studies of these phenomena, see e.g. Kim and Incecik (2017); Sang et al. (2023).

To characterise the number of unusual fuel consumption days encountered, we consider the following simple Bernoulli process[5]. Let p be the probability of unusual fuel consumption

[5]More sophisticated methods could include scenario trees, inflow forecast over the rolling planning horizon, and other techniques of adjusting probabilities and impacts of bad weather. See also Lu et al. (2013); Tu et al. (2017); Grifoll et al. (2018). As the aim of this paper is to show how the impact of fuel consumption stochasticity may impact speed and journey selection decisions, the actual mechanism that introduces this randomness is of lesser importance in the context of this paper.

happening in a single day. Then the maximum of unusual fuel consumption days is the same as the ceiling number of travel time $m = T^s$. Let the accumulative unusual fuel consumption days be $z, z \in \{0, 1, \ldots, m\}$, then the probability of z is as follows:

$$Prob(z = k) = \binom{m}{k} p^k (1-p)^{m-k}. \tag{3.3}$$

Assume random variable z happens under T_1 states, $i \in \{1, \ldots, T_1\}$. Let state ω_{zi} occur with probability p_{zi}, $\sum_{i=1}^{T_1} p_{zi} = 1$. Thus, the random outcomes of unusual fuel consumption days z are defined on a discrete probability space $\{\Omega_z, \mathcal{F}_z, P_z\}$ where $\Omega_z = \{\omega_{z1}, \ldots, \omega_{zT_1}\}$, $\mathcal{F}$ is a σ-field and $Prob_z(\omega_{zi}) = p_{zi}$.

The above assumptions about uncertain fuel consumption offer one mechanism to deal with the stochasticity about fuel consumption in operation. There are studies on the relationship between fuel consumption rate and weather conditions, including ocean waves, currents, and winds by analysing the ship speed and power performance (Skoglund et al., 2015; Tillig et al., 2018; Wang et al., 2019). However, it is acknowledged that there is no semi-empirical or theoretical model that could convincingly capture the relationship between ship speed and power, or fuel consumption rate. In such case, modelling k_r and its distribution will be a valid and effective approach to demonstrate the benefit of considering the uncertainty about fuel consumption in ship scheduling optimisation problems.

3.3.1.2 Uncertainty beyond termination time

The FPP G_0, introduced in Ge et al. (2021), captures the ship's future profit potential discounted to the ship's termination time. We now recognise that this value is an estimate, and it would be reasonable to consider it a random variable. Various sources of randomness may include: operations of the vessel itself, trade surplus when the vessel terminates at the port, worldwide shipping industry state, and other factors at the macro level. In this paper, we assume G_0 could be approximated by a well predicted distribution valid over the range of possible completion days. Otherwise, a time-dependent distribution should be considered to ensure validity. See also Section 3.5.3 for an estimation of FPP values from dry bulk earnings data.

We assume the following process . Let random variable G_0 happen under T_2 states, $j \in \{1, \ldots, T_2\}$. Let state $\omega_{G_0 j}$ occur with probability $p_{G_0 j}$, $\sum_{j=1}^{T_2} p_{G_0 j} = 1$. Thus, the random outcomes of G_0 are defined on a discrete probability space $\{\Omega_{G_0}, \mathcal{F}_{G_0}, Prob_{G_0}\}$ where $\Omega_{G_0} = \{\omega_{G_0 1}, \ldots, \omega_{G_0 T_2}\}$, $\mathcal{F}$ is a σ-field and $Prob_{G_0}(\omega_{G_0 j}) = p_{G_0 j}$.

Without loss of generality, random variables z and G_0 could alternatively also follow continuous probability distributions. Then, the probability density function for z and G_0 will be, respectively:

$$F(z) = Prob(a \leq z \leq b) = \int_a^b f(z)\, \mathrm{d}z \geq 0, \quad 0 \leq a \leq b \leq m, \tag{3.4}$$

and

$$F(G_0) = Prob(a \leq G_0 \leq b) = \int_a^b f(G_0)\, \mathrm{d}G_0 \geq 0. \tag{3.5}$$

3.3.2 $\mathcal{P}_{\Omega_z \times \Omega_{G_0}}(1,1,G_0)$

For the single leg job acceptance and economic travel time decision problem with stochastic fuel consumption rate and FPP, we define the problem category $\mathcal{P}_{\Omega_z \times \Omega_{G_0}}(1,1,G_0)$ on the basis of deterministic problem set $\mathcal{P}(1,1,G_0)$. The different activities in the journey consist of loading time, sailing time, waiting time and unloading time. Assumptions about cash flows are as in Ge et al. (2021), see also Figure 2. In particular, the shipper will receive the freight rate that was negotiated the moment the job was accepted, and the money is exchanged upon delivery at port B.

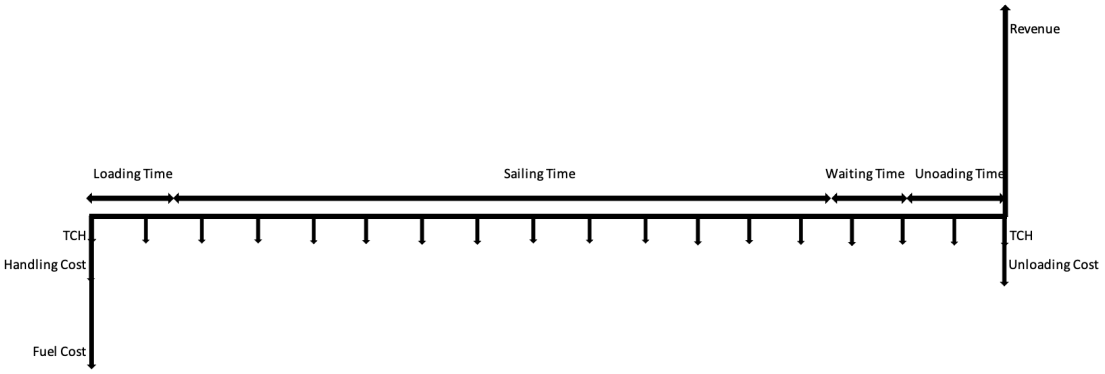

FIGURE 2: Timeline of cash flows in single leg

TABLE 3: Notation of stochastic single leg ship speed optimisation problem

Symbol	Definition
v	Average speed (nm per hour)
$v_{\min}$	Lower limit of design speed
$v_{\max}$	Higher limit of design speed
S	Sailing distance (nm)
T^l	Loading time (days)
T^s	Sailing time/Travel time (days)
T^{s*}	Optimal travel time (days)
T^w	Waiting time (days)
T^u	Unloading time (days)
T	Total time for completing the leg (days)
f^{TCH}	Daily hire rate (TCH: Time Charter Hire)
α	Opportunity cost of capital rate (per day)
$C^l(v,z)$	Loading cost
C^u	Unloading cost
C^h	Handling cost
$C^f(v,w,z)$	Fuel cost
c^f	Fuel price
R^j	Revenue of the job
$\mathbb{E}[h(T,z)]$	Expected NPV excluding the FPP
$\mathbb{E}[H(T,z,G_0)]$	Expected NPV including the FPP

Main notation is introduced in Table 3. As presented in Figure 2, the total journey time T consists of loading time T^l, sailing time T^s, waiting time T^w and unloading time T^u,

$$T = T^l + T^s + T^w + T^u. \tag{3.6}$$

There is an average speed determined by the sailing distance S and sailing time T^s,

$$v = S/(24 \cdot T^s). \tag{3.7}$$

Loading costs $C^l(v,z)$ consist of fuel cost and handling cost C^h at port A. As the fuel consumption rate is stochastic, for the scenario that unusual fuel consumption days are given by $z = \omega_{zi},\ \omega_{zi} \in \{0,1,\ldots,m\}$, the unusual fuel consumption rate is given by k_r (see Section 3.3.1.1). The loading cost is as follows:

$$C^l(v, z = \omega_{zi}) = C^h + C^f(v, w, z = \omega_{zi}), \tag{3.8}$$

where C^f is the fuel cost along the journey,

$$C^f(v, w, z = \omega_{zi}) = c^f \cdot (f(v, w, k_r) \cdot \omega_{zi} + f(v, w, k) \cdot (T^s - \omega_{zi})),\ T^s \geq \omega_{zi}. \tag{3.9}$$

Thus, the net present value for taking job from port A to port B (excluding the FPP) for scenario $z = \omega_{zi},\ \omega_{zi} \in \{0,1,\ldots,m\}$ is calculated as follows[6]:

$$h(T, z = \omega_{zi}) = (R^j - C^u) \cdot e^{-\alpha T} - C^l(v, z = \omega_{zi}) - \int_0^T f^{\mathrm{TCH}} \cdot e^{-\alpha t}\, \mathrm{d}t. \tag{3.10}$$

The expected contribution to the NPV from executing the job is thus:

$$\mathbb{E}_{z \in \Omega_z}[h(T,z)] = \sum_{i=1}^{T_1} p_{zi} \cdot h(T, z = \omega_{zi}). \tag{3.11}$$

As shown in Ge et al. (2021), the NPV for the ship must include in addition the time discounted FPP at port B at termination time T. The NPV for scenario $z = \omega_{zi},\ \omega_{zi} \in \{0,1,\ldots,m\}$, $G_0 = \omega_{G_0 j}$ is thus as:

$$H(T, z = \omega_{zi}, G_0 = \omega_{G_0 j}) = h(T, z = \omega_{zi}) + \omega_{G_0 j} \cdot e^{-\alpha T}, \tag{3.12}$$

and the expected NPV is as follows:

$$\mathbb{E}_{z \in \Omega_z, G_0 \in \Omega_{G_0}}[H(T, z, G_0)] = \sum_{j=1}^{T_2} \sum_{i=1}^{T_1} p_{zi} \cdot p_{G_0 j} \cdot H(T, z = \omega_{zi}, G_0 = \omega_{G_0 j}). \tag{3.13}$$

[6]Note that α is the cost of capital rate of the decision maker. It can be adjusted to account for inflation, see also Brealey et al. (2012).

For a risk neutral decision maker, the optimal termination time T^* is derived by maximising the expected NPV:

$$T^* = \arg\max \ \mathbb{E}_{z\in\Omega_z, G_0\in\Omega_{G_0}}[H(T,z,G_0)]. \tag{3.14}$$

3.3.3 Risk

For decision makers who are not risk neutral with respect to the risks involved in the journey, (3.14) is no longer applicable. The financial risk of a project can be defined as the probability of failing to meet a certain profit target or exceeding a set cost level, typically encountered in maximisation and minimisation problems, respectively (see also e.g. (Barbaro and Bagajewicz, 2004)).

We apply the theory of financial risk in our problem and develop the risk related to job acceptance and speed strategy under the two types of uncertainties as introduced in Section 3.3.1. The risk is defined as the probability of not meeting the profit target in the probability spaces Ω_z and Ω_{G_0}.

3.3.3.1 Short-term risk

Certain decision makers want to focus on controlling the risk on the current journey, perhaps since they need to keep the probability of a negative cash-flow position very low in order to ensure meeting e.g. loan repayments and avoid bankruptcy. For those decision makers, the risk on the long-term profitability is of much lesser importance.

The current journey profits are found as the NPV excluding the FPP (see Section 3.3.2), and in order to control the short-term risk, a minimum level μ_s is to be guaranteed. The uncertainty in the first phase comes, for example, from random unusual fuel consumption days and consequent fuel consumption rate (see Section 3.3.1.1). For an aspiration target level of profit in the short-term μ_s, the risk related to travel time T^s is then as follows:

$$\text{Risk}_{\Omega_z}(T^s, \mu_s) = Prob(h(T,z) < \mu_s), \tag{3.15}$$

where T is derived by (3.6)-(3.7). In the discrete case, the risk could be expressed by using an indicator function, see also e.g. (Guillén et al., 2005), as follows. Rewrite the risk under travel time T^s and μ_s as:

$$\text{Risk}_{\Omega_z}(T^s, \mu_s) = \sum_{i=1}^{T_1} p_{zi} \cdot \mathbb{1}_s(T^s, \mu_s), \tag{3.16}$$

where $\mathbb{1}_s$ is defined as:

$$\mathbb{1}_s(T^s, \mu_s) = \begin{cases} 1, & \text{if } h(T,z) < \mu_s, \\ 0, & \text{otherwise.} \end{cases} \tag{3.17}$$

3.3.3.2 Long-term risk

For decision makers who are willing to accept possible negative cash-flow positions in the shorter term in the pursuit of profitability, a longer-term view about their risk profile can be considered.

In the long-term case, the profit target represents the value of NPV including FPP expected by the decision maker (see Section 3.3.2). Uncertainties associated to fuel consumption rate and FPP are involved when counting the risk in the long-term (see Sections 3.3.1.1-3.3.1.2). For the aspiration level for the long-term profit target μ_l, the risk related to travel time T^s is as follows:

$$\text{Risk}_{\Omega_z \times \Omega_{G_0}}(T^s, \mu_l) = Prob(H(T, z, G_0) < \mu_l). \tag{3.18}$$

Similarly, we could use an indicator function to express risk. Rewrite the risk under travel time T^s and μ_l as follows:

$$\text{Risk}_{\Omega_z \times \Omega_{G_0}}(T^s, \mu_l) = \sum_{j=1}^{T_2} \sum_{i=1}^{T_1} p_{zi} \cdot p_{G_0 j} \cdot \mathbb{1}_l(T^s, \mu_l), \tag{3.19}$$

where $\mathbb{1}_l$ is defined as:

$$\mathbb{1}_l(T^s, \mu_l) = \begin{cases} 1, & \text{if } H(T, z, G_0) < \mu_l, \\ 0, & \text{otherwise.} \end{cases} \tag{3.20}$$

3.4 Mean-risk optimisation model and algorithm for $\mathcal{P}_{\Omega_z \times \Omega_{G_0}}(1, 1, G_0)$

Risk neutral decision makers will want to maximise expected profits. Mean-risk optimisation models, however, allow decision makers to account for risk by considering the compromise between expected values of profit and risk measures.

3.4.1 Basic mean-risk model

Mean-risk optimisation models describe the return distributions in two categories: the expected value and the value of a risk measure (Roman et al., 2007). For the choice of risk measure, Markowitz (1952) proposes the mean-variance model for a portfolio selection problem which includes the variance as the risk measure. Other risk measures, for instance, VaR and CVaR (discussed further in Section 3.4.2-3.4.3) are also widely applied in various applications (Artzner et al., 1999; Pflug, 2000; Tasche, 2002; Acerbi and Tasche, 2002).

Define $\pi(x, \omega)$ as a random monetary outcome associated to decision x under state of nature ω, and $\rho(.)$ as a risk measure. The efficient solutions for general multi-objective optimisation problems are Pareto efficient solutions. One common expression for the mean-risk model is as

follows:

$$\max_{x \in \mathcal{X}} \quad \mathbb{E}_\omega[\pi(x,\omega)] - \lambda \cdot \rho[\pi(x,\omega)], \tag{3.21}$$

where λ is a coefficient that reflects risk aversion. Another common expression is, rather than scalarising expected values and risk measures, defining a risk (tolerance) level R, giving the following expectation maximising mean-risk model:

$$\max_{x \in \mathcal{X}} \quad \mathbb{E}_\omega[\pi(x,\omega)] \tag{3.22}$$

$$s.t. \quad \rho[\pi(x,\omega)] \leq \mathrm{R} \tag{3.23}$$

Alternatively, a profit target μ is introduced. The risk minimising mean-risk model is then expressed as follows:

$$\min_{x \in \mathcal{X}} \quad \rho[\pi(x,\omega)] \tag{3.24}$$

$$s.t. \quad \mathbb{E}_\omega[\pi(x,\omega)] \geq \mu \tag{3.25}$$

The three models are equivalent for suitably chosen corresponding values of the parameters λ, R and μ, although the link between these may not be easily established in practice. The choice of model may depend on decision maker preference, and which parameter is known in the problem at hand. For problems of class $\mathcal{P}_{\Omega_z \times \Omega_{G_0}}(1,1,G_0)$ in this paper, we choose to formulate the mean-risk models in expectation maximising form.

3.4.2 Mean-risk models for $\mathcal{P}_{\Omega_z \times \Omega_{G_0}}(1,1,G_0)$ with short-term profit target

In order to meet the profit target in the short-term at a certain risk level, we develop mean-risk models in expectation maximising form based on (3.22)-(3.23). The profit target in the short-term case μ_s is established as the aspiring NPV excluding FPP, see (3.10).

3.4.2.1 The general case

For a general risk measure $\rho(\cdot)$, we define the mean-risk models with short-term profit target in expectation maximising form as follows:

$$\max_{T^s \in [T^s_{\min}, T^s_{\max}]} \quad \mathbb{E}_{z \in \Omega_z, G_0 \in \Omega_{G_0}}[H(T,z,G_0)] \tag{3.26}$$

$$s.t. \quad \rho(\mathrm{Risk}_{\Omega_z}(T^s, \mu_s)) \leq \mathrm{R} \tag{3.27}$$

Considering the optimisation model displayed in (3.26)-(3.27), the decision variable is travel time T^s. By altering the value of T^s, an optimised expected NPV including FPP could be obtained when the risk of not meeting the NPV excluding FPP at μ_s is less than or equal to risk

level R. Otherwise, there is no suitable v for which (3.27) can be met. Algorithm 1 describes the stochastic programming algorithm proposed to solve the model (3.26)-(3.27).

Algorithm 1 Solving $\mathcal{P}_{\Omega_z \times \Omega_{G_0}}(1,1,G_0)$ with short-term profit target μ_s at risk level R

Initialisation ϵ, $T^s = T^s_{\min}$;
for $T^s \leq T^s_{\max}$ **do**
  Calculate $\rho(\text{Risk}_{\Omega_z}(T^s, \mu_s))$;
  if $\rho(\text{Risk}_{\Omega_z}(T^s, \mu_s)) \leq$ R **then**
    Add T^s into decision set $\mathcal{T}^*$
    Calculate $\mathbb{E}_{z\in\Omega_z, G_0\in\Omega_{G_0}}[H(T,z,G_0)]$, $T = T^l + T^s + T^w + T^u$, see (3.6) **if** $\mathbb{E}_{z\in\Omega_z, G_0\in\Omega_{G_0}}[H(T,z,G_0)] \geq \mathbb{E}_{z\in\Omega_z, G_0\in\Omega_{G_0}}[H(T^*,z,G_0)]$ **then**
      $T^* = T$
    else
  else
    $T^s = T^s + \epsilon$;
  end
end
if $\mathcal{T}^*$ *is* $\emptyset$; **then**
  Return NA;
else
  Return T^{s*} and $\mathbb{E}_{z\in\Omega_z, G_0\in\Omega_{G_0}}[H(T^*,z,G_0)]$
end
Result: NA or $T^{s*}, \mathbb{E}_{z\in\Omega_z, G_0\in\Omega_{G_0}}[H(T^*,z,G_0)]$

3.4.2.2 The mean-VaR model

VaR indicates the *Value-at-Risk*, and is one of the instruments used to measure financial risk Duffie and Pan (1997). By using VaR in (3.26)-(3.27), the mean-VaR model with short-term profit target in expectation maximising form is written as:

$$\max_{T^s \in [T^s_{\min}, T^s_{\max}]} \quad \mathbb{E}_{z\in\Omega_z, G_0\in\Omega_{G_0}}[H(T,z,G_0)] \tag{3.28}$$

$$s.t. \quad Prob(h(T,z) < \mu_s) \leq \text{R} \tag{3.29}$$

3.4.2.3 The mean-CVaR model

It is known that VaR lacks the property of sub-additivity, and is thus not a coherent risk measure. Sub-additivity means that the joint risk cannot exceed the addition. The property of sub-additivity plays an important role when multiple investments are considered in a planning project. *Conditional Value-at-Risk* (CVaR) is an alternative, and is coherent Rockafellar et al. (2000). CVaR_R is also called Expected Shortfall (ES) at the $100 \cdot$ R% level, and describes the expected return of the project in the worst $100 \cdot$ R% of conditions.

Define $q^{\mathrm{R}}(\cdot)$ as the lower R−quantile. The lower quantile function for $h(T,z)$ is defined as follows:

$$q^{\mathrm{R}}(h(T,z)) = \inf\{x \in \mathbb{R} : Prob(h(T,z) \leq x) \geq \mathrm{R}\}. \tag{3.30}$$

Let q_h^{R} represent $q^{\mathrm{R}}(h(T,z))$. Define the CVaR at risk level R for return function, the NPV excluding FPP $h(T,z)$, as:

$$\mathrm{CVaR}_{\mathrm{R}}(h(T,z)) = -\{\mathbb{E}(h(T,z)^{\mathbb{1}_{\{h(T,z)\leq q_h^{\mathrm{R}}\}}} - q_h^{\mathrm{R}}[Prob(h(T,z) \leq q_h^{\mathrm{R}} - \mathrm{R}]\}/\mathrm{R}, \tag{3.31}$$

where $\mathbb{1}_{\{h(T,z)\leq q_h^{\mathrm{R}}\}}$ is an indicator function defined as:

$$\mathbb{1}_{\{h(T,z)\leq q_h^{\mathrm{R}}\}} = \begin{cases} 1, & h(T,z) \leq q_h^{\mathrm{R}}, \\ 0, & h(T,z) > q_h^{\mathrm{R}}. \end{cases} \tag{3.32}$$

By applying CVaR (3.31) in (3.26)-(3.27), the mean-CVaR model with short-term profit target in expectation maximising form is written as[7]:

$$\max_{T^s \in [T^s_{\min}, T^s_{\max}]} \quad \mathbb{E}_{z\in\Omega_z, G_0 \in \Omega_{G_0}}[H(T,z,G_0)] \tag{3.33}$$

$$s.t. \qquad \mathrm{CVaR}_{\mathrm{R}}(h(T,z)) \leq -\mu_s' \tag{3.34}$$

3.4.3 Mean-risk models for solving $\mathcal{P}_{\Omega_z \times \Omega_{G_0}}(1,1,G_0)$ with long-term profit target

When mean-risk models are formulated for solving the problem with a long-term profit target, uncertainties in both phases are involved when calculating the value of risk measure for given profit target μ_l and risk level R.

The model formulation for $\mathcal{P}_{\Omega_z \times \Omega_{G_0}}(1,1,G_0)$ with long-term profit target follows the way shown in Section 3.4.2. The objective function in the long-term case is the same as the short-term case (3.26). The risk function in constraint (3.27), however, is replaced by the long-term risk (3.18)-(3.19). The same substitution in Algorithm 1 is needed to solve the long-term model.

3.4.4 Decision makers' attitude to risk

Having specified the above framework of models, we can now distinguish several types of decision makers with respect to their risk tolerance levels and profit targets. Figure 3 illustrates a box model approach, distinguishing between several types of decision makers with low, medium, and high risk tolerance levels, and high, medium, low, and negative (for short-term only) profit

[7]The profit target μ_s' in CVaR differs from μ_s in VaR, see (3.29) and (3.34): μ_s describes a quantile where the probability of not meeting this quantile should not exceed R; μ_s' is the conditional expectation of the return function at the left-hand side of the quantile. The values of μ_s and μ_s' can be chosen over a wide range in applications, including negative ranges.

targets. 'LH', for example, represents a decision maker who has a low risk tolerance level and high profit target.

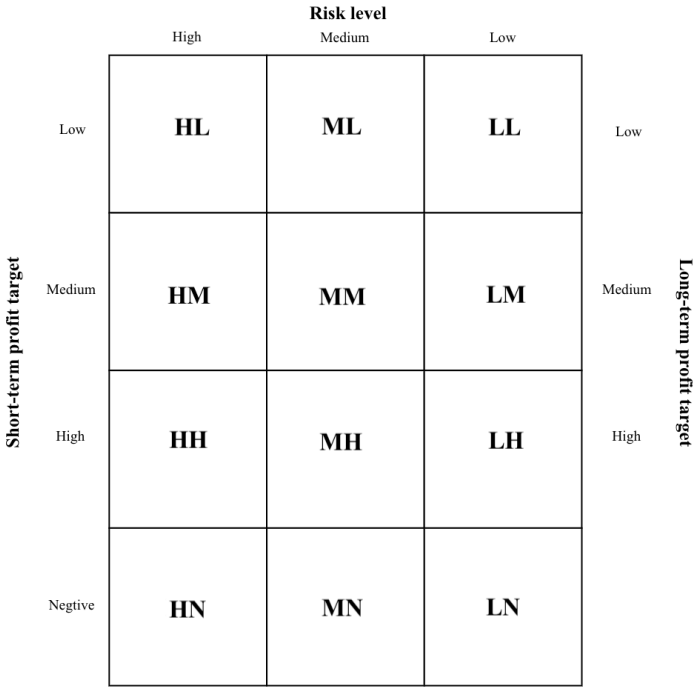

FIGURE 3: Types of profit target-risk tolerance level chart for short-term models and long-term models

There is evidence showing that the decision making behaviour about investments is affected by multiple factors, including but not limited to: company size, assets condition, liabilities, cash-flow situation and personality of the decision maker (Ingersoll and Ingersoll, 1987). For shipowners who have only a few vessels or less, the ability to take risks on any particular journey may be much lower than for large shipping firms operating many vessels across different routes and trades, who are better able to spread these risks. The former type of decision maker may thus typically have a much lower risk level compared to the latter, and may have a profit target focusing on the short term. Other factors, such as a bad cash-flow position, may require decision makers to lower their expectations about earnings obtained from the job under consideration. Such decision makers may be in the category 'LL' of Figure 3. Others, however, may have such high debts that need to be re-payed and thus may need to search for a higher profit target in the short term. However, such opportunities may perhaps come with a wider distribution (for example, on a route with bad weather highly likely) and so they may need to be prepared to take higher risk. Thus such decision makers may identify with 'MM' or 'HM' for a short-term model. Those with no debts or the opportunity to hire a ship easily, might only accept the job offer with lower risks and a higher profit target, and thus be 'LH' for short-term or 'LH' for long-term.

Some firms that have better risk spreading ability but with a focus to make money in the short-term may find affiliation with the category 'HH'. Sometimes, the low profit target can be negative

which represents a condition that the decision maker does not mind taking the risk of losing some money in the short-term to maximise the long-term profitability. Such decision makers may be in the categories 'LN', 'MN' and 'HN'.

Similar considerations leads to categories in Figure 3 applying to long-term risk. For the long-term case, decision makers concentrate on maximising an expected long-term profit and the corresponding risk of not meeting the profit target (also in the long-term), see Section 3.4.3. Profits in the short-term cannot be guaranteed when using the long-term models. However, the long-term model will incorporate the risk of bad weather and the risk of lower future profits. From the consideration of protecting the decision makers who may not be able to share risk well, in particular, for those who have debts to pay, the long-term models seem less appropriate. Nevertheless, when using these mean-risk models to evaluate different journey opportunities, the long-term model will be better able to recommend those jobs that also end up in a destination port with high profit potential. Indeed, the long-term model can also be used to evaluate a purposeful repositioning of the ship in ballast to a promising port or area of the world by incorporating the negative profit of that journey.

Furthermore, categories of decision makers with good risk spreading abilities can be represented by risk level and profit targets in the long-term as well. For example, 'HL' and 'HM' refer to types of decision makers who do not mind taking on risks and will accept a job when it reaches a low or medium profit in the long-term. 'HH', on the other hand, will be more demanding about the long-term profit target that the job is expected to reach.

3.5 Computational results and practical interpretation

Numerical experiments illustrate the proposed models and algorithms of Section 3.4, and more specifically show the impact on solutions from the following modelling features: (i) differences in decision maker's attitudes, FPP values, and fuel consumption; (ii) impact from different mean-risk models; and (iii) different (in-)coherent risk measures. In addition, we also (iv) compare with other methods from the literature; and (v) test our models using real-life data.

Before going into the detailed discussion of results, here is an overview of the experimental setup. Numerical experiments are for a *Suezmax* tanker, of which vessel characteristics can be found in Appendix A.1. Regarding (i), within the experiments for each model type, we derive and compare the optimal speed, NPV including FPP (long-term profitability) and NPV excluding FPP (short-term profitability) for different risk attitudes, see Sections 3.5.1-3.5.2 and Tables 4-7. As for (ii), four groups of experiments are prepared under the same assumptions about uncertainties. The comparison between using VaR and CVaR in short-term risk and long-term risk model is illustrated in Tables 4 to 7. For (iii), mean-VaR and mean-CVaR models with long-term risk are examined in two scenarios with the same mean but different standard deviation, see Table 8. (iv): To observe the difference with other speed optimisation methods, experiments are tested for different scenarios about the FPP and unusual fuel consumption period, see Section

3.5.4 and Table 11. Regarding (v), we test our models on data from DBE-P (Dry Bulk Earnings for Panamax), see Table 10.

3.5.1 Results for mean-VaR models

We examine the mean-VaR models considering the short-term and long-term risks formulated in Section 3.4 for the following parameter settings: $k_r = 2 \cdot k$, which indicates the fuel consumption rate during an unusual weather day is double the fuel consumption rate of a normal weather day; total unusual fuel consumption days follows a binomial distribution[8] $B(10, 0.3)$; the daily value of the FPP follows a normal distribution αG_0 (USD/day) $\sim N(20,000; 10,000^2)$. The opportunity cost of capital is set at $\alpha = 0.08$.

In the following experiments, we wish to see the impact on optimal solutions when decision makers hold different risk attitudes. Different risk attitudes are expressed through the specification of the risk level R and either the short-term profit target μ_s or long-term profit target μ_l, depending on the model type implemented.

3.5.1.1 Short-term risk model

Table 4 shows computational results including optimal speeds, the value of NPV including FPP and NPV excluding FPP when solving a mean-VaR model with short-term risk. It shows the results for a series of experiments for the following profit targets μ_s: -1.00, 0, 1.50, 2.00, 2.95, 2.96 and 3.00 million USD, and for different risk levels R: 0.05, 0.3, 0.8 and 0.999, respectively.

A short-term profit target that is negative or 0 represents the situation that the decision maker finds it acceptable to maximize the long-term profitability by accepting the risk for non-positive short-term NPV, or thus a negative cash inflow in the short term. When a positive profit target is specified in the model, the decision maker wants to minimise the risk that earnings from the currently planned journey under uncertainty would be too small. For example, if the decision maker sets a short-term profit target as 2 million USD, and only accepts to fail at 0.05 probability, the optimal speed suggested by the model (see Table 4) is 12.72 knots. The optimal expected NPV excluding FPP is 2.604 million USD, which is indeed above the target. The expected NPV including FPP is of course much higher at 93.503 million USD.

For the lower profit target values in Table 4, optimal speed seems to remain constant, however, when the profit target reaches a certain value (see $\mu_s = 2.95$ in Table 4), reducing the risk level will lead to the decrease of the optimal speed. The optimal speed will at some point approach the lowest speed of the ship $v_{\min}$ either with the decrease of the risk level or the increase of the profit target, until eventually, the feasible solution set will be empty, indicated by 'NA' in the tables. The practical meaning of 'NA' is that the model recommends to the decision maker not to undertake this journey, unless a lower short-term profit target or a more tolerant risk attitude is given.

[8] $B(x, p)$ denotes the binomial distribution with number of experiments x and success probability p. The daily value of the FPP G_0 (USD) corresponds to αG_0 (USD/day). $N(x; y^2)$ denotes normal distribution with mean x and standard deviation y.

TABLE 4: Optimal speed and NPV values from short-term mean-VaR risk model, $\alpha G_0 \sim N(20,000; 10,000^2)$, for multiple profit targets and risk levels

Profit target (μ_s) (million USD)	-1.00			
Risk level (R)	0.05	0.3	0.8	0.999
Speed (x) (knots)	12.72	12.72	12.72	12.72
NPV including FPP (H) (million USD)	93.503	93.503	93.503	93.503
NPV excluding FPP (h) (million USD)	2.604	2.604	2.604	2.604
Profit target (μ_s) (million USD)	0			
Risk level (R)	0.05	0.3	0.8	0.999
Speed (x) (knots)	12.72	12.72	12.72	12.72
NPV including FPP (H) (million USD)	93.503	93.503	93.503	93.503
NPV excluding FPP (h) (million USD)	2.604	2.604	2.604	2.604
Profit target (μ_s) (million USD)	1.50			
Risk level (R)	0.05	0.3	0.8	0.999
Speed (x) (knots)	12.72	12.72	12.72	12.72
NPV including FPP (H) (million USD)	93.503	93.503	93.503	93.503
NPV excluding FPP (h) (million USD)	2.604	2.604	2.604	2.604
Profit target (μ_s) (million USD)	2.00			
Risk level (R)	0.05	0.3	0.8	0.999
Speed (x) (knots)	12.72	12.72	12.72	12.72
NPV including FPP (H) (million USD)	93.503	93.503	93.503	93.503
NPV excluding FPP (h) (million USD)	2.604	2.604	2.604	2.604
Profit target (μ_s) (million USD)	2.95			
Risk level (R)	0.05	0.3	0.8	0.999
Speed (x) (knots)	NA	11.36	12.56	12.72
NPV including FPP (H) (million USD)	NA	93.480	93.503	93.503
NPV excluding FPP (h) (million USD)	NA	2.965	2.931	2.604
Profit target (μ_s) (million USD)	2.96			
Risk level (R)	0.05	0.3	0.8	0.999
Speed (x) (knots)	NA	10.60	12.26	12.72
NPV including FPP (H) (million USD)	NA	93.444	93.501	93.503
NPV excluding FPP (h) (million USD)	NA	2.973	2.942	2.604
Profit target (μ_s) (million USD)	3.00			
Risk level (R)	0.05	0.3	0.8	0.999
Speed (x) (knots)	NA	NA	NA	12.10
NPV including FPP (H) (million USD)	NA	NA	NA	93.499
NPV excluding FPP (h) (million USD)	NA	NA	NA	2.947

The results show that there is a narrow range of profit targets within which one can observe a reduction of optimal speed down to the lower limit before the model returns NA. Before approaching this narrow range, the optimal speed is the same, which is 12.72 knots for the tested scenario. In this range, the constraint related to risk does not affect the decision, and the solution derived by the model is the same as for a risk neutral decision maker. When the decision maker thus tests over a broad range of profit targets, none of which falls within this range where optimal speeds are sensitive to the target value, the results from the model may give the impression that results are of the 'bang-bang' type, as the optimal speed is either 12.72 knots when the problem is feasible under determined risk attitudes, or the trip is not worth undertaking (NA). This will also be the case, for example, in the Tables 5-7.

3.5.1.2 Long-term risk model

Table 5 shows optimal solutions calculated from applying different values of profit target μ_l and risk level R for mean-VaR models in the long-term case. The setting of μ_l is based on the value of expected NPV including FPP. As the FPP dominates the long-term NPV in case $\alpha G_0 \sim N(20,000; 10,000^2)$ where H is 93.503 million USD and h is 2.604 million USD, we formulate μ_l as 0, 50.00, 100.00 and 140.00 million USD in experiments to represent different decision makers who have, respectively, a zero, low, medium and high profit target in the long-term. Negative profit targets are not considered in long-term models for the obvious reason that

we assume that the decision maker wants the activity to be profitable in the long term. The risk level is formulated in the same way as experiments for the short-term model, see Section 3.5.1.1 and Table 4. Results are similar as in the short-term model in that the optimal speed will again be 12.72 knots, but the range when it transitions to not worth undertaking (NA) is of course now based on long-term risk considerations.

TABLE 5: Optimal speed and NPV values from long-term mean-VaR risk model, $\alpha G_0 \sim N(20,000; 10,000^2)$, for multiple profit targets and risk levels

Profit target (μ_l) (million USD)	0			
Risk level (R)	0.05	0.3	0.8	0.999
Speed (x) (knots)	12.72	12.72	12.72	12.72
NPV including FPP (H) (million USD)	93.503	93.503	93.503	93.503
NPV excluding FPP (h) (million USD)	2.604	2.604	2.604	2.604
Profit target (μ_l) (million USD)	50.00			
Risk level (R)	0.05	0.3	0.8	0.999
Speed (x) (knots)	NA	12.72	12.72	12.72
NPV including FPP (H) (million USD)	NA	93.503	93.503	93.503
NPV excluding FPP (h) (million USD)	NA	2.604	2.604	2.604
Profit target (μ_l) (million USD)	100.00			
Risk level (R)	0.05	0.3	0.8	0.999
Speed (x) (knots)	NA	NA	12.72	12.72
NPV including FPP (H) (million USD)	NA	NA	93.503	93.503
NPV excluding FPP (h) (million USD)	NA	NA	2.604	2.604
Profit target (μ_l) (million USD)	140.00			
Risk level (R)	0.05	0.3	0.8	0.999
Speed (x) (knots)	NA	NA	NA	12.72
NPV including FPP (H) (million USD)	NA	NA	NA	93.503
NPV excluding FPP (h) (million USD)	NA	NA	NA	2.604

3.5.2 Results for mean-CVaR models

We also designed experiments for short- and long-term mean-CVaR risk models. Assumptions about uncertainties are as in Section 3.5.1 for mean-VaR models.

3.5.2.1 Short-term risk model

Table 6 shows computational results including optimal speeds, the value of NPV including FPP and NPV excluding FPP when solving a mean-CVaR model with short-term risk.

The profit target for mean-CVaR models has a different meaning compared with mean-VaR models. Results show that the mean-CVaR model is more cautious: when the same values of μ_s and μ_s' are applied, the optimal speed calculated by the mean-CVaR model is less or equal to the one calculated by the mean-VaR model, or the model suggests NA more readily, see e.g. results for $\mu_s = 3.00$, R $= 0.999$ in Table 4 and $\mu_s' = 3.00$, R $= 0.999$ in Table 6.

3.5.2.2 Long-term risk model

Table 7 shows computational results when same value of profit target and risk level are formulated as in Table 5. When a profit target μ_l' as 100.00 million USD is determined, there is no feasible solution for all risk levels, see Table 7. Recall that, instead, 12.72 knots is suggested at risk level 0.8 and 0.999 for decision makers using mean-VaR models, see Table 5.

TABLE 6: Optimal speed and NPV values from short-term mean-CVaR risk model, $\alpha G_0 \sim N(20,000; 10,000^2)$, for multiple profit targets and risk levels

Profit target (μ_s) (million USD)	-1.00			
Risk level (R)	0.05	0.3	0.8	0.999
Speed (x) (knots)	12.72	12.72	12.72	12.72
NPV including FPP (H) (million USD)	93.503	93.503	93.503	93.503
NPV excluding FPP (h) (million USD)	2.604	2.604	2.604	2.604
Profit target (μ'_s) (million USD)	0			
Risk level (R)	0.05	0.3	0.8	0.999
Speed (x) (knots)	12.72	12.72	12.72	12.72
NPV including FPP (H) (million USD)	93.503	93.503	93.503	93.503
NPV excluding FPP (h) (million USD)	2.604	2.604	2.604	2.604
Profit target (μ'_s) (million USD)	1.50			
Risk level (R)	0.05	0.3	0.8	0.999
Speed (x) (knots)	12.72	12.72	12.72	12.72
NPV including FPP (H) (million USD)	93.503	93.503	93.503	93.503
NPV excluding FPP (h) (million USD)	2.604	2.604	2.604	2.604
Profit target (μ'_s) (million USD)	2.00			
Risk level (R)	0.05	0.3	0.8	0.999
Speed (x) (knots)	12.72	12.72	12.72	12.72
NPV including FPP (H) (million USD)	93.503	93.503	93.503	93.503
NPV excluding FPP (h) (million USD)	2.604	2.604	2.604	2.604
Profit target (μ'_s) (million USD)	3.00			
Risk level (R)	0.05	0.3	0.8	0.999
Speed (x) (knots)	NA	NA	NA	NA
NPV including FPP (H) (million USD)	NA	NA	NA	NA
NPV excluding FPP (h) (million USD)	NA	NA	NA	NA

TABLE 7: Optimal speed and NPV values from long-term mean-CVaR risk model, $\alpha G_0 \sim N(20,000; 10,000^2)$, for multiple profit targets and risk levels

Profit target (μ'_l) (million USD)	0			
Risk level (R)	0.05	0.3	0.8	0.999
Speed (x) (knots)	NA	12.72	12.72	12.72
NPV including FPP (H) (million USD)	NA	93.503	93.503	93.503
NPV excluding FPP (h) (million USD)	NA	2.604	2.604	2.604
Profit target (μ'_l) (million USD)	50.00			
Risk level (R)	0.05	0.3	0.8	0.999
Speed (x) (knots)	NA	NA	12.72	12.72
NPV including FPP (H) (million USD)	NA	NA	93.503	93.503
NPV excluding FPP (h) (million USD)	NA	NA	2.604	2.604
Profit target (μ'_l) (million USD)	100.00			
Risk level (R)	0.05	0.3	0.8	0.999
Speed (x) (knots)	NA	NA	NA	NA
NPV including FPP (H) (million USD)	NA	NA	NA	NA
NPV excluding FPP (h) (million USD)	NA	NA	NA	NA
Profit target (μ'_l) (million USD)	140.00			
Risk level (R)	0.05	0.3	0.8	0.999
Speed (x) (knots)	NA	NA	NA	NA
NPV including FPP (H) (million USD)	NA	NA	NA	NA
NPV excluding FPP (h) (million USD)	NA	NA	NA	NA

3.5.2.3 Comparisons between mean-VaR and mean-CVaR models

To compare the differences between mean-VaR and mean-CVaR models, especially in cases where a higher dispersion for the FPP is estimated, we extended the experiments for mean-risk models with long-term risk for two scenarios of the FPP. Scenario I represents $\alpha G_0 \sim N(20,000; 10,000^2)$ of which results were reported in Sections 3.5.1-3.5.2. In scenario II we use $\alpha G_0 \sim N(20,000; 12,000^2)$, i.e. the same expected value but a higher standard deviation. Experiments run for different profit targets (μ_l and μ'_l): 0, 30.00, 78.00, 100.00 million USD, and risk levels R: 0.05, 0.3, 0.8, and 0.999

Optimal speed strategies under these experiments are summarised in Table 8. For mean-VaR models, there is no difference between the two scenarios in optimal speed. Results calculated

by mean-CVaR models, however, does show differences. For the case, $\mu_l' = 30.00$ and R $= 0.3$, the suggested speed goes from 12.72 knots to infeasible when the estimated standard deviation increases, see also case $\mu_l' = 78.00$ and R $= 0.8$. The results show that CVaR is more sensitive to the tail of the distribution (see also Section 3.4).

TABLE 8: Optimal speed when applying two scenarios of FPP in mean-VaR and mean-CVaR models with long-term risk

Profit target	Risk level	Optimal speed (knots)			
μ_l, μ_l' (million USD)	R	mean-VaR		mean-CVaR	
		Scenario I[a]	Scenario II[b]	Scenario I[a]	Scenario II[b]
0	0.05	12.72	12.72	NA	NA
	0.3	12.72	12.72	12.72	12.72
	0.8	12.72	12.72	12.72	12.72
	0.999	12.72	12.72	12.72	12.72
30.00	0.05	NA	NA	NA	NA
	0.3	12.72	12.72	12.72	NA
	0.8	12.72	12.72	12.72	12.72
	0.999	12.72	12.72	12.72	12.72
78.00	0.05	NA	NA	NA	NA
	0.3	NA	NA	NA	NA
	0.8	12.72	12.72	12.72	NA
	0.999	12.72	12.72	12.72	12.72
100.00	0.05	NA	NA	NA	NA
	0.3	NA	NA	NA	NA
	0.8	12.72	12.72	NA	NA
	0.999	12.72	12.72	NA	NA

[a] $\alpha G_0 \sim N(20,000; 10,000^2)$; [b] $\alpha G_0 \sim N(20,000; 12,000^2)$.

3.5.3 Estimation of FPP for Panamax vessels

Now that we have established insight on the effects of randomness on economic parameters, we report here on how one may construct possible distributions of FPP that resemble real-world situations from market indices. In this section, we use as an example the Dry Bulk Earnings for Panamax vessels (DBE-P). DBE-P reports daily average earnings for dry bulk vessels that can transit the Panama Canal. Table 9 and Figure 4 show statistics we calculated from DBE-P values over a period of three years (2019 to 2021).

TABLE 9: Statistics calculated for DBE-P from 2019 to 2021

Year	mean (USD per day)	Std.	skewness	kurtosis
2019	13045.55	3543.38	0.125	-0.808
2020	10,203.00	2971.70	0.076	-1.062
2021	20,451.92	4628.53	-0.368	-0.719

Data source: https://www.bimco.org/news/market_analysis/2021/20210601_dry_bulk_shipping

We design numerical experiments by using statistics shown in Table 9 for constructing the distribution for FPP. Different to the assumption of normality for FPP in previous tests, historical data show none of DBE-P in 2019, 2020 and 2021 are Gaussian distributed, which would need $\tau = 0$ and $\kappa = 3$. Thus we use computed statistics from samples to establish the skew-normal distribution[9] $SN(\alpha, \xi, \omega)$ for FPP rather than the normal distribution $N(\mu, \sigma^2)$.

[9]Estimation for parameters include location parameter ξ, scale parameter ω and shape parameter α for a skew-normal distribution $SN \sim (\xi, \omega, \alpha)$ could be computed by sample mean $\hat{\mu}$, sample variance $\hat{\delta}^2$ and sample skew $\hat{\tau}$. Relevant formulas are in Appendix B.

Table 10 shows results of optimal speeds for four types of decision makers with various profit targets and risk levels for the mean-CVaR model with long-term risk. For example, using the sample of DBE-P in 2019, the skew-normal distribution is $\alpha G_0 \sim SN(11,172;\ 4,251;\ 0.9598)$, and the optimal speed suggested is 12.10 knots for the type of 'HL', 'LL' and risk neutral decision makers. The job is not suggested to be taken for decision makers who are of the types HH' and 'LH', as defined. Using 2020 data, we can see that the distribution on the FPP moves to a lower range (see also Figure 4), and thus the recommended speed reduces to 11.80 knots. In addition, the tail on the low side of the FPP is fatter, which leads the 'LL' category of decision makers to no longer finding it profitable to operate this job in this market. For 2021 data, the median has moved to higher values, which leads speeds to be higher at 12.28 knots. The tail is fairly similar to the 2019 distribution and which leads to acceptance results that are the same. Note that in reality the decisions recommended from the models can also greatly differ from year to year due to other factors changing, e.g. the cost of fuel.

TABLE 10: Optimal speed for the FPP derived from historical DBE-P for mean-CVaR models with long-term risk

Year	Estimation Distribution for FPP	Optimal speed (knots)				
		HL[a]	HH[b]	LL [c]	LH[d]	RN[e]
2019	$\alpha G_0 \sim SN(11,172;\ 4,251;\ 0.9598)$	12.10	NA	12.10	NA	12.10
2020	$\alpha G_0 \sim SN(\ 8,869;\ 3,410;\ 0.7788)$	11.80	NA	NA	NA	11.80
2021	$\alpha G_0 \sim SN(10,944;\ 6,383;\ 1.7091)$	12.28	NA	12.28	NA	12.28

[a] : R = 0.8, $\mu_l' = 30$, [b] : R = 0.8, $\mu_l' = 100$, [c] : R = 0.05, $\mu_l' = 30$, [d] : R = 0.05, $\mu_l' = 100$, [e] : Risk neutral, R = 1, $\mu_l' = 0$;

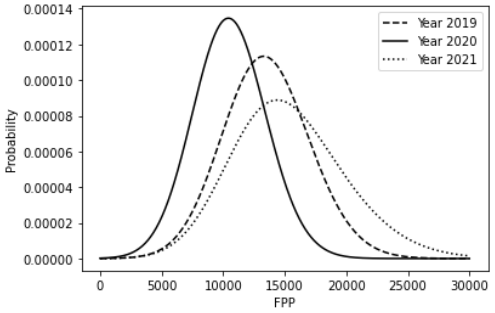

FIGURE 4: Skew-normal distributions for FPP derived from historical DBE-P from 2019 to 2021

We tested the mean-risk models for a 54,810 dwt PANAMANA bulk-carrier for one of its laden legs from Nueva Palmira to Londonderry, see Appendix A.2 for its ship characteristics. The results of these experiments show that while optimal speed values highly depend on the particular instance data, similar patterns are observed as those obtained for *Suezmax*, as in Tables 4-11. Here too, optimal speed remains constant over a range of profit targets, and only starts to decrease towards the lower speed limit within in a narrow range of profit targets above some threshold profit target, beyond which it is not worthwhile to undertake the journey, see Appendix A.3.

3.5.4 Comparison with other models

In this section, results of numerical experiments increase our insights on the optimal speed strategy when solving the problem with different speed optimisation models.

To compare with the optimal policy by using other methods, we replicate four influential speed optimisation models mentioned in Section 3.2. The model in Theocharis et al. (2019) minimises unit cost per tonne which is considered to represent the equilibrium freight rate or required freight rate (RFR), and is based on the least cost speed (LCS) economic theory of Alderton (1981). This model does not include the FPP concept, but instead looks at the current journey and ship characteristics as being representative data. Ronen (1982) and Magirou et al. (2015) have an objective to maximise net profit per unit time when making decision problems associated to speed. Especially, Magirou et al. (2015) includes the stochasticity of freight rates and maximise the expected net profit per unit time as objective function. Here, we examine their 'Stochastic freight rates â independence' model without the random effect of freight rates. We also compare with Ge et al. (2021), in which optimal speeds are derived from a model that most closely relates to the model in this paper, and includes the FPP as well but as a deterministic value, and without considering uncertainty on fuel consumption.

TABLE 11: Comparison of economic speed optimisation models

Scenarios	Optimal speed (knots)								
$k_r = 2, z \sim B(10, 0.3)$	Our paper (mean-CVaR long-term risk)					GBH	TRPH	Ronen	MPB
	HL[a]	HH[b]	LL[c]	LH[d]	RN[e]				
$\alpha G_0 \sim (0; 0)$	NA	NA	NA	NA	10.52	10.92	10.82	17	17
$\alpha G_0 \sim (10,000; 4,000^2)$	11.74	NA	NA	NA	11.74	12.26	10.82	17	17
$\alpha G_0 \sim (12,000; 4,000^2)$	11.96	NA	NA	NA	11.96	12.50	10.82	17	17
$\alpha G_0 \sim (16,000; 10,000^2)$	12.36	NA	NA	NA	12.36	12.94	10.82	17	17
$\alpha G_0 \sim (20,000; 10,000^2)$	12.72	NA	NA	NA	12.72	13.34	10.82	17	17
$\alpha G_0 \sim (20,000; 20,000^2)$	12.72	NA	NA	NA	12.72	13.34	10.82	17	17
$\alpha G_0 \sim (30,000; 10,000^2)$	13.56	13.56	NA	13.56	13.56	14.28	10.82	17	17
$\alpha G_0 \sim (50,000; 10,000^2)$	14.96	14.96	14.96	14.96	14.96	15.82	10.82	17	17
$\alpha G_0 \sim (50,000; 20,000^2)$	14.96	14.96	14.96	NA	14.96	15.82	10.82	17	17

Scenarios		Optimal speed (knots)								
$\alpha G_0 \sim N(20,000; 10,000^2)$		Our paper (mean-CVaR long-term risk)					GBH	TRPH	Ronen	MPB
		HL	HH	LL	LH	RN				
$k_r = 1$	$z = 0$	13.36	NA	NA	NA	13.36	13.34	10.82	17	17
$k_r = 2$	$z \sim B(10, 0.3)$	12.72	NA	NA	NA	12.72	13.34	10.82	17	17
$k_r = 2$	$z \sim B(10, 0.8)$	11.96	NA	NA	NA	11.96	13.34	10.82	17	17
$k_r = 2$	$z \sim B(10, 1)$	11.72	NA	NA	NA	11.72	13.34	10.82	17	17
$k_r = 3$	$z \sim B(10, 0.3)$	12.24	NA	NA	NA	12.24	13.34	10.82	17	17
$k_r = 3$	$z \sim B(10, 0.8)$	11.14	NA	NA	NA	11.14	13.34	10.82	17	17
$k_r = 3$	$z \sim B(15, 0.8)$	10.54	NA	NA	NA	10.54	13.34	10.82	17	17
$k_r = 6$	$z \sim B(10, 0.8)$	10.00	NA	NA	NA	10.00	13.34	10.82	17	17

GBH: Ge et al. (2021); TRPH: Theocharis et al. (2019); Ronen: Ronen (1982); MPB: Magirou et al. (2015).
[a] R = 0.8, $\mu'_l = 30$, [b] R = 0.8, $\mu'_l = 100$, [c] R = 0.05, $\mu'_l = 30$, [d] R = 0.05, $\mu'_l = 100$, [e] Risk neutral, $\mu'_l = 0$, R = 1; [f] this model is explained in Section 3.5.5.

Table 11 shows optimal speeds obtained by the different economic speed optimization models. For experiments in our paper, five types of risk attitudes (including the risk neutral decision maker 'RN') are considered and calculated by mean-CVaR models with long-term risk. The significance of suggested optimal speed for decision makers who hold different risk attitudes is found by comparing results within columns of 'Our paper'.

The top part of the Table 11 shows solutions for different FPP scenarios. The solution from TRPH, as the model minimises cost per tonnage regardless of potential future profitability, is unaffected by a change in FPP scenario. TRPH typically finds low speeds due to it representing the equilibrium under perfect competition between ship operators (where profits reduce to zero). Solutions from Ronen and MPB, since these models account for current freight rate revenue values on the current journeys, suggest much higher speeds, although they do not account for

and thus remain insensitive to FPP values. GBH, as that paper introduced the FPP concept, does adjust speed to the expected value of the FPP. The mean-CVaR model developed in this paper will exhibit similar characteristics as the GBH model in that optimal speeds will increase with the expected value of the FPP. However, in the mean-CVaR model the result may also be NA if there is too much risk on the FPP.

The second part of the Table 11, shows solutions for different bad weather scenarios. With increasing chance of bad weather, the optimal speed in the mean-CVaR model reduces for 'HL' and 'RN' profiles, but because the objective function accounts for the whole future of the ship, it is found not significant enough to lead to a switch to 'NA' decisions. The randomness on the FPP, however, has very different impact on the decisions. An increase in standard deviation on the FPP does not affect optimal speed, if the journey is worthwhile to undertake, but increases the likelihood of 'NA' results for a given risk profile. The other models from the literature reported in the table are not affected by the bad weather risk on the current journey. This also explains why the optimal speeds in GBH, a model that does not account for higher fuel cost risks, are somewhat higher than in our mean-CVaR models that do account for this risk.

To summarise, the mean-risk models developed strengthen the robustness of decisions by dealing with stochasticities during execution and after termination time. By using the concept of FPP introduced in GBH, optimal speed on a journey depends on the judgement of the decision maker about what the future holds for this ship. An optimistic decision maker will thus arrive at a higher speed than a pessimistic one. The mean-risk models developed can be viewed as extensions of the deterministic GBH model, which allows them to account for the risk associated with randomness on the cost of executing the current journey, and randomness on the future profit potential when arriving at the destination port. Which of these risks are most important is to be decided by the decision maker. Short-term models as developed can help those who need to manage the risk on the current journey primarily, and we have provided several examples of possible situations in Section 3.5.5 in which this viewpoint can make good sense. Long-term models can serve organisations that are less bound to avoiding short-term losses on individual ships and journeys: they can use long-term expected profitability goals for their risk assessments.

3.5.5 Why using NPV models?

While the NPV approach is an accepted part of financial decision theory, one may wonder whether the additional mathematical complexity is worth considering for problems as formulated in this paper.

This is an important question that has been addressed recently in Ge et al. (2021) (see in particular Table 2 and Section 5 in that paper), and Beullens et al. (2023) (see in particular Section 4 and Table 11). These authors have carefully demonstrated the value of NPV modelling for ship speed optimisation.

In this section, we briefly offer intuition behind some of these results, and show that they also apply to this context of mean-risk models under uncertainty. The optimisation problem without regard of the time value of money and the ship's future would arguably arrive at the following objective function:

$$\max \mathbb{E}_{z\in\Omega_z}[\text{Net profit}], \tag{3.35}$$

where the net profit is defined as the total of revenues minus all the costs relevant to the carrier. In a single journey from port A to port B with a targeted total travel time T and associated speed v, for scenario $z = \omega_{zi}$, $\omega_{zi} = \{0, 1, \ldots, m\}$, we would arrive at:

$$\text{Net profit}(T, z = \omega_{zi}) = R^j - C^u - C^l(v, z = \omega_{zi}) - f^{\text{TCH}} \cdot T, \tag{3.36}$$

where R^j is the total freight revenue earned on this journey, C^u is the unloading cost, C^l is the loading cost including fuel cost, f^{TCH} is the daily hire rate, see also (3.6-3.8) and Section 3.3.2. Note that R^j and C^u are constants and not influencing the optimisation.

The question now arises whether we should proceed optimising based on this function. The T that maximises this function affects profits that can be earned by this ship on future journeys throughout the year, but these are not accounted for in (3.36). This approach would thus only work if the ship is chartered for this single journey only, and is returned to the owner at completion in port B. (See also Theorem 1, part (I) and (II) in Beullens et al. (2023).) This approach is similar to what is deployed in the TRPH model of Table 11.

Indeed, computational results are calculated for the model (3.35) under the different scenarios considered in Table 11. When using (3.36), the optimal solution is accepting the job and sail at the speed that ranges from 10.66 knots down to 10.04 knots, depending on the weather scenario. This suggested speed is somewhat lower than TRPH mainly due to that model not considering uncertainty on fuel consumption.

When the decision maker wishes to use the ship after this journey is completed, an approach based on (3.36) is thus conceptually wrong. Because future profits are ignored, these models will typically find speeds that are much too low. The approach taken in this paper recognises that the current speeds of the ship affects the future, see (3.12), through discounting this future based on the time of completion of the current work. This typically increases recommended speeds of the ship significantly by 0.5 to several knots depending on how bright the economic future looks[10], compare e.g. RN with TRPH in Table 11.

[10]One knot faster may reduce a journey taking 24 days down to 22 days, for example. This may not seem like much, but on an ongoing basis the repeated use of a speed 1 knot different to optimal may lead to significant monetary losses that can easily amount to 0.3 to 0.5 million USD per year in the Suezmax example.

An alternative approach that does not use the NPV framework would seek to maximize net profit per journey day:

$$\text{Net daily profit}(T, z = \omega_{zi}) = \frac{R^j - C^u - C^l(v, z = \omega_{zi}) - f^{\text{TCH}} \cdot T}{T}. \tag{3.37}$$

At first sight this approach concentrates on this particular journey only, and thus it would seem that again this model does not account for profits the ship could earn on *future* journeys. As shown in Beullens et al. (2023) (Theorem 1, (III)-(V)), however, this is not true since they show that optimal speeds obtained will be equivalent to those obtained from a model in which one assumes that this journey is infinitely repeated under the same economic conditions. The model therefore does account for the future; only a very specific one. This approach is in spirit what is used in the methods Ronen and MPB in Table 11.

When using (3.37), the optimal solution is accepting the job and sail at the speed in a range from close to 17 knots down to below 11 knots depending on the predicted weather scenario, results that are only close to Ronen and MPB for perfect weather scenarios.

Assuming the same economic conditions as they are on a day during this journey (and when travelling at this particular speed as found by the model) could be unrealistic because the ship is likely to proceed after unloading in port B with a journey of a different profit structure (for example, a ballast leg back to port A). Much better results with this method are obtained when considering a round-trip journey.

Even then, the approach can be unrealistic because economic conditions in the future will change. If the economic conditions in the future are considered better than today, it would seem natural for the decision maker to want the ship to do the currently considered job in a somewhat shorter total time, and thus for the ship to speed up. Alternatively, if the future looks bleak one may want to slow down the ship. But such future profit prospects are not accounted for in models with objective functions similar to (3.37). Many tramp ships also do not undertake round-trip journeys. Differences in recommended ship speeds between such models and the NPV models can amount to several knots, compare e.g. RN with Ronen in Table 11.

By using an NPV formulation as in Section 3.3 of this paper, the model can account for different possible futures and is not restricted to journeys of a particular structure. As shown in Table 11 in Beullens et al. (2023), both classic assumptions implicitly adopted in above formulations (3.36) and (3.37) as well as many other plausible futures can be modelled.

It is also clear from Table 11 that these results from model (3.35) in general differ greatly from the results obtained with an NPV model, such as GBH and the NPV models developed in this paper.

In summary, it is clear from this discussion that the model used greatly influences the results obtained, and if one uses a particular model the underlying assumptions should be well understood. The question of whether NPV modelling is worthwhile can perhaps be viewed a matter of

preference. In our view, however, the increased flexibility and accuracy of the approach would trump the additional complexity of the method.

3.6 Model extensions: late payment risks

A model that accounts for risk allows for the inclusion and due consideration of various kinds of risks, while deterministic models or models maximizing expected profits cannot do so. In this section, we illustrate with an example how the model established in Sections 3.3-3.4 can be extended to accommodate for more realistic payment structures, including late payment penalties.

Payment structures as agreed in the contract between the carrier (our decision maker) and the shipper (the customer) can vary. In Nuzio, for example, we are given the following examples: In a 'freight prepaid' arrangement, the shipper pays the carrier within, say, 15 days from shipment, while in a 'freight collect' payment, this could be 15 days from delivery. They also provide examples what could happen if payments are late, including a case where if the shipper fails to pay and the carrier is forced to employ an outside source to collect, then penalties may increase up to 6 or 7 times the original fee.

Term A: partially 'shipment', partially 'delivery' and failure-to-pay penalty

We can interpret the payment structure implemented in our basic model described in Section 3.3 thus as a 'collect' payment on the day of delivery. In this section we show how to extend the model to allow for a generalized payment structure, referred to as Term A, in which a fraction is prepaid, the remainder is collect, and where there are failure-to-pay penalties. This will accommodate the above mentioned payment structures derived from Nuzio. For a more general treatment of how NPV models enable the inclusion of generalized payment structures, see also Beullens and Janssens (2014).

We introduce the following notation and assumptions, see also Figure 5. According to the agreed contract, the shipper pays the fraction $\beta_s \cdot R^j$ for total freight charges after shipment from port A within B_s days. The remaining fraction $\beta_d \cdot R^j = (1-\beta_s) \cdot R^j$ is paid within B_d days after delivery. Failure to pay within the negotiated period results an additional penalty $l_A \cdot R^j$ at most B_{lA} days after the deadline. For simplicity, take $\beta_s = 0$.

Assume the actual payment is $\tilde{\beta_d} \cdot R^j$ at time $\tilde{B_d}$. Note that $\tilde{\beta_d}$ and $\tilde{B_d}$ should be considered random variables for the decision maker. The ability of shippers to make payments in line with the contract is affected by their short-term liquidity and cash-flow coverage ratio (Kavussanos and Visvikis, 2009). The rate of failure to pay penalty and clearance days are also formulated as random variables that are denoted by $\tilde{l_A}$ and $\tilde{B_{lA}}$ to represent the case when shippers are insolvent and are not able to pay the rest of the freight penalty charges. Define the probability space for random variables involved in payments including $\tilde{\beta_d}$, $\tilde{B_d}$, $\tilde{l_A}$, $\tilde{B_{lA}}$ by $\{\Omega_{\tilde{\beta_d}}, \mathcal{F}_{\tilde{\beta_d}}, Prob_{\tilde{\beta_d}}\}$,

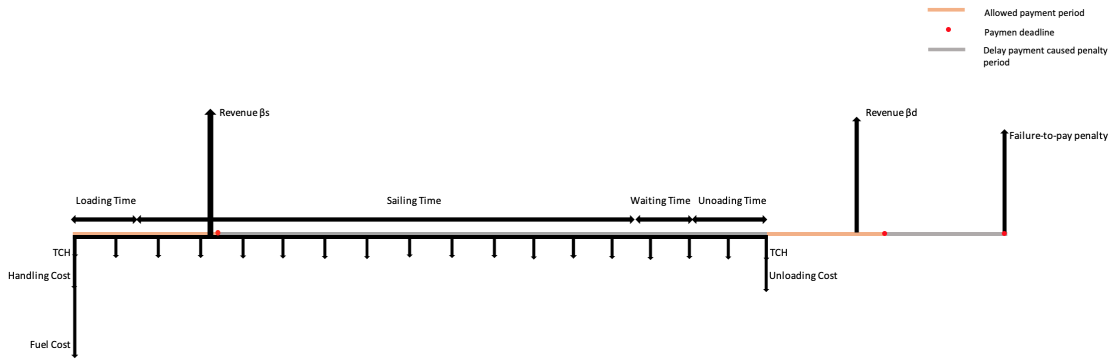

FIGURE 5: Timeline of cash flows in single leg under payment Term A

$\{\Omega_{\tilde{B_d}}, \mathcal{F}_{\tilde{B_d}}, Prob_{\tilde{B_d}}\}$, $\{\Omega_{\tilde{l_A}}, \mathcal{F}_{\tilde{l_A}}, Prob_{\tilde{l_A}}\}$, and $\{\Omega_{B\tilde{_{lA}}}, \mathcal{F}_{B\tilde{_{lA}}}, Prob_{B\tilde{_{lA}}}\}$, respectively[11]. Incidentally, liquidity, cash flow coverage and solvency of a shipping company are considered to be highly correlated to each other (Merikas et al., 2011; Ayoush et al., 2021). Thus, we simplify the probability space of all random variables about payments and failure to pay penalty by a joint space Ω_B, where $\Omega_B = \Omega_{\tilde{\beta_d}} \otimes \Omega_{\tilde{B_d}} \otimes \Omega_{\tilde{l_A}} \otimes \Omega_{B\tilde{_{lA}}}$. Define the vector $B = \prec \tilde{\beta_d}, \tilde{B_d}, \tilde{l_A}, B\tilde{_{lA}} \succ$. The expected NPV for taking the job from port A to port B excluding counting the FPP at port B is:

$$\mathbb{E}_{z\in\Omega_z, B\in\Omega_B}[h(T,z,B)] = \sum_{i=1}^{T_1}\sum_{j=1}^{T_B} p_{zi}\cdot p_{Bj}\cdot h(T,z=\omega_{zi},B=\omega_{Bj}), \tag{3.38}$$

where $h(T,z=\omega_{zi},B=\omega_{Bj})$ is the NPV for a particular scenario:

$$\begin{aligned} h(T,z=\omega_{zi},B=\omega_{Bj}) = \tilde{\beta_d}\cdot R^j\cdot e^{-\alpha(T+\tilde{B_d})} + (1-\tilde{\beta_d})\cdot(1+\tilde{l_A})\cdot R^j\cdot e^{-\alpha(T+\tilde{B_d}+\tilde{B_{lA}})} \\ -C^u\cdot e^{-\alpha T} - C^l(v,z=\omega_{zi}) - \int_0^T f^{\mathrm{TCH}}\cdot e^{-\alpha t}\,\mathrm{d}t, \end{aligned} \tag{3.39}$$

where $z = \omega_{zi}$, $\omega_{zi} \in \{0,1,\ldots,m\}$, and $B = \omega_{Bj} = \prec \tilde{\beta_d}_j, \tilde{B_d}_j, \tilde{l_A}_j, \tilde{B_{lA}}_j \succ$. These new equations for short-term profit can now be applied into the models of Sections 3.3-3.4.

Short-term risk now involves assessing the trustworthiness of shippers, and risk averse decision makers will tend to want to avoid shippers that are more likely to pay late or not at all (default risk).

There are other possible contractual arrangements of which many, it seems to us, can be modelled in this framework. Carriers may propose a contract in which payment has to be completed

[11] Detailed description about how to define a random variable and its probability space involved in payments is demonstrated as follows for $B\tilde{_{lA}}$: assume random variable $B\tilde{_{lA}}$ happens under $T_{B\tilde{_{lA}}}$ states, $i \in \{1,\ldots,T_{B\tilde{_{lA}}}\}$. Let state $\omega_{T_{B\tilde{_{lA}}}}$ occur with probability $p_{B\tilde{_{lA}}}$, $\sum_{i=1}^{T_{B\tilde{_{lA}}}} p_{B\tilde{_{lA}}} = 1$. Thus, the random outcomes of when the remaining freight charges are received are defined on a discrete probability space $\{\Omega_{B\tilde{_{lA}}}, \mathcal{F}_{B\tilde{_{lA}}}, Prob_{B\tilde{_{lA}}}\}$ where $\Omega_{B\tilde{_{lA}}} = \{\omega_{B\tilde{_{lA}}1},\ldots,\omega_{B\tilde{_{lA}}T_{B\tilde{_{lA}}}}\}$, $\mathcal{F}$ is a σ-field and $Prob_{B\tilde{_{lA}}}(\omega_{B\tilde{_{lA}}i}) = p_{B\tilde{_{lA}}i}$.

before the start of unloading, with a clause that goods could be used as collateral in case of failure-to-pay. If shippers accept this kind of contract, it would lower the risks for the carrier compared to Term A above. The shipper also signals through this that they are in a strong financial position and may attract more carriers interested in the job, which then may put them in a stronger negotiation position.

For further research, one can also investigate how to include risks related to late delivery penalties. This is a complex area that often involves legal proceedings in which it has to be determined who is to blame for the delays. Finally, each of the parties could also take out insurance against various risks and such knowledge could in principle also become integrated into mean-risk models.

3.7 Conclusions

The problem of optimal (average) ship speed from an economic perspective is a well-studied area in the maritime literature. Most of the existing studies in the tramp shipping literature either consider deterministic conditions or maximise expected profits. In this chapter we extend this literature by considering mean-risk models that can account for the differences in risk attitude of decision makers. The decision problem now naturally extends to include also the option for the decision maker to not accept the job under evaluation. While the models developed focus on the assessment of a single potential journey, they are ideally used when wanting to compare a set of potential journeys and select the one that best meets the particular decision maker's aptitude to risk.

In deciding on the speed of the ship, the models capture the trade-off between profits made from the current job, and the future profit potential when the ship completes the current job in the destination port. A fast speed means higher fuel consumption but the revenues of the current job arrive sooner (when paid on collect), and vice versa. The future profit potential depends on the attractiveness of the ship being in the destination port and the time when it becomes available for the next job. This trade-off is elegantly captured through application of the Net Present Value method introduced in Ge et al. (2021); the models in this paper extend this deterministic framework to a stochastic setting as to allow the study of risk-related aspects of decision making. We illustrated the method through both VaR and CVaR approaches. We also presented algorithms for finding optimal solutions to these models.

The two sources of randomness used in most of in this paper are (1) fuel consumption increases due to bad weather days, (2) daily earnings reflecting the profit potential in the destination port are drawn from a distribution. We believe these two sources of uncertainty are both very important in the decision process. We have proposed mechanisms to calculate values for (1) in Section 3.3.1.1 and (2) in Section 3.5.3. These methods have been chosen because of their simplicity; through further research these methods are likely to be improved, or replaced by better methods. However these methods themselves were not the focus of this paper; instead

the focus here is on demonstrating the impact of these sources of uncertainty on the decision making process and results.

The impact of uncertainty depends on the type of decision maker. The short-term models, on the one hand, can help those who need to manage the risk on the current journey primarily. The main source of uncertainty here is the impact of fuel consumption. The impact from the future profit potential is mainly through its expected value: a higher value will tend to speed up the ship, affecting its fuel consumption and risk impact from bad weather. Long-term models, on the other hand, can serve organisations that are less bound to avoiding short-term losses on individual ships and journeys: they can use long-term expected profitability goals for their risk assessments. The whole distribution of the future profit potential could impact the acceptance of a job; its mean affecting the speed on the job, while bad weather forecasts will lower speed values.

The nature of the solutions returned by the mean-risk optimisation models captures some important aspects of real-life decision making under risk. Models that do not include risk recommend the job that has the highest expected profit (or NPV), but may also carry too much risk. If things go well, undertaking the job will give the decision maker a high profit. However, operating a vessel in practice is full of uncertainties. The stochasticities and leading risks should be well considered before chasing the high profit. Our model provides a risk profile of NPV excluding and including FPP rather than an individual optimal solution. Results derived by our model can accommodate decision makers with various concerns about risk measures, risk tolerance levels, and profit targets.

The models developed have certain limitations that point towards fruitful avenues for further research. Uncertainties during the journey can be modelled in different ways with respect to not only weather impact but also, e.g., fuel price or ship maintenance conditions. The FPP characterisation should ideally be fine-tuned so as to better reflect port-specific and route-specific freight market data. In some markets, of e.g. dry bulk goods, seasonality will lead to the time-dependency of the FPP. As illustrated Section 3.6, the models lends themselves towards consideration of more specific payment and other contractual arrangements, and trustworthiness of parties – another important area of risk.

Chapter 4

A Framework of Markov Decision Processes for Economic Ship Routing and Scheduling Problems

Chapter 3 establishes the mean-risk optimisation models to include stochasticity at different dimensions in decision process and risk attitudes. In this chapter, we consider the additional complication that not all the information about stochasticity is well known at the beginning of the planning horizon, while on the other hand information updates do reduce uncertainty during the decision process. In this chapter, the dynamics of the information for fuel consumption rate, port congestion and FPP are modelled to be updated through the decision process. A framework of Markov decision processes (MDPs) for obtaining the optimal routes, waypoints and speeds is established.

Given the nature of sailing and the unique features of tramp shipping, the decision-maker who is the carrier in a shipping contract may face more uncertainties from the natural environment, port, and shipping market simultaneously. These uncertainties are mostly changing over time and will affect the arrival time or unloading time at the destination port, which may also cause a delay in delivery. This paper aims to develop a method of dynamic stochastic programming, more specifically, a framework of MDP to incorporate the stochasticities beyond and after terminating at the destination port, as well as the information updating through the decision process, for solving a ship routing and scheduling problem. In this study, the decision-maker expects to maximise the long-term profitability, which includes not only the profit obtainable from the current journey but also the profitability after termination. We employ the approach of Net Present Value (NPV) and exploit the Future Profit Potential (FPP) to represent profitability after completing the current journey. The model is established in 3D states that include the spatial and temporal constituents of the vessel and solved by the value iteration algorithm. Subsequently, a simulation-enhanced value iteration (SEVI) is proposed to generate the distribution profile of NPV in the short- and long-term for decision-makers with a variety of risk attitudes. Numerical

experiments show the methods proposed in this paper generate a higher NPV under a wide range of scenarios under risk. Experiments in reference to alternative delivery time-window offer insights into how to secure an ideal delivery time-window before reaching agreement with consideration of risk attitudes and long-term profitability.

4.1 Introduction

Ship Routing and Scheduling Problems (SRSPs) are a type of optimisation problem in shipping that aims to help the decision makers optimise sailing routes and schedules. Given the variety of shipping modes, vessels, contracts, cargoes to transport, etc., the model formulation of the problem could be different. For example, the problem concentrating on liner shipping generally aims to keep an ideal delivery frequency under certain contracts, payment terms, and time windows (Wang and Meng, 2012b). While, for tramp ships, decision-makers can either be the ship owner or the charterer involved in a time- or voyage-chartered contract. Decision makers are responsible for selecting profitable jobs and making decisions about sailing routes and speeds to maximise the profit or minimise the cost based on their will. Due to above flexibility during decision-making process, more uncertainties came along that will impact the cost, profit, and delivery time and finally influence the performance of optimal solutions in the real world.

Maritime transport and trade systems have faced challenges from the variety of uncertainties, that working singly or in combination, leading to increased volatility and risk in the shipping market. Tramp shipping market, which handles over 75 percent of cargo volumes in international maritime trade and usually deal with dry bulk cargo like coal, grains, and minerals. The performance of freight markets in tramp shipping is highly corresponding to the Baltic Dry Index (BDI) which measures the average cost of dry bulk material transportation across more than 23 routes (on Trade and Development). During last two years, BDI reached an over 13-year high of 5526 points at September of 2021, and fell to 538 points at February 2023 [12]. The fluctuation from bulk cargo freight markets not only impact the profitability for the current journey undertaken by the decision maker in tramp shipping, but also plays a vital role for future profitability that obtainable after completing the job at the destination port (Ge et al., 2021).

In addition to the volatility in freight markets, uncertainties during the sailing process and after calling at ports, such as dynamic weather conditions and fuel costs, and rising port congestion also cause the risk of delay and affect profitability (Fagerholt et al., 2010a; Alvarez et al., 2011; Schinas and Stefanakos, 2012; Magirou et al., 2015; Guan et al., 2017). The information about the above uncertainties is usually not well studied at the beginning of the journey but will become more clear over time. For example, oceanic weather conditions are considered the main factor that causes speed loss or a higher fuel consumption rate if keeping the same speed level (speed over ground) (Yu et al., 2017; Hinnenthal and Clauss, 2010). The prediction of oceanic weather conditions is 80 percent correct 7 days behind and will fall to 50 percent if it is 10 days behind. Directly using the weather predictions in an optimisation model to optimise routes and speeds for

[12] The data is collected from a public resource: https://tradingeconomics.com/commodity/baltic.

a tramp shipping journey, which usually takes more than a month, is unrealistic and inefficient. Similarly, in the estimation of port congestion and freight markets, updating the information through the decision process are likewise necessary.

With the vital role of tramp shipping in maritime trade as well as the nature of ever-changing stochasticities, considering the technique of stochastic dynamic programming has become requisite in solving Tramp Ship Routing and Scheduling Problems (TSRSPs). We propose a stochastic dynamic programming model that embraces an information updating procedure to optimise ship routing and scheduling. Decision makers aim to optimise the profitability in the long term, which distinguishes from maximising the profit (from the job undertaken), which represents the profitability in the short term and does not consider the potential profitability after terminating at the destination port. The job consists of a single-leg which starts from port A and ends at port B with a required delivery time window, which is a soft time window which could be negotiable when the scheduling is in advance the journey (Fagerholt, 2001). Delivery completed outside the time window will cause a late of delivery penalty, and possibly impact the profitability of the vessel as well as the business of the decision maker in the future (Nakandala et al., 2013).

To establish the framework of MDP for solving the TSRSPs proposed, preliminary work is demonstrated as follows step by step: 1. initialise the waypoints and routes based on the grand circle route between two ports into stages; 2. create 3D states backward from the termination states that are affiliated with the termination waypoint to the starting states that are affiliated with the starting waypoint. Each state includes the latitude, longitude, and time from the starting time of the decision process; 3. formulate the stochasticities, including oceanic weather conditions at all states, waiting time, and Future Profit Potential (FPP) at the destination port. The framework of MDP for TSRSPs is established afterwards, which integrates the space of 3D states, actions, likelihood, reward functions, and a continuously time-discounted rate. Subsequently, an adjusted value iteration algorithm is formulated to derive optimum solution for risk-neutral decision makers and a simulation-enhanced value iteration algorithm (SEVI) for decision makers have a variety of risk tolerance levels, profit target in short- or long-term.

The purpose of the proposed framework of MDP in solving TSRSPs is threefold. It provides feasibility to solve ship routing and scheduling problems that include stochasticities that are not only time-dependent but also need to be updated over time; it offers possibilities to take the decision makers' risk attitudes into account by extending the framework to a simulation-based decision-making problem. The risk performance of simulated NPV in the short- and long-term as well as the intuitive graphs are suggested rather than a single optimal solution; it develops a framework that is able to integrate other assumptions (structure of uncertainties, delivery time), objectives (maximise gross profit or minimise carbon emissions), or be applied to analyse the robustness of decisions under fluctuating fuel prices and freight rates.

The paper is structured as follows. Relevant studies are reviewed in Section 4.2. Preliminary works are prepared in Section 4.3 before moving forward to establish the framework of the MDP for TSRSPs. The stochasticities are formulated with the frequency of updating in Section

4.4. The framework of MDP is presented in Section 4.5. Value iteration and SEVI algorithms are proposed in Section 4.6. Numerical experiments are presented in Section 4.7. Section 4.8 provides discussions of conclusions and future research,

4.2 Literature review

In this section, we review the literature of dealing with the uncertainties in TSRSPs. In addition, we also review the literature of applying stochastic programming, dynamic programming, and stochastic dynamic programming in SRSPs.

Tramp shipping, as a shipping mode that is similar to taxi service for cargo, are more flexible in operations. The routing and scheduling problems in tramp shipping are dynamic and stochastic in nature (Christiansen and Fagerholt, 2014; Ksciuk et al., 2023). In previous studies, uncertainties are addressed for following aspects: (i) sailing times; (ii) weather conditions; (iii) freight markets; (iv) service times; and others.

For (i), the stochastic sailing time is usually modelled as a result of (ii) at different levels, which is also called as weather routing and scheduling problems (WRSPs). Zis et al. (2020) provides a thorough review about ship weather routing. Weather data including wind and wave is considered as uncertainties in WRSPs with an objective of minimising fuel consumption (Lo and McCord, 1998; Ballou et al., 2008; Du et al., 2015; Lu et al., 2015; Bentin et al., 2016; Perera and Soares, 2017); Skoglund et al. (2015) proves that including the uncertainties of weather conditions in weather routing problems can improves controlling the risk of delay; multi-objective technique is applied under a variety of oceanic weather conditions to compromise the fuel cost and risk of sailing safety (Krata and Szlapczynska, 2018; Zaccone et al., 2018), fuel consumption and time (Varelas et al., 2013; Vettor and Soares, 2016; Sidoti et al., 2016), or fuel consumption, time, and avoidance of insecure areas (Szlapczynska, 2015). Li et al. (2022b) proposes a budget-bounded robust model to reflect the uncertainty budget schemes in liner ship routing and scheduling problems. Azaron and Kianfar (2003) considers the variations of weather conditions in a continuous time Markov process. In the model presented in this paper, uncertainties of (i) and (ii) are considered together. Information about (ii) at different regions are represented by a prior distribution and will be incrementally revealed through the decision process. (ii) is the main resources that will cause an uncertain (i).

The uncertainties of (i) and (iv) are also considered together in some studies (Christiansen and Nygreen, 2005; Wang and Meng, 2012a; Agra et al., 2013). Additionally, (iv) receives more concerns in liner shipping compared to in the field of tramp shipping. Vessels in liner shipping attempt to leave enough transit time at ports to ensure the required delivery frequency or to complete the job within the time window. Although the application of this paper is set to tramp shipping, an uncertain service time at ports is also taken into account to face rising difficulties in unforeseen strikes, port congestion, and shortages of labours (on Trade and Development).

The fluctuation in (iii) could influence the profitability of a tramp ship twofold. Firstly, the freight rates of the journey vary with the demand and supply of transporting the type of cargo from one port (which is not necessarily the port where the vessel is currently) to another port. Transport demand is considered to be influenced by the spot market, the cargo, and the trade surplus of the cargo between ports. The transport supply, however, is determined by the status of the competition among similar types of tramp ships at the demand port. Secondly, FPP represents the potential profitability after accomplishing the job at the destination port. For a voyage-chartered vessel that should be returned at the initial port, there is no FPP that needs to be considered. For a time-chartered vessel, future profitability should be taken into account (Ge et al., 2021). Song et al. introduces a stochastic FPP when optimising the decision about job acceptance and economic travel time. In this paper, stochastic FPP is taken into account and performed as dynamic information that will be revealed over time. Besides, Lindstad et al. (2013) provides an analysis of vessel's speed under different levels of (ii) and (iii). Hwang et al. (2008) proposes to use model to reduce the variance of profit under a fluctuated spot markets.

In general, SRSPs and Speed Optimisation Problems (SOPs) are able to be formulated as Shortest Path Problems (SPPs), i.e. Fagerholt (2001) and Fagerholt et al. (2010b) use SPPS to minimise cost, sailing times, fuel consumption, or emissions. However, SPPs only work when information is well-known beforehand and deterministic. Otherwise, stochastic programming is required: Magirou et al. (2015) develops the freight rates in the freight market through a continuous time Markov chain model and optimises the sailing speed and operating sequence with an objective maximising profit; Wang et al. (2018a) uses approximation technique to optimise the sailing speed and bunker purchasing strategy under stochastic bunker price; Li et al. (2022a) applies a two-stage stochastic programming model for TSRSPs with uncertain cargo availability.

Some studies also consider applying dynamic programming when solving SRSPs. Forward dynamic programming is utilised in weather routing and scheduling problems for breaking the problem down into a series of simpler problem-solving steps (Wei and Zhou, 2012; Shao et al., 2012; Zaccone et al., 2018). Three-dimensional dynamic programming is considered in Wang et al. (2019) and Shin et al. (2020) for minimising either fuel consumption, cost, or emissions in WRSPs. We argue that the advantages of using dynamic programming in WRSPs and SRSPs are limited due to the fact that not all information can be well predicted, and some of them, i.e., 3D Dijkstra's algorithm, cannot deal with the negative function as it leads to a negative edge weight in the graph. Both limitations lead to the fact that these methods cannot be applied to solve the problem proposed in this paper.

More than one type of uncertainties are involved in the decision process of routing and scheduling for tramp ships. Most of the parameter values associated with these sources of uncertainties cannot be well known or estimated by the decision maker at the beginning of the planning horizon. It leads to sub-optimal solutions when the problem is formulated by deterministic models. In stochastic models they may be more accurately represented but now the issue is that

updated information will need to be integrated in the decision process. It thus requires a dynamic stochastic formulation, i.e. MDP with dynamic information updates, for the routing and scheduling optimisation models.

The contributions of this chapter are: (1) propose the framework of MDPs for solving the SRSPs in tramp shipping with uncertainties from oceanic weather conditions, port, and freight markets that are all updated in the decision system frequently; (2) incorporate the perspective of risk attitudes by introducing a SEVI that provides a distribution of NPV in the short- and long-term, both in an intuitive way or calculated by risk measures; and (3) consider soft delivery time-window as an alternative.

4.3 Preliminaries

Preliminary work is required before employing the MDP in further steps. Assume the vessel is prepared to undertake the voyage from port A to port B. There is no predefined route requested by the shipper or the contract. In other words, the decision maker could take any possible route as long as the voyage was completed by the stipulated delivery time at port B. The initialisation for waypoints and routes with the consideration of time, also known as ready to departure time, is called 3D ship routine and scheduling (Wei and Zhou, 2012; Wang et al., 2019). The ship's 2D state includes a spatial coordinate, as (x, y), while the ship's 3D state is denoted by (x, y, t), where t is the ship's ready to departure time.

The generation of 3D states for a journey between two ports requires following information: location of the departure port and the destination port, delivery time window stipulated by the contract, geographical environment of the possible sailing area, vessel's characteristics, and service rate of the ports. The process of generation starts from initialising possible sailing are and 2D states (waypoints) based on the great circle route from the departure port to the destination port (Fagerholt and Lindstad, 2007). To include the uncertainty of waiting time at the ports, we expand the waypoint of a port to 2 waypoints, depends on its role in the journey. For the departure port A, two waypoints are developed to represent the state of the vessel 'at port A before loading' and 'at port A after loading and ready to departure'. These two waypoints have the same 2D state, which is $[x_A, y_A]$. Similarly, for the destination port B, two waypoints are developed to represent the state of the vessel 'at port B before berthing' and 'at port B after completing the delivery'. Both of the waypoints have the same 2D state $[x_B, y_B]$[13].

For each of waypoint on the great circle route, a line that is vertical relative to the great circle route could be drawn. Then a series of waypoints on these vertical lines could be determined. An initialised sailing area and waypoints are drawn and shown in Figure 6 as follows:

[13]To distinguish the 3D states for these waypoints defined for the ports, we define the 3D states in the order in which they actually occur. The state that occurred first has no superscript "'" in its temporal vector. For example, $[x_A, y_A, t_A]$ denotes the 3D state for the waypoint 'at port A before loading' and $[x_A, y_A, t_{A'}]$ denotes the 3D state for the waypoint 'at port A after loading and ready to departure'.

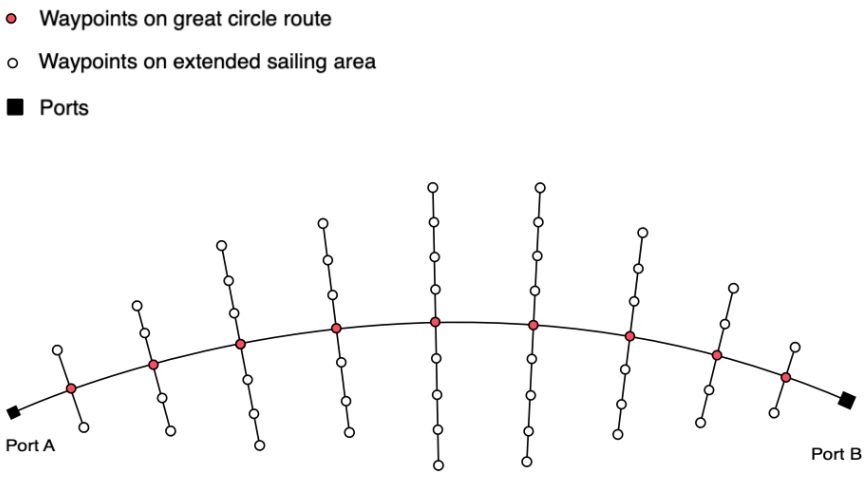

FIGURE 6: Initialisation of possible sailing area and waypoints based on the great circle route between port A and port B

After generating all possible 2D states of the journey, 3D states could be generated by discretising the 2D states backward. Assume the delivery time window is denoted by $[T^{ED}, T^{LD}]$, where T^{ED} is the earliest delivery time by contract, and T^{LD} is the negotiated latest delivery time. The latest late of delivery time is denoted by T^{LLD} [14]. Thus, if the temporal discretisation is established on a standard of one day, possible 3D states for the destination port, which is also the last waypoint on the great circle route, could be written as $[x_B, y_B, t_{B'}]$, where $t_{B'} = T^{ED}, T^{ED}+1, \ldots, T^{LLD}$ [15]. The time window for the waypoint of the destination port 'before berthing' is considered as $[T^{ED} - \overline{T^{w_B}}, T^{LLD}]$ where $\overline{T^{w_B}}$ denotes the maximum of estimation for waiting time at port B. Thus, 3D states for the waypoint could be written as $[x_B, y_B, t_B]$, where $t_B = T^{ED} - \overline{T^{w_B}}, T^{ED} - \overline{T^{w_B}} + 1, \ldots, T^{LLD}$.

The temporal discretisation of the destination port shows that the earliest ready to departure time and the latest ready to departure time of the target waypoint should be calculated before applying a temporal precision to generate the 3D states. For each of waypoints except the destination port and the departure port, we define for the waypoint w, its ready to departure time window is denoted by $[T^{EDp}, T^{LDp}]$, where $T_w^{EDp} = \min_{\forall w'}\{T_{w'}^{EDp} - d_{ww'}/24 \cdot v_{max}\}$, which is the minimum among all possible waypoints at the next stage substract the shortest travelling time between w and w'. And, $T^{LDp} = \max_{\forall w'}\{T_{w'}^{LDp} - d_{ww'}/24 \cdot v_{min}\}$ is the maximum among all possible waypoints at the next stage substract the longest travelling time between w and w'. Finally, possible 3D states for the waypoint w could be written as $[x_w, y_w, t_w]$, where $t_w = T^{EDp}, T^{EDp}+1, \ldots, T^{LDp}$. The temporal discretisation follows above mentioned process go backward from the waypoint of the destination port until the waypoint of the departure port. For the waypoint of the departure port A 'ready to departure', discretised 3D states could be

[14] The role of the latest late delivery time in a contract is to allow the delay when it is not outside a certain period. Relevant terms and conditions about latest late delivery time also explain the liability and penalty under all considered circumstances. Deliveries beyond the latest delivery time are usually not acceptable.

[15] The delivery time by contract, and the latest late delivery time are considered all as calendar days.

written as $[x_A, y_A, t_{A'}]$, where $t_{A'} = T^{EDp}, T^{EDp}+1, \ldots, T^{LDp}$. And for the waypoint of the departure port A 'before loading', discretised 3D states could be written as $[x_A, y_A, t_A]$, where $t_A = 0, 1, \ldots, T^{LDp}$. The lowest bound of the ready to departure time is restricted to 0 to avoid being negative.

We summarise the sailing process as a N stages decision process, where N denotes the number of waypoints on the great circle route, including two waypoints for the departure port A and the destination port B, separately. Define the series of waypoints at stage i, $i \in \{0, \ldots, N\}$ is denoted by P_{ij}, where $j \in \{0, \ldots, j(i)\}$. Then, the total number of waypoint for stage i is known by $j(i)+1$. After discretising all possible 3D states of the vessel based on the waypoints, the 3D states for each waypoint P_{ij} could be written as $[x_{P_{ij}}, y_{P_{ij}}, t_{P_{ij}}]$, where $t_{P_{ij}}$ is a number within the waypoint's defined time window. For the convenience of understanding, we write the waypoint at the departure port before loading, $[x_{P_{00}}, y_{P_{00}}, t_{P_{00}}]$, also as $[x_A, y_A, t_A]$; and write the waypoint at the departure port after loading and ready to departure $[x_{P_{10}}, y_{P_{10}}, t_{P_{10}}]$ also as $[x_A, y_A, t'_A]$. Similar to the 3D states derived from the two waypoints of the destination port B[16].

4.4 Stochasticity

Factors from various aspects are considered in this study with regard to their impacts on the decision-making process about T-SRSPs. Firstly, oceanic weather conditions consisting of winds, waves, and currents are acknowledged as the main reasons that cause additional resistance. The average speed at which a ship is propelled forward by consuming an equal amount of fuel per unit time varies under different weather conditions. The various average speeds will cause an unexpected travelling time towards the planned next waypoint. We attribute the uncertainty of the oceanic weather conditions to stochastic sailing time. Secondly, the uncertainty about potential profitability after terminating at destination port B is represented by the FPP. The FPP is time-sensitive and will be impacted by the delay in delivery. Finally, an uncertain port waiting time also contributes to the termination time, which will lead to different FPP and NPV in the long term. Possible situations that could potentially cause unusual waiting times at ports include port congestion, labour shortages at ports, and so on.

We introduce the above stochasticity as random variables in our model and update the observations of the stochasticity through the whole decision process. The formulation for the stochasticities is given in the following sections.

4.4.1 Oceanic weather conditions

The oceanic weather conditions are considered the main factor that impacts the ship's performance. There are a lot of studies that concentrate on the oceanic weather modelling in the area of marine meteorology (Zis et al., 2020). For the WRSPs and SRSPs, various weather conditions are considered the main reason to cause additional fuel consumption or increase the risk

[16] States that represent the vessel at port B before berthing, $[x_{P_{N-1,0}}, y_{P_{N-1,0}}, t_{P_{N-1,0}}]$ could be written by $[x_B, y_B, t_B]$; and the state of the vessel at port B after completing the delivery, $[x_{P_{N0}}, y_{P_{N0}}, t_{P_{N0}}]$, could be written by $[x_B, y_B, t'_B]$, too.

of delay for ships in liner shipping. Some studies show the influence of oceanic weather conditions could either be advantageous or hazardous to the ship performance[17]. On the side of time consumed for sailing from waypoint i to j, advantageous oceanic weather conditions may help the vessel travel 'faster' (speed on ground) when the same level of marine engine power was supplied. Meanwhile, hazardous weather conditions will cause a longer travelling time than normal weather conditions. We conclude the impact of various oceanic weather conditions are evaluated through a hidden process as shown in Figure 7:

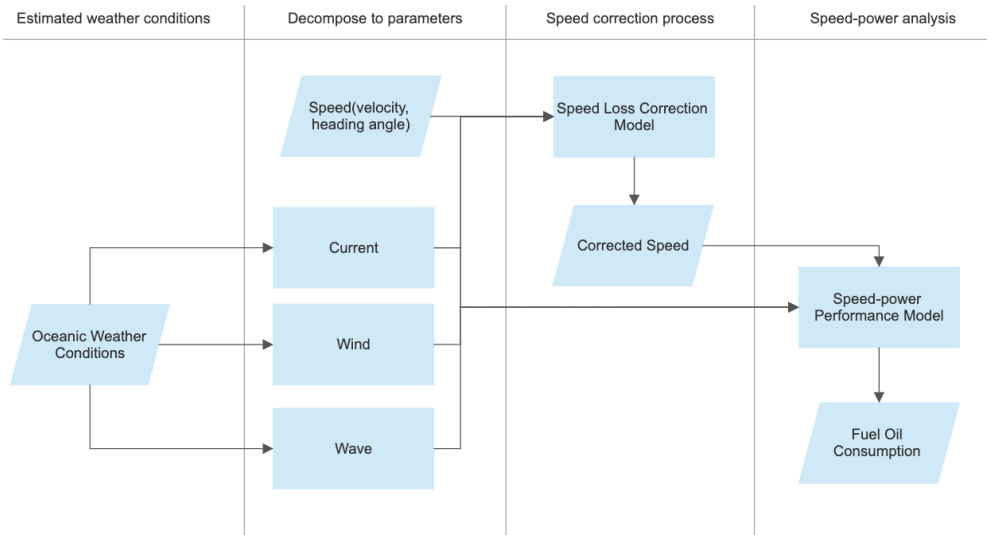

FIGURE 7: Interpretation from oceanic weather conditions to fuel oil consumption rate

As shown in Figure 7, the weather condition could be known either as a deterministic value or a distribution which depends on the assumptions of the problem. The data-set about weather conditions could be decomposed to wind, wave, current as a parameter vector W as follows:

$$W = ([H_s, T_z, S_w(H_s, T_z)], C, [V_{wu}, V_{wv}]), \tag{4.1}$$

where $[H_s, T_z, S_w(H_s, T_z)]$ denotes the coefficients about wave height, wave period, and wave spectrum, respectively. C denotes the coefficient of current. And $[V_{wu}, V_{wv}]$ are wind direction and velocity. Based on the speed loss model, a different speed through water v will be resulted under W due to the weather caused extra resistance. Here, we consider the oceanic weather conditions at various level will result a new travelling time. Assume the decision maker plans to let the vessel sail from state $[x_{P_{ij}}, y_{P_{ij}}, t_{P_{ij}}]$ to state $[x_{P_{i+1j'}}, y_{P_{i+1j'}}, t_{P_{i+1j'}}]$. The corresponding action is $[\overrightarrow{P_{ij}P_{i+1j'}}, t_{P_{i+1j'}} - t_{P_{ij}}]$. The average speed could be derived by:

$$v = L_{\overrightarrow{P_{ij}P_{i+1j'}}} / (t_{P_{i+1j'}} - t_{P_{ij}}), \tag{4.2}$$

where $L_{\overrightarrow{P_{ij}P_{i+1j'}}}$ is the length of the segment $P_{ij}P_{i+1j'}$. The average speed in (4.2) is an estimation when the ocean is assumed as the calm water. According to the speed-loss model illustrated, we

[17] Zis et al. (2020) explains that depending on the path it takes, the current could lead the ship's speed to increase or decrease.

summarise the effect of W on v can be interpreted by a coefficient k_W. Then, the average speed under weather condition W after considering the speed loss is denoted by v_W as follows:

$$v_W = k_W \cdot v. \tag{4.3}$$

Thus, for the same length of the segment $P_{ij}P_{i+1j'}$, when a different weather condition occurs, the actual travelling time consumed by the vessel will differ from the time previously planned to be used. The actual arrival time at waypoint $[x_{P_{i+1j'}}, y_{P_{i+1j'}}]$ under W could be obtained by:

$$t_{P_{i+1j'}} = L_{\overrightarrow{P_{ij}P_{i+1j'}}}/v_w + t_{P_{ij}}, \tag{4.4}$$

where v_w could be found in (4.3).

For a deterministic observation of W, a fixed travelling time $t_{P_{i+1j'}}$ between two waypoints can be estimated. However, the laden leg of a tramp ship usually takes more than a month while the oceanic weather cannot be predicted for such long period. It results that the information about oceanic weather conditions along the whole journey is hardly to be known as a deterministic observation. Wang et al. (2019) updates the weather information as an observation each time when the vessel approaches a new waypoint. We propose the information about oceanic weather conditions could be described by a random variable with its probability distribution. The random variable could either be formulated to be discrete or continuous.

Also, we consider to update the information about oceanic weather conditions based on an updating frequency. The updating frequency needs to be determined according to the stipulated delivery time of the voyage, the number of stages N, and the accuracy of the weather prediction. Assume the updating frequency for the weather is defined as u_W, $u_W \in \{1, 2, \ldots, N\}$. The information about weather will be updated when the vessel approaches stage $u_W, 2 \cdot u_W, \ldots,$ until the end of the voyage which terminates at stage N. The information set includes historical data for all states at approached stages, and distributions of oceanic weather conditions for all states at stages in the rest of the voyage. Define the newest updated information set about oceanic weather conditions at state $s = [x_{P_{ij}}, y_{P_{ij}}, t_{P_{ij}}]$ as $\mathbb{I}_W(s)$, which could be written as:

$$\mathbb{I}_W(s) = \mathbb{I}_W(s)^{past} \oplus \mathbb{I}_W(s)^{future}, \tag{4.5}$$

where $\oplus$ means to concatenate two matrices as two rows of a matrix. Here, $\mathbb{I}_W(s)^{past}$ denotes the matrix which includes certain information about oceanic weather conditions for states at the approached stages, or states those time elements are greater than $t_{P_{ij}}$. In numerical experiments, we also put 'infeasible states' into $\mathbb{I}_W(s)^{past}$. The 'infeasible states' indicates those states that

are infeasible to be approached according to the current state $s = [x_{P_{ij}}, y_{P_{ij}}, t_{P_{ij}}]$.

$$\mathbb{I}_W(s)^{past} = \begin{bmatrix} s_1^{past} & k_W(s_1^{past}) & 1 \\ \vdots & \vdots & \vdots \\ s_{N_{past}}^{past} & k_W(s_{N_{past}}^{past}) & 1 \end{bmatrix}, \tag{4.6}$$

where columns of $\mathbb{I}_W(s)^{past}$ denote the past state itself, its weather coefficient, and its probability, respectively. The total number of past states is denoted by N_{past}. Then, $\mathbb{I}_W(s)^{future}$ denotes the information set about oceanic weather conditions for the rest of the states, which could be written as:

$$\mathbb{I}_W(s)^{future} = \begin{bmatrix} s_1^{future} & k_W(s_1^{future}) & f_W(s_1^{future}) \\ \vdots & \vdots & \vdots \\ s_{N_{future}}^{future} & k_W(s_{N_{future}}^{future}) & f_W(s_{N_{future}}^{future}) \end{bmatrix}, \tag{4.7}$$

where the first column and the second column of $\mathbb{I}_W(s)^{future}$ denote the future state itself, its weather coefficient, and its probability density function (PDF) $f_W(\cdot)$, respectively. The total number of future states is denoted by N_{future}. Assume for a future state $s_j^{future}, j \in \{1, \ldots, N_{future}\}$, its weather coefficient is described by a random variable $k_W(s_j^{future})$. For a discretely distributed $k_W(s_j^{future})$, define its sample space as $\Omega_{k_W(s_j^{future})}$. Then for $\omega \in \Omega_{k_W(s_j^{future})}$, its probability is given by $Prob(\omega, k_W(s_j^{future})) = f_W(\omega | k_W(s_j^{future}))$. There needs to be as follows:

$$\sum_{\forall \omega \in \Omega_{k_W(s_j^{future})}} Prob(\omega, k_W(s_j^{future})) \equiv 1. \tag{4.8}$$

For a continuously distributed $k_W(s_j^{future})$, there needs to be as follows:

$$\int_{-\infty}^{+\infty} f_W(k_W(u | s_j^{future}))\mathrm{d}u \equiv 1. \tag{4.9}$$

4.4.2 Waiting time

The waiting time for the harbour is not a definite value. On the contrary, port operations, staff allocation, supply and demand of transported commodities, fuel prices, etc. may cause fluctuations in port waiting times. When the model introduces a deterministic waiting time, fluctuations in the port time may cause delay of delivery, especially when a strict time window is given, and finally result in losses. In this case, even if the ship sails at the planned optimal speed and path and arrives at the destination port nearby on time, a longer waiting time than the estimation can lead to a delay of delivery.

Thus, we introduce the waiting time at the port as a random variable. For a voyage from port A to port B, waiting time at port A is known as a certain value as the vessel starts the journey at port A from the start of the decision process. Whereas the waiting time at port B could change during the decision process and is time-dependent. Define the waiting time for the vessel at state $s = [x_B, y_B, t_B]$ as a random variable $T^{w_B}(s)$, which could either be discretely distributed or continuously distributed. For a discretely distributed $T^{w_B}(s)$, the PDF of $T^{w_B}(s)$ is defined by $f_Q(T^{w_B}(s))$. Define its sample space as $\Omega_{T^{w_B}(s)}$. Then for $\omega \in \Omega_{T^{w_B}(s)}$, its probability is given by $Prob(\omega, T^{w_B}(s)) = f_Q(\omega | T^{w_B}(s))$. There needs to be as follows:

$$\sum_{\forall \omega \in \Omega_{T^{w_B}(s)}} Prob(\omega, T^{w_B}(s))) \equiv 1. \tag{4.10}$$

For a continuously distributed T^{w_B}, there needs to be as follows:

$$\int_{-\infty}^{+\infty} f_Q(T^{w_B}(s)))\mathrm{d}u \equiv 1. \tag{4.11}$$

The PDF of a continuously distributed T^{w_B} is defined by:

$$Prob(a < T^{w_B}(s) \leq b) = F_Q(b) - F_Q(a), \quad a < b, \tag{4.12}$$

where F_Q denotes the cumulative distribution function (CDF) of $T^{w_B}(s)$. Similar to the information updating process for the oceanic weather conditions, the knowledge of estimated waiting time at port B will be updated along the decision process. Define the updating frequency for the waiting time as u_{Q_B}, $u_{Q_B} \in \{1, 2, \ldots, N\}$. The information about weather will be updated when the vessel approaches stage $u_{Q_B}, 2 \cdot u_{Q_B}, \ldots$, until the waiting time at port B becomes a well known information, in other words, could be observed, at stage N.

4.4.3 FPP

To describe the uncertainty about the future profit potential after arriving at the destination port, a stochastic dynamic FPP is introduced. Compared to the oceanic weather conditions and waiting times, FPP plays the role of strategic planning rather than day-to-day planning. When FPP is high, decision makers seeking long-term profitability prefer to embark on the voyage. In such a case, the short-term NPV and ocean weather conditions have a small impact on the decision-making process about job acceptance, while the actual sailing routes and speeds may be disturbed. Examination of such scenarios had been proved in Chapter 3.

Define the daily value of the FPP G_0 (USD) corresponds to a random variable αG_0 (USD/-day), which is formulated as state dependent random variable. When the vessel is at state $s = [x_B, y_B, t'_B]$, define the daily value of FPP as a random variable $\alpha G_0(s)$ which could either be discretely distributed or continuously distributed. For a discretely distributed $\alpha G_0(s)$, the PDF of $\alpha G_0(s)$ is defined by $f_{\mathrm{FPP}}(\alpha G_0(s))$. Define its sample space as $\Omega_{\alpha G_0(s)}$. Then for $\omega \in \Omega_{\alpha G_0(s)}$, its probability is given by $Prob(\omega, \alpha G_0(s)) = f_{\mathrm{FPP}}(\omega | \alpha G_0(s))$. There needs to

be as follows:

$$\sum_{\forall \omega \in \Omega_{\alpha G_0(s)}} Prob(\omega, \alpha G_0(s))) \equiv 1. \tag{4.13}$$

For a continuously distributed $\alpha G_0(s)$, there needs to be as follows:

$$\int_{-\infty}^{+\infty} f_{\text{FPP}}(\alpha G_0(s)))\mathrm{d}u \equiv 1. \tag{4.14}$$

The PDF of a continuously distributed $\alpha G_0(s)$ is defined by:

$$Prob(a \leq \alpha G_0(s) \leq b) = F_{\text{FPP}}(b) - F_{\text{FPP}}(a), \quad a < b, \tag{4.15}$$

where F_{FPP} denotes the CDF of $\alpha G_0(s)$. Along the decision-making process, knowledge of the estimated daily value of the FPP G_0 at port B will be updated, much to the information updating procedure for oceanic weather conditions and waiting time at Section 4.4.1-4.4.2. Given the updating frequency for the αG_0 as u_{FPP_B}, $u_{\text{FPP}_B} \in \{1, 2, \ldots, N\}$. The information about the FPP will be updated when the vessel approaches stage $u_{\text{FPP}_B}, 2 \cdot u_{\text{FPP}_B}, \ldots$, until the FPP at port B becomes a well known information, in other words, could be observed, at stage N.

The PDF of αG_0 is defined as:

$$Prob(a < \alpha G_0 \leq b) = F_{\alpha G_0}(b) - F_{\alpha G_0}(a), \quad a < b, \tag{4.16}$$

where $F_{\alpha G_0}$ denotes the CDF of αG_0.

Because of the time discretisation for states, continuous waiting time is not able to be employed in the further model establishments unless the adjustment of time, i.e. rounding up or discretising the distribution of waiting time. In the following, we will model the MDPs under the assumption that the FPP is continuously distributed, the waiting time is discretely distributed, and the oceanic weather conditions are discretely distributed. It is worth noting that since the distribution of FPP only involves the computation of the value function in the termination stage, the continuous property of its distribution does not conflict with the time discretisation of the whole model. A discussion of this can be found in Section 4.6.

4.5 Markov Decision Processes and decision makers

4.5.1 A framework of MDPs

Given the problem described in Section 4.3, we are able to formulate a framework of MDP in this section. The MDP is defined by $\mathcal{M} = \langle \mathbf{S}, \mathbf{A}, \mathbf{L}, R, \alpha \rangle$. For any state s in the state set $\mathbf{S}$, there is $s = [x, y, t]$. The state includes the longitude x, latitude y and time t. For a voyage with distinct departure port A, destination port B, vessel characteristics and contract, waypoints and states could be initialised by following the discretisation procedures in Section 4.3. Assume the

decision process was divided into N stages, the set of states is defined by:

$$\mathbf{S} = \bigcup_{i=0}^{N} \bigcup_{j=0}^{j(i)} S_{P_{ij}}, \tag{4.17}$$

where $S_{P_{ij}}$ denotes the set of states that derived by the the waypoint P_{ij}. As explained earlier, $i = 0$, $i = 1$, $i = N-1$ and $i = N$ indicate state $[x_A, y_A, t_A]$, $[x_A, y_A, t'_A]$, $[x_B, y_B, t_B]$ and $[x_B, y_B, t'_B]$, respectively. The set of actions $\mathbf{A}$ consists of the next state planned to be reached from the current state. Since the defined state consists of both spatial and temporal elements, an action in the action set consists of the following target waypoint in relation to the current waypoint geographically, and the time planned to be taken to reach the following target waypoint. Define the action as $a = [\theta_x, \theta_y, \Delta t]$, where θ_x and θ_y denote the geographical relation between current state s and the following target waypoint s'. The time planned for sailing from s to s' is denoted by Δt.

Actions are required to be undertaken when the vessel is at stage $1, \ldots, N-2$. If the vessel is at stage 0 or stage $N-1$, only a result of waiting time will be seen. Thus, the action set $\mathbf{A}$ is defined by:

$$\mathbf{A} = \bigcup_{i=1}^{N-2} \bigcup_{j=0}^{j(i)} A_{P_{ij}}, \tag{4.18}$$

where $A_{P_{ij}}$ denotes the set of actions for the waypoint P_{ij}.

The likelihood space is denoted by $\mathbf{L}$ which includes the stochasticity about oceanic weather conditions, waiting time and FPP. Define the likelihood space as follows:

$$\mathbf{L} = \bigcup_{i=0}^{N} \bigcup_{j=0}^{j(i)} \bigcup_{\forall s \in S_{P_{ij}}} L(s), \tag{4.19}$$

where $L(s) = \{\mathbb{I}_W(s), T^{W_B}(s), \alpha G_0(s)\}$ indicates the likelihood space for a state s in state set $S_{P_{ij}}$ for the waypoint P_{ij}. Each of the element in a likelihood space $L(s)$ plays a role as transition probability matrix as in traditional MDPs. Assume the current state of the vessel is $s = [x_{P_{ij}}, y_{P_{ij}}, t_{P_{ij}}]$, let $i = 1, \ldots, N-2$. And the likelihood function about oceanic weather conditions is known as $\mathbb{I}_W(s)$, see (4.5)-(4.7). Assume the decision maker takes a, $a = [\theta_x, \theta_y, \Delta t]$ defined in the action set $\mathbf{A}$. Then the following target waypoint is determined, while the time consumed to reach the waypoint is probabilistic and could be estimated through the likelihood space. Let $s' = [x', y', t']$ denotes the next state, there should be $x' = x + \theta_x$ and $y' = y + \theta_y$. Azaron and Kianfar (2003) proposes the transition time is also a function of the environmental variable of the nodes (states). Here, we consider the possible t' and its corresponding probability could be found by applying the information set about oceanic weather conditions as follows:

$$\hat{\Delta t} = \tilde{k_W}([x', y'] | [x, y], s) \cdot \Delta t, \tag{4.20}$$

where $\tilde{k_W}([x',y']|[x,y],s)$ indicates the approximately coefficient of weather effect between waypoint $[x,y]$ and $[x',y']$ for an information set $\mathbb{I}_W(s)$, which is updated at state s. The formula of $\tilde{k_W}(\cdot)$ is given by: $\tilde{k_W}([x',y']|[x,y],s) = (k_W([x,y]|s) + (k_W([x',y']|s))/2$.

$$Prob(\hat{\Delta t}) = f_W(k_W([x',y']|s)), \tag{4.21}$$

where $f_W(k_W([x',y']|s))$ could be found in $\mathbb{I}_W(s)$. Thus, possible next states and related probabilities can be concluded as:

$$\langle s', Prob(s')\rangle = \langle [x',y',t+\hat{\Delta t}], Prob(\hat{\Delta t})\rangle. \tag{4.22}$$

When the vessel is at stage $N-1$, there is no action about sailing required to be undertaken, and the stochasticity of waiting time will get the vessel transit from state $s = [x_B, y_B, t_B]$ to $s' = [x_B, y_B, t'_B]$, where t'_B is probabilistic and depends on $T^{W_B}(s)$. Possible next states and related probabilities can be concluded as:

$$\langle s', Prob(s')\rangle = \langle [x_B, y_B, t_B+\omega], Prob(\omega, T^{W_B}(s))\rangle, \quad \omega \in \Omega_{T^{W_B}(s)}. \tag{4.23}$$

And for the likelihood space about FPP, it will not transfer the vessel's state, such as the oceanic weather condition or waiting time at the destination port. We assume the FPP is involved in computing the reward function.

In conventional MDPs, the reward function is formulated to evaluate the direct benefits, costs, or contributions related to certain decision moments, where the reward function could be either depends on states or the state-action pair (Puterman, 2014). The discount factor is introduced to distinguish the instant reward and future reward. Specifically, a discount factor smaller than 1 could improve the convergence for certain algorithms, or for a MDP defined on infinite time horizon. In this framework of MDPs, we assume the reward function is defined on the state-action-state pair $R : \mathbf{S} \times \mathbf{A} \times \mathbf{S} \to \mathbb{R}$ on a finite time horizon. The reward of transferring from state s to state s' by taking action a will be denoted by $R(s,a,s')$. The discount factor α performs as the continuous interest rate corresponding to the limit length zero. It allows the reward function and cumulative reward to be calculated as time-discounted rather than stage-discounted [18].

The reward function is applied to calculate net present value (NPV) during each stage by applying a discount factor α back to the start time of the stage. Assume the vessel was at state s and transferred to state s' by taking action a. Cash flows happened during this transition process are denoted by a cash flow function $\mathrm{CF}(\tau)$, where τ indicates the time consumed in the transition. Then, the reward function is calculated by:

$$\mathrm{R}(s,a,s') = \int_0^{\tau} \mathrm{CF}(\sigma)\cdot e^{-\alpha\sigma}\mathrm{d}\sigma. \tag{4.24}$$

[18] The discount rate in conventional MDPs could also be considered time discounted or approximately time discounted when the time consumed at each stage is equivalent.

Specifically, the structure of cash flows in a laden leg for tramp ships is shown in Figure 8. The cash-flow structures also depend on on the assumptions of bunkering strategies, payment of delivery, late delivery penalty, etc. In this paper, we assume fuel costs are calculated based on the bunker price at the bunkering time at the departure port A. The delivery fee will be paid on time after the completion of unloading at the destination port. Delivery on time is not obligatory. A late of delivery penalty and possible demurrage fees will be fined after assigning blame according to the terms and conditions associated with the contract. Meanwhile, we formulate the FPP will be influenced by the late of delivery due to the on-time performance is considered as a factor which influence the charterer's reputation. Relevant discussions about the impact of late of delivery and FPP on decisions about ship's routing and scheduling can be found in Section 4.7.

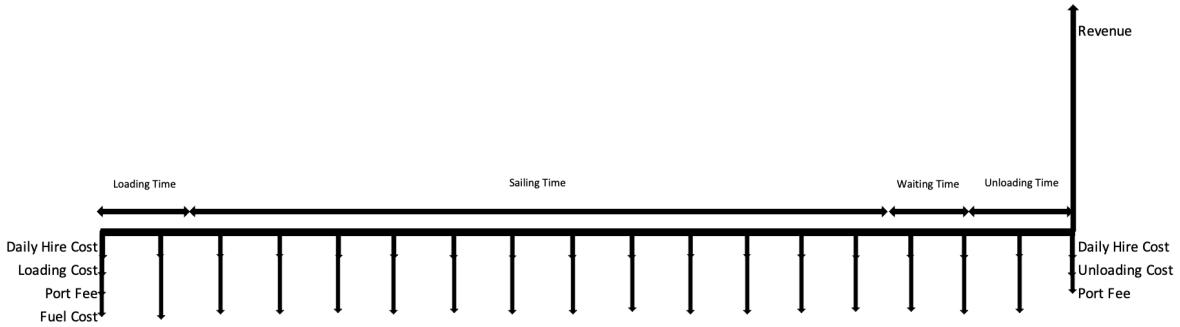

FIGURE 8: Timeline of cash-flows for a laden leg

For the structure of cash-flows shown in Figure 8, the reward function (4.24) could be written more specifically for loading process, sailing process and unloading process. For the transition from initial state $s = [x_A, y_A, t_A]$ to state $s' = [x_A, y_A, t'_A]$ which indicates the vessel is at port A ready to departure, no action was required to be undertaken. The reward function is defined by:

$$\mathrm{R}(s = [x_A, y_A, t_A], a = \varnothing, s' = [x_A, y_A, t'_A]) = -\int_{t_A}^{t'_A} f^{\mathrm{TCH}} \cdot e^{-\alpha\sigma} \mathrm{d}\sigma - C^l - \mathrm{PF}^A, \quad (4.25)$$

where f^{TCH} denotes the daily hire rate, C^l denotes the loading cost, and PF^A denotes the port fees at port A. After the departure from port A, the vessel starts the sailing. For the transition from state $s = [x_{P_{ij}}, y_{P_{ij}}, t_{P_{ij}}]$ to state $s' = [x_{P_{i+1,j'}}, y_{P_{i+1,j'}}, t_{P_{i+1,j'}}]$ by taking action $a = [\theta_x, \theta_y, \Delta t]$, where $i = 1, \ldots, N-2$, the reward function is defined by:

$$\mathrm{R}(s = [x_{P_{ij}}, y_{P_{ij}}, t_{P_{ij}}], a = [\theta_x, \theta_y, \Delta t], s' = [x_{P_{i+1,j'}}, y_{P_{i+1,j'}}, t_{P_{i+1,j'}}]) = \quad (4.26)$$

$$-\int_{t_{P_{ij}}}^{t_{P_{i+1,j'}}} f^{\mathrm{TCH}} \cdot e^{-\alpha\sigma} \mathrm{d}\sigma - C^f (t_{P_{i+1,j'}} - t_{P_{ij}}) \cdot e^{\alpha t_{P_{ij}}}, \quad (4.27)$$

The 'adverse' time discounted $e^{\alpha t_{P_{ij}}}$ is for calculating the fuel cost according to the bunkering time, rather than the consuming time. As we assume the fuel cost has been paid as a lump sum

at port A. The fuel cost $C^f(t)$ is a function of time given as follows:

$$C^f(t) = c^f \cdot f(v, w), \tag{4.28}$$

where c^f indicates the unit fuel price, and $f(v, w)$ is the fuel consumption function introduced by Psaraftis and Kontovas (2014).

$$f(v, w) = k \cdot (p + v^g)(w + A)^h, \tag{4.29}$$

where v denotes the average sailing speed, w denotes the deadweight tonnage carried. A denotes the lightweight tonnage of the ship, while the values of the parameters p, g, h depend on the ship's characteristics and its condition. The average speed v here is calculated by the sailing distance divided by the actual sailing time. Let $S(P_{ij}P_{i+1,j'})$ denotes the distance between waypoint P_{ij} and $P_{i+1,j'}$. Then the average speed v is:

$$v = S(P_{ij}P_{i+1,j'})/(24 \cdot (t_{P_{i+1,j'}} - t_{P_{ij}})). \tag{4.30}$$

Lastly, for the transition from state $s = [x_B, y_B, t_B]$ to state $s' = [x_B, y_B, t'_B]$, no action was required to be undertaken. The reward function is defined by:

$$\begin{aligned} \mathrm{R}(s = [x_B, y_B, t_B], a = \varnothing, s' = [x_B, y_B, t'_B]) = \quad & -\int_{t_B}^{t'_B} f^{\mathrm{TCH}} \cdot e^{-\alpha\sigma} \mathrm{d}\sigma \\ & +(R - C^u - \mathrm{PF}^B) \cdot e^{-\alpha(t'_B - t_B)}. \end{aligned} \tag{4.31}$$

where R denotes the total revenue, C^u denotes the unloading cost, and PF^B denotes the port fees at port B. The notation of symbols in the framework of MDPs is concluded in Table 12 as follows:

4.5.2 Decision makers

To distinguish decision makers with different risk attitudes, define the risk level as R, and the profit target as μ. The profit target could be defined either for short-term profit or long-term profit, equivalent to, NPV excluding the FPP (h) or NPV including the FPP (H). Compared to risk-neutral decision makers, we suppose decision makers who are risk-averse have a lower risk tolerance level for a certain profit target or cost budget. However, the concept of being risk-averse is relative. We can assume that a decision maker is more risk-averse than another decision maker when they face the same decision problem. But it is difficult to generally define the risk attitudes of this decision maker when other decision problems are taken into account. Meanwhile, the object of being risk-averse may differ among decision makers.

Thus, two types of risk-averse decision makers will be discussed in this section. The first type is introduced as risk-averse in short-term profitability (*Averse-short*), and the other type as risk-averse for long-term profitability (*Averse-long*) [19]

TABLE 12: Notation of symbols in the framework of MDPs for T-SRSPs

Symbol	Definition
$\mathcal{M}$	Markov decision process, $\mathcal{M} = \langle \mathbf{S}, \mathbf{A}, \mathbf{L}, R, \alpha \rangle$
$\mathbf{S}$	Discrete state space $\mathbf{S}$ is composed by the set of states $S_{P_{ij}}$ derived by the waypoint P_{ij}. Each state $s = [x, y, t]$ in a set of states $S_{P_{ij}}$ is defined by longitude x, latitude y and time t. See (4.17).
$\mathbf{A}$	Discrete action space $\mathbf{A}$ is composed by the set of actions $A_{P_{ij}}$ derived by the waypoint P_{ij}. Each action $a = [\theta_x, \theta_y, \Delta t]$ in a set of states $A_{P_{ij}}$ is defined by the geographical relation between current state s and the following target waypint s' denoted by θ_x and θ_y, and the time planned for sailing from s to s' denoted by Δt. See (4.18).
$\mathbf{L}$	Likelihood space $\mathbf{L}$ is composed by the set of likelihood space $L(s)$ for a state s, where $L(s) = \{\mathbb{I}_W(s), T^{W_B}(s), \alpha G_0(s)\}$ includes the stochasticity of oceanic weather conditions, waiting time and FPP for state s. See (4.19) - (4.23).
$\mathrm{R}(s, a, s')$	Reward function which computes the cash-flow functions led by transferring from state s to state s' by taking action a at a discount rate α. Formulas of $\mathrm{R}(s, a, s')$ at different stages are given in (4.24)-(4.31).
$\mathrm{Q}(s, a)$	Action-value function computes the expected value of all possible results lead by taking action a at state s. See (4.37).
$\mathrm{V}(s)$	Value function for state s which is the maximum of all action-value functions $Q(s, a)$ for the state s and associated action a. Formulas of $\mathrm{V(s)}$ at different stages are given in (4.32), (4.34), (4.38), and (4.40).
$\mathrm{V}^*(s)$	The maximum of value function for states s at the stage. Formulas of $\mathrm{V}^*(s)$ at different stages are given in (4.33), (4.36), (4.39), (4.42).
ψ	Policy $\psi = (\psi_0, \ldots, \psi_{N-1})$ is defined by a sequence of the policies of stage i from 0 to $N-1$.
ψ^*	Policy ψ is optimal if and only if at all stages it satisfies (4.43).
H^*	The expected NPV including FPP at the destination port after applying the optimal policy ψ^*.
h^*	The expected obtained NPV from completing the voyage after applying the optimal policy ψ^*.

4.6 Algorithms

The value iteration algorithm and SEVI are introduced to solve the MDP with updated information. Methods are applicable to provide decision-makers with a variety of risk attitudes to intuitively observe the distribution of NPV, either in the short- or long-term.

4.6.1 Value iteration algorithm

After establishing the framework for the MDPs, we propose to use the value iteration algorithm, also known as Backward induction algorithm to solve the problem. The value iteration algorithm is one of the basic dynamic programming algorithms used to determine the optimum strategy for a Markov decision process. The optimum strategy is recursively selected by taking an action at a state at each stage that gives the maximum of expected rewards attributed to action at this

state and the discounted maximum of the discounted accumulative reward for the next decision stage.

Thus, following up the way of finding the optimum strategy, we start from the the terminal stage N. Set the current stage in iteration as $i = N$, the value function for states $s \in S_{P_{Nj(N)}}$ is given by the expected value of the FPP:

$$V(s) = \mathbb{E}[\alpha G_0(s)], \quad s = [x_B, y_B, t'_B], \quad \text{and} \quad s \in S_{P_{Nj(N)}}. \tag{4.32}$$

The maximum of value function for states at stage N is given by:

$$V^*(s) = \max_{\forall s \in S_{P_{Nj(N)}}} V(s),. \tag{4.33}$$

As no action is required to be undertaken during the transition from stage $N-1$ to N, the value function for state at stage $i = N-1$ should be calculated by:

$$V(s) = \sum_{\forall s' \in S_{P_{Nj(N)}}} [\mathrm{R}(s, \varnothing, s') \cdot Prob(t'_B - t_B, T^{w_B}(s)) + V(s') \cdot e^{-\alpha(t'_B - t_B)}], \tag{4.34}$$

$$\text{for} \quad s = [x_B, y_B, t_B], \quad s \in S_{P_{N-1,j(N-1)}}; \quad s' = [x_B, y_B, t'_B], \quad \text{and} \quad s' \in S_{P_{Nj(N)}}. \tag{4.35}$$

where $R(s, \varnothing, s')$ refers to (4.31). The maximum of value function for states at stage $N-1$ is given by:

$$V^*(s) = \max_{\forall s \in S_{P_{N-1,j(N-1)}}} V(s). \tag{4.36}$$

For $i = N-2, \ldots, 1$, an action-value function is defined by:

$$\begin{aligned} Q(s_{P_{ij}}, a_{P_{ij}}) &= \textstyle\sum_{\forall s_{P_{i+1,j'}} \in S_{P_{i+1,j'}}} \mathbb{E}[\mathrm{R}(s_{P_{ij}}, a_{P_{ij}}, s_{P_{i+1,j'}}) + V(s_{P_{i+1,j'}}) \cdot e^{-\alpha(t_{P_{i+1,j'}} - t_{P_{ij}})}] \\ &= \textstyle\sum_{\forall s_{P_{i+1,j'}} \in S_{P_{i+1,j'}}} [\mathrm{R}(s_{P_{ij}}, a_{P_{ij}}, s_{P_{i+1,j'}}) \cdot Prob(t_{P_{i+1,j'}} - t_{P_{ij}}) + V(s_{P_{i+1,j'}}) \cdot e^{-\alpha(t_{P_{i+1,j'}} - t_{P_{ij}})}], \\ &\quad \text{for} \quad s_{P_{ij}} = [x_{P_{ij}}, y_{P_{ij}}, t_{P_{ij}}], \quad s_{P_{ij}} \in S_{P_{ij}}; \quad a_{P_{ij}} = [\theta_x, \theta_y, \Delta t], \quad \text{and} \quad a_{P_{ij}} \in A_{P_{ij}}. \end{aligned} \tag{4.37}$$

The action-value function represent an expected value of all possible results lead by taking action $a_{P_{ij}}$ at state $s_{P_{ij}}$. During the decision period $N-1$ to 1, the expectation is applied to the probability space of random oceanic weather conditions, see (4.37). The probability of having a weather condition which results the transition to $s_{P_{i+1,j'}}$ is denoted by $Prob(t_{P_{i+1,j'}} - t_{P_{ij}})$ or $Prob(\hat{\Delta}t)$, see (4.20)-(4.22). The value function is calculating by:

$$V(s_{P_{ij}}) = \max_{\forall a_{P_{ij}} \in A_{P_{ij}}} Q(s_{P_{ij}}, a_{P_{ij}}). \tag{4.38}$$

Then the optimum value function for states at stage i is given by:

$$V^*(s) = \max_{\forall s \in S_{P_{ij}}} V(s). \tag{4.39}$$

The value functions are recursively calculated for all states from stage $N-1$ to 1. Finally, the value function for states at stage $i = 0$ is given by:

$$V(s) = \sum_{\forall s' \in S_{P_{10}}} [\mathrm{R}(s, \varnothing, s') \cdot Prob(t'_A - t_A, T^{w_A}(s)) + V(s') \cdot e^{-\alpha(t'_A - t_A)}], \tag{4.40}$$

$$\text{for} \quad s = [x_A, y_A, t_A], \quad s \in S_{P_{00}}; \quad s' = [x_A, y_A, t'_A], \quad \text{and} \quad s' \in S_{P_{10}}. \tag{4.41}$$

where $\mathrm{R}(s, \varnothing, s')$ refers to (4.25). The maximum of value function for states at the initial stage 0 is given by:

$$V^*(s) = \max_{\forall s \in S_{P_{00}}} V(s). \tag{4.42}$$

So far, (4.32)-(4.25) shows how to compute the value function for all states using the Backward induction algorithm on a given certain probability space considered for an initialised problem, which includes all stochasticities considered in Section 4.4. It allows the decision maker to make decisions forward, from the initial stage 0 to the terminated stage N for a case where there are no new information inflows into the decision system [20]. For models that take into account the updating information set in the decision-making process, the optimum strategy cannot be determined by following the computed value functions. Instead, the problem needs to be solved iteratively based upon the updating frequency for the information and current state using the above Backward induction algorithm to determine the optimum strategy.

The optimal policy is denoted by ψ^*, where the policy $\psi = (\psi_0, \ldots, \psi_{N-1})$ is an optimal policy if and only if at all stages it satisfies:

$$\mathrm{Supp}(\psi_i) \subseteq \arg\max_{a_{P_{ij}} \in A_{P_{ij}}} Q(s_{P_{ij}}, a_{P_{ij}}), i = 0, \ldots, N-1. \tag{4.43}$$

[20] The Backward induction algorithm described in (4.32)-(4.25) could be employed to a problem that assumes the information set about stochasticity will not be updated through the decision process.

Algorithm 2 Value iteration algorithm for solving MDPs with updating information (Risk-neutral T-SRSPs)

Initialisation: the framework of MDP, $\mathcal{M} = \langle \mathbf{S}, \mathbf{A}, \mathbf{L}, R, \alpha \rangle$, where $\mathbf{L}$ contains the likelihood space about weather condition $\mathbf{I}_W$, waiting time T^{W_B} and αG_0;the vessel starts the journey from stage $l = 0$, which indicates the state $s = [x_A, y_A, t_A]$; the whole NPV including FPP to $H^* = 0$, the whole NPV excluding FPP to $h^* = 0$.

while $l \leq N$ **do**

Let the value iteration starts from the stage $i \to N$;

Calculate the value function for all states at stage N, the optimum value function for states at stage N by following (4.32)-(4.33), respectively;

Let $i \to N-1$, and calculate the value function for all states at stage $N-1$, the optimum value function for states at stage $N-1$ by following (4.34)-(4.36), respectively;

for $i = N-2, \ldots, 1$ **do**

Calculate Action-value function, value function and the optimum value function by following (4.37)-(4.39), respectively;

Let $i \to i-1$

end

Calculate the value function and optimum value function for $i \to 0$ by following (4.40)-(4.42);

Determine a policy $\psi = (\psi_0, \ldots, \psi_N)$ is optimum if it satisfies (4.43);

Choose the lth element in ψ, ψ_l^* as the optimum strategy for current stage l;

The vessel transits to state $s' = [x_{P_{l+1j'}}, y_{P_{l+1j'}}, t_{P_{l+1j'}}]$ with a simultaneously reward R_l;

Calculate $H^* = H^* + R_l \cdot e^{\alpha \Delta t}$; calculate $h^* = h^* + R_l \cdot e^{\alpha \Delta t}$ if $l < N$, otherwise let $h^* = h^*$;

the information space $\mathbf{L}$ according to the current state (time). The framework of MDP $\mathcal{M} = \langle \mathbf{S}, \mathbf{A}, \mathbf{L}, R, \alpha \rangle$ will be correspondingly updated as well;

Let $l \to l+1$.

end

Result: Return an optimum strategy sequence $\psi^* = (\psi_1^*, \ldots, \psi_N^*)$, the NPV including FPP H^*, and the NPV excluding FPP under the optimum strategy h^*.

The Algorithm 2 shows the value iteration algorithm for finding the optimum strategy in a MDP with updating information, especially for decision makers who are risk neutral. After applying the value iteration algorithms N times along the decision process, the accumulative reward function, which is also the NPV including FPP will be maximised [21] For risk-averse or risk-taking decision makers, the risk in the decision process should be assessed when maximising the NPV including FPP.

[21] It is acknowledged that the optimum strategy ψ^* is hardly likely to become a global optimum when the information involves not only transition probability but also the calculation of reward function and accumulative reward. Thus, we clarify that the optimum strategy actually represents the best selection of actions under a certain updated information pattern.

We propose that the risk in the decision process can be evaluated in a simulation-based way as follows: simulate the certain information updated pattern by employing the Algorithm 2 multiple times. Use the simulation results to establish distributions of the NPV including FPP (H^*) or the NPV excluding FPP (h^*). After applying a risk measure to the distribution, the risk performance could be detected and compared with the decision makers' long-term profit target (H^*) or short-term profit target (h^*). More about simulation process can be found in Section 4.6.2.

4.6.2 Simulation-enhanced value iteration algorithm (SEVI)

In the risk-neutral value iteration algorithm, the information for all past and the current decision stages are deterministic while the information for all future decision stages are represented by stochastic distributions. Meanwhile, the deterministic information for the current stage is often derived from the stochastic information about this stage from the previous stage.

Thus, SEVI is developed by integrating a random sampling process. The deterministic value of information for the current stage is generated by the random sampling from the distribution of it from the information set in previous stage. The process of updating information is consistent with the flow of information into decision-making systems in practice. At the beginning of the decision-making stage, the information except for the first few stages is vague that represented by a wide distribution, but over time, as the decision-making stage is approached, the distribution of random variables in the stages corresponding to the concentration of information will be gradually narrowed down.

Let the information space updates by an exactly same pattern every time in a simulation run, which ensures the updating frequencies for all stochasticities are same, and the distributions of random variables keep the same as well. The optimum strategy for a simulation run is denoted by $\bar{\psi}$. Run the simulation for N_{Simul} times, then the results of simulation is denoted by $\bar{\Psi} = \{\bar{\psi}_1, \ldots, \bar{\psi}_{N_{\text{Simul}}}\}$. And correspondingly, the NPV including FPP and NPV excluding FPP for each run are denoted by $\bar{H^*} = \{\bar{H^*}_1, \ldots, \bar{H^*}_{N_{\text{Simul}}}\}$, and $\bar{h^*} = \{\bar{h^*}_1, \ldots, \bar{h^*}_{N_{\text{Simul}}}\}$, as multiset[22], respectively. Given the simple random sampling process is unbiased, the simulation run times could be interpreted to the number of times an element appears in the multiset.

$$\sum_{\bar{H_j^*} \in \bar{H^*}} \mathbb{1}_{\bar{H_i^*}}(\bar{H_j^*}). \tag{4.44}$$

The frequency of $\bar{H^*}_i, i = 1, \ldots, N_{\text{Simul}}$ can be written as:

$$\frac{1}{N_{\text{Simul}}} \cdot \sum_{\bar{H_j^*} \in \bar{H^*}} \mathbb{1}_{\bar{H_i^*}}(\bar{H_j^*}). \tag{4.45}$$

[22]We clarify $\bar{H^*}$ and $\bar{h^*}$ should be defined as multiset rather than set. Due to a set does not include multiplicities that cannot be avoid during the simulation process.

Then, let $f(\bar{H^*})$ denotes the probability density function for $\bar{H^*}$, and $F(\bar{H^*})$ denotes the cumulative density function for $\bar{H^*}$. The probability function for $\bar{h^*}$ can be developed by following the same way. Thus, the number of times an element $\bar{h_i^*}$ appears in the multiset $\bar{h^*}$ is:

$$\sum_{\bar{h_j^*} \in \bar{h^*}} \mathbb{1}_{\bar{h_i^*}}(\bar{h_j^*}). \tag{4.46}$$

The frequency of $\bar{h^*}_i$, $i = 1, \ldots, N_{\text{Simul}}$ can be written as:

$$\frac{1}{N_{\text{Simul}}} \cdot \sum_{\bar{h_j^*} \in \bar{h^*}} \mathbb{1}_{\bar{h_i^*}}(\bar{h_j^*}). \tag{4.47}$$

4.7 Numerical experiments

In this section, we will base on a test route for *PANAMANA* vessel which undertakes a journey from Nueva Palmira (departure port A) to Londonderry (destination port B) to examine models proposed above. The total estimated length of the route is 8293 nm. The characteristics of the vessel could be found in Table 28 in Appendix A. The number of decision stages in the model can be adapted to the specifics of the problem. For example, for the test route considered in this section, if the great circle route is divided equally into N parts, then the length of route of each segment on the grand circle route is $8293/N$. If we consider making decisions about route choice and speed in these N segments referred to as the design speed limit for the vessel, the updating frequency of the oceanic weather conditions will become $8293/(24 \cdot N \cdot v_{\max})$ to $8293/(24 \cdot N \cdot v_{\min})$ days[23]. Results shown in this section are from experiments with seven stages, and five of them are relevant to routing and scheduling decisions. It allows information about oceanic weather conditions to be updated at a frequency in the range of 3.5 to 7 days.

The waypoints and feasible routes generated for the problem when the total number of stages is set to seven are created as follows:

The earliest arrival time and latest arrival time for all waypoints are able to be derived after taking the uncertainties about waiting time and oceanic weather conditions into account. Table 13 shows the original arrival time window, and the adjusted arrival time window according to a 0.5 days delivery time precision for all waypoints. Then, 3D states could be generated by time-discretising the waypoints by its adjusted arrival time window. For example, the adjusted arrival time window for waypoint $[0, 0]$ is $[0, 25.0]$, its 3D states are: $[0, 0, 0]$, $[0, 0, 0.5]$, $\ldots$, $[0, 0, 24.5]$, $[0, 0, 25.0]$.

Besides, the ordinal number of waypoints, the distance matrix, and some parameters assumed in the contract are shown in Appendix C. Parameters not explained in the following sections are

[23] As we expand waypoints at two ports into four waypoints, there are two stages in the whole decision process that are irrelevant to routing and scheduling decisions. Thus, to ensure an updating frequency in the range of $[8293/(24 \cdot N \cdot v_{\max}), 8293/(24 \cdot N \cdot v_{\min})]$, the total number of stages is $N + 2$.

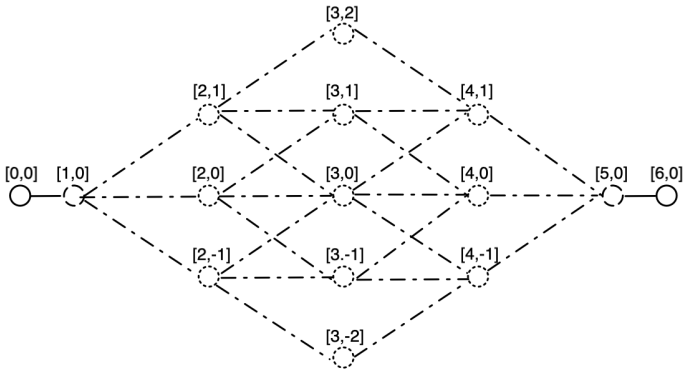

FIGURE 9: Initialised waypoints and feasible routes when the number of stage is 7

TABLE 13: Arrival time window for the waypoints when the number of stage is 7

Waypoint	Arrival time window (original)	Arrival time window (adjusted)
[0, 0]	[0, 24.72]	[0, 25.0]
[1, 0]	[0, 25.45]	[0, 25.5]
[2, -1]	[1.93, 28.47]	[1.5, 28.5]
[2, 0]	[2.48, 29.03]	[2.0, 29.5]
[2, 1]	[1.93, 28.47]	[1.3, 28.3]
[3, -2]	[6.06, 31.50]	[6.0, 31.50]
[3, -1]	[6.62, 32.05]	[6.5, 32.5]
[3, 0]	[6.06, 32.61]	[6.0, 33.0]
[3, 1]	[6.62, 32.05]	[6.5, 32.5]
[3, 2]	[6.06, 31.50]	[6.0, 31.50]
[4, -1]	[10.20, 35.63]	[10.0, 36.0]
[4, 0]	[10.75, 36.19]	[10.5, 36.5]
[4, 1]	[10.20, 35.63]	[10.0, 36.0]
[5, 0]	[14.33, 39.77]	[14.0, 40.0]
[6, 0]	[14.56, 40.00]	[14.5, 40.0]

considered as fixed numbers rather than control variables in the numerical experiments in this paper. The information of this part of the parameters are also displayed in Appendix C.

The delivery time is set to 40 days after the start time of the decision process[24]. Assume the shipper allows a late of delivery after the delivery time as long as a late of delivery penalty is paid by the charterer or a third party, i.e. an insurance party, with regard to the period of lateness. Besides, a delivery time window will be regulated in the form of terms or in the contract before the shipment starts. The FPP will be used in calculating the NPV including FPP after the vessel terminates at the destination port, but only when the shipment is completed within the delivery time window. For a delivery outside the delivery time window, a reduced FPP will be applied (Tan et al., 2022).

To calculate the NPV including FPP and the optimum strategy for the entire decision process, we employ the random generator when updating observations in the information set. Thus, the results of experiments should be analysed under a specific initial information set (distributions) and observations (value), which are obtained through the decision process.

[24]The start time of the decision process is defined by t_A in the model. For convenience, let $t_A = 0$ in this section. The delivery time stipulated on the contract usually indicates the time specified in a required shipment; the charterer reserves the right to cancel or reject the cargo if the delivery completes after the time specified.

4.7.1 Results for risk-neutral decision makers: experiments for Algorithm 2

In this section, we show results of experiments for solving an optimum strategy in MDPs for risk-neutral decision makers in the formulated T-SRSPs. Experiments are designed into several parts: 1. *Benchmark*; 2. changing the expectations of stochasticities including oceanic weather conditions k_W, the waiting time at the destination port T^{w_B}, and the daily value of the FPP αG_0; 3. changing the shape of distributions of stochasticities while keeping their expectations the same. For a delivery time-window which is 32 to 34 in days, results are shown in Table 14.

TABLE 14: Summary of experiments results when applying Algorithm 2 for risk-neutral decision makers under different scenarios

Scenarios	States track	Optimum strategy		Arrival time	Delayed or early	NPV excluding FPP (million USD)	NPV including FPP (million USD)
		Actions track	Suggested speed				
Benchmark	[0, 0, 0.0][1, 0, 1.0] [2, 1, 7.5][3, 1, 17.0] [4, 1, 24.0][5, 0, 31.5] [6, 0, 33.5]	$[1,0,\varnothing][1,1,7.0]$ $[1,0,6.5][1,0,5.0]$ $[1,-1,8.0][1,0,\varnothing]$	(14.25, 13.29, 17.28, 12.47)	33.5	×	0.5398	91.12
Weather mean-	[0, 0, 4.5][1, 0, 5.5] [2, 0, 11.5][3, 0, 18.0] [4, 0, 26.5][5, 0, 31.5] [6, 0, 33.5]	$[1,0,\varnothing][1,0,6.5]$ $[1,0,6.5][1,0,7.5]$ $[1,0,5.0][1,0,\varnothing]$	(13.29, 13.29, 11.52, 17.28)	33.5	×	0.5864	91.17
Weather mean+	[0, 0, 0.0][1, 0, 1.0] [2, -1, 7.5][3, -1, 15.5] [4, -1, 24.5][5, 0, 32.0] [6, 0, 34.0]	$[1,0,\varnothing][1,-1,6.5]$ $[1,0,5.5][1,0,5.0]$ $[1,1,6.0][1,0,\varnothing]$	(15.35, 15.71, 15.71, 16.62)	34.0	×	0.4686	91.04
FPP mean-	[0, 0, 0.0][1, 0, 1.0] [2, 1, 7.5][3, 1, 17.0] [4, 1, 24.0][5, 0, 31.5] [6, 0, 33.5]	$[1,0,\varnothing][1,1,7.0]$ $[1,0,6.5][1,0,5.0]$ $[1,-1,8.0][1,0,\varnothing]$	(14.25, 13.29, 17.28, 12.47)	33.5	×	0.5398	45.83
FPP mean+	[0, 0, 0.0][1, 0, 1.0] [2, 1, 7.5][3, 1, 17.0] [4, 1, 24.0][5, 0, 31.5] [6, 0, 33.5]	$[1,0,\varnothing][1,1,7.0]$ $[1,0,6.5][1,0,5.0]$ $[1,-1,8.0][1,0,\varnothing]$	(14.25, 13.29, 17.28, 12.47)	33.5	×	0.5398	136.4
Waiting time mean-	[0, 0, 0.0][1, 0, 1.0] [2, 1, 8.0][3, 1, 17.5] [4, 1, 24.5][5, 0, 31.5] [6, 0, 32.5]	$[1,0,\varnothing][1,1,7.5]$ $[1,0,6.5][1,0,5.0]$ $[1,-1,7.5][1,0,\varnothing]$	(13.30, 13.29, 17.28, 13.30)	32.0	×	0.5673	91.18
Waiting time mean+	[0, 0, 0.0][1, 0, 1.0] [2, 1, 7.5][3, 1, 17.5] [4, 1, 24.5][5, 0, 31.0] [6, 0, 33.5]	$[1,0,\varnothing][1,1,7.0]$ $[1,0,7.0][1,0,5.0]$ $[1,-1,7.0][1,0,\varnothing]$	(14.25, 12.34, 17.28, 14.25)	33.5	×	0.5173	91.10

The discrete distribution for scenarios indicate: *Weather mean-* $\sim [0.8, 0.9, 1, 1.2]$; *Weather mean+* $\sim [0.8, 1.2, 1.6, 2.0]$; *FPP mean-* $\sim [-10000, 0, 10000, 20000]$; *FPP mean+* $\sim [10000, 20000, 30000, 40000]$; *Waiting time mean-*$\sim [0, 2, 4, 8]$; *Waiting time mean+* $\sim [8, 16, 24, 48]$

Optimum results for a scenario (rows 2 to 8) as shown in Table 14 can be interpreted as follows: the states track shows 3D states of the vessel during the decision process, i.e., the states track for *Benchmark* indicates the vessel starts the loading process at port A at time zero, completes all preparations, and leaves port A at time 1.0 (days), arrives at waypoint $[2,1]$, $[3,1]$, $[4,1]$, $[5,0]$ at time 7.5, 17.0, 24.0, and 31.5 (days), respectively. Then the vessel starts to wait for unloading at port B and completes all unloading and delivery processes at time 33.5 (days). We call the vessel terminates at the destination port B at 32.5 (days) relevant to the initial time of 0 (days) of the decision process; the actions track shows the optimum actions obtained at each state, i.e., the actions track for *Benchmark* indicates the vessel does not need to take actions at state $[0,0,0.0]$. Then, at states $[1,0,1.0]$, $[2,1,7.5]$, $[3,1,17.0]$ and $[4,1,24.0]$, the vessel is suggested to move forward to the neighbour waypoint at the next stage within 7.0, 6.5, 5.0, and 8.0 days, respectively. Likewise, the vessel does not need to take actions at state $[5,0,31.5]$; the suggested speed is corresponding stated for the suggested time consumed for the following sailing leg, i.e., the suggested speed for *Benchmark* indicates the vessel needs to travel at speed 14.25 knots from waypoint $[1,0]$ to $[2,1]$ to avoid being late, and for the rest of the sailing segment, the suggested speed are 13.29 knots, 17.28 knots, 12.47 knots, respectively; the arrival

time represents the time that the vessel completed the delivery and ready for undertaking the next job; the status of delay can be determined by comparing the arrival time and the demanded delivery time; the NPV excluding FPP and the NPV including represent the actual NPV which is calculated by applying the actual observations about stochasticies, including a really got FPP.

By comparing the optimum strategies and results for *Benchmark* and categorised scenarios about oceanic weather condition, including *Weather mean-* and *Weather mean+*, we conclude: 1. having a non ideal estimations of oceanic weather conditions, vessels are more likely to sail as early as possible to avoid possible delays due to bad weathers. On the contrary, having a milder weather condition in estimations may change the vessel's starting time for loading and preparations, while it may also allow the vessel to alter its sailing speed, which is due to the time dependency of weather conditions. See rows of *Benchmark*, *Weather mean-*, and *Weather mean+*, first states in their column 'States track', and their column 'Suggested speed'; 2. having various oceanic weather conditions can change the NPV excluding FPP due to fuel consumption are varied environment and sailing speed. However, the vessel aims to complete the delivery on time in order to avoid extra costs including demurrage fees, late of delivery penalty, and a loss of FPP, which leads to the FPP will not change so long as the arrival time is within the delivery time-window. Considering the FPP dominates the NPV including FPP when it is closely estimated by the daily hire rate, there is no significant differences among scenarios *Benchmark*, *Weather mean-*, *Weather mean+*, *Waiting time mean+*, and *Waiting time mean-*, due to there are no delay or early deliveries under these scenarios.

Optimum strategies for *Benchmark*, *FPP mean-* and *FPP mean+* are the same in Table 14. It is caused by the FPP, which is time-dependent and established as a random variable related to the delivery time. If the arrival time actually lies within the range defined by the delivery time-window, the FPP will be the value as estimated; otherwise, a loss of delay will be applied to deriving a reduced FPP. Thus, although the mean value of FPP changes, the optimum strategy for *Benchmark* already provides the best decisions for making the best NPV excluding FPP and a maximum of FPP, which leads to the same optimum strategies, the same NPV excluding FPP and various NPV including FPP.

Experiments also reveal that the expected estimation of waiting time at destination port B will influence the optimum strategy, including optimum actions and suggested speeds. When the expectation of waiting time at port B increases by around 1 day, the average speed in optimum strategy will have a prompt of 0.31 knots. It is explained that the ship tries its best to arrive at the destination port within the specified delivery window to achieve the best FPP and NPV including FPP. When a longer waiting time is expected, vessels will tend to start preparations and leave from the departure port earlier when there is a slack in starting time, or, alternatively, change the sailing routes and schedules. See comparisons among *Benchmark*, *Waiting time mean-*, and *Waiting time mean+*.

4.7.2 Simulation-based value iteration algorithm for risk-averse decision makers

Furthermore, experiments are designed to examine the optimum strategy for risk-averse decision makers in this section. As illustrated in Section 4.5.2, we distinguish risk-averse decision makers into two categories with regards to their willingness to control the risk for profit in the long-term (*averse-long*) or in the short-term (*averse-short*). For these two types of risk-averse decision makers, a simulation-based value iteration algorithm is employed for building the distributions of NPV including FPP and NPV excluding FPP under groups of risk levels, scenarios about stochasticities, and problem settings.

We show the results of simulations run 100 times and 1,000 times for *Benchmark*. Each run of simulation generates the actual oceanic weather conditions, waiting time, and FPP randomly based on the same initial information set and information set in updating. Generated random observations will be updated in the information set and implemented to derive optimum policies for further stages. For each run, a result profile that includes states track, policy track, NPV excluding FPP and NPV including FPP will be obtained. We investigate the performance of $\bar{H}^*$ and $\bar{h^*}$ by applying *Value-at-Risk* (VaR) and *Conditional-Value-at-Risk* (CVaR) with various levels of risk tolerance, results for a 100 run times and 1,000 run times could be found in Table 15 and Table 16, respectively.

TABLE 15: Risk performance of a 100 run times simulation when applying value iteration algorithm under scenario *Benchmark*

Risk tolerance level	NPV excluding FPP (million USD)		NPV including FPP (million USD)	
	VaR	CVaR	VaR	CVaR
0.01	-0.1902	-0.1902	-0.1902	-0.1902
0.05	0.1358	0.0468	45.38	18.15
0.10	0.2501	0.1143	45.52	31.80
0.20	0.3379	0.2084	45.14	38.69

TABLE 16: Risk performance of a 1000 run times simulation when applying value iteration algorithm under scenario *Benchmark*

Risk tolerance level	NPV excluding FPP (million USD)		NPV including FPP (million USD)	
	VaR	CVaR	VaR	CVaR
0.01	0.0606	0.0005	-44.74	-44.89
0.05	0.2656	0.1595	0.5410	-11.41
0.10	0.3512	0.2439	45.30	-4.022
0.20	0.4546	0.3313	45.80	20.81

The performance of $\bar{H}^*$ and $\bar{h^*}$ under different risk measures and risk tolerance levels should be compared with the decision makers' profit targets, i.e., from Table 16, a decision maker who can accept the probability of not achieving a 0.2 million USD of NPV excluding FPP as 0.1 can be satisfied by undertaking the job (without making changes of the delivery window); a decision maker who can accept the probability of having a positive NPV including FPP as 0.05 or 0.1 can be satisfied when applying VaR, while, not when applying CVaR. Results in Table 15-16 can also be interpreted by confidential level and profit targets, i.e., for a decision maker who is willing to make sure the NPV excluding FPP is higher than 0.25 million USD and the the NPV

including FPP is higher than 45 million USD both at confidential level 90%, the simulation results from 100 run times and 1,000 run times both indicate the job can satisfy the decision maker's demand when VaR is applied.

In cases where decision makers do not have clear profit targets or risk tolerance levels, graphical distributions of NPV excluding FPP and NPV including FPP can also be helpful. Histograms of NPV excluding FPP, NPV including FPP of 100 run times, and NPV including FPP of 1,000 run times are shown in Figure 4.10(a)-4.12(b), respectively. By observing the visualised distribution, it is possible to see in which area the data is concentrated, i.e., the distribution of NPV including FPP in Figure 4.12(b) is concentrated on the right side of the figure between 75 million USD and 100 million USD, and also between 40 million USD and 60 million USD. Considering the simulation results by looking at both the plots of distribution and performances under various risk measures and tolerance levels is more effective, especially for decision makers who do not have a strict risk appetite or have that risk aversion in the short or long term.

Meanwhile, there are possibilities that decision makers' own risk attitudes and profit targets cannot be satisfied by acknowledging the risk performance and histograms of a simulation with abundant run times. For example, a decision maker who needs to pay a debt by month or by season have to consider whether the earnings obtained from the job is enough to pay the debt on time, also the associated risk. The earnings are reflected by the NPV excluding FPP in this paper. If the decision maker completed the journey with a NPV excluding FPP over his or her lowest re-pay level, the business could be continued. Otherwise a failure-to-pay penalty will be charged until the decision maker has ability to pay debt based on an additional penalty rate. The worst case will be the decision maker becomes insolvent and go bankrupt. For example, assume there is a decision maker who needs to pay a debt at least 0.1 million USD 34 days after the journey starts, 5 percent failure rate could be known from Table 16. For the same reason, when a higher profit target is required, more risks should be undertaken, otherwise the job will not be suggested under current assumptions.

The model is able to be extended to determine an ideal delivery time-window before stipulating the contract. Relevant experiments are shown in Section 4.7.4.

4.7.3 Comparison with other methods

Then, we compare our methods with some other methods that proposed for solving SRSPs and are applicable for tramp ships: 1. The 3D-Dijkstra's algorithm which minimises the fuel consumption proposed by Wang et al. (2019); 2. The improved A* algorithm which minimises the path cost introduced by Shin et al. (2020). The path cost could be fuel cost or Estimated Time of Arrival (ETA); 3. The 3D Bellman-Ford algorithm which maximises the gross profit. 4. The mean-risk optimisation problem introduced by [Paper 1] which maximises the expected NPV including FPP under risk. These methods are either considered in a dynamic decision environment, or with stochasticity, or with updating information, but not all of them. While the framework of MDPs and value iteration algorithms for MDPs with updating information that

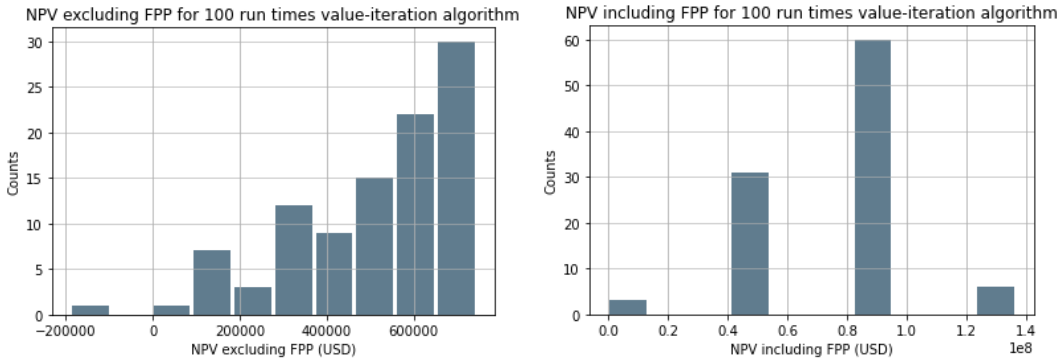

(a) NPV excluding FPP (b) NPV including FPP

FIGURE 10: Histogram of NPV for a 100 run times simulation when applying value iteration algorithm under scenario *Benchmark*

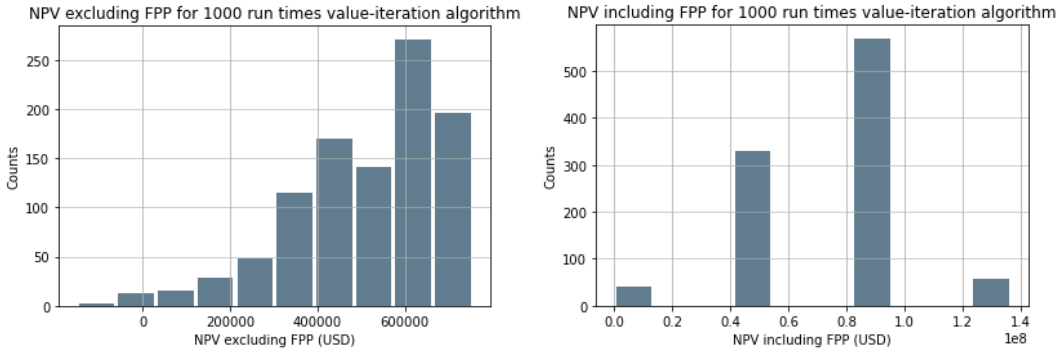

(a) NPV excluding FPP (b) NPV including FPP

FIGURE 11: Histogram of NPV for a 1000 run times simulation when applying value iteration algorithm under scenario *Benchmark*

proposed by this paper are able to solve the T-SRSPs in a dynamic stochastic decision environment with updating information. Comparisons among methods with regards to the features of dynamics, stochasticity, updating information, and objectives are given in Table 17 as follows:

TABLE 17: Comparisons of methods that are applicable to solve T-SRSPs

Method	Dynamics	Stochasticity	Updating information	Objectives
Value iteration algorithm for MDPs with updating information (this paper)	✓	Oceanic weather conditions, FPP, Waiting time at the destination port	Information updated at the beginning of each stage as distribution	Maximise expected NPV including FPP under risk
3D-Dijkstra's algorithm Wang et al. (2019)	✓	×	Information updated at the beginning of each stage as certain value	Minimise fuel cost
Improved A* algorithm Shin et al. (2020)	✓	×	Information updated at the beginning of each stage as certain value	Minimise fuel cost or ETA
3D Bellman-Ford algorithm	✓	×	Information updated at the beginning of each stage as certain value	Maximise gross profit
Stochastic programming (Chapter 3)	×	Oceanic weather conditions, FPP	×	Maximise expected NPV including FPP under risk

The 3D Dijkstra's algorithm proposed by Wang et al. (2019) and the improved A* algorithm

introduced by Shin et al. (2020) consider the objective of optimising as minimising fuel consumption, or fuel cost, or ETA. The improved A* algorithm is an effective algorithm that adds a heuristic cost function to evaluate the expected cost of travelling from the current node to the target node. Thus, as an algorithm that is established based on Dijkstra's algorithm, A* algorithm improves computational space and time, especially when the problem only asks for the shortest path from a single source to a single destination. The optimal solutions produced by these two methods are the same when minimising the fuel cost.

Meanwhile, both methods are not applicable to solve the T-SRSPs with the objective of maximising profit, whether or not the profit is considered NPV, due to the fact that they cannot solve the graph with negative edge weights. Sometimes, longest path problems could be solved by using Dijkstra's algorithm or Dijkstra's algorithm-based algorithms, such as the A* algorithm, by switching from maximising path length to minimising negative path length when the path lengths are all denoted by negative values. Otherwise, algorithms that are able to find the shortest path, whether or not the edge weights are positive, should be considered. The Bellman-Ford algorithm solves the shortest path problem from a single source to all other nodes and allows the existence of negative edge weights if there are no negative cycles within the graph Ford (1956); Bellman (1958). Thus, the 3D Bellman-Ford algorithm with the objective of maximising the gross profit are also considered in the model comparisons under the problem setting in this paper.

As shown in Table 18, methods are compared under scenarios same as described in Table 14. In Table 18, *MDP-UI* represents the value iteration algorithm adopted to solve the Markov decision processes with updating information for T-SRSPs proposed in this paper; *3DD* indicates the 3D Dijkstra's algorithm introduced by Wang et al. (2018a); and, *3DBF* is the 3D Bellman-Ford algorithm considered in this paper. Each row of experiment contains the name of scenario, method, and results about the states track (the state of vessel in space and temporal), optimum strategy, arrival time, the condition of delay or early, and the performance of actual NPV excluding FPP (million USD) and NPV including FPP (million USD), respectively.

Three dynamic methods with updating information (*MDP-UI*, *MDP-UI* and *3DBF*) could change routes and schedules when the expectation of weather conditions changed. However, *MDP-UI* always has the highest NPV including FPP when compared to the results from others under the same scenario. It is not only because the objective of *MDP-UI* is maximising the expected NPV including FPP, but also attribute to the assessment of uncertainties in *MDP-UI* is from the distributions of random variables rather than certain estimation value (or mean value). The actual arrival time after delivery among methods demonstrates *MDP-UI* adjusts the routes and speeds when the estimation of future changes that avoids the vessel arrives outside the *MDP-UI*. While, other methods, only use the mean value of estimations about weather conditions, waiting time and FPP to adjust their decisions, still have a relatively high probability to fail to deliver within the negotiated time-window and being required to pay a demurrage fee and late of delivery penalty. A loss of FPP will also be applied in such cases as explained in Section 4.7.4. Case

TABLE 18: Summary of experiments results for risk-neutral decision makers when applying different scenarios and methods

Scenario	Method	States track	Optimum strategy		Arrival time	Delayed or early	NPV excluding FPP (million USD)	NPV including FPP (million USD)
			Actions track	Suggested speed				
Benchmark	*MDP-UI*	[0, 0, 0.0][1, 0, 1.0] [2, 1, 7.5][3, 1, 17.0] [4, 1, 24.0][5, 0, 31.5] [6, 0, 33.5]	$[1,0,\varnothing][1,1,7.0]$ $[1,0,6.5][1,0,5.0]$ $[1,-1,8.0][1,0,\varnothing]$	(14.25, 13.29, 17.28, 12.47)	33.5	×	0.5398	91.12
	3DD	[0, 0, 0.0][1, 0, 1.0] [2, 1, 8.5][3, 1, 16.0] [4, 1, 24.5][5, 0, 32.5] [6, 0, 34.5]	$[1,0,\varnothing][1,1,7.5]$ $[1,0,7.5][1,0,8.5]$ $[1,-1,8.0][1,0,\varnothing]$	(13.30, 11.52, 10.16, 12.47)	34.5	✓	0.4090	45.69
	3DBF	[0, 0, 0.0][1, 0, 1.0] [2, 1, 8.0][3, 1, 14.5] [4, 1, 23.0][5, 0, 31.0] [6, 0, 33.0]	$[1,0,\varnothing][1,1,7.0]$ $[1,0,6.5][1,0,8.5]$ $[1,-1,8.0][1,0,\varnothing]$	(14.25, 14.29, 10.16, 12.47)	33	×	0.4661	91.06
Weather mean-	*MDP-UI*	[0, 0, 4.5][1, 0, 5.5] [2, 0, 11.5][3, 0, 18.0] [4, 0, 26.5][5, 0, 31.5] [6, 0, 33.5]	$[1,0,\varnothing][1,0,6.5]$ $[1,0,6.5][1,0,7.5]$ $[1,0,5.0][1,0,\varnothing]$	(13.29, 13.29, 11.52, 17.28)	33.5	×	0.5864	91.17
	3DD	[0, 0, 0.0][1, 0, 1.0] [2, 0, 7.0][3, 0, 14.0] [4, 0, 21.0][5, 0, 28.0] [6, 0, 30.0]	$[1,0,\varnothing][1,0,6.0]$ $[1,0,7.0][1,0,7.0]$ $[1,0,7.0][1,0,\varnothing]$	(14.40, 12.34, 12.34, 12.34)	30	✓	0.6788	46.00
	3DBF	[0, 0, 0.0][1, 0, 1.0] [2, 0, 7.0][3, 0, 13.5] [4, 0, 20.0][5, 0, 27.0] [6, 0, 29.0]	$[1,0,\varnothing][1,0,6.0]$ $[1,0,6.5][1,0,6.5]$ $[1,0,7.0][1,0,\varnothing]$	(14.40, 13.29, 13.29, 12.34)	29.0	✓	0.6782	46.01
Weather mean+	*MDP-UI*	[0, 0, 0.0][1, 0, 1.0] [2, -1, 7.5][3, -1, 15.5] [4, -1, 24.5][5, 0, 32.0] [6, 0, 34.0]	$[1,0,\varnothing][1,-1,6.5]$ $[1,0,5.5][1,0,5.0]$ $[1,1,6.0][1,0,\varnothing]$	(15.35, 15.71, 15.71, 16.62)	34.0	×	0.4686	91.04
	3DD	[0, 0, 0.0][1, 0, 1.0] [2, -1, 9.0][3, -1, 17.5] [4, -1, 26.0][5, 0, 35.5] [6, 0, 37.5]	$[1,0,\varnothing][1,-1,8.0]$ $[1,0,8.5][1,0,8.5]$ $[1,1,9.5][1,0,\varnothing]$	(12.47, 10.16, 10.16, 10.50)	37.5	✓	0.0550	0.0550
	3DBF	[0, 0, 0.0][1, 0, 1.0] [2, -1, 7.5][3, -1, 14.5] [4, -1, 23.0][5, 0, 31.5] [6, 0, 33.5]	$[1,0,\varnothing][1,-1,6.5]$ $[1,0,7.0][1,0,8.5]$ $[1,1,8.5][1,0,\varnothing]$	(15.35, 12.34, 10.16, 11.74)	33.5	×	0.4335	91.02
Waiting time mean-	*MDP-UI*	[0, 0, 0.0][1, 0, 1.0] [2, 1, 8.0][3, 1, 17.5] [4, 1, 24.5][5, 0, 31.5] [6, 0, 32.5]	$[1,0,\varnothing][1,1,7.5]$ $[1,0,6.5][1,0,5.0]$ $[1,-1,7.5][1,0,\varnothing]$	(13.30, 13.29, 17.28, 13.30)	32.0	×	0.5673	91.18
	3DD	[0, 0, 0.0][1, 0, 1.0] [2, 1, 8.5][3, 1, 16.0] [4, 1, 24.5][5, 0, 32.5] [6, 0, 33.0]	$[1,0,\varnothing][1,1,7.5]$ $[1,0,7.5][1,0,8.5]$ $[1,-1,8.0][1,0,\varnothing]$	(13.30, 11.52, 10.16, 12.47)	33.0	×	0.5236	91.12
	3DBF	[0, 0, 0.0][1, 0, 1.0] [2, 1, 8.0][3, 1, 14.5] [4, 1, 23.0][5, 0, 30.5] [6, 0, 31.0]	$[1,0,\varnothing][1,1,7.0]$ $[1,0,6.5][1,0,8.5]$ $[1,-1,7.5][1,0,\varnothing]$	(14.25, 13.29, 10.16, 13.30)	31.0	✓	0.4893	45.81
Waiting time mean+	*MDP-UI*	[0, 0, 0.0][1, 0, 1.0] [2, 1, 7.5][3, 1, 17.5] [4, 1, 24.5][5, 0, 31.0] [6, 0, 33.5]	$[1,0,\varnothing][1,1,7.0]$ $[1,0,7.0][1,0,5.0]$ $[1,-1,7.0][1,0,\varnothing]$	(14.25, 12.34, 17.28, 14.25)	33.5	×	0.5173	91.10
	3DD	[0, 0, 0.0][1, 0, 1.0] [2, 1, 8.5][3, 1, 16.0] [4, 1, 24.5][5, 0, 32.5] [6, 0, 35.0]	$[1,0,\varnothing][1,1,7.5]$ $[1,0,7.5][1,0,8.5]$ $[1,-1,8.0][1,0,\varnothing]$	(13.30, 11.52, 10.16, 12.47)	35.0	✓	0.3956	45.67
	3DBF	[0, 0, 0.0][1, 0, 1.0] [2, 1, 7.5][3, 1, 14.0] [4, 1, 22.5][5, 0, 30.5] [6, 0, 33.0]	$[1,0,\varnothing][1,1,6.5]$ $[1,0,6.5][1,0,8.5]$ $[1,-1,8.0][1,0,\varnothing]$	(15.35, 13.29, 10.16, 12.47)	33.0	×	0.4832	91.08

MDP-UI: Markov Decision processes with updating information proposed and solved by value iteration algorithm (Algorithm 2) in this paper; *3DD*: 3D Dijkstra's algorithm Wang et al. (2018a); *3DBF*: 3D Bellman-Ford algorithm .

that completes the delivery early or late, except in the scenario of *Weather mean-*, the NPV excluding FPP and the NPV including FPP followed are lower than the case under same scenario but completes delivery within the delivery time-window [25].

When the expectation of waiting time at port B increases, *MDP-UI* adjusts the sailing speeds of segments based on weather conditions in the newest updated information set, while other methods do not. The speeding up is not an equally or proportionally increased speed for segments. *MDP-UI* is able to reschedule the actions in the most economic way. By comparing the suggested speed between *Benchmark* : *MDP-UI* to *Waiting time mean+* : *MDP-UI*, the sailing route stays the same. The suggested speed in second segment from waypoint $[2,1]$ to $[3,1]$

[25] *MDP-UI* has a lower NPV excluding FPP when compared to *3DD* and *3DBF* under the scenario *Weather mean-*, which is due to the latter two methods have different objectives with the method proposed in this paper. The difference indicates the difference of a continuous daily hire cost in time-chartered tramp ships. Let T denotes the termination time, for a $TCH = 26500$, $TCH^{365}_{T=33.5} = 884498$; $TCH^{365}_{T=30} = 792392$; and $TCH^{365}_{T=29} = 766062$. The difference between a $T = 33.5$ and $T = 30$ is 92106, which is approximately the difference between 0.6788 million and 0.5863 million, as shown in Scenario *Weather mean-*.

decreases from 13.29 to 12.34, and the suggested speed in last segment from waypoint $[4,1]$ to $[5,0]$ increases from 12.29 to 14.25. It is caused by the actual weather condition at $[3,1]$ is worse than expected; a lower speed could be helpful in saving fuel consumption and fuel costs. Then, for waypoints $[4,1]$ and $[5,0]$, weather conditions are better than expected, when the information set becomes available, a higher speed in the last segment is derived to make sure the vessel will arrive at port B with enough waiting time spared before the upper delivery window.

4.7.4 Alternative delivery time-window

To help decision makers who are not satisfied with the risk performance of NPV that derived from current delivery time-window, we extend our model to compare some alternative delivery time-windows for the decision maker to make further decisions. We conclude two types or alternatives, expand the delivery time-window, or change the contract date. In experiments shown earlier in this section, the delivery time window is assumed as $[32,34]$ days after the starting time of the decision process. Any delivery outside the time-window will cause a demurrage fee (whether when early or delayed), a late of delivery penalty (only when delayed), and a loss of FPP. Alternatives are provided based on the original time-window as: (i). expand the time-window to $[31,35]$ days, the length of the window increases from 2 days to 4 days; (ii-a). keeps the length of the window as 2 days, move the window to $[34,36]$ days; (ii-b). move the window to $[36,38]$ days. For these alternatives, simulation of 100 runs are independently completed. Results of risk performance and histograms are given in Table 19-21 , Figure 12-14, respectively for alternative (i), (ii-a), and (ii-b), and are compared to the results derived from original delivery time-window, Table 15 and Figure 10, respectively.

TABLE 19: Risk performance of a 100 run times simulation for alternative delivery time-window (i)

Risk tolerance level	NPV excluding FPP (million USD)		NPV including FPP (million USD)	
	VaR	CVaR	VaR	CVaR
0.01	-0.0374	-0.0374	0.1425	0.1425
0.05	0.2302	0.0990	45.27	18.28
0.10	0.3214	0.1913	45.79	31.93
0.20	0.4250	0.2834	90.86	45.67

The risk performance of NPV displayed in Table 19 is better than the results shown in Table 15 at all risk tolerance levels. The $\text{VaR}_{0.05}$ of NPV obtained from completing the journey itself increases from 0.1358 million USD to 0.2302 million USD. The failure rate of not reaching a specific short-term profit target (NPV excluding FPP) when applying CVaR decreases, dropping approximately 5 percent for a 0.1 million target and 10 percent for a 0.20 million target. From the aspect of long-term profitability, the frequency of having a NPV including FPP over 80 million USD rises by 17 percent. Alternative delivery time-window (i) seems to be a better choice, whether for risk-averse decision makers who have a demand for short-term NPV or decision makers who desire long-term NPV.

For alternative (ii-a) that postpones the time-window for 2 days, we found the performance of NPV excluding FPP is improved for risk tolerance levels of 0.01, 0.05, 0.10, and 0.20 whether

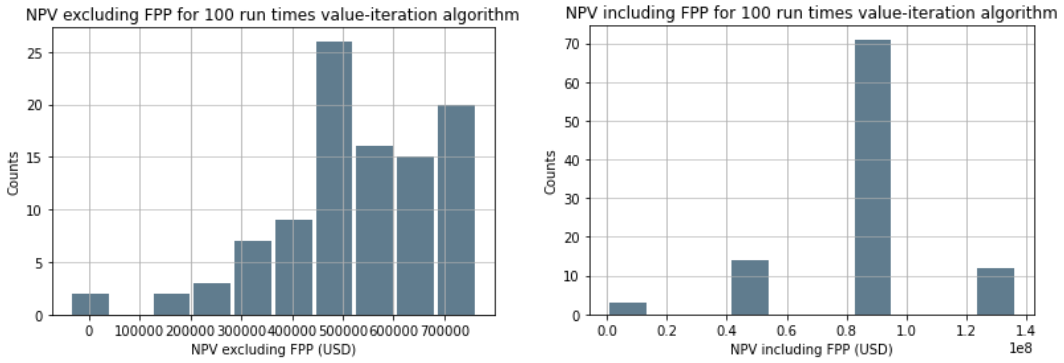

(a) NPV excluding FPP (b) NPV including FPP

FIGURE 12: Histogram of NPV for a 100 run times simulation for alternative delivery time-window (i)

TABLE 20: Risk performance of a 100 run times simulation for alternative delivery time-window (ii-a)

Risk tolerance level	NPV excluding FPP (million USD)		NPV including FPP (million USD)	
	VaR	CVaR	VaR	CVaR
0.01	-0.0422	-0.0422	-44.99	-44.99
0.05	0.2018	0.1430	0.2475	-8.858
0.10	0.2676	0.1964	45.45	-4.274
0.20	0.3109	0.2427	45.61	20.62

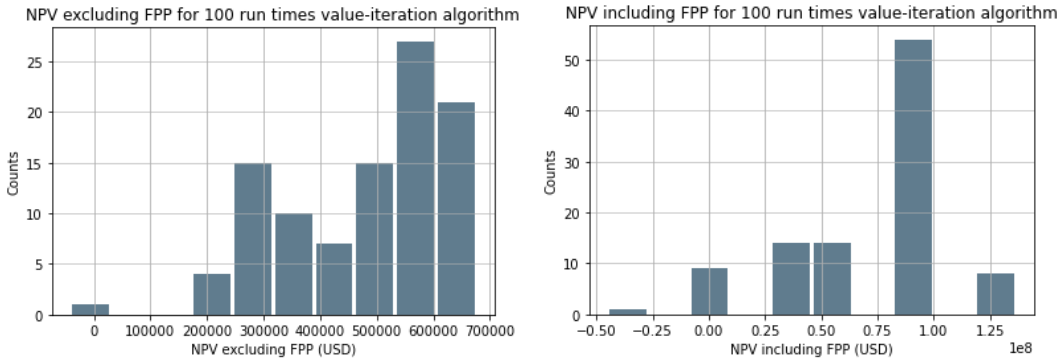

(a) NPV excluding FPP (b) NPV including FPP

FIGURE 13: Histogram of NPV for a 100 run times simulation for alternative delivery time-window (ii-a)

TABLE 21: Risk performance of a 100 run times simulation for alternative delivery time-window (ii-b)

Risk tolerance level	NPV excluding FPP (million USD)		NPV including FPP (million USD)	
	VaR	CVaR	VaR	CVaR
0.01	-0.0217	-0.0217	-45.25	-45.25
0.05	0.0967	0.0283	0.1033	-18.04
0.10	0.3016	0.1233	45.54	9.216
0.20	0.3566	0.2302	45.75	27.43

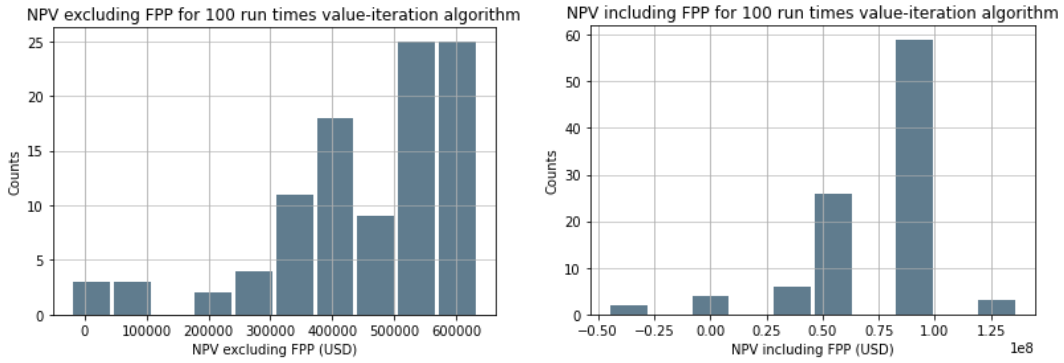

(a) NPV excluding FPP (b) NPV including FPP

FIGURE 14: Histogram of NPV for a 100 run times simulation for alternative delivery time-window (ii-b)

VaR or CVaR is applied. There is no significant difference in the performance of NPV including FPP between (ii-a) and the original delivery time-window. For alternative (ii-b) that postpones the time-window for 4 days, the performance of NPV excluding FPP is less acceptable at risk tolerance levels 0.01 and 0.05. The performance of NPV including FPP is less satisfactory at risk tolerance levels of 0.01, 0.05, 0.10, and 0.20 whether VaR or CVaR is applied. Thus, alternative (ii-a) seems to be a good choice for risk averse decision makers with a short-term profit target but not for decision makers who desire long-term NPV.

Optimal strategies for alternatives (i), (ii-a), and (ii-b) are given in Table 22 as follows:

TABLE 22: Summary of experiments results when applying Value iteration algorithm to the MDP framework with different delivery time-window

Delivery time-window	States track	Optimum strategy		Arrival time	Delayed or early	NPV excluding FPP (million USD)	NPV including FPP (million USD)
		Actions track	Suggested speed				
[32, 34]	[0, 0, 0.0][1, 0, 1.0] [2, 1, 7.5][3, 1, 17.0] [4, 1, 24.0][5, 0, 31.5] [6, 0, 33.5]	$[1, 0, \varnothing][1, 1, 7.0]$ $[1, 0, 6.5][1, 0, 5.0]$ $[1, -1, 8.0][1, 0, \varnothing]$	(14.25, 13.29, 17.28, 12.47)	33.5	×	0.5398	91.12
(i): [31, 35]	[0, 0, 0.0][1, 0, 1.0] [2, 1, 8.0][3, 1, 17.5] [4, 1, 24.5][5, 0, 30.5] [6, 0, 32.5]	$[1, 0, \varnothing][1, 1, 7.5]$ $[1, 0, 6.5][1, 0, 5.0]$ $[1, -1, 6.5][1, 0, \varnothing]$	(13.30, 13.30, 17.28, 15.35)	32.5	×	0.5274	91.13
(ii-a): [34, 36]	[0, 0, 0.0][1, 0, 1.0] [2, 1, 8.5][3, 1, 18.5] [4, 1, 25.5][5, 0, 33.5] [6, 0, 35.5]	$[1, 0, \varnothing][1, 1, 8.0]$ $[1, 0, 7.0][1, 0, 5.0]$ $[1, -1, 8.5][1, 0, \varnothing]$	(12.47, 12.34, 17.28, 11.74)	35.5	×	0.4742	91.02
(ii-b): [36, 38]	[0, 0, 0.0][1, 0, 1.0] [2, 1, 9.5][3, 1, 19.5] [4, 1, 27.5][5, 0, 35.5] [6, 0, 37.5]	$[1, 0, \varnothing][1, 1, 8.0]$ $[1, 0, 7.0][1, 0, 5.5]$ $[1, -1, 8.5][1, 0, \varnothing]$	(12.47, 12.34, 15.71, 11.74)	37.5	×	0.4609	90.96

Experiments are derived by applying the scenario *Benchmark*. There is no delayed or early delivery under all delivery time-window when applying the value iteration algorithm proposed by this paper. For a wider time-window, such as (i), the risk of not completing the delivery on time is reduced, thus the arrival time is optimised over the time-window $[31, 35]$ and determined by 32.5 days in the example. A postponed delivery time-window, such as (ii-a) and (ii-b), the average speed of the overall journey is reduced by 1 knot and 1.35 knots, compared to the average speed of $[32, 34]$, respectively. Intuitively, postponing the delivery time-window

is beneficial to decision makers when the estimation of fuel oceanic consumption rates under weather conditions is higher or the waiting time at the destination port becomes longer. In the opposite direction, moving the delivery time-window ahead of schedule could be a better choice.

In practice, the cost and relevant risks of negotiating a new delivery time-window with the shipper should be evaluated and taking in to account when comparing the expected return and risk performances.

4.8 Conclusion

This chapter introduces the framework of MDPs for solving SRSPs in tramp shipping. The problem is a general SRSPs in tramp shipping that the decision maker is responsible to make decisions about ship's operation, including sailing routes and speed, as well as the planned departure time and arrival time. Delivery outside the time window will cause extra cost and lost the future potential profitability. There are several underlying elements that may cause a fluctuation of the estimated arrival time, that includes ship's operation, environmental factors, port congestion, and so on, while most of these elements are changing over time. This study formulates decisions about ship's motion (direction to next waypoint) and corresponding speed as actions in MDP, and uncertainties about weather conditions and time consumed at port as random variables.

There are abundant studies of SRSPs, either in operational research or in the marine engineering community. Conventional optimisation modelling in both fields usually connects the uncertainties from environmental factors, i.e., winds, waves, and currents, to the objective of minimising fuel consumption or carbon emissions. Dynamic programming is adapted to solve this type of WRSPs by updating the parameters of weather conditions with certain predictions and re-optimising the problem over time. We point out certain limitations of these methods in the literature and conclude them as follows: (1) ignore the journey in tramp shipping, which usually takes a month or longer, while the accuracy of predictions for oceanic weather significantly decreases after a week; (2) inefficiency when maximising profit; and (3) a shortage of considering the diversity of risk attitudes for decision makers.

The framework established by this paper improves (1) by the formulation of stochasticies, see Section 4.4; (2) by the advantage of MDP; and (3) by value iteration and EHVI, see Section 4.6. For decision makers who are risk-neutral or are not familiar with their own tolerance level and profit targets, the value iteration algorithm could be employed to generate optimum solutions, while the EHVI could provide an intuitive NPV analysis by showing the histogram of NPV under a number of simulation run times, see Table 14, and Figure 10-11. For decision makers with certain risk attitudes, a summary of risk performance is a better option.

The contributions of this chapter are as follows: (1) a framework of MDPs is proposed for solving the SRSPs in tramp shipping with uncertainties from oceanic weather conditions, port, and freight markets that are all updated in the decision system frequently; (2) the perspective

of risk attitudes is implemented by introducing a SEVI that provides a distribution of NPV in the short- and long-term, both in an intuitive way or calculated by risk measures; and (3) a soft delivery time-window can be considered as an alternative.

The advantages of applying MDP are addressed in numerical experiments under many scenarios in Section 4.7. Results reveal that applying the method in this paper has a higher opportunity to achieve better profitability in the long-term. It also mitigates the risk of delay or arriving earlier than the contractual delivery time. We also find that when altering the distribution of uncertainties, the method in this paper is able to adjust the decisions and provide new solutions, while methods that use certain information rather than distribution cannot.

We consider that future research could possibly be extended to include, but not be limited to, the following directions: First, risk-constrained MDPs could include risks from environmental perspectives, i.e., carbon emissions, or ECAs. Specific constraints among time windows, safety factors, carbon costs, or similar strict requirements could be added to the MDPs. Second, soft constraints may also be considered one of the objectives of value iterations. Assume more than one parallel MDP, each of which has a unique objective function represented by a reward function. Solving methods for multi-objective optimisation problems can be further introduced to find the optimal policy. Third, the estimation of weather conditions, FPP, fuel prices, and waiting times can be further modelled by Bayesian information.

Chapter 5

Payment Structures, NPV Analysis and Letters of Credit in Tramp Shipping

As illustrated in Chapter 2, non-payment risk is omitted in the mathematical modelling for tramp ship optimisation problems. However, payment amount and/or payment time may not be as agreed and thus may impact the cash-flows for shipper, carrier and consignee. When discussing the objective of carriers in tramp shipping, the total profit, i.e. revenue minus the total cost related to sailing route, speed and outer environment (Ronen, 1982; Magirou et al., 2015; Norstad et al., 2011), or in format of NPV (Ge et al., 2021), also see Chapter 4 and 5, all assume that the revenue could be received in full and on time, for example, when the carrier presents the Bill of Lading at the destination port. In this chapter, we propose the payment structures when non-payment risk exists.

Conventional speed optimisation problems in tramp shipping determine the freight revenue as constant after the decision maker decided to undertake the job, which leads to the objective function being formulated to minimise the total, or maximise the profit, in total or per day. All of these assume there is no payment delay or non-payment during the transaction period and do not consider the time value of money. Neither of which holds true in reality. This chapter develops a Net Present Value (NPV) model to generally describe payment structures under a variety of freight payment terms, including Freight Prepaid (FP) and Freight Collect (FC), and shipment terms, including Free-on-Board Origin (FOB-O), Free-on-Board Destination (FOB-D), Cost and Freight (CFR), Cost, Insurance, and Freight (CIF) (Gorton, 2009; Baughen, 2018). We demonstrate the cash-flows are symmetric when all parties have extended trust when conducting business activities with each other, which means there is no non-payment risk with freight charges. While the trust among all parties is weaker than extended trust, i.e., basic trust or guarded trust, additional monitoring mechanisms are required to assure all parties are liable to comply with the contract. Letter of Credit (LC), as a financial instrument that has been widely used in international trade, is discussed in this paper, especially for the transaction for freight charges. Variations in Letters of Credit are addressed in the payment structure. Computational

results reveal that when the unit freight rate is determined, Red Clause Letters of Credit (RCLC) are more advantageous than other types of LC, i.e., Irrevocable Confirmed Letters of Credit (ICLC), and Letters of Credit at sight (LC at sight), especially when the carrier has inadequate liquidity cash flows. Whereas, decisions of taking LC at sight first-order stochastic dominate RCLC when the time period of asymmetric cash-flows for RCLC first-order stochastic dominates LC at sight.

5.1 Introduction

A recurring problem in international commodities trading is that buyers and sellers are concerned about whether the other party will be able to fulfil the contractual obligations. This problem becomes more difficult to resolve when the trading parties come from different countries due to litigation in a foreign country may be time-consuming, expensive, and without a guarantee of success. A simple example is that a purchaser of a certain amount of goods would prefer not to pay a distant seller the price of the products without confirmation that the required items will be supplied in accordance with the contract. However, a seller would want to get paid before relinquishing control of his items (Clarke et al., 2017). Under this background, the documentary credits and independent guarantees are motivated to be developed (Enonchong, 2007; Todd, 2013).

Guarantees of Letters of Credit (LC) are not limited to trading but are also used for certain performance of services (Joseph, 1977; Deak, 1980). This paper considers cases where the freight charges in tramp shipping are paid by LC or its variations. The problem is described as follows: the shipper (who could be the same party as the seller in international trade), the consignee (who could be the same party as the buyer in international trade), and the carrier have made an agreement on transport itself. Freight payment terms define who pays the freight charge and the type of payment terms, including combinations of Free on Board (FOB), Cost and Freight (CFR), and Cost, Insurance, and Freight (CFI); and Freight Prepaid (FP) and Freight Collect (FC). However, the party who is liable to pay freight charges may negotiate with the carrier to complete the transaction of freight payments by LC rather than using an opening account, a cheque, or others. Under such a case, the party who is liable to pay freight charges becomes the 'buyer' for shipping services, and the carrier becomes the 'seller' to provide services. By utilising the LC, on the one hand, the shipper or consignee will have guarantees that the freight charges won't be paid until the carrier provides proof (usually the clean BoL) that he or she has fulfilled the duties assigned to him or her under the terms of their shipping contract. On the other hand, the carrier is guaranteed to be paid by a third-party (usually a bank) after showing the proof which is ready to be examined (Dolan, 2007; Carr and Stone, 2013).

This paper elucidates the origins of the willingness of LC to pay freight charges: (a). the lack of extended trust among parties involved in the shipment; (b). the party who is liable to pay freight charges would potentially have better management of cash flows; and (c). the non-payment risk is reduced for the carrier. Respectively, contents of payment structures under business that

parties share extended trust and weaker trust support are shown in Section 5.3-5.4 to demonstrate (a). NPV analysis for the shipper or consignee under different payment structures are shown in Section 5.3-5.4 to support (b); and (c) is supported by the content about LC in Section 5.5.1-5.5.2.

The main contribution of this paper could be concluded as follows: firstly, a variety of freight payment terms are described by a general payment structure model and employed by the approach of NPV; secondly, the non-payment risk is addressed by considering the business in shipping when all parties have an extended trust and a relatively weaker trust. We further prove that documentary credit, such as LC, is not necessary in an extended trust business as there is a non-payment risk. In contrast, LC will be taken into account to reduce the wide range of risks raised by the party entitled to the ownership of cargo and the carrier, by which means the cost of the transaction will be increased owing to the lower level of trust; thirdly, for weaker trust business with LC, we discuss a wide range of options for LC and provide analysis about NPV for the carrier. To the best of our knowledge, this paper first addresses terms and clauses about freight charges in the field of admiralty law using mathematical models. The NPV analysis and discussions about non-payment risk could help carriers better choose terms and clauses before negotiating the agreements. Also, our model provides insights for professionals in the shipping industry about how to select the best freight charge terms for different types of carriers.

5.2 Literature review

The International Chamber of Commerce (ICC) built a collection of pre-defined commercial terminology known as the Incoterms, or International Commercial Terminology, with respect to international commercial law. Since the establishment of the first version of Incoterms in 1923, it has been developed several times, and the newest set[26], Incoterms 2020, is the ninth version, having been published on September 10, 2019. According to Incoterms 2020, terms such as FOB, CFR, and CIF define the point that the responsibility of taking care of cargoes is transferred from the seller (usually the same party as the shipper) to the buyer (usually the same party as the consignee). Both terms are popularly chosen in the international shipping markets; moreover, certain advantages are accompanied by both terms. In CFR, sellers are liable to deal with the delivery process, which includes packaging, organising the transporting process, securing the cargoes' value until the cargoes are well delivered and received by the buyer. CIF is similar to CFR except the seller is required to buy insurance to mitigate the risk of damages or losses for the cargoes during transit. The complex handling process reveals CIF and CFR are more suitable for sellers with more professions in the shipping market, such as large companies. Buyers also prefer to buy CIF or CFR when they lack expertise in the delivery process. FOB, as another common term of the 11 International commerce terms (Incoterms), consists of 'FOB Origin' and 'FOB Destination'. The attached word of place defines where the ownership of cargoes will be transferred and who will take responsibility to replace the damaged or lost items. For example, 'FOB Origin' defines that ownership of cargoes is transferred to the

[26] Available at: *https://iccwbo.org/business-solutions/incoterms-rules/incoterms-2020*.

buyer once the shipment starts, and the buyer is obliged to take care of the cargoes from damage or loss. 'FOB Destination' defines the title of cargoes as being reserved by the seller, and the buyer takes the responsibility to replace the damages and losses until cargoes are received by the buyer at the predetermined destination.

Buying FOB, CFR and CIF does not mean all additional costs that occurred during the no-liability period will be exempt. Sellers and buyers, who also play the roles of shipper and consignee, respectively, should follow the obligations attributed to themselves according to the BoL. A general case is that the buyer bought the CFR and let the seller take charge of the transportation process; however, as the consignee, he or she does not suspect the condition of the cargo and record the problem neither at the time of delivery nor at the soonest possible time at the warehouse. In such cases, if the buyer finds there are any loss or damage to cargoes, the freight claims cannot be accomplished due to the failure to perform the obligation stipulated in the BoL about checking the status of cargoes during the delivery process. The seller does not have to pay for the loss or damage to cargo. Another case is found in disputes about who pays demurrage fees. If the lateness of cargo collection, loss or damage is caused by the shipper who did not provide correct consignment information in detail, shippers are liable to compensate the carrier for the demurrage fee (including the extra cost), daily hire cost, and loss of profitability; compensate the buyer for the freight claim.

The most common Incoterms used in tramp shipping is FOB, which could be further subdivided into FOB Origin Freight Collect (FOB-O-FC), FOB Origin Freight Prepaid (FOB-O-FP), FOB Origin Freight Prepaid Charge Back (FOB-O-FPCB), FOB Destination Freight Collect (FOB-D-FC), FOB Destination Freight Prepaid (FOB-D-FP), and FOB Destination Freight Collect Allowed (FOB-D-FCA) with the feature of payment plan. CFR and CIF are sometimes used in practice too, and the freight charges are always prepaid by one party between the shipper and consignee. We conclude the characteristics of all considered combinations of terms and freight payments, which include: who pays for freight charges; who bears freight charges (additional costs happened during shipment); who owns cargo in transit (during shipment); and who files claims, if there are any, in Table 23, respectively.

TABLE 23: Characteristics of terms and freight payment discussed in this paper

Terms	Freight payment	Scheduled freight charges	Additional freight charges	Ownership of cargoes in transit	Files claims	Cargo insurance
FOB-O	FC	CNEE	CNEE	CNEE	CNEE	✓
FOB-O	FP	SHPR	SHPR	CNEE	CNEE	✓
FOB-O	FPCB	SHPR	CNEE	CNEE	CNEE	✓
FOB-D	FC	CNEE	CNEE	SHPR	SHPR	✓
FOB-D	FP	SHPR	SHPR	SHPR	SHPR	✓
FOB-D	FCA	CNEE	SHPR	SHPR	SHPR	✓
CIF	FP	SHPR	SHPR	CNEE	CNEE	✓
CFR	FP	SHPR	SHPR	CNEE	CNEE	×

[1]CNEE: Consignee; SHPR: Shipper; FOB-O: Free-on-Board Origin; FC: Freight Collect; FP: Freight Prepaid; FPCB: Freight Prepaid Charge Back; FOB-D: Free-on-Board Destination; FCA: Freight Collect Allowed. Cargo insurance is forced into the price of cargoes.

The difference between CIF and CFR in the aspect of freight charges are, the shipper is obligated to buy cargo insurance in CIR, while in CFR the shipper is not. There are multitudes of types of marine insurance in the shipping market. In this paper, we mainly discuss two types of

insurance in payment structure that will be introduced in further sections: freight insurance and cargo insurance. Of the two, the former is purchased by the freight forwarder (same as the carrier in tramp shipping) to make sure that forwarders are protected from legal liability in cases where faults or negligence contribute to lost or damaged goods. And when loss or damage during the transportation process happen, the claim will be based on the weight of the cargo. Whereas the latter is meant to protect the interests of the owner of the cargo, which could be the shipper or the consignee, depending on the terms [27]. And the value will be claimed as the commercial value of the cargoes.

For a time-chartered carrier in tramp shipping, freight insurance could be bought for the coverage as time-based, voyage-based, or a combination of both. More classifications will not be addressed in this paper. We simplify the modelling of payment structures for freight insurance and cargo insurance in Section 5.3-5.4 as follows: the freight insurance is always bought by the carrier as voyage-based after the BoL is agreed upon by three parties; the cost of insuring the cargo during shipment is already factored into the price of the actual cargoes. When the loss or damage that happens during the shipment is eligibly covered by cargo insurance and freight insurance, the party who files the claim must provide information about the shipment itself, the type of loss or freight damage, the amount of the freight claim or estimate, and the demand for payment within the claim period as indicated on the BoL. Besides, supporting documents are required to be provided, such as the original BoL, proof of the paid freight bill, proof of the value of the commodities lost or damaged, and inspection reports. The party who lacks submission of documents may cause a delay in the inspection or receipt of claims. The price of cargo insurance will not be covered since it is not the goal of this study to explore the cash flows between demand and supply between seller and buyer. The insurance fee discussed in further sections is for freight insurance.

LC is commonly used as a financial instrument that plays the role of a guarantee issued by a bank or equivalent third-party organisation that assures the seller (either for goods or services) that they will receive the payment on time and with the correct amount regardless of the buyer's ability to pay in full. There are several variations of LC to work for divergent needs and purposes (Harfield, 1985). Focusing on the enforceability of credit offered, there are revocable and irrevocable letters of credit. The former allows the issuing bank to change or revoke the credit at any moment without providing the seller with prior notice. And the latter requires all parties involved in a LC, including the buyer, issuing bank, seller, and any confirming bank, to consent to the changes before they are made. According to whether the credit is guaranteed by another bank (also called a confirming bank), if the issuing bank fails to pay the amount in full, LCs are divided into confirmed and unconfirmed letters of credit. Besides, there are transferable and non-transferable letters of credit, letters of credit at sight, and a red clause letters of credit. It is obvious that revocable letters of credit lack the security that the carrier needs; thus, UCP 600

[27] Although the object being protected is more than often interpreted as the shipper, sender, or manufacturer, we consider there is an alignment between ownership and title of claim. When ownership is transferred from one party to another during shipment, the title of the claim in certain insurance policies should be passed on simultaneously.

demonstrates that the LC should only be permissible in irreversible forms [28]. Unconfirmed letters of credit are rarely used in practice due to the same reason. This paper assumes the LC used and agreed by all parties are a confirmed irrevocable letter of credit, it implicitly ensures the payment will sent either by the issuing bank, or confirming bank after carrier present essential documentations.

We further discuss the at sight letters of credit and red clause letters of credit in Section 5.5. The former requests the issuing bank completes payments as soon as the carrier presents the proof delivery (BoL). The latter establishes an obligation on the issuing bank to provide partial payments to the carrier before the shipment starts. Compared to general LC, the carrier may receive the freight payment sooner under at-sight letters of credit. And red clause letters of credit seem to correspond more to the specific application in tramp shipping, while the carriers need to consume a large amount of money for bunkering at the departure port before the shipment. The cost of bunkering accounted for approximately 42 percent of the total operating cost when the bunker price was assumed to be 300 USD per tonne (Stopford, 2008; Stefanakos and Schinas, 2014). The last half-yearly and yearly averages of global bunker prices are 665.50 and 698 USD per tonne, respectively[29]. A higher percentage is able to be deducted from the increased unit bunker price, which means the carrier needs to advance more before finally getting paid the freight charges that include the total cost of shipping. The partially cash-in-advance in red clause letters of credit allows the carrier to use the money to bunker fuels or pay for daily hire costs beforehand, presenting the BoL (Hinkelman, 2003). It provides more opportunities for carriers who do not have sufficient money to support the basic operation of shipping and undertake jobs.

To the best of our knowledge, this paper seems to be the first to develop the different payment terms for freight charges in shipping using mathematical models and employ the approach of NPV to discuss which is the most advantageous term for carriers. There are some studies that investigate Trade Credit Insurance (TCI), which is used as a protection by suppliers to avoid default risk against credit buyers in supply chain management (Yang et al., 2021). However, the contracts and LC discussed in this paper are based on a different framework where the LC is not only chosen as an additional security but also involved by underlying payment terms.

5.3 NPV employed payment structure analysis for extended trust business

In the business of shipping, the terms of payment of freight are generally categorised as FP and FC, depending on the party paying the freight and the time of payment. Assume the shipper needs to transport a batch of cargoes of size Q from port A to port B. The consignee expect to collect the amount of Q cargoes at port B at time T. The taxonomy, quantity of cargoes,

[28] UCP 600 are the latest revision of the Uniform Customs and Practice that govern the operation of letters of credit. Available at :*http://static.elmercurio.cl/Documentos/Campo/2011/09/06/2011090611422.pdf*

[29] The data is collected from *https://shipandbunker.com/prices/av/global/av-glb-global-average-bunker-price*; the half-yearly data is collected from 10-04-2023 to 10-10-2023; the yearly data is collected from 10-10-2022 to 10-10-2023.

destination are all specified in the legal document 'Bill of Lading' (BoL), that is issued by the shipper, carrier, and consignee together. These obligations and responsibilities of each of the three parties involved in a transaction are as well outlined in BoL. The carrier plans the voyage and secures the cargo in accordance with the BoL and aims to complete delivery within the predetermined delivery time window. Additional terms may indicate the liability and responsibility as a supplement, i.e. FOB, CFR, CIF, insurance document, etc. Some of them had been discussed in Section 5.2.

The extended trust business is defined to describe the situation that there is three parties in the BoL have extended trust with each other, and there is no payment delay or non-payment happens during the transaction period. Extended trust is proposed in (Brenkert, 1998a,b) to describe a type of trust between parties with partnership in business which enables organisations to participate in more intricate relationships, which allows for the reduction of monitoring systems, resulting in more adaptable and economical agreements for both parties. It leads to no need to consider counterparty credit exposure during the transaction period as the transparency of itself. Paying certain premium to invoke clearinghouse or buying insurance about freight payments is unfavourable for parties with extended trust. While, some other types of insurances, such as public liability insurance and workers compensation insurance may still be required by the local law or the shipper. The carrier warrants to the shipper that obligatory insurances will be purchased.

We develop a general payment structure to include the terms addressed in Table 23 after considering the main difference in payment structure among these: the party who files the claim should be the same as the owner of the cargo during shipment, which is either the shipper or the consignee; scheduled freight charges or additional freight charges may be paid by different parties separately or together.

If the freight payment is FC, carrier bills the freight charges once after the shipment and will be paid by the consignee or together with the shipper depends on it is FC or FCA. Let t^{bill3} denotes the time that carrier send the bill, and t^{bill3_c} denotes the time that the party who is liable to pay the bill completes the payment. Similarly, for FP, define the carrier bills the scheduled freight charges at time t^{bill1} and the additional freight charges at time t^{bill2}. Let t^{bill1_c} and t^{bill2_c} denote the time that the party who is liable to pay the bill completes the payment. Then, all payment terms could be represented by a matrix about freight payment as follows:

$$\beta = \begin{bmatrix} \beta_{11} & \beta_{12} \\ \beta_{21} & \beta_{22} \\ \beta_{31} & \beta_{32} \end{bmatrix}, \tag{5.1}$$

where when $i = 1, 2$:

$$\beta_{i1} = \begin{cases} 1, & \text{for shipper liable to pay bill i in full,} \\ 0, & \text{otherwise,} \end{cases} \tag{5.2}$$

and,

$$\beta_{i2} = \begin{cases} 1, & \text{for consignee liable to pay bill j in full,} \\ 0, & \text{otherwise.} \end{cases} \tag{5.3}$$

and when $i = 3$,

$$\beta_{i1} = \begin{cases} R^{add}/(R^j + R^{add}), & \text{for shipper liable to pay the part of additional freight charges in bill 3,} \\ 0, & \text{otherwise.} \end{cases} \tag{5.4}$$

$$\beta_{i2} = \begin{cases} R^j/(R^j + R^{add}), & \text{for consignee liable to pay the part of scheduled freight charges in bill 3,} \\ 0, & \text{otherwise.} \end{cases} \tag{5.5}$$

Furthermore, depends on who owns the cargo during shipment and files the claim, define a matrix about insurance claim as follows:

$$\gamma = \begin{bmatrix} \gamma_1 & \gamma_2 \end{bmatrix}. \tag{5.6}$$

where:

$$\gamma_1 = \begin{cases} 1, & \text{for shipper liable to file claim,} \\ 0, & \text{otherwise,} \end{cases} \tag{5.7}$$

and,

$$\gamma_2 = \begin{cases} 1, & \text{for consignee liable to file claim,} \\ 0, & \text{otherwise.} \end{cases} \tag{5.8}$$

Thus, we are able to conclude all terms addressed in Table 23 by different β and γ. Specifically, for FOB-O-FC, the β and γ is written by:

$$\beta = \begin{bmatrix} 0 & 0 \\ 0 & 0 \\ 0 & 1 \end{bmatrix}, \quad \gamma = \begin{bmatrix} 0 & 1 \end{bmatrix}. \tag{5.9}$$

For FOB-O-FP, CIF-FP, and CFR-FP, the β and γ is written by:

$$\beta = \begin{bmatrix} 1 & 0 \\ 1 & 0 \\ 0 & 0 \end{bmatrix}, \quad \gamma = \begin{bmatrix} 0 & 1 \end{bmatrix}. \tag{5.10}$$

For FOB-O-FPCB, the β and γ is written by:

$$\beta = \begin{bmatrix} 1 & 0 \\ 0 & 1 \\ 0 & 0 \end{bmatrix}, \quad \gamma = \begin{bmatrix} 0 & 1 \end{bmatrix}. \tag{5.11}$$

For FOB-D-FC, the β and γ is written by:

$$\beta = \begin{bmatrix} 0 & 0 \\ 0 & 0 \\ 0 & 1 \end{bmatrix}, \quad \gamma = \begin{bmatrix} 1 & 0 \end{bmatrix}. \tag{5.12}$$

For FOB-D-FP, the β and γ is written by:

$$\beta = \begin{bmatrix} 0 & 1 \\ 0 & 1 \\ 0 & 0 \end{bmatrix}, \quad \gamma = \begin{bmatrix} 1 & 0 \end{bmatrix}. \tag{5.13}$$

For FOB-D-FCA, the β and γ is written by:

$$\beta = \begin{bmatrix} 0 & 0 \\ 0 & 0 \\ R^{add}/(R^j + R^{add}) & R^j/(R^j + R^{add}) \end{bmatrix}, \quad \gamma = \begin{bmatrix} 1 & 0 \end{bmatrix}. \tag{5.14}$$

Thus, the general payment structure and NPV could be given for all parties involved. A stream of events is shown as follows:

It is notable that the stream of events as shown in Figure 15 does not mean the strict sequence of events in temporal. For example, the time when shipper completes payment for bill 1 could later than when sailing starts, or even later than sailing ends, so long as the time difference between t^{bill1_c} and t^{bill1_b} is less than the latest payment period allowed in bill 1. For example, if carrier requires the shipper completes the payment no later than 30 days after receival of the bill 1, there is:

$$t^{bill1_b} \leq t^{bill1_c} \leq t^{bill1_b} + 30/365. \tag{5.15}$$

More generally, define the carrier actually requires the shipper completes the payment no later than L^{bill1} and L^{bill2} days after receival of the bill 1 and bill 2, separately, there are:

$$t^{bill1_b} \leq t^{bill1_c} \leq t^{bill1_b} + L^{bill1}/365, \tag{5.16}$$

and,

$$t^{bill2_b} \leq t^{bill2_c} \leq t^{bill2_b} + L^{bill2}/365. \tag{5.17}$$

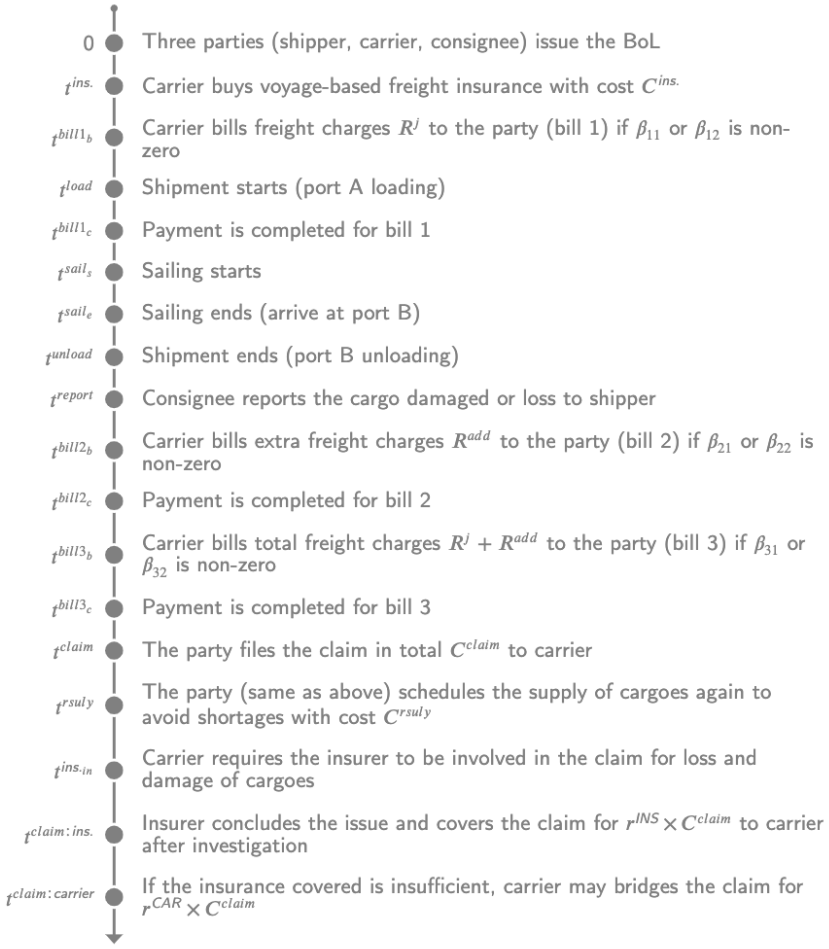

FIGURE 15: A general stream of events applicable for multiple terms

Similarly, for the bill 3 under FC, define the party who is liable to pay the bill should complete the payment no later than L^{bill3} days after receival of the bill 3, there is:

$$t^{bill3_b} \leq t^{bill3_c} \leq t^{bill3_b} + L^{bill3}/365. \tag{5.18}$$

The items may be inspected by the consignee, who has the right to reject them if they are damaged or differ from the description. The inspection needs to be accomplished at the soonest possible time and location; regularly, this happens to be the consignee's warehouse or place of business. The consignee ought to check the cargo for loss or damage at the time of delivery and record any problems on the delivery receipt; this will be used as proof to support the claim. The party who takes the responsibility to files the claim if there is any should be reach out the carrier within L^{claim} days after the delivery, where L^{claim} is indicated by the insurance policy. After receiving the claim, the carrier is compulsory to move the case to insurer for further investigation [30]. Meanwhile, the insurer is required to close the issue within L^{ivcl} days after receiving the

[30] In practice, if the carrier does not buy freight insurance, the claim will only be covered by carrier liability coverage, there will be no insurer involved. The claim must be satisfactory in that: loss or damage is noted at BoL; the carrier's negligence is proven; the value of cargoes is proven; and the claim is filed within the period.

claim. Constraints of above time limit are expressed as follows:

$$t^{unload} \leq t^{report} \leq t^{unload} + L^{claim}/365, \tag{5.19}$$

and,

$$t^{INS_{in}} \leq t^{claim:ins.} \leq t^{INS_{in}} + L^{ivcl}/365. \tag{5.20}$$

Due to the assumption of market, cash-in and cash-out happens simultaneously when one party completes the payment to another party. Then, based on the stream of events as shown above, we present a symmetric cash-flows for all three parties involved have extended trust in Figure 16.

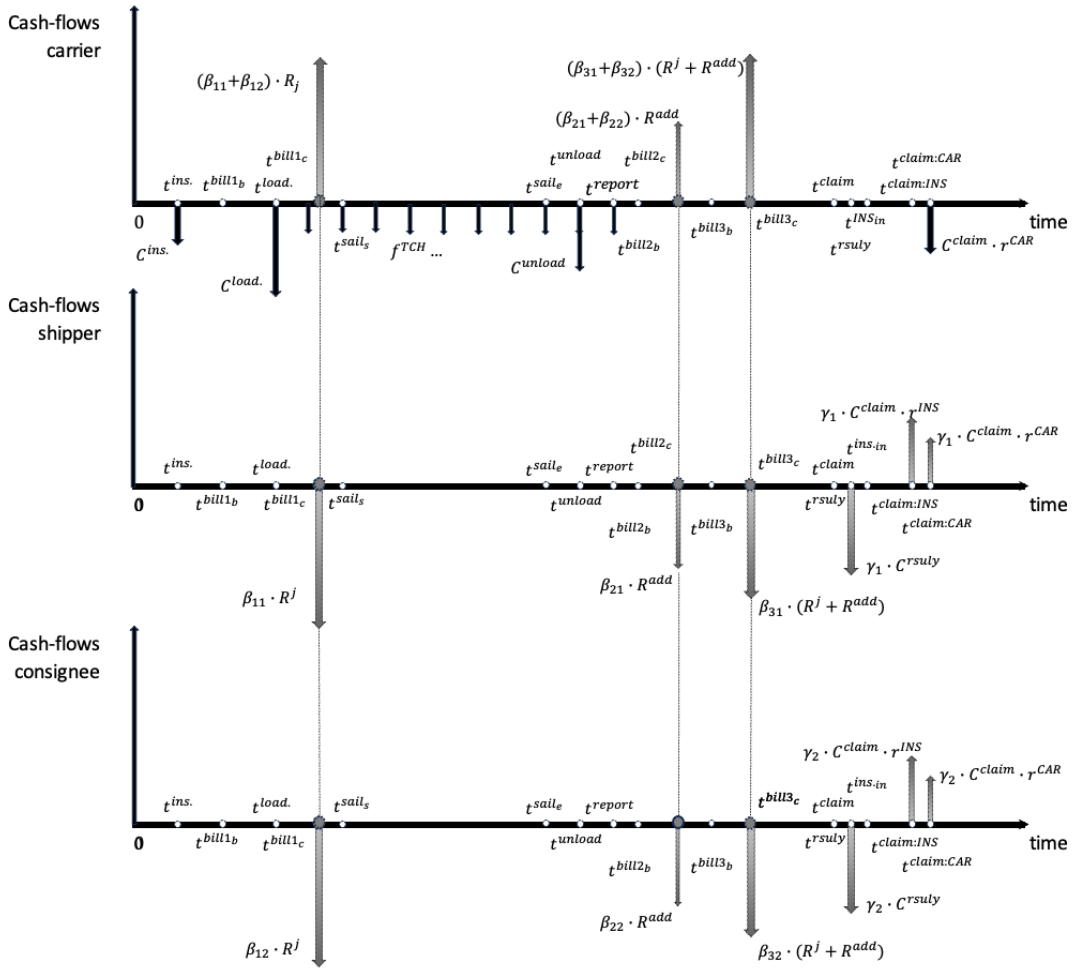

FIGURE 16: A symmetric cash-flows for carrier, shipper and consignee under general terms and extended trust

It is notable the dashed line in Figure 16 does indicates the payments have zero delay. Beullens and Janssens (2014) explains the symmetric payment is a conventional payment structure. When the shipper pays out bills of freight charges, the carrier receives the money 'immediate' and 'in

full'. It is the perfect results when no clearinghouse is involved. The NPV for carrier (*CAR*), shipper (*SHPR*), and consignee (*CNEE*) is given as follows[31]:

$$\begin{aligned}\mathrm{NPV}_{CAR} = \quad & -C^{ins.} \cdot e^{-\alpha t^{ins.}} - C^{load} \cdot e^{-\alpha t^{load}} - \int_{t^{load}}^{t^{report}} f^{TCH} \cdot e^{-\alpha t} \mathrm{d}t + (\beta_{11} + \beta_{12}) \cdot R^{j} \cdot e^{-\alpha t^{bill1_c}} \\ & -C^{unload} \cdot e^{-\alpha t^{unload}} + (\beta_{21} + \beta_{22}) \cdot R^{add} \cdot e^{-\alpha t^{bill2_c}} + (\beta_{31} + \beta_{32}) \cdot (R^{j} + R^{add}) \cdot e^{-\alpha t^{bill3_c}} \\ & -C^{claim} \cdot r^{CAR} \cdot e^{-\alpha t^{claim:CAR}},\end{aligned} \tag{5.21}$$

$$\begin{aligned}\mathrm{NPV}_{SHPR} = \quad & -\beta_{11} \cdot R^{j} \cdot e^{-\alpha t^{bill1_c}} - \beta_{21} \cdot R^{add} \cdot e^{-\alpha t^{bill2_c}} - \beta_{31} \cdot (R^{j} + R^{add}) \cdot e^{-\alpha t^{bill3_c}} - \gamma_1 \cdot C^{rsuly} \cdot e^{-\alpha t^{rsuly}} \\ & +\gamma_1 \cdot C^{claim} \cdot r^{INS} \cdot e^{-\alpha t^{claim:INS}} + \gamma_1 \cdot C^{claim} \cdot r^{CAR} \cdot e^{-\alpha t^{claim:CAR}},\end{aligned} \tag{5.22}$$

$$\begin{aligned}\mathrm{NPV}_{CNEE} = \quad & -\beta_{12} \cdot R^{j} \cdot e^{-\alpha t^{bill1_c}} - \beta_{22} \cdot R^{add} \cdot e^{-\alpha t^{bill2_c}} - \beta_{32} \cdot (R^{j} + R^{add}) \cdot e^{-\alpha t^{bill3_c}} - \gamma_2 \cdot C^{rsuly} \cdot e^{-\alpha t^{rsuly}} \\ & +\gamma_2 \cdot C^{claim} \cdot r^{INS} \cdot e^{-\alpha t^{claim:INS}} + \gamma_2 \cdot C^{claim} \cdot r^{CAR} \cdot e^{-\alpha t^{claim:CAR}}.\end{aligned} \tag{5.23}$$

5.4 NPV employed payment structure analysis for weaker-trust business

Models presented in Section 5.3 assume the party who is obliged to pay freight charges or bear additional freight fees always fulfils and has the ability to fulfil the contractual obligations. However, in practice, it is not always true. The risk of delay in payment, failure to pay, or one of the two parties between the shipper and consignee going bankrupt and not having the ability to fulfil the obligation anymore does exist, whereas the carrier cannot ignore it. We conclude the risk relevant to the above scenarios as 'payment risk'.

In this section, we introduce the NPV employed payment structures under the weaker-trust business. We mainly discuss the potential payment risk, specifically the situation that the party who is liable to pay the freight charges cannot fulfil or loses the ability to fulfil the contractual obligation about paying on time, specifically, without the letter of credit for the unpaid freight charges. Such an unpaid bill will affect the carrier's cash flow and possibly change the vessel's further business (when return or re-delivery is required in some cases). We summarise that there are generally two cases of late payment: one is represented by the bill being paid later than the time negotiated but still being cleared at time t^{odc}(usually at an overdue rate r^{od}), the other is that the payment is not cleared. In practice, if the carrier faces the latter situation, according to the contract and terms that indicate the ownership of cargoes, the carrier may need to transport the cargo back to the initial port (return) or reschedule the delivery (re-delivery), or in some cases, have the right to dispose of cargoes (usually when the value of the cargo is not high or not worth

[31] Under FTB, $(\beta_{i1} + \beta_{i2}) \equiv 1$ for $i = 1, 2, 3$.

transporting back to the departure port). For the shipper and consignee, an overdue bill will affect the claim process either under cargo insurance or freight insurance.

For business that parties has weaker trust, $\beta_{i1} + \beta_{i2}$ is unnecessarily equals to 1, which is written as:

$$0 \leq \beta_{i1} + \beta_{i2} \leq 1, \quad i = 1, 2, 3. \tag{5.24}$$

Define payments made later than the last bill's deadline as R_j^{late} at time t_j^{late}, $j = 1, 2, \ldots, n$. The series of payment made after $t^{bill3_b} + L^{bill_3}/365$ is for paying the outstanding bill. Thus, define the amount of outstanding bill as R^{os}, which is:

$$R^{os1} = (1 - \beta_{11} - \beta_{12}) \cdot R^j, \tag{5.25}$$

$$R^{os2} = (1 - \beta_{21} - \beta_{22}) \cdot R^{add}, \tag{5.26}$$

$$R^{os3} = (1 - \beta_{31} - \beta_{32}) \cdot (R^j + R^{add}), \tag{5.27}$$

and the corresponding overdue time is defined by t^{osi} where $i = 1, 2, 3$ as follows:

$$t^{osi} = \mathbb{1}_{1-\beta_{i1}-\beta_{i2}>0} = \begin{cases} t^{billi_b} + L^{billi}/365, & \text{if} \quad 1 - \beta_{i1} - \beta_{i2} > 0, \\ 0, & \text{otherwise.} \end{cases} \tag{5.28}$$

The remaining amount of outstanding bill is denoted by:

$$R^{aosi} = \begin{cases} R^{osi}, & \text{for} \quad i = 1 \\ R^{osi} + R^{aosi-1} \cdot (1 + r^{od}/365)^{t^{aosi} - t^{aosi-1}}, & \text{for} \quad i = 2, 3 \\ R^{aosi-1} \cdot (1 + r^{od}/365)^{t^{aosi} - t^{aosi-1}} - (\gamma_1 + \gamma_2) \cdot R_{i-3}^{late}, & \text{for} \quad i = 4, \ldots, n. \end{cases} \tag{5.29}$$

The corresponding time for R^{aosi} is denoted by t^{aosi} and written as follows:

$$t^{aosi} = \begin{cases} t^{osi} & \text{for} \quad i = 1, 2, 3, \\ t_{i-3}^{late}, & \text{for} \quad i = 4, \ldots, n. \end{cases} \tag{5.30}$$

If all bills about freight charges are cleared before due date, there is no further payment about freight charges afterwards. This constraint is expressed by:

$$R_j^{late} \equiv 0, \quad \text{if} \quad R^{aos3} = 0, \quad \text{where} \quad j = 1, 2, \ldots, n. \tag{5.31}$$

Also, in case the initial bills were overdue, once the outstanding bill is cleared, there should not be payment made from other party afterwards, it is written as:

$$R_j^{late} \equiv 0, \quad \text{if} \quad R^{aosj+2} = 0, \quad \text{where} \quad j = 2, \ldots, n. \tag{5.32}$$

Consider that the period for which the shipping contract is valid is L^{max} after than the shipment starts, the last payment accounted should be completed before time $t^{load} + L^{max}$. We show the asymmetric cash-flows for carrier, shipper and consignee under general terms and weaker trust in Figure 17.

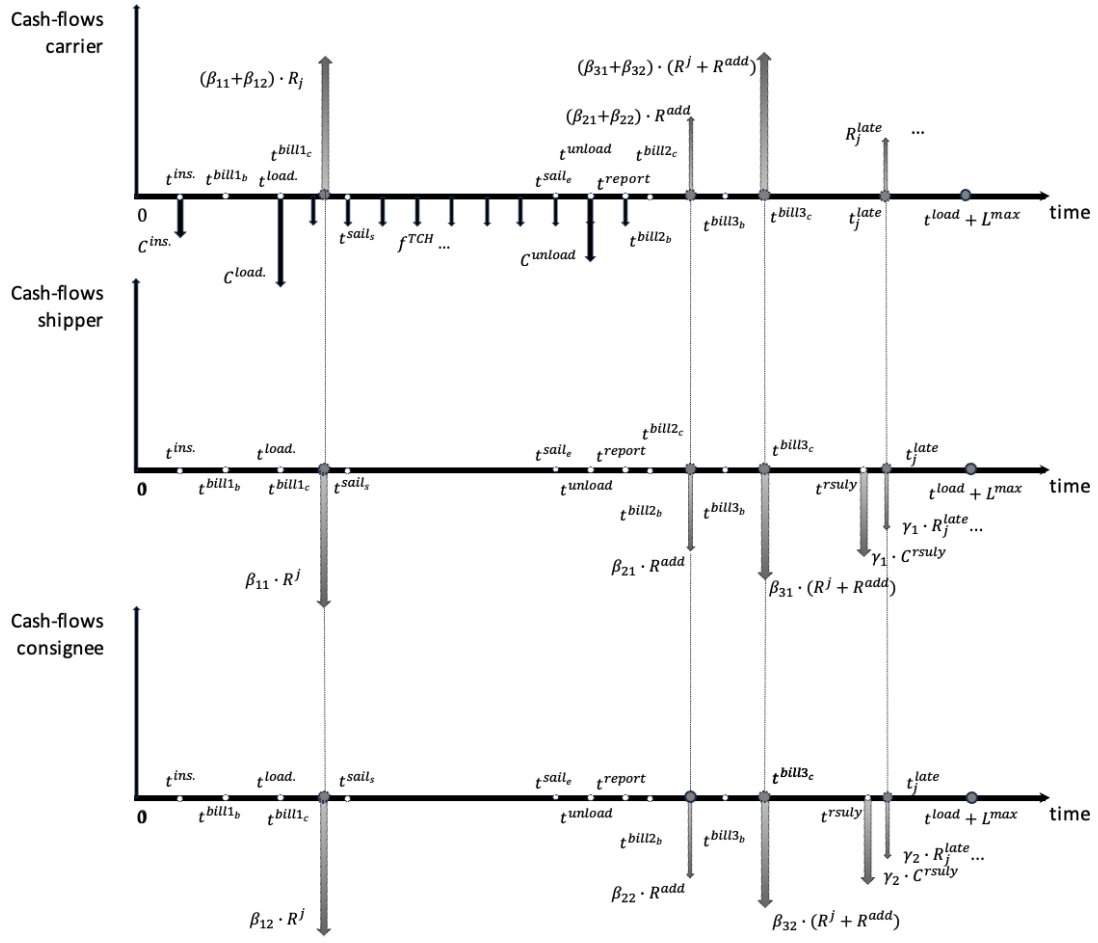

FIGURE 17: A symmetric cash-flows for carrier, shipper and consignee under general terms and weaker trust

The NPV for carrier, shipper, and consignee is given as follows:

$$\begin{aligned} \text{NPV}_{CAR} = \quad & -C^{ins.} \cdot e^{-\alpha t^{ins.}} - C^{load} \cdot e^{-\alpha t^{load}} - \int_{t^{load}}^{t^{report}} f^{TCH} \cdot e^{-\alpha t} \mathrm{d}t + (\beta_{11} + \beta_{12}) \cdot R^j \cdot e^{-\alpha t^{bill1_c}} \\ & -C^{unload} \cdot e^{-\alpha t^{unload}} + (\beta_{21} + \beta_{22}) \cdot R^{add} \cdot e^{-\alpha t^{bill2_c}} + (\beta_{31} + \beta_{32}) \cdot (R^j + R^{add}) \cdot e^{-\alpha t^{bill3_c}} \\ & + \textstyle\sum_{j=1,\ldots,n} (\gamma_1 + \gamma_2) \cdot R_j^{late} \cdot e^{-\alpha t_j^{late}}, \end{aligned} \tag{5.33}$$

$$\begin{aligned}\mathrm{NPV}_{SHPR} = \quad & -\beta_{11}\cdot R^{j}\cdot e^{-\alpha t^{bill1_c}} - \beta_{21}\cdot R^{add}\cdot e^{-\alpha t^{bill2_c}} - \beta_{31}\cdot (R^{j}+R^{add})\cdot e^{-\alpha t^{bill3_c}} \\ & -\gamma_1\cdot C^{rsuly}\cdot e^{-\alpha t^{rsuly}} - \textstyle\sum_{j=1,\dots,n}\gamma_1\cdot R_j^{late}\cdot e^{-\alpha t_j^{late}},\end{aligned} \tag{5.34}$$

$$\begin{aligned}\mathrm{NPV}_{CNEE} = \quad & -\beta_{12}\cdot R^{j}\cdot e^{-\alpha t^{bill1_c}} - \beta_{22}\cdot R^{add}\cdot e^{-\alpha t^{bill2_c}} - \beta_{32}\cdot (R^{j}+R^{add})\cdot e^{-\alpha t^{bill3_c}} \\ & -\gamma_2\cdot C^{rsuly}\cdot e^{-\alpha t^{rsuly}} - \textstyle\sum_{j=1,\dots,n}\gamma_2\cdot R_j^{late}\cdot e^{-\alpha t_j^{late}}.\end{aligned} \tag{5.35}$$

There are multiple methods to deal with the payment risk, including wisely choosing terms depending on different types of business partners, investigating the business partners independently or by a third-party agency, asking for LC if the bill has not been cleared when the party collects cargo at the destination port, purchasing trade credit insurance, or any combination of them. For example, if the shipper or consignee who is liable to pay freight charges chooses to pay by an LC, the bank that issued the LC will pay the carrier about the remaining freight charges if the shipper or consignee fails to do so[32]. According to the pricing policy for the LC, the bank will authorise or determine the credit amount on the LC through a full investigation of the applicant's creditworthiness and financial situation, such as cash liquidity, credit, and so on.

From the perspective of protecting the interests of the shipper, consignee, and carrier, LC allows a delay in freight charges flowing into the carrier's account, whereas the risk of unpaid invoices could be avoided. In order to unlock the service of the LC, the party who pays freight charges needs to foot the fees by themselves or spread the cost with other parties. The NPV model and some discussions of the value of LC will be addressed in Section 5.5.

5.5 Letters of Credit in weaker trust business

In this section, we consider employing the method of NPV in the payment structures of a single journey in tramp shipping with LC. As mentioned in Section 5.2, LC has a lot of variation according to its security, revocability, pay-in-advance and transferability. Due to UCP 600 have suggested the revocable and unconfirmed letters of credit are not recommended in practice, we will only address irrevocable confirmed letters of credit (ICLC), letters of credit at sight (LC at sight), and red clause letters of credit (RCLC).

Generally, LC plays a role as a guarantee of payments with certain benefits: The LC issued by the bank is trusted by all parties in the transaction, and its trustworthiness is much greater than that of ship brokers which leads to more effective protection; 2. LC ensures the safety of transactions and reliably avoids non-payment in the event that one of the parties defaults on payments or goes bankrupt, as the bank will be required to cover the full or remaining amount of the freight

[32] In practice, if the carrier has doubts about the creditworthiness of the bank that issued the LC, a confirmed LC will be requested as an extra protection; in case the first bank fails to do so, the second bank will take the obligation to pay.

charges. From the perspective of carriers, having an LC reduces the risk of unpaid invoices and loss of revenue. From the shipper's or consignee's side, it also protects their interests and avoids the situation where cargoes are not delivered but the freight charges are already transferred to the carrier's account (usually under freight prepaid); 3. LC potentially advances the liquidity of freight markets. Without the involvement of LC, carriers, shippers, and consignees will be more cautious about entering the market, starting business, and building partnerships with someone who has not yet established collaboration, i.e. evidence about trustworthiness is one of key factors when choosing business partners (Wuyts and Geyskens, 2005; Holloway and Parmigiani, 2016).

Considering the liabilities for all parties involved in a tramp shipping commission with provisions about freight charges being paid by LC, the payment structures for ICLC, LC at sight, and Red Clause LC are different. The asymmetric payment structures are shown for the underlying terms in Section 5.5.1.

5.5.1 ICLC and LC at sight: asymmetric payment structures without cash-in-advance

Consider the case where three parties made an agreement for a shipment that the party who pays freight charges should provide a LC if the freight charges has not been cleared at negotiated payment time. Same party takes the duty of getting the LC issued by the bank. The LC is singly approved for this transaction and will only be valid within a certain period. Let the amount explicitly authorised by the bank is CDT^{fc}, and the cost of obtaining this LC is denoted by $r^{\mathrm{LC}^{fc}} \cdot \mathrm{CDT}^{fc}$, which depends on the type of LC utilised, the applicant's credit history, safeguarding provisions, bank, and so on. Let $L^{\mathrm{LC}_c^{fc}}$ denotes the length of period that the carrier receives the LC and make the payment done by presenting necessary documents to the bank. Figure 18 shows the procedure for using LC as a payment method in practical shipping when LC is an ICLC or LC at sight. The procedures for using these two types of LC are no different whereas $L^{\mathrm{LC}_c^{fc}}$ may be varied.

The dashed line implies that the issuing bank is not necessarily the different bank from the confirming bank; thus, the carrier could either present the BoL to the issuing bank or the confirming bank, or even both. The same sequence number for payment includes cases where the applicant pays the freight charges to the issuing bank on time or defaults on payment. The carrier will get paid no matter which case happens.

According to Figure 18 and variables established for LC, we conclude key time points contain: the shipper or consignee request the ICLC or LC at sight at time $t^{\mathrm{LC}_a^{fc}}$, the issuing bank sends credit to the confirming bank $t^{\mathrm{CDT}}_{IB/CB}$, shipment starts t^{load}, shipment ends t_e^{sail}, carrier present the BoL $t^{CAR_{\mathrm{BoL}}}$, the shipper or consignee pays the freight charges to the issuing bank $t^{fc}_{(party)/IB}$, confirming bank pays the carrier $t^{fc}_{CB/CAR}$. Then, an asymmetric cash-flows for the party who request an LC about freight charges, issuing bank, confirming bank, and carrier is shown in Figure 19.

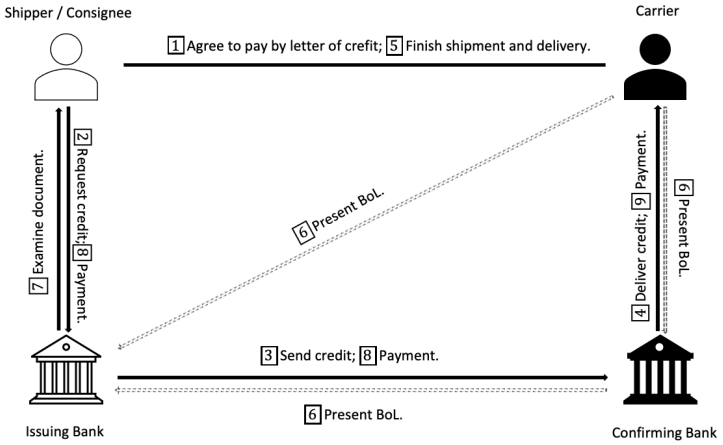

FIGURE 18: The procedures for using ICLC or LC at sight in a shipment

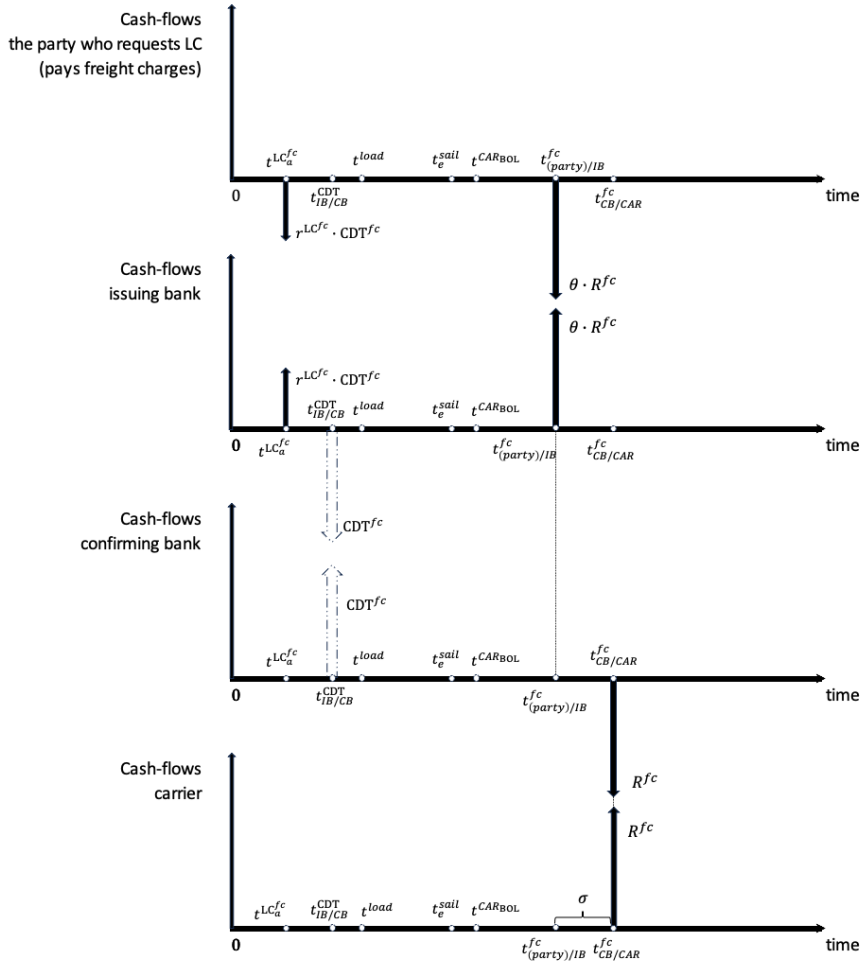

FIGURE 19: An asymmetric cash-flows for the party who request an ICLC or LC at sight about freight charges, issuing bank, confirming bank, and carrier

In Figure 19, dashed arrow represents the credit in the amount of CDT^{fc} authorised by issuing bank to confirming bank due to the latter taking the role of paying the freight charges to the

carrier after examining the BoL. In cases where the issuing bank is also the confirming bank, the dashed arrows could be eliminated and the solid arrows should be combined into one cash-flows. The cost of shipping in cash-flows for the carrier is left out in Figure 19 due to the same structure as Figure 17. After carrier presents the BoL, the party who request LC is liable to pay corresponding amount R^{fc} to the LC issuing bank. Let $\theta \cdot R^{fc}$ denotes the actual amount paid, where $0 \leq \theta \leq 1$. We point out the time period $\sigma = t^{fc}_{CB/CAR} - t^{fc}_{(party)/IB}$ potentially causes the asymmetric cash-flows when LC is used in business with weaker trust among parties. The unit of σ here could either be in days or years, as long as when time discounting the cash-flows σ should be converted to σ in years due to the α is a yearly based opportunity cost rate.

Compare asymmetric cash-flows paid by or not paid by LC, $\sigma = 0$ indicates the latter, while $\sigma > 0$ represents the former. The NPV about freight charges for the party who pays freight charges and the carrier is given as follows:

$$\mathrm{FC}^{\mathrm{LC}}_{(party)} = -r^{\mathrm{LC}^{fc}} \cdot \mathrm{CDT}^{fc} \cdot e^{-\alpha t^{\mathrm{LC}^{fc}_a}} - \theta \cdot R^{fc} \cdot e^{-\alpha t^{fc}_{(party)/IB}}, \tag{5.36}$$

and,

$$\begin{aligned} \mathrm{FC}^{\mathrm{LC}}_{CAR} &= R^{fc} \cdot e^{-\alpha t^{fc}_{CB/CAR}} \\ &= R^{fc} \cdot e^{-\alpha (t^{fc}_{(party)/IB} + \sigma)} \\ &= R^{fc} \cdot e^{-\alpha t^{fc}_{(party)/IB}} \cdot e^{-\alpha \sigma}. \end{aligned} \tag{5.37}$$

Subsequently, the NPV for carrier is written by:

$$\begin{aligned} \mathrm{NPV}^{\mathrm{LC}}_{CAR} = \quad & -C^{ins.} \cdot e^{-\alpha t^{ins.}} - C^{load} \cdot e^{-\alpha t^{load}} - \int_{t^{load}}^{t^{report}} f^{TCH} \cdot e^{-\alpha t} \mathrm{d}t - C^{unload} \cdot e^{-\alpha t^{unload}} \\ & + R^{fc} \cdot e^{-\alpha t^{fc}_{(party)/IB}} \cdot e^{-\alpha \sigma} - C^{claim} \cdot r^{CAR} \cdot e^{-\alpha t^{claim:CAR}}. \end{aligned} \tag{5.38}$$

To compare the difference of total freight charges and NPV in consequence by various σ, we define:

$$\triangle \mathrm{FC}^{\mathrm{LC}}_{CAR} = \mathrm{FC}^{\mathrm{LC}}_{CAR}|_{\sigma} - \mathrm{FC}^{\mathrm{LC}}_{CAR}|_{\sigma=0}, \tag{5.39}$$

and

$$\triangle \mathrm{NPV}^{\mathrm{LC}}_{CAR} = \mathrm{NPV}^{\mathrm{LC}}_{CAR}|_{\sigma} - \mathrm{NPV}^{\mathrm{LC}}_{CAR}|_{\sigma=0}. \tag{5.40}$$

To examine the impact of σ in payment structures where freight charges are paid by ICLC or LC at sight on the carrier's cash flow condition, experiments are designed, as shown in Table 24. We find that both freight charges calculated as NPV and total NPV for carriers will be affected by the value of σ. When σ increases from 0 to 30 days, the carrier will bear a loss of NPV of 0.1 million USD under the example. The difference in freight charges calculated as NPV and total NPV are consistent, which is caused by σ being the only variable relevant to freight charges under ICLC or LC at sight. Considering the issuing bank should pay carrier 'at sight' of

TABLE 24: Numerical results for different σ in payment structures that freight charges are paid by ICLC or LC at sight

Instance (in days)	$\mathrm{FC}^{\mathrm{LC}}_{CAR}$ $Eq.(5.37)$	$\triangle\mathrm{FC}^{\mathrm{LC}}_{CAR}$ $Eq.(5.39)$	$\mathrm{NPV}^{\mathrm{LC}}_{CAR}$ $Eq.(5.38)$	$\triangle\mathrm{NPV}^{\mathrm{LC}}_{CAR}$ $Eq.(5.40)$
1 ($\sigma = 0$)	13.532	-	15.220	-
2 ($\sigma = 10$)	13.498	-0.033	15.187	-0.033
3 ($\sigma = 20$)	13.465	-0.066	15.154	-0.066
4 ($\sigma = 30$)	13.432	-0.100	15.121	-0.100
5 ($\sigma = 40$)	13.399	-0.133	15.088	-0.133

[1]The speed $v = 12$ knots; the opportunity cost of capital rate per year $\alpha = 0.08$; results are given in million USD.

BoL, σ under LC at sight should be smaller than equivalent conditions under ICLC. Define two distributions for random variables σ are denoted by $F^{\text{LC at sight}}$ and F^{ICLC}, correspondingly, the distributions of the utility function $\mathrm{NPV}^{\mathrm{LC}}_{CAR}$ are given by $G^{\text{LC at sight}}$ and G^{ICLC},

Lemma 5.1. *$G^{\text{LC at sight}}$ first-order stochastically dominates G^{ICLC} if F^{ICLC} first-order stochastically dominates $F^{\text{LC at sight}}$.*

Proof. ($\Leftarrow$) The condition that F^{ICLC} first-order stochastically dominates $F^{\text{LC at sight}}$ is equivalent to $F^{\text{ICLC}}(\sigma) \leq F^{\text{LC at sight}}(\sigma)$, $\forall\sigma$; and $\exists\sigma$, $F^{\text{ICLC}}(\sigma) < F^{\text{LC at sight}}(\sigma)$. Further, $\mathrm{NPV}^{\mathrm{LC}}_{CAR}$ could be simplified to $\mathrm{NPV}^{\mathrm{LC}}_{CAR}(\sigma) = a + b \cdot e^{-\alpha\sigma}$, where $a < 0$, $b > 0$, $\alpha > 0$, $\sigma \geq 0$. Thus, $\mathrm{NPV}^{\mathrm{LC}}_{CAR}$ is continuous, strictly decreasing and convex, there is:

$$\forall\sigma, \quad G^{\text{ICLC}}(\sigma) = Pr(\mathrm{NPV}^{\mathrm{LC}}_{CAR}(\sigma^{\text{ICLC}}) \leq \sigma') \geq Pr(\mathrm{NPV}^{\mathrm{LC}}_{CAR}(\sigma^{\text{LC at sight}}) \leq \sigma') = G^{\text{LC at sight}}(\sigma), \tag{5.41}$$

and,

$$\exists\sigma, \quad G^{\text{ICLC}}(\sigma) = Pr(\mathrm{NPV}^{\mathrm{LC}}_{CAR}(\sigma^{\text{ICLC}}) \leq \sigma') > Pr(\mathrm{NPV}^{\mathrm{LC}}_{CAR}(\sigma^{\text{LC at sight}}) \leq \sigma') = G^{\text{LC at sight}}(\sigma), \tag{5.42}$$

then clearly, $G^{\text{LC at sight}}$ first-order stochastically dominates G^{ICLC}.

□

An example for Lemma 5.1 is when F^{ICLC} and $F^{\text{LC at sight}}$ are both discrete (also called as state-wise dominance). Let $F^{\text{LC at sight}} = (0, 0.2; 10, 0.5; 20, 0.2; 30, 0.1)$, and $F^{\text{ICLC}} = (0, 0.1; 10, 0.3; 20, 0.4; 30, 0.1; 40, 0.1)$. It is obvious that F^{ICLC} first-order stochasticaly dominates $F^{\text{LC at sight}}$. We calculated G^{ICLC} and $G^{\text{LC at sight}}$ according to Eq. (5.38). The Cumulative Density Function (CDF) for F^{ICLC}, $F^{\text{LC at sight}}$, G^{ICLC} and $G^{\text{LC at sight}}$ are shown in Table 25 as follows:

TABLE 25: $F^{\text{LC at sight}}$, G^{ICLC}, $G^{\text{LC at sight}}$, F^{ICLC}, and corresponding CDF

σ	$F^{\text{LC at sight}}$	CDF of $F^{\text{LC at sight}}$	F^{ICLC}	CDF of F^{ICLC}	$\sigma' = \mathrm{NPV}^{\mathrm{LC}}_{CAR}(\sigma)$	$G^{\text{LC at sight}}$	CDF of $G^{\text{LC at sight}}$	G^{ICLC}	CDF of G^{ICLC}
0	0.2	0.2	0.1	0.1	15.220	0.2	1	0.1	1
10	0.5	0.7	0.3	0.4	15.187	0.5	0.8	0.3	0.9
20	0.2	0.9	0.4	0.8	15.154	0.2	0.3	0.4	0.6
30	0.1	1	0.1	0.9	15.121	0.1	0.1	0.1	0.2
40	0	1	0.1	1	15.088	0	0	0.1	0.1

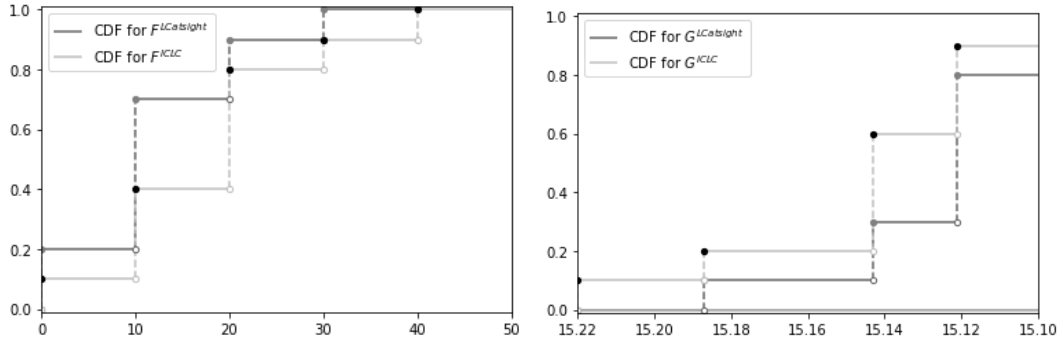

(a) CDF for $F^{\text{LC at sight}}$ and F^{ICLC}

(b) CDF for $G^{\text{LC at sight}}$ and G^{ICLC}

FIGURE 20: Plot of CDF for $F^{\text{LC at sight}}$, F^{ICLC}, $G^{\text{LC at sight}}$ and G^{ICLC}

The relationship of first-order stochastically dominance between F^{ICLC} and $F^{\text{LC at sight}}$, $G^{\text{LC at sight}}$ and G^{ICLC} is shown in Figure 5.20(a) and 5.20(b), respectively. In practice, σ for LC at sight is at least no larger than for ICLC, under the same circumstances. It implies that the distribution of the latter is first-order stochastically dominant over the former, and Lemma 5.1 is applicable.

Notably, we discuss the existence of anchor point in the NPV in the payment structure model that freight charges are paid by LC? The anchor point is introduced by Beullens and Janssens (2011) as an arbitrary moment in the future, chosen to coincide with the start or end of some activity, that does not change with a change in any of the policy variables or other parameters in the model. We discuss that the time point that receives freight charges is not an anchor point due to the small gap that exists between: carrier present BoL; IB or CB examine BoL; party pays IB; IB pays carrier. So, it is not an anchor point. However, in payment structures for tramp shipping paid with LC, parties are all acknowledged that carrier will receive the payment about freight charges at before time $t^{fc}_{CB/CAR}$ regardless the activity of shipper or consignee due to the term is irrecoverable. When the LC is additional confirmed, the activity of the first issuing bank is also negligible.

5.5.2 Red Clause LC: asymmetric payment structures with cash-in-advance

Unlike the payment structures for ICLC or LC at sight, Red Clause LC (RCLC) enables the carrier under the term to receive part of the credit before showing the BoL. We emphasise that this feature of cash-in-advance potentially benefits carriers because, although the operation cost for travel is included in the freight charges, carriers should bear the cost at first and wait to get paid after the documentary proof is issued by the bank. It implicitly requires the carrier to have enough money to support bunkering and the following daily operating costs.

Let the total amount of documentary credit issued by the bank be CDT^{fc}, the cost of obtaining the RCLC is denoted by $r^{\text{RCLC}^{fc}} \cdot \text{CDT}^{fc}$. The RCLC agreed by all parties involved has provisions about when and under what conditions the carrier is able to receive the specific amount from the bank. Let the possible receipt happen at $t^{fci}_{CB/CAR}$ with corresponding amount R^{fci}, where $i = 1, 2$ in usual cases. $t^{fc1}_{CB/CAR}$ could be any moment after the RCLC issued by the

issuing bank; $t^{fc1}_{CB/CAR} < t^{fc2}_{CB/CAR}$, and $t^{fc2}_{CB/CAR}$ usually indicates a time point that the BoL has been presented to the bank and, after being examined, is ready to be paid. Due to the RCLC is assumed to be irrevocable and confirmed, R^{fci} is invariant with the actual payment condition of the party who is liable to complete the payment. Thus, let R^{fc} denotes the total amount of freight charges, $R^{fci} = \theta_i \cdot R^{fc}$, for $i = 1,2$, $\theta_i \in (0,1)$, and $\sum \theta_i \equiv 1$, $\forall i$. For the cash outflow for the party who request to pay by RCLC, let the time of it is denoted by $t^{fci}_{party/IB}$ with corresponding amount $R^{fci}_{party/IB}$, where $i = 1,2$; $R^{fci}_{party/IB} = \eta_i \cdot R^{fc}$, for $i = 1,2$, $\eta_i \in [0,1]$, and $\sum \eta_i \leq 1$, $\forall i$. We say $\theta_i \leq \eta_i$ is not a necessary condition here due to the party may use valuable assets as collateral and not requisite to pay the issuing bank before confirming bank pay the carrier.

Figure 21 shows the procedure for using RCLC as a payment method in practical shipping. Compared to Figure 18, there is a payment being sent to the carrier before the shipment has been finished and showed the BoL to be examined. Then, we show an asymmetric cash-flows for all parties involved in the shipment with RCLC in Figure 22.

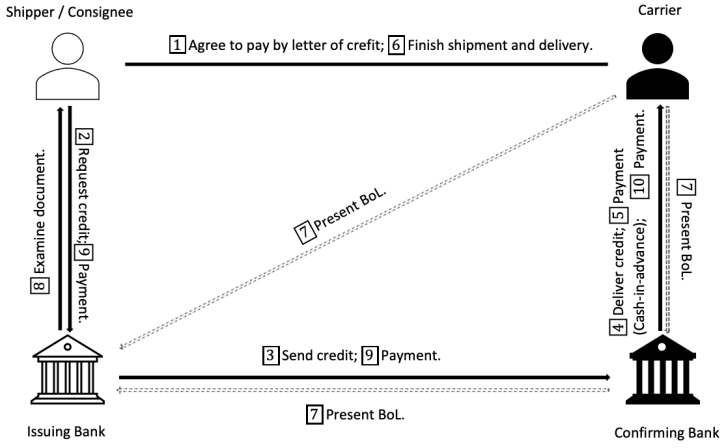

FIGURE 21: The procedures for using RCLC in a shipment

The cash inflows about freight charges are calculated by:

$$\begin{aligned} \mathrm{FC}^{\mathrm{LC}}_{CAR} &= \theta_1 \cdot R^{fc} \cdot e^{-\alpha t^{fc1}_{CB/CAR}} + +\theta_2 \cdot R^{fc} \cdot e^{-\alpha t^{fc2}_{CB/CAR}} \\ &= \theta_1 \cdot R^{fc} \cdot e^{-\alpha t^{fc1}_{CB/CAR}} + \theta_2 \cdot R^{fc} \cdot e^{-\alpha t^{fc2}_{(party)/CAR}} \cdot e^{-\alpha\sigma}, \end{aligned} \tag{5.43}$$

and, the NPV for carrier is written by:

$$\begin{aligned} \mathrm{NPV}^{\mathrm{LC}}_{CAR} = \; & -C^{ins.} \cdot e^{-\alpha t^{ins.}} - C^{load} \cdot e^{-\alpha t^{load}} - \int_{t^{load}}^{t^{report}} f^{TCH} \cdot e^{-\alpha t} \mathrm{d}t + \theta_1 \cdot R^{fc} \cdot e^{-\alpha t^{fc1}_{CB/CAR}} \\ & -C^{unload} \cdot e^{-\alpha t^{unload}} + \theta_2 \cdot R^{fc} \cdot e^{-\alpha t^{fc2}_{CB/CAR}} - C^{claim} \cdot r^{CAR} \cdot e^{-\alpha t^{claim:CAR}} \\ = \; & -C^{ins.} \cdot e^{-\alpha t^{ins.}} - C^{load} \cdot e^{-\alpha t^{load}} - \int_{t^{load}}^{t^{report}} f^{TCH} \cdot e^{-\alpha t} \mathrm{d}t + \theta_1 \cdot R^{fc} \cdot e^{-\alpha t^{fc1}_{CB/CAR}} \\ & -C^{unload} \cdot e^{-\alpha t^{unload}} + \theta_2 \cdot R^{fc} \cdot e^{-\alpha t^{fc2}_{(party)/CAR}} \cdot e^{-\alpha\sigma} - C^{claim} \cdot r^{CAR} \cdot e^{-\alpha t^{claim:CAR}}. \end{aligned} \tag{5.44}$$

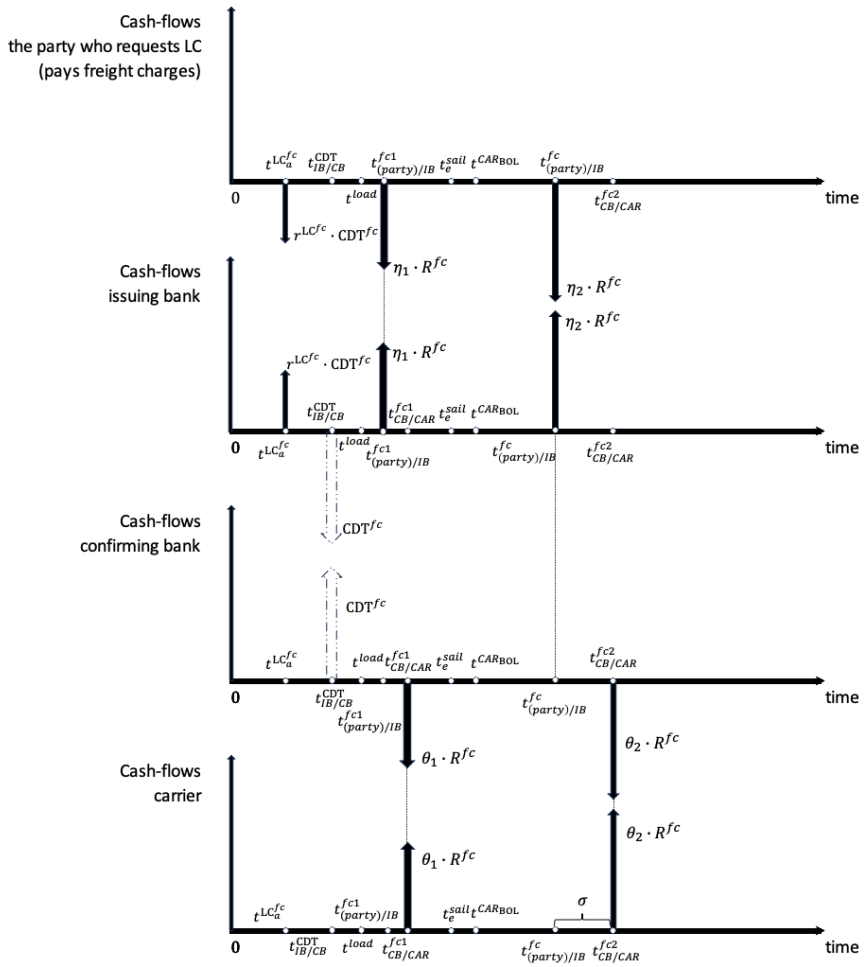

FIGURE 22: An asymmetric cash-flows for the party who request a RCLC about freight charges, issuing bank, confirming bank, and carrier

The values of θ_1 and θ_2 could be prior agreed upon and determined by all parties involved, while the σ is still randomised and uncertain. A series of numerical examples are shown to illustrate that when θ_1 and θ_2 are given as different combinations, how could freight charges differently perform. Two cases that when θ_1 and θ_2 are given by its boundary value is: when $\theta_1 = 0$ and $\theta_2 = 100\%$, the payment structure is equivalent to the ICLC when the σ is equally distributed under the ICLC and RCLC; also, when $\theta_1 = 100\%$, and $\theta_2 = 0$, the payment structure could be taken as the 'freight prepaid' but without non-payment risk. To show the difference between ICLC and RCLC ($\theta_1 \neq 0$, and $\theta_2 \neq 1$), we define:

$$\Delta \mathrm{FC}^{\mathrm{RCLC}}_{CAR}(\theta_1, \theta_2) = \mathrm{FC}^{\mathrm{RCLC}}_{CAR}|_{\sigma;\theta_1,\theta_2} - \mathrm{FC}^{\mathrm{LC}}_{CAR}|_{\sigma}, \tag{5.45}$$

$$\Delta \mathrm{NPV}^{\mathrm{RCLC}}_{CAR}(\theta_1, \theta_2) = \mathrm{NPV}^{\mathrm{RCLC}}_{CAR}|_{\sigma;\theta_1,\theta_2} - \mathrm{NPV}^{\mathrm{LC}}_{CAR}|_{\sigma}, \tag{5.46}$$

that are difference in freight charges and NPV, respectively. Then, numerical results for different combinations of θ_1 and θ_2 are given in Table 26.

TABLE 26: Numerical results for different combinations of θ_1 and θ_2 in payment structures that freight charges are paid by RCLC: σ is fixed to 10 days

Instance (in percentage)		FC^{LC}_{CAR} *Eq.*(5.43)	$\triangle FC^{LC}_{CAR}$ *Eq.*(5.39)	NPV^{LC}_{CAR} *Eq.*(5.44)	$\triangle NPV^{LC}_{CAR}$ *Eq.*(5.40)
θ_1	θ_2				
0	100%	13.498	-	15.187	-
10%	90%	13.511	0.013	15.200	0.013
30%	70%	13.524	0.026	15.213	0.026
50%	50%	13.563	0.065	15.252	0.065
70%	30%	13.589	0.091	15.278	0.091
90%	10%	13.615	0.116	15.304	0.116
100%	0	13.628	0.129	15.317	0.129

[1]The speed $v = 12$ knots; the opportunity cost of capital rate per year $\alpha = 0.08$; $t^{fc1}_{CB/CAR}$ is assumed to be equal to t^{load}.

From Table 26, there is an increment in freight charges or NPV for carriers when the proportional of θ_1 is increased. We find that RCLC is a more beneficial option to carriers compared to ICLC due to an earlier cash inflow before showing the BoL does improve the cash-flow condition and a certain higher NPV. The instance of $\theta_1 = 10\%$, and $\theta_2 = 90\%$ could usually be considered as the deposit in practical business.

5.6 Conclusion

Optimisation problems in tramp shipping consider optimising the objective from the view of decision makers, either on behalf of the shipowner or the time-charterer, which is actually the carrier in the shipping contract. A lot of studies in the field of tramp ship routing and scheduling problems determine the objective function as maximising profit per journey, per day calculated as net profit or NPV (Ronen, 1982; Norstad et al., 2011; Magirou et al., 2015; Ge et al., 2021). All these studies assume that the carrier will receive the revenue from freight charges on time and in the correct amount. However, in practice, it is not always true. A receipt of payment for goods less than or later than stipulated is a common occurrence in actual shipping. Such instances may affect the carrier's following operations in the shipping market or make the carrier involved in litigation and consume more time and effort to deal with the unresolved issue, as well as weaken the cash-flow liquidity. Thus, how to wisely select terms about freight payments and choose risk management tools are quite important in decision-making problems for carrier.

In Section 3.6, we consider the timeline of cash flows with non-payment risk for a single-leg journey in tramp shipping and briefly introduce two different payment structures. In this paper, we further discuss the payment structures under a wide range of freight payment contracts and terms. We conclude that terms including FOB-O, FOB-D, CIF, and CFR mainly decide when the title of ownership changes from shipper to consignee, who files a claim for cargo insurance if there is any loss or damage to cargo, and who pays the cargo insurance. On the other side, terms of freight payment determine who pays the scheduled freight charges and additional freight charges. These characteristics of payment are summarised into a general payment structure for the carrier, shipper, and consignee in this paper.

In contrast to businesses with extended trust, the payment structure for businesses with weaker trust, in which cases of delay in payment or non-payment are incorporated, is also formulated in this paper. The NPV for the carrier, shipper, and consignee involved in business with two different types of trust is shown and compared. The non-payment risk in businesses with weaker trust is a consequence of counterparty risk. In practice, this type of risk could be mitigated by a third-party institute, i.e., the central bank, acting as the intermediary to guarantee the payment time and amount. This paper discusses different LCs and employs the approach of NPV to analyse the payment structures under a certain LC, particularly for the carrier. We find that there is a first-order stochastic dominance between the LC at sight and the ICLC. The dominance could be explained as: when the time period of asymmetric cash flows for ICLC first-order stochastic dominates the LC at sight, choosing LC at sight is a better decision than choosing ICLC due to a higher NPV being followed up.

Moreover, we compare RCLC with ICLC and find that under the same estimation of the time period σ, RCLC is a more beneficial option to carriers because part of the freight charges will be paid before the shipment is completed and the carrier shows the BoL, which is considered a cash-in-advance. Some numerical experiments are given to prove the effect of different percentages of this cash-in-advance on a Suezmax example. We show the cash flows of payment structures without documentary credit are symmetric, either for businesses with extended transactions or weaker trust. Whereas freight charges paid by documentary credit, such as the different types of LC presented in this paper, cause the cash flows of payment structures to be asymmetric.

Chapter 6

Conclusions

Throughout the whole thesis, we have addressed three main topics in decision-making problems in tramp shipping. Topics are independent of each other but also connectable in future research or applications. We will conclude the main contributions and find them chapter by chapter.

In Chapter 3, we modelled the speed optimisation problem in tramp shipping by mean-risk optimisation model, and answered research questions 1-3 by addressing the risk of not achieving the NPV, excluding and including the FPP for decision makers with various risk attitudes. The decision makers are categorised based on their risk tolerance level and profit target, whether short- or long-term. The mean-risk optimisation models with short- or long-term NPV constraints are designed to solve job acceptance and economic speed for different decision makers.

Results are not only focusing on optimising speed (equivalent to the economic travel time), but also provide insights on decisions of job acceptance, which is new to the literature. The novelty of the concept provided in this paper are threefold: (1) our model consider two sources of randomness including fuel consumption increases due to bad weather days, and daily earnings reflecting the profit potential in the destination port and both of them are drawn from a distribution. These two stochasticity, that are both very important in the decision process, had not been discussed in literature and are caught as a certain research gap; (2) we show the impact of uncertainty depends on the type of decision maker. The short-term models, on the one hand, can help those who need to manage the risk on the current journey primarily. The main source of uncertainty here is the impact of fuel consumption. The impact from the future profit potential is mainly through its expected value: a higher value will tend to speed up the ship, affecting its fuel consumption and risk impact from bad weather. Long-term models, on the other hand, can serve companies that are less bound to avoiding short-term losses on individual ships and journeys: they can use long-term expected profitability goals for their risk assessments. The whole distribution of the future profit potential could impact the acceptance of a job; its mean affecting the speed on the job, while bad weather forecasts will lower speed values; (3) the solutions returned by the mean-risk optimisation models captures some important aspects of real-life decision making under risk, particularly, from the decision maker's own risk attitudes. The model

does not offer a single best answer; rather, it offers a risk profile of NPV with and excluding FPP. Decision-makers with different worries about risk metrics, risk tolerance levels, and profit objectives might use the model's results to their advantage.

The objective function is also determined as maximising profitability in the long term in Chapter 4. Nevertheless, we amplify the considerations of stochasticities throughout the decision process. In Chapter 4, research questions 4-5 are answered by establishing the problem for solving the ship routine and scheduling that is applicable for a day-to-day or hour-to-hour plan. Information, including oceanic weather conditions, port congestion, and FPP, is modelled into random variables with distributions that are updated over time. A framework for MDP is established based on 3D states that include the spatial and temporal constituents of the vessel. We develop a value iteration algorithm to incorporate the features of information, and then a simulation-enhanced value iteration (SEVI) is proposed to generate the distribution profile of NPV in the short- and long-term for decision-makers with a variety of risk attitudes. We find that applying the MDP is able to achieve better profitability in the long term compared to other methods. It also mitigates the risk of delay or arriving earlier than the contractual delivery time. We also find that when altering the distribution of uncertainties, the method in this paper is able to adjust the decisions and provide new solutions, while methods that use certain information rather than distribution cannot. At the end of this chapter, we extend the model to help decision makers who are not satisfied with the risk performance of NPV derived from the current delivery time window. Results discovered in numerical experiments for alternatives to delivery time-window reveal that postponing the delivery time-window is beneficial to decision makers when the estimation of fuel oceanic consumption rates under weather conditions is higher or the waiting time at the destination port becomes longer. In the opposite direction, moving the delivery time-window ahead of schedule could be a better choice.

Chapter 3 and Chapter 4 mainly concentrate on how to optimise the profitability of the decision maker by operating the ship by evaluating different jobs, scheduling the ship's routes and speeds, or delivery time window. Both topics belong to the speed optimisation problems due to the speed (equivalent to economic travel time) being optimised. And the latter also belongs to ship routing and scheduling problems because the solutions are more precisely given based on the number of stages initialised. For example, for a 7 stage problem formulated for a single-leg journey with 8293 nm, the solutions will be updated once a week; when the number of stages increases to 11, the solutions will be updated every three days. We propose the third topic on the basis of the first two, by considering the lack of considering non-payment risk when calculating the revenue of freight charges. Thus, in Chapter 5, we develop a general model of freight payment for the shipper, consignee, and carrier within a shipping contract. The non-payment risk is addressed by taking into account the business in shipping when all parties have an extended trust and a somewhat weaker trust. A common payment structure model is utilised to clarify an assortment of product payment conditions. We further demonstrate that the extended trust industry does not require documented credit, such as LC, since there is a danger of non-payment. Thirdly, for weaker trust business with LC, we discuss a broad spectrum of risks raised by the party entitled

to the ownership of the cargo and the carrier, which will result in an increase in the transaction's cost because of the lower level of trust. Research questions 6-7 are answered step by step for a wide range of freight payment terms and letters of credit. The NPV analysis for the main counterparty involved in the freight payment is discussed.

In summary, this research offer insights of helping decision makers with various risk attitudes to make decision at different dimensions. Before stipulating the contract with other parties involved in the potential shipping market, proper payment terms and documentary credits could be carefully compared by using the model introduced in Chapter 5. When comparing several potential jobs or repositioning legs start from current port to others, mean-risk optimisation models in Chapter 3, could be selected according to the risk tolerance level and desire of profit in short- or long-term. The most profitable job will be suggested with an economic travel time for the decision maker. More technical sailing strategies such as routes of waypoints and sailing speeds are able to be generated by implementing the dynamic information update process involved in the framework of MDP and SEVI, as demonstrated in Chapter 4.

The limitations of this research can be concluded by having paid less attention that perhaps would be desirable to the effect of emissions zones in shipping, i.e. different sailing speed boundary in ECAs. Secondly, potential profit of saving CO_2 emissions might become more important in future decision making and thus should be incorporated in future work. Applying SEVI sometimes costs considerable computational time of more than one hour when the number of stages or state space inflate. Still, this seems acceptable in the light of the overall decision processes involved.

The potential directions of future research are given as follows: risks from environmental viewpoints, such as carbon emissions or ECAs, may be included in risk-constrained MDPs. The MDPs might include specific limitations on time limits, safety considerations, carbon prices, or other stringent criteria; one of the goals of value iterations may also include soft limitations. Assume that there are several simultaneous MDPs, each with a different objective function symbolised by a reward function. To determine the best course of action, further multi-objective optimisation problem solving techniques can be used. Bayesian information may be used to better model the assessment of weather conditions, FPP, fuel costs, and waiting times; risk analysis could be provided; the non-payment risk could be incorporated into the speed optimisation model either in the mean-risk optimisation model (Chapter 3), or MDP (Chapter 4); multi-objective optimisation models could be considered as the basement for dealing with the speed optimisation problem with environmental prospects.

References

Abadie, L.M., Goicoechea, N., 2019. Powering newly constructed vessels to comply with eca regulations under fuel market prices uncertainty: Diesel or dual fuel engine? Transportation Research Part D: Transport and Environment 67, 433–448.

Abdelwahab, W.M., Sargious, M., 1990. Freight rate structure and optimal shipment size in freight. Logistics and Transportation Review 26, 271.

Acerbi, C., Tasche, D., 2002. On the coherence of expected shortfall. Journal of Banking & Finance 26, 1487–1503.

Adland, R., Cariou, P., Wolff, F.C., 2020. Optimal ship speed and the cubic law revisited: Empirical evidence from an oil tanker fleet. Transportation Research Part E: Logistics and Transportation Review 140, 101972.

Agarwal, R., Ergun, Ö., 2008. Ship scheduling and network design for cargo routing in liner shipping. Transportation Science 42, 175–196.

Agra, A., Christiansen, M., Figueiredo, R., Hvattum, L.M., Poss, M., Requejo, C., 2013. The robust vehicle routing problem with time windows. Computers & Operations Research 40, 856–866.

Alderton, P., 1981. The optimum speed of ships. The Journal of Navigation 34, 341–355.

Alvarez, J.F., Tsilingiris, P., Engebrethsen, E.S., Kakalis, N.M., 2011. Robust fleet sizing and deployment for industrial and independent bulk ocean shipping companies. INFOR: Information Systems and Operational Research 49, 93–107.

Anderson, E.J., 2013. Business risk management: models and analysis. John Wiley & Sons.

Appelgren, L.H., 1969. A column generation algorithm for a ship scheduling problem. Transportation Science 3, 53–68.

Appelgren, L.H., 1971. Integer programming methods for a vessel scheduling problem. Transportation Science 5, 64–78.

Artzner, P., Delbaen, F., Eber, J.M., Heath, D., 1999. Coherent measures of risk. Mathematical Finance 9, 203–228.

Aydin, N., Lee, H., Mansouri, S.A., 2017. Speed optimization and bunkering in liner shipping in the presence of uncertain service times and time windows at ports. European Journal of Operational Research 259, 143–154.

Ayoush, M.D., Toumeh, A.A., Shabaneh, K.I., 2021. Liquidity, leverage, and solvency: What affects profitability of industrial enterprises the most. Investment Management and Financial Innovations 18, 249–259.

Azaron, A., Kianfar, F., 2003. Dynamic shortest path in stochastic dynamic networks: Ship routing problem. European Journal of Operational Research 144, 138–156.

Ballou, P., Chen, H., Horner, J.D., 2008. Advanced methods of optimizing ship operations to reduce emissions detrimental to climate change, in: OCEANS 2008, IEEE. pp. 1–12.

Barbaro, A., Bagajewicz, M.J., 2004. Managing financial risk in planning under uncertainty. AIChE Journal 50, 963–989.

Barnhart, C., Laporte, G., 2006. Handbooks in operations research and management science: Transportation. Elsevier.

Baughen, S., 2018. Shipping law. Routledge.

Bausch, D.O., Brown, G.G., Ronen, D., 1998. Scheduling short-term marine transport of bulk products. Maritime Policy & Management 25, 335–348.

Behrens, K., Gaigné, C., Thisse, J.F., 2009. Industry location and welfare when transport costs are endogenous. Journal of Urban Economics 65, 195–208.

Behrens, K., Picard, P.M., 2011. Transportation, freight rates, and economic geography. Journal of International Economics 85, 280–291.

Bellman, R., 1958. On a routing problem. Quarterly of Applied Mathematics 16, 87–90.

Benford, H., 1981. A simple approach to fleet deployment. Maritime Policy and Management 8, 223–228.

Bentin, M., Zastrau, D., Schlaak, M., Freye, D., Elsner, R., Kotzur, S., 2016. A new routing optimization tool-influence of wind and waves on fuel consumption of ships with and without wind assisted ship propulsion systems. Transportation Research Procedia 14, 153–162.

Besbes, O., Savin, S., 2009. Going bunkers: The joint route selection and refueling problem. Manufacturing & Service Operations Management 11, 694–711.

Beşikçi, E.B., Arslan, O., Turan, O., Ölçer, A.I., 2016. An artificial neural network based decision support system for energy efficient ship operations. Computers & Operations Research 66, 393–401.

Beullens, P., Ge, F., Hudson, D., 2023. The economic ship speed under time charter contractâa cash flow approach. Transportation Research Part E: Logistics and Transportation Review 170, 102996.

Beullens, P., Janssens, G.K., 2011. Holding costs under push or pull conditions–the impact of the anchor point. European Journal of Operational Research 215, 115–125.

Beullens, P., Janssens, G.K., 2014. Adapting inventory models for handling various payment structures using net present value equivalence analysis. International Journal of Production Economics 157, 190–200.

Bichou, K., 2008. Security and risk-based models in shipping and ports: Review and critical analysis .

Branch, A.E., 2012. Economics of shipping practice and management. Springer Science & Business Media.

Brealey, R.A., Myers, S.C., Allen, F., Mohanty, P., 2012. Principles of corporate finance. Tata McGraw-Hill Education.

Brenkert, G.G., 1998a. Trust, business and business ethics: an introduction. Business Ethics Quarterly 8, 195–203.

Brenkert, G.G., 1998b. Trust, morality and international business. Business Ethics Quarterly 8, 293–317.

Brown, G.G., Graves, G.W., Ronen, D., 1987. Scheduling ocean transportation of crude oil. Management Science 33, 335–346.

Buzzell, R.D., Chussil, M.J., 1985. Managing for tomorrow. Sloan Management Review (pre-1986) 26, 3.

Carr, I., Stone, P., 2013. International trade law. Routledge.

Chen, C., Shiotani, S., Sasa, K., 2013. Numerical ship navigation based on weather and ocean simulation. Ocean Engineering 69, 44–53.

Choi, Y.M., Joo, H.K., Park, Y.K., 2011. Do dividend changes predict the future profitability of firms? Accounting & Finance 51, 869–891.

Christiansen, M., Fagerholt, K., 2014. Chapter 13: Ship routing and scheduling in industrial and tramp shipping, in: Vehicle Routing: Problems, Methods, and Applications, Second Edition. SIAM, pp. 381–408.

Christiansen, M., Fagerholt, K., Ronen, D., 2004. Ship routing and scheduling: Status and perspectives. Transportation Science 38, 1–18.

Christiansen, M., Nygreen, B., 2005. Robust inventory ship routing by column generation, in: Column Generation. Springer, pp. 197–224.

Clarke, M.A., Hooley, R.J., Munday, R.J., Sealy, L.S., Turner, P., Tettenborn, A., 2017. Commercial law: Text, cases, and materials. Oxford University Press.

Cook Jr, V.J., 1985. The net present value of market share. Journal of Marketing 49, 49–63.

Deak, N.L., 1980. Letters of credit (documentary credit). NYL Sch. J. Int'l & Comp. L. 2, 229.

Dolan, J., 2007. The law of letters of credit. THE LAW OF LETTERS OF CREDIT, 4th edition, John F. Dolan, AS Pratt & Sons , 07–36.

Du, Y., Meng, Q., Wang, Y., 2015. Budgeting fuel consumption of container ship over round-trip voyage through robust optimization. Transportation Research Record 2477, 68–75. doi:.

Duffie, D., Pan, J., 1997. An overview of value at risk. Journal of derivatives 4, 7–49.

Dulebenets, M., Golias, M., Mishra, S., 2017. The green vessel schedule design problem: consideration of emissions constraints. Energy Systems 8, 761–783.

Enonchong, N., 2007. The problem of abusive calls on demand guarantees. Lloyd's Maritime & Commercial Law Quarterly 1, 83–106.

Fagerholt, K., 2001. Ship scheduling with soft time windows: An optimisation based approach. European Journal of Operational Research 131, 559–571.

Fagerholt, K., 2004. A computer-based decision support system for vessel fleet schedulingâexperience and future research. Decision Support Systems 37, 35–47.

Fagerholt, K., Christiansen, M., Hvattum, L.M., Johnsen, T.A., Vabø, T.J., 2010a. A decision support methodology for strategic planning in maritime transportation. Omega 38, 465–474.

Fagerholt, K., Laporte, G., Norstad, I., 2010b. Reducing fuel emissions by optimizing speed on shipping routes. Journal of the Operational Research Society 61, 523–529.

Fagerholt, K., Lindstad, H., 2007. Turborouter: An interactive optimisation-based decision support system for ship routing and scheduling. Maritime Economics & Logistics 9, 214–233.

Fama, E.F., French, K.R., 2000. Forecasting profitability and earnings. The Journal of Business 73, 161–175.

Ford, L.R., 1956. Network flow theory .

Gao, Y., Sun, Z., 2023. Tramp ship routing and speed optimization with tidal berth time windows. Transportation Research Part E: Logistics and Transportation Review 178, 103268.

Gatica, R.A., Miranda, P.A., 2011. Special issue on latin-american research: a time based discretization approach for ship routing and scheduling with variable speed. Networks and Spatial Economics 11, 465–485.

Ge, F., Beullens, P., Hudson, D., 2021. Optimal economic ship speeds, the chain effect, and future profit potential. Transportation Research Part B: Methodological 147, 168–196.

Gidado, U., 2015. Consequences of port congestion on logistics and supply chain in african ports. Developing Country Studies 5, 160–167.

Gorton, L., 2009. The liability for freight. Stockholm Institute for Scandinavian Law , 38–18.

Goulielmos, A.M., Psifia, M.E., 2011. Forecasting short-term freight rate cycles: do we have a more appropriate method than a normal distribution? Maritime Policy & Management 38, 645–672.

Grifoll, M., de Osés, F.M., Castells, M., 2018. Potential economic benefits of using a weather ship routing system at short sea shipping. WMU Journal of Maritime Affairs 17, 195–211.

Grønhaug, R., Christiansen, M., Desaulniers, G., Desrosiers, J., 2010. A branch-and-price method for a liquefied natural gas inventory routing problem. Transportation Science 44, 400–415.

Grullon, G., Michaely, R., Benartzi, S., Thaler, R.H., 2005. Dividend changes do not signal changes in future profitability. The Journal of Business 78, 1659–1682.

Guan, F., Peng, Z., Chen, C., Guo, Z., Yu, S., 2017. Fleet routing and scheduling problem based on constraints of chance. Advances in Mechanical Engineering 9, 1687814017743026.

Guillén, G., Mele, F., Bagajewicz, M., Espuna, A., Puigjaner, L., 2005. Multiobjective supply chain design under uncertainty. Chemical Engineering Science 60, 1535–1553.

Harfield, H., 1985. Who does what to whom: The letter-of-credit mechanism. UCCLJ 17, 291.

Hinkelman, E.G., 2003. A Short Course in International Payments: How to Use Letters of Credit, D/P and D/A Terms, Prepayment, Credit, and Cyberpayments in International Transactions. World trade press.

Hinnenthal, J., Clauss, G., 2010. Robust pareto-optimum routing of ships utilising deterministic and ensemble weather forecasts. Ships and Offshore Structures 5, 105–114.

Holloway, S.S., Parmigiani, A., 2016. Friends and profits donât mix: The performance implications of repeated partnerships. Academy of Management Journal 59, 460–478.

Holtrop, J., Mennen, G., 1982. An approximate power prediction method. International Shipbuilding Progress 29, 166–170.

Huang, G.C., Liano, K., Pan, M.S., 2006. Do stock splits signal future profitability? Review of Quantitative Finance and Accounting 26, 347–367.

Hwang, H.S., Visoldilokpun, S., Rosenberger, J.M., 2008. A branch-and-price-and-cut method for ship scheduling with limited risk. Transportation Science 42, 336–351.

IMO, 2014. Third imo greenhouse gas study 2014. URL: https://www.imo.org/en/OurWork/Environment/Pages/Greenhouse-Gas-Studies-2014.aspx.

IMO, 2021. IMO's work to cut GHG emissions from ships.

Ingersoll, J.E., Ingersoll, J.E., 1987. Theory of financial decision making. volume 3. Rowman & Littlefield.

Jewson, S., Brix, A., 2005. Weather derivative valuation: the meteorological, statistical, financial and mathematical foundations. Cambridge University Press.

Jing, L., Marlow, P.B., Hui, W., 2008. An analysis of freight rate volatility in dry bulk shipping markets. Maritime Policy & Management 35, 237–251.

Joseph, C.E., 1977. Letters of credit: The developing concepts and financing functions. Banking Lj 94, 816.

Kavussanos, M.G., Alizadeh-M, A.H., 2002. Seasonality patterns in tanker spot freight rate markets. Economic Modelling 19, 747–782.

Kavussanos, M.G., Visvikis, I.D., 2009. Shipping derivatives and risk management. Springer.

Kim, Mingyu, O.H.O.T.S.D., Incecik, A., 2017. Estimation of added resistance and ship speed loss in a seaway. Ocean Engineering , 465–476.

Kim, S.H., Lee, K.K., 1997. An optimization-based decision support system for ship scheduling. Computers & Industrial Engineering 33, 689–692.

Kleinrock, L., 1975. Theory, volume 1, queueing systems.

Koekebakker, S., Adland, R., Sødal, S., 2006. Are spot freight rates stationary? Journal of Transport Economics and Policy (JTEP) 40, 449–472.

Koekebakker, S., Adland, R., Sødal, S., 2007. Pricing freight rate options. Transportation Research Part E: Logistics and Transportation Review 43, 535–548.

Kontovas, C.A., 2014. The green ship routing and scheduling problem (gsrsp): a conceptual approach. Transportation Research Part D: Transport and Environment 31, 61–69.

Krata, P., Szlapczynska, J., 2018. Ship weather routing optimization with dynamic constraints based on reliable synchronous roll prediction. Ocean Engineering 150, 124–137.

Ksciuk, J., Kuhlemann, S., Tierney, K., Koberstein, A., 2023. Uncertainty in maritime ship routing and scheduling: A literature review. European Journal of Operational Research 308, 499–524.

Kuhlemann, S., Ksciuk, J., Tierney, K., Koberstein, A., 2021. The stochastic liner shipping fleet repositioning problem with uncertain container demands and travel times. EURO Journal on Transportation and Logistics 10, 100052.

Kulkarni, K., Goerlandt, F., Li, J., Banda, O.V., Kujala, P., 2020. Preventing shipping accidents: Past, present, and future of waterway risk management with baltic sea focus. Safety Science 129, 104798.

Kwon, Y., 2008. Speed loss due to added resistance in wind and waves. Nav Archit 3, 14–16.

Li, M., Fagerholt, K., Schütz, P., 2022a. Stochastic tramp ship routing with speed optimization: analyzing the impact of the northern sea route on co 2 emissions. Annals of Operations Research , 1–25.

Li, M., Xie, C., Li, X., Karoonsoontawong, A., Ge, Y.E., 2022b. Robust liner ship routing and scheduling schemes under uncertain weather and ocean conditions. Transportation Research Part C: Emerging Technologies 137, 103593.

Lin, Y.H., Fang, M.C., Yeung, R.W., 2013. The optimization of ship weather-routing algorithm based on the composite influence of multi-dynamic elements. Applied Ocean Research 43, 184–194.

Lindstad, H., Asbjørnslett, B.E., Jullumstrø, E., 2013. Assessment of profit, cost and emissions by varying speed as a function of sea conditions and freight market. Transportation Research Part D: Transport and Environment 19, 5–12. doi:.

Lintner, J., 1956. Distribution of incomes of corporations among dividends, retained earnings, and taxes. The American Economic Review 46, 97–113.

Lo, H.K., McCord, M.R., 1998. Adaptive ship routing through stochastic ocean currents: General formulations and empirical results. Transportation Research Part A: Policy and Practice 32, 547–561.

Lu, R., Turan, O., Boulougouris, E., 2013. Voyage optimisation: prediction of ship specific fuel consumption for energy efficient shipping, in: Low Carbon Shipping Conference, London, pp. 1–11.

Lu, R., Turan, O., Boulougouris, E., Banks, C., Incecik, A., 2015. A semi-empirical ship operational performance prediction model for voyage optimization towards energy efficient shipping. Ocean Engineering 110, 18–28.

Magirou, E.F., Psaraftis, H.N., Bouritas, T., 2015. The economic speed of an oceangoing vessel in a dynamic setting. Transportation Research Part B: Methodological 76, 48–67.

Mallidis, I., Despoudi, S., Dekker, R., Iakovou, E., Vlachos, D., 2018. The impact of sulphur limit fuel regulations on maritime supply chain network design. Annals of Operations Research , 1–19.

Mansouri, S.A., Lee, H., Aluko, O., 2015. Multi-objective decision support to enhance environmental sustainability in maritime shipping: a review and future directions. Transportation Research Part E: Logistics and Transportation Review 78, 3–18.

Markowitz, H., 1952. The utility of wealth. Journal of political Economy 60, 151–158.

Meng, Q., Wang, S., Lee, C.Y., 2015. A tailored branch-and-price approach for a joint tramp ship routing and bunkering problem. Transportation Research Part B: Methodological 72, 1–19.

Meng, Q., Wang, T., Wang, S., 2012. Short-term liner ship fleet planning with container transshipment and uncertain container shipment demand. European Journal of Operational Research 223, 96–105.

Merikas, A.G., Polemis, D., Triantafyllou, A., et al., 2011. Mergers and acquisitions in the shipping industry. Journal of Applied Business Research (JABR) 27, 9–22.

Merkel, A., Kalantari, J., Mubder, A., 2022. Port call optimization and co2-emissions savings–estimating feasible potential in tramp shipping. Maritime Transport Research 3, 100054.

Miola, A., Ciuffo, B., Giovine, E., Marra, M., 2010. Regulating air emissions from ships: the state of the art on methodologies, technologies and policy options. JRC Reference Reports .

Nakandala, D., Samaranayake, P., Lau, H.C., 2013. A fuzzy-based decision support model for monitoring on-time delivery performance: A textile industry case study. European journal of operational research 225, 507–517.

Nissim, D., Ziv, A., 2001. Dividend changes and future profitability. The Journal of Finance 56, 2111–2133.

Norstad, I., Fagerholt, K., Laporte, G., 2011. Tramp ship routing and scheduling with speed optimization. Transportation Research Part C: Emerging Technologies 19, 853–865.

Notteboom, T., Cariou, P., 2009. Fuel surcharge practices of container shipping lines: Is it about cost recovery or revenue making, in: Proceedings of the 2009 international association of maritime economists (IAME) conference, IAME Copenhagen, Denmark. pp. 24–26.

Notteboom, T.E., Vernimmen, B., 2009. The effect of high fuel costs on liner service configuration in container shipping. Journal of Transport Geography 17, 325–337.

Nuzio, A., . PAY ON TIME, OR ELSE! - UNDERSTANDING FREIGHT CARRIER PAYMENT TERMS. Website. URL: https://www.linkedin.com/pulse/pay-time-else-understanding-freight-carrier-payment-terms-nuzio/.

Oceanic, N., of Commerce, A.A.U.D., . Weather forecasting: How reliable are weather forecasts? URL: https://scijinks.gov/forecast-reliability/.

Ottaviano, G., Tabuchi, T., Thisse, J.F., 2002. Agglomeration and trade revisited. International Economic Review 43, 409–435.

Pastra, A., Zachariadis, P., Alifragkis, A., 2021. The role of slow steaming in shipping and methods of co 2 reduction, in: Sustainability in the Maritime Domain. Springer, pp. 337–352.

Perakis, A., Bremer, W., 1992. An operational tanker scheduling optimization system: background, current practice and model formulation. Maritime Policy & Management 19, 177–187.

Perakis, A.N., 1985. A second look at fleet deployment. Maritime Policy and Management 12, 209–214.

Perakis, A.N., Papadakis, N., 1987a. Fleet deployment optimization models. part 1. Maritime Policy & Management 14, 127–144.

Perakis, A.N., Papadakis, N., 1987b. Fleet deployment optimization models. part 2. Maritime Policy & Management 14, 145–155.

Perera, L.P., Soares, C.G., 2017. Weather routing and safe ship handling in the future of shipping. Ocean Engineering 130, 684–695.

Pewsey, A., 2000. Problems of inference for azzalini's skewnormal distribution. Journal of Applied Statistics 27, 859–870.

Pflug, G.C., 2000. Some remarks on the value-at-risk and the conditional value-at-risk, in: Probabilistic constrained optimization. Springer, pp. 272–281.

Poongodi, T., Muthulakshmi, S., 2013. Control chart for waiting time in system of (m/m/1):(?/fcfs) queuing model. International Journal of Computer Applications 63.

Preinreich, G.A., 1940. The economic life of industrial equipment. Econometrica: Journal of the Econometric Society , 12–44.

Pruyn, J., Kana, A., Groeneveld, W., 2020. Analysis of port waiting time due to congestion by applying markov chain analysis, in: Maritime Supply Chains. Elsevier, pp. 69–94.

Psaraftis, H.N., Kontovas, C.A., 2014. Ship speed optimization: Concepts, models and combined speed-routing scenarios. Transportation Research Part C: Emerging Technologies 44, 52–69.

Puterman, M.L., 2014. Markov decision processes: discrete stochastic dynamic programming. John Wiley & Sons.

Rockafellar, R.T., Uryasev, S., et al., 2000. Optimization of conditional value-at-risk. Journal of risk 2, 21–42.

Roman, D., Darby-Dowman, K., Mitra, G., 2007. Mean-risk models using two risk measures: a multi-objective approach. Quantitative Finance 7, 443–458.

Ronen, D., 1982. The effect of oil price on the optimal speed of ships. Journal of the Operational Research Society 33, 1035–1040.

Ronen, D., 1983. Cargo ships routing and scheduling: Survey of models and problems. European Journal of Operational Research 12, 119–126.

Ronen, D., 1993. Ship scheduling: The last decade. European Journal of Operational Research 71, 325–333.

Ronen, D., 2011. The effect of oil price on containership speed and fleet size. Journal of the Operational Research Society 62, 211–216.

Sang, Y., Ding, Y., Xu, J., Sui, C., 2023. Ship voyage optimization based on fuel consumption under various operational conditions. Fuel 352, 129086.

Schinas, O., Stefanakos, C.N., 2012. Cost assessment of environmental regulation and options for marine operators. Transportation Research Part C: Emerging Technologies 25, 81–99.

Shao, W., Zhou, P., Thong, S.K., 2012. Development of a novel forward dynamic programming method for weather routing. Journal of Marine Science and Technology 17, 239–251.

Shin, Y.W., Abebe, M., Noh, Y., Lee, S., Lee, I., Kim, D., Bae, J., Kim, K.C., 2020. Near-optimal weather routing by using improved a* algorithm. Applied Sciences 10, 6010.

Sidoti, D., Avvari, G.V., Mishra, M., Zhang, L., Nadella, B.K., Peak, J.E., Hansen, J.A., Pattipati, K.R., 2016. A multiobjective path-planning algorithm with time windows for asset routing in a dynamic weather-impacted environment. IEEE Transactions on Systems, Man, and Cybernetics: Systems 47, 3256–3271.

Skoglund, L., Kuttenkeuler, J., Rosén, A., Ovegård, E., 2015. A comparative study of deterministic and ensemble weather forecasts for weather routing. Journal of Marine Science and Technology 20, 429–441.

Song, Y., Beullens, P., Hudson, D., . Job acceptance and economic travel time of a tramp ship under risk. Transportation Research Part E: Logistics and Transportation Review (Under Review) .

Stefanakos, C.N., Schinas, O., 2014. Forecasting bunker prices; a nonstationary, multivariate methodology. Transportation Research Part C: Emerging Technologies 38, 177–194.

Stopford, M., 2008. Maritime economics 3e. Routledge.

Szlapczynska, J., 2015. Multi-objective weather routing with customised criteria and constraints. The Journal of Navigation 68, 338–354.

Talley, W.K., 2006. Port performance: an economics perspective. Research in Transportation Economics 17, 499–516.

Talley, W.K., 2013. Maritime transportation research: topics and methodologies. Maritime Policy & Management 40, 709–725.

Tan, Z., Zhang, M., Shao, S., Liang, J., Sheng, D., 2022. Evasion strategy for a coastal cargo ship with unpunctual arrival penalty under sulfur emission regulation. Transportation Research Part E: Logistics and Transportation Review 164, 102818.

Tasche, D., 2002. Expected shortfall and beyond. Journal of Banking & Finance 26, 1519–1533.

Taylor, J.S., 1923. A statistical theory of depreciation: Based on unit cost. Journal of the American Statistical Association 18, 1010–1023.

Terborgh, G.W., et al., 1949. Dynamic equipment policy .

Theocharis, D., Rodrigues, V.S., Pettit, S., Haider, J., 2019. Feasibility of the northern sea route: The role of distance, fuel prices, ice breaking fees and ship size for the product tanker market. Transportation Research Part E: Logistics and Transportation Review 129, 111–135.

Tillig, F., Ringsberg, J.W., Mao, W., Ramne, B., 2018. Analysis of uncertainties in the prediction of shipsâ fuel consumption–from early design to operation conditions. Ships and Offshore Structures 13, 13–24.

Todd, P., 2013. Bills of lading and bankers' documentary credits. Taylor & Francis.

on Trade, U.N.C., Development, . Review of maritime transport 2022. United Nations Conference on Trade and Development. URL: https://unctad.org/node/39387.

Tu, E., Zhang, G., Rachmawati, L., Rajabally, E., Huang, G.B., 2017. Exploiting ais data for intelligent maritime navigation: A comprehensive survey from data to methodology. IEEE Transactions on Intelligent Transportation Systems 19, 1559–1582.

Varelas, T., Archontaki, S., Dimotikalis, J., Turan, O., Lazakis, I., Varelas, O., 2013. Optimizing ship routing to maximize fleet revenue at danaos. Interfaces 43, 37–47.

Vettor, R., Soares, C.G., 2016. Development of a ship weather routing system. Ocean Engineering 123, 1–14.

Walther, L., Rizvanolli, A., Wendebourg, M., Jahn, C., 2016. Modeling and optimization algorithms in ship weather routing. International Journal of e-Navigation and Maritime Economy 4, 31–45.

Wang, H., Mao, W., Eriksson, L., 2019. A three-dimensional dijkstra's algorithm for multi-objective ship voyage optimization. Ocean Engineering 186, 106131.

Wang, K., Yan, X., Yuan, Y., Jiang, X., Lin, X., Negenborn, R.R., 2018a. Dynamic optimization of ship energy efficiency considering time-varying environmental factors. Transportation Research Part D: Transport and Environment 62, 685–698.

Wang, S., Meng, Q., 2012a. Liner ship route schedule design with sea contingency time and port time uncertainty. Transportation Research Part B: Methodological 46, 615–633.

Wang, S., Meng, Q., 2012b. Sailing speed optimization for container ships in a liner shipping network. Transportation Research Part E: Logistics and Transportation Review 48, 701–714.

Wang, S., Meng, Q., Liu, Z., 2013. Bunker consumption optimization methods in shipping: A critical review and extensions. Transportation Research Part E: Logistics and Transportation Review 53, 49–62.

Wang, Y., Meng, Q., 2020. Semi-liner shipping service design. Transportation Science 54, 1288–1306.

Wang, Y., Meng, Q., Kuang, H., 2018b. Jointly optimizing ship sailing speed and bunker purchase in liner shipping with distribution-free stochastic bunker prices. Transportation Research Part C: Emerging Technologies 89, 35–52.

Wei, S., Zhou, P., 2012. Development of a 3d dynamic programming method for weather routing. TransNav: International Journal on Marine Navigation and Safety of Sea Transportation 6, 79–85.

Wen, M., Pacino, D., Kontovas, C., Psaraftis, H., 2017. A multiple ship routing and speed optimization problem under time, cost and environmental objectives. Transportation Research Part D: Transport and Environment 52, 303–321.

Wen, M., Ropke, S., Petersen, H.L., Larsen, R., Madsen, O.B., 2016. Full-shipload tramp ship routing and scheduling with variable speeds. Computers & Operations Research 70, 1–8.

Wong, E.Y., Tai, A.H., Lau, H.Y., Raman, M., 2015. An utility-based decision support sustainability model in slow steaming maritime operations. Transportation Research Part E: Logistics and Transportation Review 78, 57–69.

Wu, L., Wang, S., Laporte, G., 2021. The robust bulk ship routing problem with batched cargo selection. Transportation Research Part B: Methodological 143, 124–159.

Wuyts, S., Geyskens, I., 2005. The formation of buyer–supplier relationships: detailed contract drafting and close partner selection. Journal of Marketing 69, 103–117.

Xu, J., Liu, D., 2012. Queuing models to improve port terminal handling service. Systems Engineering Procedia 4, 345–351.

Yang, S.A., Bakshi, N., Chen, C.J., 2021. Trade credit insurance: Operational value and contract choice. Management Science 67, 875–891.

Yao, Z., Ng, S.H., Lee, L.H., 2012. A study on bunker fuel management for the shipping liner services. Computers & Operations Research 39, 1160–1172.

Yu, B., Wang, K., Wang, C., Yao, B., 2017. Ship scheduling problems in tramp shipping considering static and spot cargoes. International Journal of Shipping and Transport Logistics 9, 391–416.

Zaccone, R., Ottaviani, E., Figari, M., Altosole, M., 2018. Ship voyage optimization for safe and energy-efficient navigation: A dynamic programming approach. Ocean Engineering 153, 215–224.

Zis, T.P., Psaraftis, H.N., Ding, L., 2020. Ship weather routing: A taxonomy and survey. Ocean Engineering 213, 107697.

Appendix A

Vessel characteristics and economic parameters applied in experiments

A.1 Suezmax

Table 27 includes vessel characteristics and economic parameters used in experiments for typical *Suezmax* vessel. Data are collected or adapted from Stopford (2008).

TABLE 27: Vessel characteristics for Suezmax

Definition (Symbol)	Number	Unit	Desciption
IMO number	9401805	-	Unique seven-digit vessel number the company issues to each vessel, preceded by the letters IMO
S	6,382	nm	Estimated route length
$v_{\min}$	10	knot	Lower bound of speed limit
$v_{\max}$	17	knot	Higher bound of speed limit
DWT^{cap}	157,880	dwt	Ship capacity
DWT^{dsg}	146,900	dwt	Ship design weight
DWT^{lgt}	49,000	dwt	Ship lightweight
DWT^{bal}	54,500	dwt	Ballast tank capacity
$r^{\mathrm{f}}_{\min}$	0.3	-	Minimum fillrate
Q^l	1,200,000	unit	Loading quantity
f^{TCH}	20,000	USD per day	Daily hire rate
R	0.5	USD per barrel per 1000nm	Unit revenue
k	3.91×10^{-6}	-	Fuel consumption function parameter
p	381	-	Fuel consumption function parameter
g	3.1	-	Fuel consumption function parameter
α	0.08	-	Opportunity cost of capital rate per year
r^l	3,000	m^3 per hour	Loading rate
r^u	3,000	m^3 per hour	Discharging rate
T^w	48	hour	Waiting time includes queuing and berthing time
c^f	63	USD per tonne	Main bunker fuel price
$c^{f_{aux}}$	590	USD per tonne	Auxiliary fuel price
c^p	300,000	USD per single entry	Fixed Port Access Costs
c^l	4,000	USD per hour	Loading charge
c^u	4,000	USD per hour	Unloading charge

A.2 PANAMANA

Table 28 includes vessel characteristics and economic parameters used in experiments for *PANAMANA* which belongs to the category of *Panamax* vessel. Data are obtained directly from

https://www.sea.live. Parameters about fuel consumption are calculated by solving a nonlinear function when substituting groups of loading weight, speed, and fuel consumption per day which are found from the same data source.

TABLE 28: Vessel characteristics for PANAMANA

Definition (Symbol)	Number	Unit	Desciption
S	8,293	nm	Route length from Nueva Palmira to Londonderry
$v_{\min}$	10	knot	Lower bound of speed limit
$v_{\max}$	19.3	knot	Higher bound of speed limit
DWT^{cap}	54,810	dwt	Ship capacity
DWT^{dsg}	50,425	dwt	Ship design weight
DWT^{lgt}	39,258	dwt	Ship lightweight
DWT^{bal}	54,500	dwt	Ballast tank capacity
$r^{\text{f}}_{\min}$	0.3	-	Minimum fillrate
Q^l	122,000	unit	Loading quantity
f^{TCH}	26,500	USD per day	Daily hire rate
R	0.5	USD per unit per 1000nm	Unit revenue
k	5.81×10^{-9}	-	Fuel consumption function parameter
p	3,275,000	-	Fuel consumption function parameter
g	5.32	-	Fuel consumption function parameter
α	0.08	-	Opportunity cost of capital rate per year
r^l	3,000	m^3 per hour	Loading rate
r^u	3,000	m^3 per hour	Discharging rate
T^w	48	hour	Waiting time includes queuing and berthing time
c^f	63	USD per tonne	Main bunker fuel price
$c^{f_{aux}}$	590	USD per tonne	Auxiliary fuel price
c^p	300,000	USD per single entry	Fixed Port Access Costs
c^l	4,000	USD per hour	Loading charge
c^u	4,000	USD per hour	Unloading charge

A.3 Experiment results for PANAMANA

Table 29 shows computational results solved by mean-CVaR model with long-term risk for increasing profit target (in long-term) and risk level. Before approaching the narrow range of constraints, optimal speed will not be influenced by the amount of profit target or risk level, which is observable from cases $\mu_l' = 0,\ 55$ for $\text{R} = 0.05,\ 0.3,\ 0.8,\ 0.999$. The narrow profit target range for risk level $\text{R} = 0.05$ is $\mu_l' \in (55.46, 55.47)$. Within this range, optimal speed decreases from 16.52 knots to the lower speed limit which is 10 knots and finally becomes not feasible, which is shown as 'NA' in the table. We also observe the narrow profit target range for $\text{R} = 0.8$ is $\mu_l' \in (109.34, 109.36)$.

Table 30 shows optimal speeds suggested to different types of decision makers under various FPP. The distribution of FPP is constructed based on the TCH and average CV value between 2019 and 2021 for DBE-P, see Tables 9-10. The difference between optimal speeds suggested for decision makers that hold different risk attitudes mainly depends on the expectation of FPP's distribution.

TABLE 29: Optimal speed and NPV values when applying multiple profit targets and risk levels in mean-CVaR model with long-term risk, $\alpha G_0 \sim N(26,500; 6,625^2)$, for PANAMANA

Model Type: Mean-CVaR with long-term risk			E	26,500
Risk measure ($\rho(\cdot)$))	CVaR		SD	6,625
Profit target (μ_l') (million USD)	0			
Risk level (R)	0.05	0.3	0.8	0.999
Speed (x) (knots)	16.52	16.52	16.52	16.52
NPV including FPP (H) (million USD)	119.470	119.470	119.470	119.470
NPV excluding FPP (h) (million USD)	-1.095	-1.095	-1.095	-1.095
Profit target (μ_l') (million USD)	55			
Risk level (R)	0.05	0.3	0.8	0.999
Speed (x) (knots)	16.52	16.52	16.52	16.52
NPV including FPP (H) (million USD)	119.470	119.470	119.470	119.470
NPV excluding FPP (h) (million USD)	-1.095	-1.095	-1.095	-1.095
Profit target (μ_l') (million USD)	55.465			
Risk level (R)	0.05	0.3	0.8	0.999
Speed (x) (knots)	16.05	16.52	16.52	16.52
NPV including FPP (H) (million USD)	119.468	119.470	119.470	119.470
NPV excluding FPP (h) (million USD)	-0.936	-1.095	-1.095	-1.095
Profit target (μ_l') (million USD)	55.4656			
Risk level (R)	0.05	0.3	0.8	0.999
Speed (x) (knots)	15.84	16.52	16.52	16.52
NPV including FPP (H) (million USD)	119.465	119.470	119.470	119.470
NPV excluding FPP (h) (million USD)	-0.933	-1.095	-1.095	-1.095
Profit target (μ_l') (million USD)	80			
Risk level (R)	0.05	0.3	0.8	0.999
Speed (x) (knots)	NA	16.52	16.52	16.52
NPV including FPP (H) (million USD)	NA	119.470	119.470	119.470
NPV excluding FPP (h) (million USD)	NA	-1.095	-1.095	-1.095
Profit target (μ_l') (million USD)	109.3506´			
Risk level (R)	0.05	0.3	0.8	0.999
Speed (x) (knots)	NA	NA	16.44	16.52
NPV including FPP (H) (million USD)	NA	NA	119.470	119.470
NPV excluding FPP (h) (million USD)	NA	NA	-9.443	-1.095
Profit target (μ_l') (million USD)	110			
Risk level (R)	0.05	0.3	0.8	0.999
Speed (x) (knots)	NA	NA	NA	16.52
NPV including FPP (H) (million USD)	NA	NA	NA	119.470
NPV excluding FPP (h) (million USD)	NA	NA	NA	-1.095

TABLE 30: Optimal speed when applying multiple scenarios of FPP and risk attitudes in mean-CVaR model with long-term risk for PANAMANA

Scenarios	Optimal speed				
$k_r = 2, z \sim B(10, 0.3)$	LH[a]	HH[b]	LL [c]	HL [d]	RN [e]
$\alpha G_0 \sim (-10,000; 2,500^2)$	NA	NA	NA	NA	NA
$\alpha G_0 \sim (0; 0)$	NA	NA	NA	NA	NA
$\alpha G_0 \sim (13,250; 3,312.5^2)$	15.86	NA	15.86	NA	15.86
$\alpha G_0 \sim (26,500; 6,625^2)$	16.52	16.52	16.52	16.52	16.52
$\alpha G_0 \sim (39,750; 9,937.5^2)$	17.06	17.06	17.06	17.06	17.06

[a] $\mu_l' = 30$, R = 0.8, [b] $\mu_l' = 80$, R = 0.8, [c] $\mu_l' = 30$, R = 0.3,, [d] $\mu_l' = 80$, R = 0.3, [e] Risk neutral, $\mu_l' = 0$, R = 1.

Appendix B

Estimation formulas for skewed-normal distribution $SN \sim (\alpha, \xi, \omega)$

Assume statistics obtained from sample data are given by sample mean $\hat{\mu}$, sample variance $\hat{\delta}^2$ and sample skewness $\hat{\tau}$. Based on the method of maximum likelihood estimation introduced in Pewsey (2000), there are:

$$|\eta| = \sqrt{\frac{\pi}{2} \cdot \frac{|\hat{\tau}|^{2/3}}{|\hat{\tau}|^{2/3} + ((4-\pi)/2)^{2/3}}}, \tag{B.1}$$

$$\eta = \frac{\alpha}{\sqrt{1+\alpha^2}}, \tag{B.2}$$

where the estimator for shape parameter $\hat{\alpha}$ could be solved. Also, according to the distribution function, the mean and variance could be found by:

$$\omega = \sqrt{\frac{\pi\hat{\delta}^2}{\pi - 2\eta^2}}, \tag{B.3}$$

$$\xi = \hat{\mu} - \omega\eta\sqrt{\frac{2}{\pi}}. \tag{B.4}$$

Appendix C

Initialisation for Chapter 4

The ordinal numbers for the waypoints shown above in Figure 9 are written as: The distance

TABLE 31: Ordinal number for the waypoints when the total number of stages is 7

Ordinal number	Waypoint
1	[0, 0]
2	[1, 0]
3	[2, -1]
4	[2, 0]
5	[2, 1]
6	[3, -2]
7	[3, -1]
8	[3, 0]
9	[3, 1]
10	[3, 2]
11	[4, -1]
12	[4, 0]
13	[4, 1]
14	[5, 0]
15	[6, 0]

matrix of the waypoints shown above is defined by:

$$
\mathrm{A}_{15\times 15} = \begin{pmatrix}
0 & 0 & +\infty & +\infty & +\infty & +\infty & +\infty & +\infty & +\infty & +\infty \\
+\infty & +\infty & +\infty & +\infty & +\infty & & & & & \\
+\infty & 0 & 2393.98 & 2073.25 & 2393.98 & +\infty & +\infty & +\infty & +\infty & +\infty \\
+\infty & +\infty & +\infty & +\infty & +\infty & & & & & \\
+\infty & +\infty & 0 & +\infty & +\infty & 2393.98 & 2073.25 & 2393.98 & +\infty & +\infty \\
+\infty & +\infty & +\infty & +\infty & +\infty & & & & & \\
+\infty & +\infty & +\infty & 0 & +\infty & +\infty & 2393.98 & 2073.25 & 2393.98 & +\infty \\
+\infty & +\infty & +\infty & +\infty & +\infty & & & & & \\
+\infty & +\infty & +\infty & +\infty & 0 & +\infty & +\infty & 2393.98 & 2073.25 & 2393.98 \\
+\infty & +\infty & +\infty & +\infty & +\infty & & & & & \\
+\infty & +\infty & +\infty & +\infty & +\infty & 0 & +\infty & +\infty & +\infty & +\infty \\
2393.98 & +\infty & +\infty & +\infty & +\infty & & & & & \\
+\infty & +\infty & +\infty & +\infty & +\infty & +\infty & 0 & +\infty & +\infty & +\infty \\
2073.25 & 2393.98 & +\infty & +\infty & +\infty & & & & & \\
+\infty & +\infty & +\infty & +\infty & +\infty & +\infty & +\infty & 0 & +\infty & +\infty \\
2393.98 & 2073.25 & 2393.98 & +\infty & +\infty & & & & & \\
+\infty & +\infty & +\infty & +\infty & +\infty & +\infty & +\infty & +\infty & 0 & +\infty \\
+\infty & 2393.98 & 2073.25 & +\infty & +\infty & & & & & \\
+\infty & +\infty & +\infty & +\infty & +\infty & +\infty & +\infty & +\infty & +\infty & 0 \\
+\infty & +\infty & 2393.98 & +\infty & +\infty & & & & & \\
+\infty & +\infty & +\infty & +\infty & +\infty & +\infty & +\infty & +\infty & +\infty & +\infty \\
0 & +\infty & +\infty & 2393.98 & +\infty & & & & & \\
+\infty & +\infty & +\infty & +\infty & +\infty & +\infty & +\infty & +\infty & +\infty & +\infty \\
+\infty & 0 & +\infty & 2073.25 & +\infty & & & & & \\
+\infty & +\infty & +\infty & +\infty & +\infty & +\infty & +\infty & +\infty & +\infty & +\infty \\
+\infty & +\infty & 0 & 2393.98 & +\infty & & & & & \\
+\infty & +\infty & +\infty & +\infty & +\infty & +\infty & +\infty & +\infty & +\infty & +\infty \\
+\infty & +\infty & +\infty & 0 & 0 & & & & & \\
+\infty & +\infty & +\infty & +\infty & +\infty & +\infty & +\infty & +\infty & +\infty & +\infty \\
+\infty & +\infty & +\infty & +\infty & 0 & & & & &
\end{pmatrix}.
$$

Let the a_{ij} represents an element in row i and column j in distance matrix $\mathbf{A}$, $a_{ij} \to +\infty$ indicates the inaccessibility from waypoint i to j, where i and j are the ordinal number of waypoints that could be found in Table 32. And, $a_{ij} = 0$ means the distance between the waypoint and itself or their location information are the same, i.e. $[0,0]$ and $[1,0]$ or $[5,0]$ and $[6,0]$. When $a_{ij} > 0$ and $a_{ij} \in \mathbb{R}$, sailing from waypoint i to j is supposed to be accessible and the length of the sailing is a_{ij}.

Initialisation

The ordinal numbers for the waypoints shown above in Figure 9 are written as: The distance matrix of the waypoints shown above is defined by:

TABLE 32: Ordinal number for the waypoints when the total number of stages is 7

Ordinal number	Waypoint
1	[0, 0]
2	[1, 0]
3	[2, -1]
4	[2, 0]
5	[2, 1]
6	[3, -2]
7	[3, -1]
8	[3, 0]
9	[3, 1]
10	[3, 2]
11	[4, -1]
12	[4, 0]
13	[4, 1]
14	[5, 0]
15	[6, 0]

$$
\mathrm{A}_{15\times 15} = \begin{pmatrix}
0 & 0 & +\infty & +\infty & +\infty & +\infty & +\infty & +\infty & +\infty & +\infty \\
+\infty & +\infty & +\infty & +\infty & +\infty & & & & & \\
+\infty & 0 & 2393.98 & 2073.25 & 2393.98 & +\infty & +\infty & +\infty & +\infty & +\infty \\
+\infty & +\infty & +\infty & +\infty & +\infty & & & & & \\
+\infty & +\infty & 0 & +\infty & +\infty & 2393.98 & 2073.25 & 2393.98 & +\infty & +\infty \\
+\infty & +\infty & +\infty & +\infty & +\infty & & & & & \\
+\infty & +\infty & +\infty & 0 & +\infty & +\infty & 2393.98 & 2073.25 & 2393.98 & +\infty \\
+\infty & +\infty & +\infty & +\infty & +\infty & & & & & \\
+\infty & +\infty & +\infty & +\infty & 0 & +\infty & +\infty & 2393.98 & 2073.25 & 2393.98 \\
+\infty & +\infty & +\infty & +\infty & +\infty & & & & & \\
+\infty & +\infty & +\infty & +\infty & +\infty & 0 & +\infty & +\infty & +\infty & +\infty \\
2393.98 & +\infty & +\infty & +\infty & +\infty & & & & & \\
+\infty & +\infty & +\infty & +\infty & +\infty & +\infty & 0 & +\infty & +\infty & +\infty \\
2073.25 & 2393.98 & +\infty & +\infty & +\infty & & & & & \\
+\infty & +\infty & +\infty & +\infty & +\infty & +\infty & +\infty & 0 & +\infty & +\infty \\
2393.98 & 2073.25 & 2393.98 & +\infty & +\infty & & & & & \\
+\infty & +\infty & +\infty & +\infty & +\infty & +\infty & +\infty & +\infty & 0 & +\infty \\
+\infty & 2393.98 & 2073.25 & +\infty & +\infty & & & & & \\
+\infty & +\infty & +\infty & +\infty & +\infty & +\infty & +\infty & +\infty & +\infty & 0 \\
+\infty & +\infty & 2393.98 & +\infty & +\infty & & & & & \\
+\infty & +\infty & +\infty & +\infty & +\infty & +\infty & +\infty & +\infty & +\infty & +\infty \\
0 & +\infty & +\infty & 2393.98 & +\infty & & & & & \\
+\infty & +\infty & +\infty & +\infty & +\infty & +\infty & +\infty & +\infty & +\infty & +\infty \\
+\infty & 0 & +\infty & 2073.25 & +\infty & & & & & \\
+\infty & +\infty & +\infty & +\infty & +\infty & +\infty & +\infty & +\infty & +\infty & +\infty \\
+\infty & +\infty & 0 & 2393.98 & +\infty & & & & & \\
+\infty & +\infty & +\infty & +\infty & +\infty & +\infty & +\infty & +\infty & +\infty & +\infty \\
+\infty & +\infty & +\infty & 0 & 0 & & & & & \\
+\infty & +\infty & +\infty & +\infty & +\infty & +\infty & +\infty & +\infty & +\infty & +\infty \\
+\infty & +\infty & +\infty & +\infty & 0 & & & & &
\end{pmatrix}.
$$

Let the a_{ij} represents an element in row i and column j in distance matrix $\mathbf{A}$, $a_{ij} \to +\infty$ indicates the inaccessibility from waypoint i to j, where i and j are the ordinal number of waypoints that could be found in Table 32. And, $a_{ij} = 0$ means the distance between the waypoint and itself or their location information are the same, i.e. $[0,0]$ and $[1,0]$ or $[5,0]$ and $[6,0]$. When $a_{ij} > 0$ and $a_{ij} \in \mathbb{R}$, sailing from waypoint i to j is supposed to be accessible and the length of the sailing is a_{ij}.

Appendix D

Payment structure under FTB by terms

We describe the payment structure models for following combinations of terms and freight payment: 1. FOB-O-FC; 2. FOB-O-FP, CIF-FP, and CFR-FP [33]; 3. FOB-O-FPCB; 4. FOB-D-FC; 5. FOB-D-FP; 6. FOB-D-FCA.

D.1 Freight prepaid under fully trusted business (FP under FTB)

Carriers send bills of freight charges to the party who takes the responsibility paying the freight charges before shipment with an allowable paying period. The party who takes the responsibility of paying the additional shipping fees could be different from the one pays for previous bill. We conclude the payment structure for multiply terms that are freight prepaid in Section D.1.1-D.1.3.

D.1.1 FOB-O-FP, CIF-FP, and CFR-FP

According to Table 23, for FOB-O-FP, CIF-FP, and CFR-FP, shipper is liable to pay freight charges as well as any possible ancillary charges that arise in transit. Of the two the latter will be billed to the shipper individually and should be cleared within the allowed clearing period after the consignee receives the cargo. While the former is billed before the shipment and should be paid within the allowed payment period by the shipper. The stream of event is shown in Figure 23.

Then, we present a symmetric cash-flows for carrier, shipper and consignee in Figure 24.

It is notable the dashed line in above figure does indicates the payments have zero delay. (Beullens and Janssens, 2014) explains the symmetric payment is a conventional payment structure.

[33] As the cost of cargo insurance is usually included in the price of cargo and should be considered in the payment structure of demand of supply, these three terms and freight payment has the same characteristics as stated in Table 23.

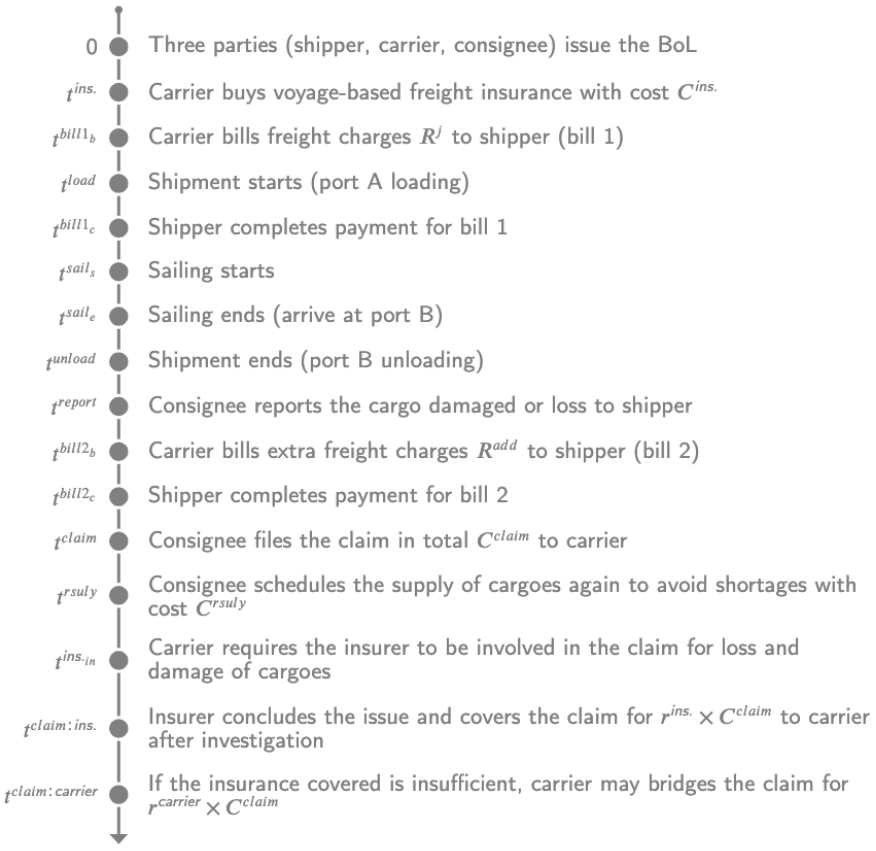

FIGURE 23: Stream of events for FOB-O-FP, CIF-FP, and CFR-FP

When the shipper pays out bills of freight charges, the carrier receives the money 'immediate' and 'in full'. It is the perfect results when no clearinghouse is involved. The NPV for carrier, shipper, and consignee is given as follows:

$$\begin{aligned} \text{NPV}_{carrier} = \quad & -C^{ins.} \cdot e^{-\alpha t^{ins.}} - C^{load} \cdot e^{-\alpha t^{load}} - \int_{t^{load}}^{t^{report}} f^{TCH} \cdot e^{-\alpha t} \mathrm{d}t + R^j \cdot e^{-\alpha t^{bill1_c}} \\ & -C^{unload} \cdot e^{-\alpha t^{unload}} + R^{add} \cdot e^{-\alpha t^{bill2_c}} - C^{claim} \cdot r^{carrier} \cdot e^{-\alpha t^{claim:carrier}}, \end{aligned} \tag{D.1}$$

$$\text{NPV}_{shipper} = \quad -R^j \cdot e^{-\alpha t^{bill1_c}} - R^{add} \cdot e^{-\alpha t^{bill2_c}}, \tag{D.2}$$

$$\text{NPV}_{consignee} = \quad -C^{rsuly} \cdot e^{-\alpha t^{rsuly}} + C^{claim} \cdot r^{ins.} \cdot e^{-\alpha t^{claim:ins.}} + C^{claim} \cdot r^{carrier} \cdot e^{-\alpha t^{claim:carrier}}. \tag{D.3}$$

D.1.2 FOB-O-FPCB

The consignee is obliged to pay the additional freight charges that arise in transit. Thus, the stream of events for FOB-O-FPCB could be obtained by altering the definitions of t^{bill2_b} and

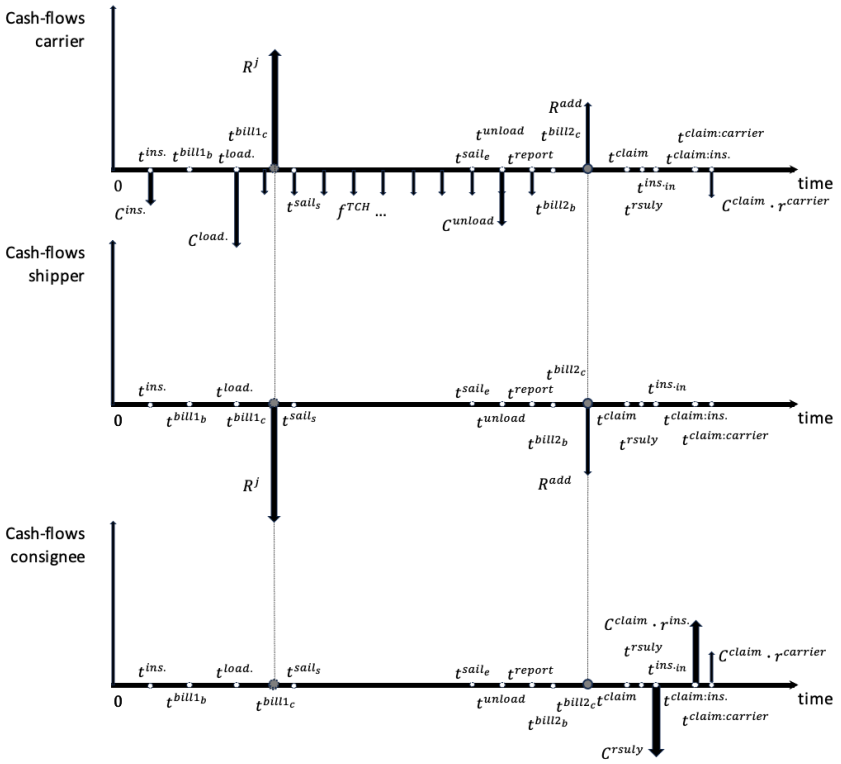

FIGURE 24: A symmetric cash-flows for carrier, shipper and consignee in FOB-O-FP, CIF-FP, and CFR-FP under FTB

t^{bill2_c} to 'Carrier bills extra freight charges R^{add} to consignee (bill 2)', 'Consignee completes payment for bill 2', respectively. And the others keep the same. We leave out the full stream of events for FOB-O-FPCB due to the minor changes. The symmetric cash-flows for carrier, shipper and consignee is shown in Figure 25 as follows:

There is no change in cash-flows for carrier between Figure 24 and Figure 25, thus the NPV of carrier in FOB-O-FPCB under FTB is also written as (D.1). The NPV for shipper, and consignee is given as follows:

$$\text{NPV}_{shipper} = \quad -R^j \cdot e^{-\alpha t^{bill1_c}}, \tag{D.4}$$

$$\begin{aligned}\text{NPV}_{consignee} = \quad & -C^{rsuly} \cdot e^{-\alpha t^{rsuly}} - R^{add} \cdot e^{-\alpha t^{bill2_c}} + C^{claim} \cdot r^{ins.} \cdot e^{-\alpha t^{claim:ins.}} \\ & + C^{claim} \cdot r^{carrier} \cdot e^{-\alpha t^{claim:carrier}}.\end{aligned} \tag{D.5}$$

D.1.3 FOB-D-FP

The shipper is obliged to pay and bear freight charges, and file the claim if there is any. The stream of event is shown in Figure 26.

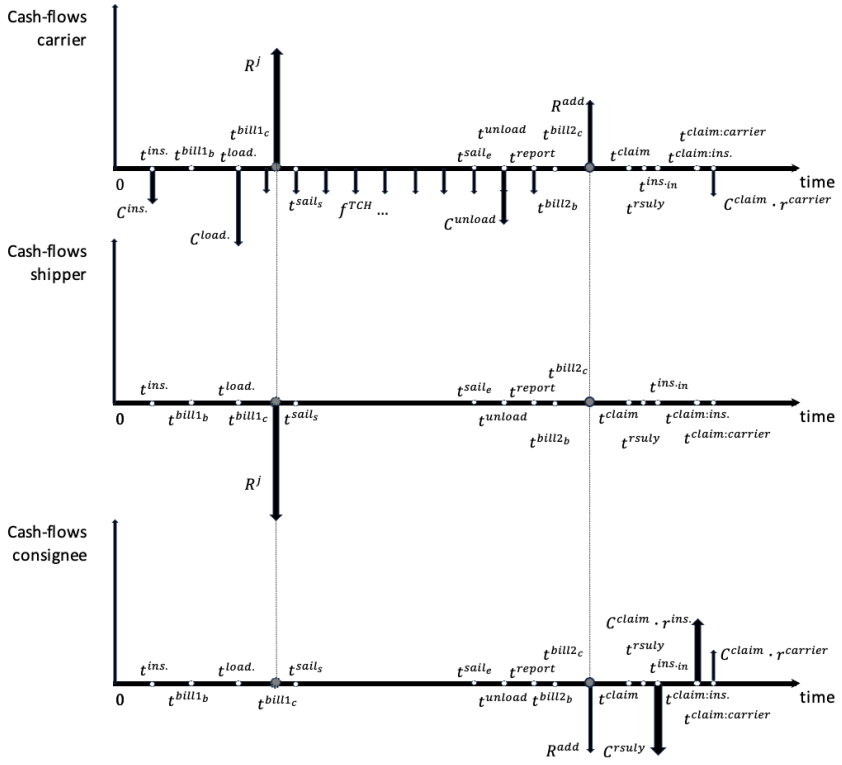

FIGURE 25: A symmetric cash-flows for carrier, shipper and consignee in FOB-O-FPCB under FTB

FIGURE 26: Stream of events for FOB-D-FP under FTB

The shipper should take the responsibility to help consignee reschedule supply of cargoes if loss and damage happened in transit. It is due to the title of cargoes belongs to shipper until it is delivered to consignee, which is different with other freight prepaid terms discussed in Section D.1.1 and D.1.2. Thus the cost of rescheduling supply of demand is altered from C^{rsuly} to C^{comp}, corresponding time is altered from t^{rsuly} to t^{comp}. It also results that shipper is responsible to file claims. The symmetric cash-flows for carrier, shipper and consignee is shown in Figure 27 as follows:

There is no change in cash-flows for carrier between Figure 24, Figure 25, and Figure 27, thus the NPV of carrier in FOB-D-FP under FTB is also written as (D.1). The NPV for shipper, and consignee is given as follows:

$$\begin{aligned}\text{NPV}_{shipper} = \quad & -R^j \cdot e^{-\alpha t^{bill1_c}} - C^{comp} \cdot e^{-\alpha t^{comp}} - R^{add} \cdot e^{-\alpha t^{bill2_c}} + C^{claim} \cdot r^{ins.} \cdot e^{-\alpha t^{claim:ins.}} \\ & + C^{claim} \cdot r^{carrier} \cdot e^{-\alpha t^{claim:carrier}},\end{aligned} \tag{D.6}$$

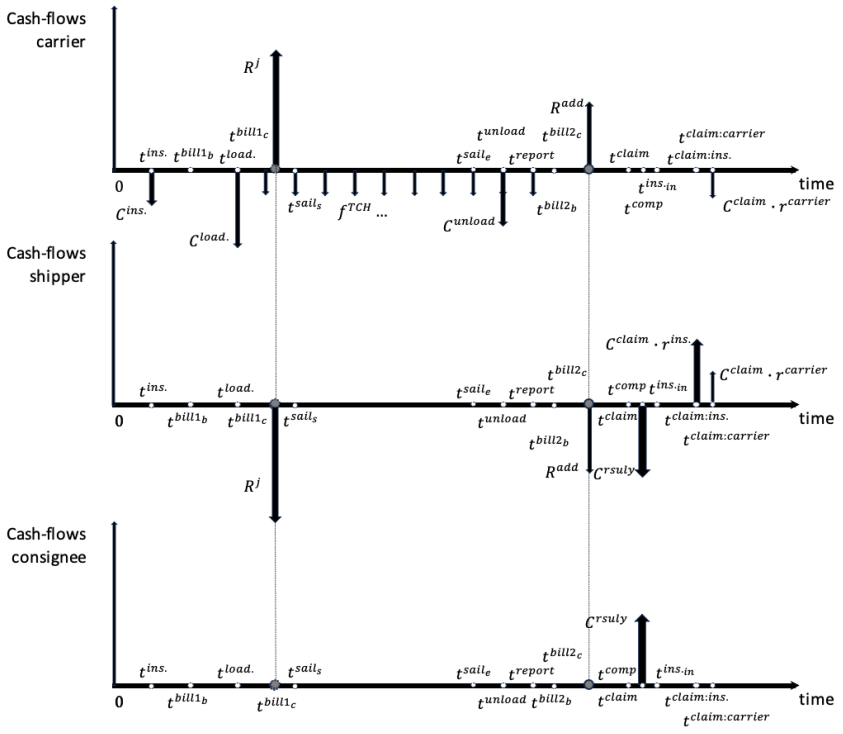

FIGURE 27: A symmetric cash-flows for carrier, shipper and consignee in FOB-D-FP under FTB

$$\text{NPV}_{consignee} = \quad C^{comp} \cdot e^{-\alpha t^{comp}}. \tag{D.7}$$

D.2 Freight collect under fully trusted business (FC under FTB)

The consignee who collects the cargo is obligated to pay the agreed freight charges under FC. Specifically, additional fees are bore by the consignee in FOB-O-FC and FOB-D-FC or by the shipper in FOB-D-FCA. Bills are sent to the party who is liable to make the payment after the cargoes are delivered. The payment structure for multiply terms that are freight collect in Section D.2.1-D.2.3.

D.2.1 FOB-O-FC

Consignee is liable to pay and bear the freight charges and file the claim if there is any. The symmetric cash-flows for carrier, shipper and consignee in FOB-O-FC under FTB is shown in Figure 29.

From the above symmetric cash-flows, the consignee pays the freight charges and additional fees $R^j + R^{add}$ at time t^{bill_c}, and the carrier receives the equal payment immediately. The shipper disclaims any responsibility for damage or loss in transit or reschedule supply in order to avoid a shortage. Thus, there is no cash-flows for shipper in FOB-O-FC under FTB. The NPV for carrier, shipper, and consignee is given as follows:

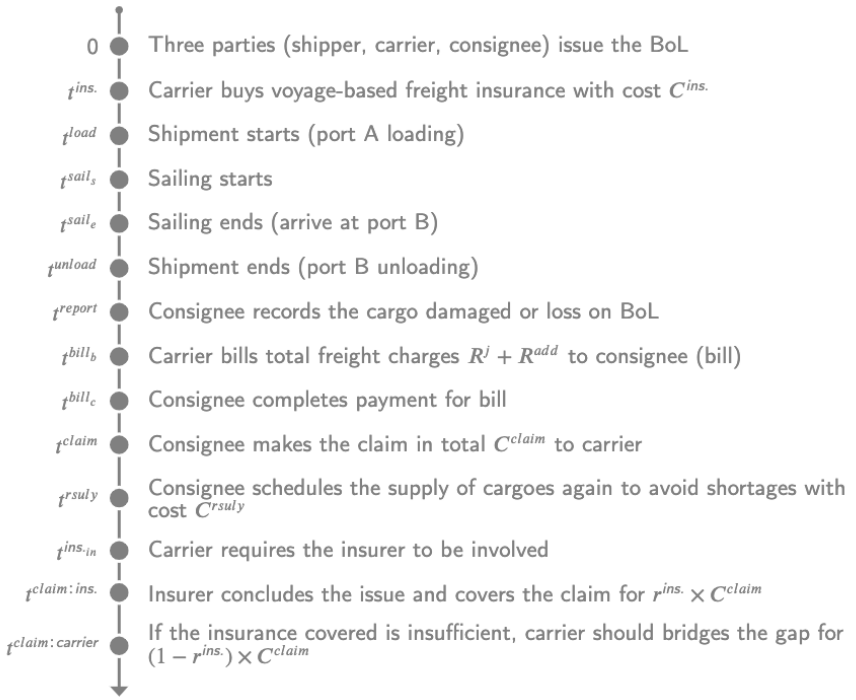

FIGURE 28: Stream of events for payment structures for FOB-O-FC under FTB

$$\begin{aligned} \text{NPV}_{carrier} = \quad & -C^{ins.} \cdot e^{-\alpha t^{ins.}} - C^{load} \cdot e^{-\alpha t^{load}} - \int_{t^{load}}^{t^{report}} f^{TCH} \cdot e^{-\alpha t} \mathrm{d}t - C^{unload} \cdot e^{-\alpha t^{unload}} \\ & + (R^j + R^{add}) \cdot e^{-\alpha t^{bill_c}} - C^{claim} \cdot r^{carrier} \cdot e^{-\alpha t^{claim:carrier}}, \end{aligned} \tag{D.8}$$

$$\text{NPV}_{shipper} = \quad 0 \tag{D.9}$$

$$\begin{aligned} \text{NPV}_{consignee} = \quad & -(R^j + R^{add}) \cdot e^{-\alpha t^{bill_c}} - C^{rsuly} \cdot e^{-\alpha t^{rsuly}} + C^{claim} \cdot r^{ins.} \cdot e^{-\alpha t^{claim:ins.}} \\ & + C^{claim} \cdot r^{carrier} \cdot e^{-\alpha t^{claim:carrier}}. \end{aligned} \tag{D.10}$$

D.2.2 FOB-D-FC

The difference between FOB-D-FC and FOB-O-FC is that the shipper owns the cargoes in transit until delivered to consignee and takes the responsibility to file the claim if there is any. Thus, in the stream of events for payment structures for FOB-D-FC, the party who takes action at time t^{claim}, t^{rsuly} should be altered to 'shipper' rather than 'consignee'. The symmetric cash-flows for carrier, shipper and consignee in FOB-D-FC under FTB is shown in Figure 30.

The NPV for carrier in FOB-D-FC under FTB is also written as (D.8). The NPV for shipper, and consignee is given as follows:

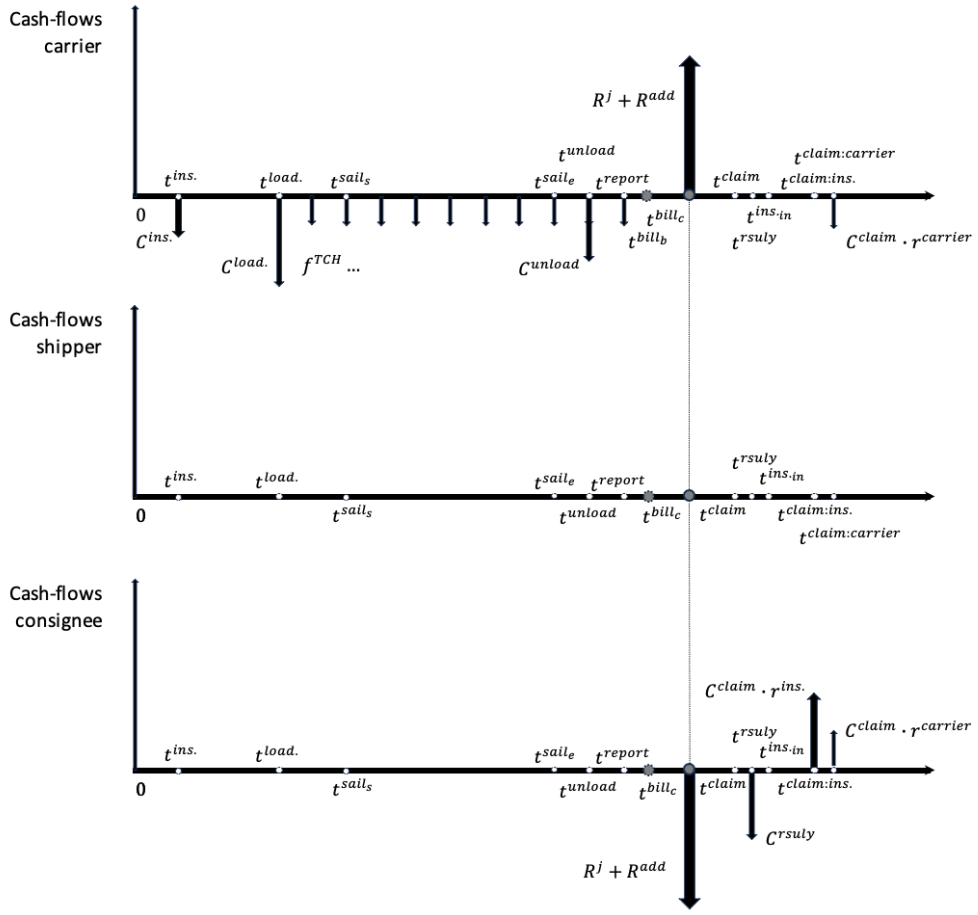

FIGURE 29: A symmetric cash-flows for carrier, shipper and consignee in FOB-O-FC under FTB

$$\text{NPV}_{shipper} = \quad -C^{rsuly} \cdot e^{-\alpha t^{rsuly}} + C^{claim} \cdot r^{ins.} \cdot e^{-\alpha t^{claim:ins.}} + C^{claim} \cdot r^{carrier} \cdot e^{-\alpha t^{claim:carrier}}, \tag{D.11}$$

$$\text{NPV}_{consignee} = \quad -(R^j + R^{add}) \cdot e^{-\alpha t^{bill_c}}. \tag{D.12}$$

D.2.3 FOB-D-FCA

The shipper bears the additional freight charges in FOB-D-FCA and takes the responsibility to file the claim if there is any. The steam of events for payment structures for FOB-D-FCA under FTB is shown in Figure 31.

The NPV for carrier in FOB-D-FC under FTB is also written as (**??**). The NPV for shipper, and consignee is given as follows:

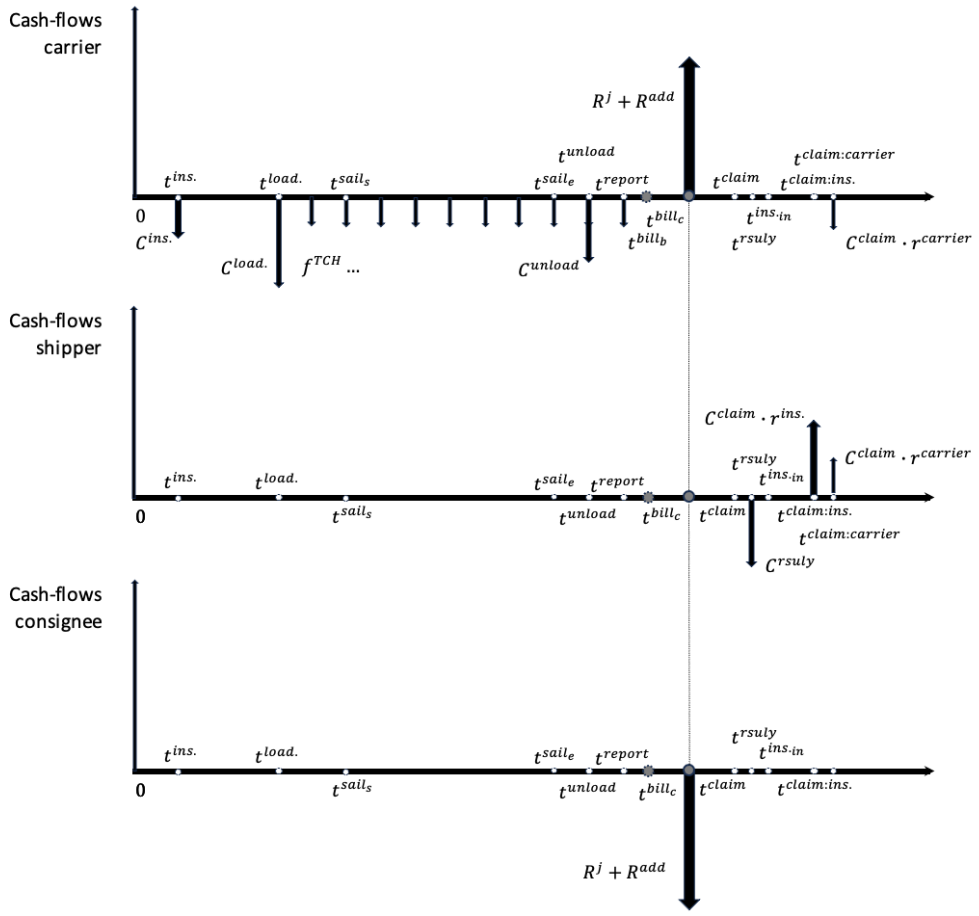

FIGURE 30: A symmetric cash-flows for carrier, shipper and consignee in FOB-D-FC under FTB

$$\text{NPV}_{shipper} = -R^{add} \cdot e^{-\alpha t^{bill_c}} - C^{rsuly} \cdot e^{-\alpha t^{rsuly}} + C^{claim} \cdot r^{ins.} \cdot e^{-\alpha t^{claim:ins.}} + C^{claim} \cdot r^{carrier} \cdot e^{-\alpha t^{claim:carrier}}, \tag{D.13}$$

$$\text{NPV}_{consignee} = -R^{j} \cdot e^{-\alpha t^{bill_c}}. \tag{D.14}$$

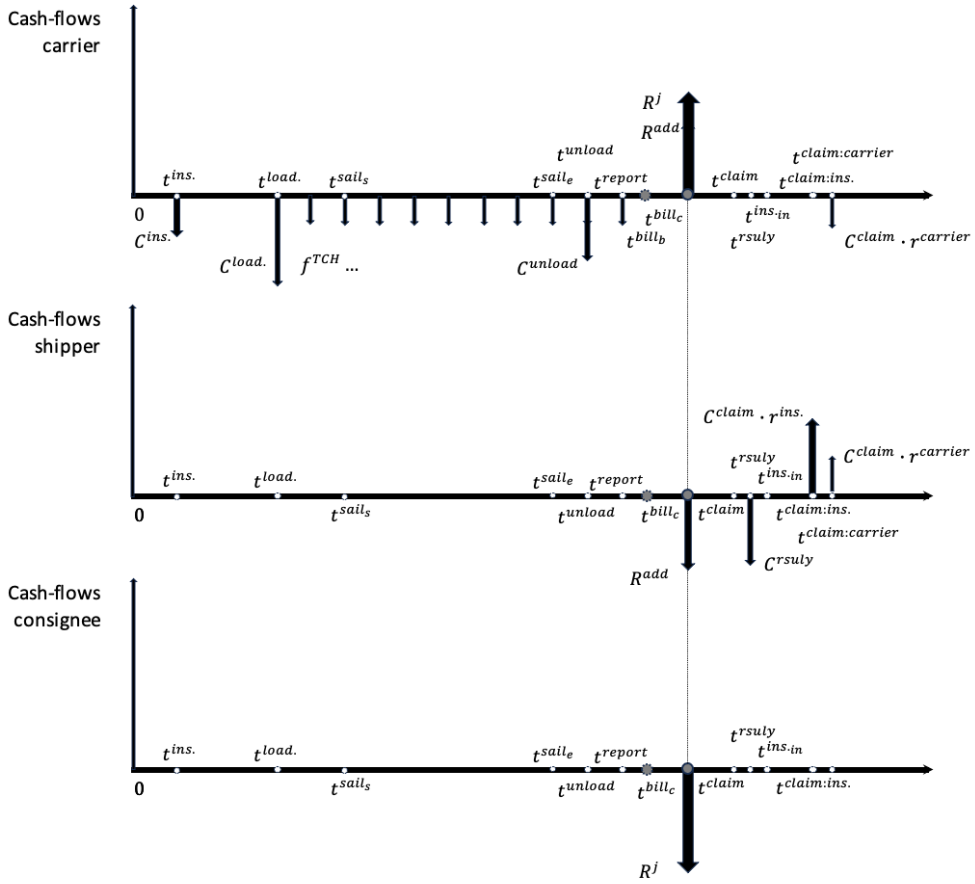

FIGURE 31: A symmetric cash-flows for carrier, shipper and consignee in FOB-D-FCA under FTB

Appendix E

Port congestion and a model for queuing system

Our problem incorporates the uncertainties involved in port congestion into two parts: before and after berthing in the port. Both parts comprise multiple reasons that may cause the port congestion. For the part before berthing the port, possible causative factors include the berth is occupied by other ships due to low service rate, wrong queuing signals, damage to the entry route for ships due to bad weather or maintenance. For the part after berthing the port, possible causative factors include labour shortages for handling cargoes and ship maintenance.

To calculate the waiting time consumed by port congestion before and after berthing in the port P, we develop general queuing models that include the queuing process before berthing as well as the queuing process while waiting for services Xu and Liu (2012). Assume the queuing system for port P is as follows:

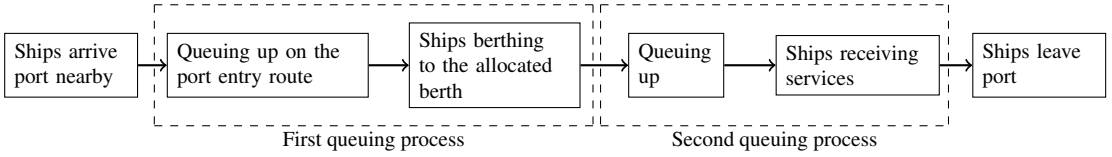

FIGURE 32: Queuing systems for vessels entering at port P

The first queuing process within the overall queuing system for port P is the ship should wait to arrive at the allocated berth. For most international ports, vessels are allocated to different areas of the port for following operations depending on the type of cargo they carry. For example, Figure 33 shows the map of Rotterdam with several segment ports where zones labelled in red are for vessels that transport dry bulk[34].

As the allocated berth is fixed for the vessel, the number of servers is 1. The first queuing process is a M/M/1 queuing mode. Assume that for the port P, ship arrivals occur at a rate of

[34]Picture source: https://rotterdamtransport.com/maps-port-of-rotterdam/gallery-2.

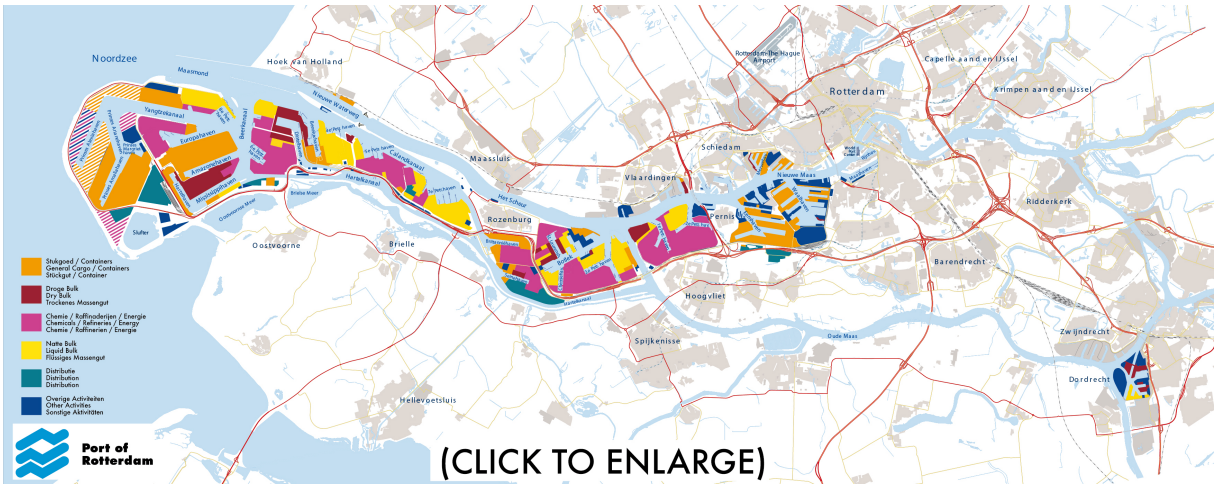

FIGURE 33: Map with segment port of Rotterdam

λ_P^b per hour on average, while service of berth occurs at a rate of μ_P^b per hour on average [35]. Ship arrival processes follow the Poisson distribution, while handling service times follow the negative exponential distribution. The ships will line up to berth based on the scheduled route as soon as they arrive at the port nearby. The utilisation factor is defined as:

$$\rho^b = \frac{\lambda_{\mathrm{P}}^b}{\mu_{\mathrm{P}}^b}, \tag{E.1}$$

for $\rho^b < 1$, the queuing system is in equilibrium. The expected waiting time for vessel in the first queuing system at port P is:

$$E[T_{pc}^b(\mathrm{P})] = \frac{1/\mu_{\mathrm{P}}^b}{1-\rho^b}, \tag{E.2}$$

where $T_{pc}^b(\mathrm{P})$ denotes the vessel's waiting time in the first queue and the service time for berthing at port P.

After arriving at the allocated berth, the ship should enter the second queuing process for further services, including unloading, ship maintenance, bunkering, and loading before leaving the port. Assume there are c servers for this segment port, the second queuing process is a M/D/c queuing model. Assume for the allocated segment port, ship arrivals occur at a rate of λ_{P}^h per hour on average. Ship arrival processes follow the Poisson distribution. There is a deterministic service time $\mathrm{D}_{\mathrm{P}}^h$ for each server (the service rate is $\mu_{\mathrm{P}}^h = 1/D_{\mathrm{P}}^h$). The ships will get ready for handling services once after they complete the berth. The utilisation factor is defined as:

[35] The average service time of berth is the time consumed for completing the berth for a ship at port P on average, which is expressed as $1/\mu_P^b$ hour.

$$\rho^h = \frac{\lambda_{\mathrm{P}}^h}{c\mu_{\mathrm{P}}^h} = \frac{\lambda_{\mathrm{P}}^h D_{\mathrm{P}}^h}{c}, \tag{E.3}$$

for $\rho^h < 1$, the queuing system is in equilibrium. The waiting time for services at berth at port P is defined as $T_{pc}^h(\mathrm{P})$. The cumulative density function for $T_{pc}^h(\mathrm{P})$ is as follows:

$$F(T_{pc}^h(\mathrm{P})) = \int_0^\infty F(x + T_{pc}^h(\mathrm{P}) - D_{\mathrm{P}}^h) \frac{(\lambda_{\mathrm{P}}^h)^c x^{c-1}}{(c-1)!} e^{-\lambda_{\mathrm{P}}^h x} \, \mathrm{d}x, \; y \geq 0. \tag{E.4}$$

As the waiting time is a non-negative variable, the expected waiting time for vessel in the second queuing system at port P could be written as:

$$E[T_{pc}^h(\mathrm{P})] = \int_0^\infty (1 - F(T_{pc}^h(\mathrm{P}))) \, \mathrm{d}T_{pc}^h(\mathrm{P}). \tag{E.5}$$

The queuing systems designed above for port congestion operate under the underlying concept of time independence (Kleinrock, 1975; Poongodi and Muthulakshmi, 2013). However, it does not imply that the data on port congestion is static and will not be updated over time during the decision-making process. For each port in the shipping network, the factors affecting port congestion are treated as discrete data.

To summarise, the time dependence of these parameters restricts the use of classic MDP in model formulation. Because t in MDP indicates phase rather than actual time. The transition from time t to time $t+1$ does not correspond to the clock moving forward in one unit, which is different from the meaning of time in our problem. In the economic ship routing and scheduling problem, on the one hand, we need to know time more precisely for a more accurate estimation of uncertainty. On the other hand, the NPV and FPP is also calculated based on time. For the above reasons, we recommend using time-dependent MDP (TMDP) for model establishment.

Appendix F

Ocean weather prediction and fuel consumption

Wind is covered in ocean weather predictions, like on land. Ocean weather, or ocean weather predictions, includes information about: (i) wind speed and direction; (ii) wave heights, directions, and periods. For instance, the main features of the *WAVEWATCH III* (WW3) weather forecast data consist of longitude, latitude, wind speed (m/s), wind direction, wave height, wave direction, and wave period.

The total resistance of the ship in calm water is estimated by the well-known Holtrop and Mennenâs method Holtrop and Mennen (1982). (Kwon, 2008) proposes an added resistance model for estimating the loss of speed due to added resistance caused by irregular ocean weather conditions. (Lu et al., 2013) concludes the speed loss for a Suez-Max oil tanker. The expressions are written as:

$$\frac{\triangle\, v}{v_1} \times 100\% = C_\beta C_U C_{Form} \tag{F.1}$$

$$\triangle\, v = v_1 - v_2 \tag{F.2}$$

$$v_2 = v_1 \cdot (1 - \frac{C_\beta C_U C_{Form}}{100\%}) \tag{F.3}$$

where $\triangle\ v$ is the speed difference, v_1 denotes design speed in calm water conditions, and v_2 denotes the ship's speed in selected weather conditions. The direction reduction coefficient, speed reduction coefficient and ship form coefficient are denoted by C_β, C_U, and C_{Form}.

We choose the optimal sailing speed (v_2) for each leg of the journey rather than the optimal design speed (v_1) for our study. We are more concerned with how much fuel needs to be consumed in order to sail at the desired speed in specific marine weather conditions than how much the weather will depletes the speed. We adopt the fuel consumption rate function introduced by (Psaraftis and Kontovas, 2014), which is written as:

$$F(v, w) = k(p + v^g)(w + A)^h, \tag{F.4}$$

where v is the average sailing speed , w is the deadweight tonnage carried, and k represents the ocean weather coefficient. The value of the coefficients k, p, g, and h depends on the features of the ship and its characteristics, whereas parameter A represents the ship's lightweight tonnage [36]. The v in (F.4) indicates ship's speed in selected weather conditions, which is v_2 in (F.1-F.3). Thus, the fuel consumption rate for sailing at speed v at sea under a specific ocean weather condition, represented by coefficients C_β, C_U, and C_{Form}, is as follows:

$$F(v, w, C) = k(p + (\frac{v}{1 - C})^g)(w + A)^h, \quad C = \frac{C_\beta C_U C_{Form}}{100\%}. \tag{F.5}$$

The calculations for the total fuel consumption and the NPV will be more precise owing to applying (F.5). The process of calculating the fuel consumption for the leg depends on the ocean weather observations and predictions. Generally, features involved in the prediction will be updated through time along the scheduled route. (Lin et al., 2013) proposes to use the linear interpolation over space and over time for obtaining the ocean weather condition when the location and time are given. The ocean weather forecast data could be acquired from the WW3, and the location could be obtained from ETOPO1. Assume for the scheduled route, the ship will arrive at location (φ, λ) at time t. In case the data can not be obtained directly due to the time or distance intervals of forecast data, the interpolation method will be applied. The linear interpolation over space is written as:

$$Z = Z_{P_1} + (Z_{P_2} - Z_{P_1})\frac{(\lambda - \lambda_1)}{(\lambda_2 - \lambda_1)}, \tag{F.6}$$

$$Z_{P_1} = Z_{11} + (Z_{21} - Z_{11})\frac{(\varphi - \varphi_1)}{(\varphi_2 - \varphi_1)}, \tag{F.7}$$

[36] In our previous study (Paper 1), we altered the coefficient k to k_r for considering the impact of irregular ocean weather conditions. The reason of abandoning the measure in this study is due to the problem scale had been expanded to a transport network rather than a single journey.

$$Z_{P_2} = Z_{12} + (Z_{22} - Z_{12})\frac{(\varphi - \varphi_1)}{(\varphi_2 - \varphi_1)}. \tag{F.8}$$

where Z denotes the data at location (φ, λ). Z_{11}, Z_{12}, Z_{21}, and Z_{22} denote the data at four locations (φ_1, λ_1), (φ_1, λ_2), (φ_2, λ_1), and (φ_2, λ_2) that they are surrounding (φ, λ). The linear interpolation over time is written as:

$$Z = Z_{t_1} + (Z_{t_2} - Z_{t_1})\frac{(t - t_1)}{(t_2 - t_1)}, \tag{F.9}$$

where Z_{t_1} and Z_{t_2} represent the data from the same location (φ, λ) at time t_1 and t_2. In this way, for any given location and time, ocean weather forecast data can be obtained directly from the database or calculated according to the above interpolation methods. The ocean weather forecast data can then be transferred into coefficients C_β, C_U, and C_{Form} by using the method introduced by (Lu et al., 2013). Finally, the fuel consumption rate for the selected weather condition could be determined using (F.5).

Appendix G

Political and legislative factors

Due to high demand in seaborne trade and calling in environmental protection and sustainable development. IMO implemented series of regulations to control the emission load of NOx, SOx, CO_2 and specifically ECA for fulfilling different requirements of the emission load regionally. For facing the ECA and other regulations, there are some deals comes up that conclude using LNG the new green fuel, using low-sulphur marine diesels or installing a scrubber, sailing longer routes or reducing speed in ECAs to avoid burning more expensive fuel. Abadie and Goicoechea (2019) combined above three options under the scenario that ECA regulations may change and parts of shipping routes will become ECA control area. According to the information provided in this paper, current ECA regulations from IMO requires emission of Sulphur and NOx as follows in Table 33,

TABLE 33: ECA regulations about Sulphur and NOx before and after 2020

Categories of Emission	ECAs	non-ECAs
Sulphur before 2020	0.10% m/m	3.50% m/m
Sulphur after 2020	0.10% m/m	0.50% m/m
NOx at 2000rpm engine speed	2g/KWh	8g/KWh

where the sulphur in non-ECAs will decreased from 3.5% m/m to 0.5% m/m. The model they established contains options such as installing duel engine, installing diesel engine, installing scrubber and not installing scrubber. Numerical experiment results show that duel engine is obviously needed with consideration of current ECA policy. Meanwhile, allowing the opportunity to install scrubber is quite necessary in different scenarios due to the potential risk that present non-ECA route will become ECA in some day.

Schinas and Stefanakos (2012) illustrated the impact of environmental policy in emission control areas(ECA) among policy-makers, researchers and operators. The sulphur limits regulated in MARPOL Annex VI can be concluded as follows: where the global sulphur limits decrease from 4.5% m/m to 3.5% m/m on 1 January 2012, drop to 0.5% m/m on 1 January 2020. For SOx ECA, there is a decrease from 1.5% m/m to 1.0% m/m on 1 January 2010 and another decrease from 1.0% m/m to 0.1% m/m.

Miola et al. (2010) summarised the European Marine Safety Agency (EMSA) as five points, increase in fuel price, model involvement fluctuated, environmental effectiveness in cost, alternatives such as scrubber and LNG and impacts ranges in different routes type and goods. Changes in the regulations strike the maritime shipping markets. From the view of the operator, operational decisions should be made in two categories, the first one is the amount of ship to buy or charter, the second one is how could the size of the ship meet the market condition (Schinas and Stefanakos, 2012). Wang et al. (2013) concluded research in bunker consumption optimisation problem to three types, minimising the fuel consumption cost, minimising total manipulation cost, joint contribution between operators and maritime corporations. Kontovas (2014) proposed the idea of 'Green Ship Routing and Scheduling Problem' (GSRSP) and pointed out the attention in GSRSP will keep the increase in future years. Mansouri et al. (2015) provided a review of research in the scope of multi-objectives optimisation in maritime optimisation, decision support system for maritime shipping and environmental sustainability in maritime shipping. They also pointed out the necessity to take environmental sustainability as one of the objectives in the maritime shipping optimisation. Dulebenets et al. (2017) added environmental regulations as constraints in the mixed integer non-linear mathematical model and the numerical experiments shown the effectiveness of solver CPLEX in constraining emissions in scheduling. Mallidis et al. (2018) evaluated the influence of environmental regulations to decision support system which formulated by mixed integer linear programming. Abadie and Goicoechea (2019) proposed navigation speed adjustment and port skipping as two options for the same problem and set the objective function as minimising the total profit loss.